Contribution of *guanine nucleotide binding protein beta polypeptide 3 (GNB3)* and

lymphocyte activation gene 3 (LAG-3) to HIV susceptibility and immune dysfunction

by

Jennifer A. Juno

A Thesis submitted to the Faculty of Graduate Studies of

The University of Manitoba

in partial fulfillment of the requirements of the degree of

Doctor of Philosophy

Department of Medical Microbiology

University of Manitoba

Winnipeg

Abstract

Host genetics play an important role in regulating susceptibility to infectious diseases, including the human immunodeficiency virus (HIV). A polymorphism in a G protein signaling gene (*GNB3*) previously associated with rapid HIV disease progression is found at high frequencies among African populations, yet its impact on HIV acquisition and disease progression is unknown. The *GNB3* gene is located on chromosome 12 near the *CD4* gene, as well the gene encoding the regulatory protein lymphocyte activation gene 3 (LAG-3). The goal of this thesis was to characterize the impact of *GNB3* genotype on risk of HIV acquisition and disease progression, as well as the relevance of LAG-3 expression to immune exhaustion during HIV infection. Because G proteins are involved in HIV entry and replication in T cells, polymorphisms affecting G protein signaling, such as *GNB3 C825T*, could dramatically alter susceptibility to HIV infection, viral replication and rates of disease progression. Similarly, the expression of the inhibitory protein LAG-3 could, like other exhaustion markers, mediate increasing immune dysfunction during chronic infection. Both GNB3 and LAG-3 could represent targets for therapeutic intervention to slow disease progression or restore lymphocyte function among HIV-infected individuals.

Surprisingly, our studies showed that *GNB3* genotype was not associated with the risk of HIV acquisition in either a female sex worker or perinatal transmission cohort. Disease progression and immune activation among healthy and HIV-infected women were also independent of *GNB3* genotype. While the RNA splicing events typically associated with the presence of the *GNB3 825T* allele could not be detected among cohort participants,

differences in LAG-3 expression were observed between women of differing *GNB3* genotypes.

In this cohort, LAG-3 expression on T cells, NK cells and iNKT cells in the peripheral blood was significantly increased among HIV+ women compared to healthy controls, and was not decreased by antiretroviral therapy. The increase in LAG-3 expression was greatest on NK and iNKT cells, an innate lymphocyte subset capable of rapid and robust cytokine production upon stimulation with CD1d-restricted lipid ligands. Lymphocytes derived from the female genital mucosa, the site of HIV acquisition in the female sex worker cohort, expressed significantly higher levels of LAG-3 compared to peripheral blood, suggesting a role for LAG-3 in regulating mucosal immunity, particularly on double negative (CD4-CD8-) T cells.

Finally, we demonstrated that iNKT cells derived from HIV-infected women exhibited significantly lower IFNγ production compared to healthy controls upon lipid stimulation, which inversely correlated with iNKT LAG-3 expression. Lipid stimulation of PBMC from HIV+ and ARV-treated women also demonstrated perturbations in the secretion of multiple cytokines and chemokines, suggesting that iNKT function is not restored following ART. Together, these data imply that LAG-3 may play an important role in regulating iNKT function during chronic HIV infection. Blocking LAG-3 signaling could therefore restore components of innate immunity that are not improved by current ART, as well as alter HIV susceptibility at the female genital tract, making LAG-3 an attractive target for future therapeutics and viral eradication strategies.

Dedication

This thesis is dedicated to my mother, a woman who embodies more strength, intelligence and love than anyone I know. Any success I attain in life is undoubtedly a result of your support and encouragement. I am so proud to be your daughter.

Acknowledgements

I would like to take this opportunity to thank everyone who has made this thesis possible, whether directly or indirectly. If I accidentally forget someone, please forgive me and know that I am grateful to everyone who contributed to my graduate studies.

First, I have to thank my advisor Dr. Keith Fowke. It was clear from the moment I set foot in the lab that your passion for science went far beyond the research, and your dedication to teaching and training has always been central to my success in the lab. I'm so glad I made the choice to work right here, in this very department.

I would also like to thank my past and present committee members, Dr. Jody Berry, Dr. Aaron Marshall and Dr. Xi Yang. You have always been supportive of my project and offered assistance whenever it was required. Although he was not on my committee, I would also like to thank Dr. Blake Ball for his willingness to provide feedback and support on my project and scientific career. Your insights have always been valuable.

Without the assistance of the support staff in the department, I would not have been able to navigate the forms, guidelines, ordering procedures or numerous other issues. Thank you to Sharon, Angie (for always remaining calm and collected when dealing with panicked students), Jude, Eva and Tash.

Similarly, most of my experiments would not have been successful without the support of our dedicated technicians. At the beginning of my degree, John Rutherford, Leslie Slaney and Ian McLean were invaluable sources of information. Thank you to Sue for her on-going organization of level 2 and everything related to cell culture, and to Adrienne and Syeda for their assistance.

The community of my fellow students and post-docs is what made everything tolerable on a daily basis. Thank you to everyone who passed through the Fowke lab during my studies: Paul, Connor, Yoav, Julius, Catherine, Andrew, Courtney, Abdi, Julie, Genevieve, Matt and Kelsi. Thank you also to all the members of the Plummer/Ball labs for your support and contributions. I am especially grateful to Cat for teaching me all things flow-related, and Genevieve for our debates and discussions. Thank you Jill, for solving my ELISA problems and generally keeping my experiments on the right track. Thank you to Lyle for every conversation over beers, all your advice, and for being an excellent Nairobi tour guide and friend. Finally, thank you to Andrew for being an eager student and an even better friend. Stressful times are always less so with you in the lab.

My project would not have been possible without the assistance of everyone at the University of Nairobi and Majengo clinic. Thank you to Joshua and Julius for your support, and Tony for your never-ending quest to provide us with internet access. Thank you to Jane, Irungu, Anne and Kyoko for your invaluable assistance with samples. I would also like to thank CIHR, the IID&GHTP and MHRC for scholarship funding. I am forever indebted to the participants of the cohort for generously donating blood and CMCs for all aspects of my project.

I would also like to thank Matt, Leta and Amanda for being supportive friends from afar, even when they have no idea what I'm doing. I miss you guys, and I think of you often.

To the people who have meant the most in my life, there truly are no words to express your importance in everything I do. Thank you grama, for always being interested in my work, and papa, I think of you often. Thank you to my mom, who has enthusiastically bragged about every accomplishment I've ever achieved. I will forever be grateful to Caitlin for years of support and encouragement that will never be forgotten. Jill, thank you for just about everything under the sun. I am a better person for knowing you, and there's nothing I can say you don't already know. Finally, thank you to Ian – for your support, for trying so valiantly to read this thesis, and for being my partner in life. No matter where we go or what we do, I look forward to spending my life with you at my side.

Table of Contents

List of Figures

List of Tables

1. Introduction

1.1 Current State of the HIV Pandemic

Globally, more than 35 million people are infected with the human immunodeficiency virus (HIV), which is the causative agent of acquired immunodeficiency syndrome (AIDS) (1). Current estimates suggest that at least 2 million new infections and 1.6 million deaths occurred in 2012 (1), emphasizing that the HIV/AIDS pandemic remains one of the most significant global public health issues today. Despite the scale up of interventions such as voluntary male circumcision and increased condom promotion and distribution, new prevention and treatment interventions are sorely needed, particularly among vulnerable populations. The aim of this thesis is to characterize the role of genetics and immune markers in regulating susceptibility to HIV infection and subsequent disease progression.

Although a worldwide health concern, the HIV pandemic has been particularly devastating in sub-Saharan Africa. The estimated adult HIV prevalence across this region is 4.7%, with Kenya reporting a higher than average prevalence of 6.1% (1). Notably, HIV prevalence among women aged 15 – 24 is more than twice that of men the same age. Female sex workers (FSW), in particular, represent a vulnerable population with high HIV incidence compared to the general population (2). In Kenya, HIV-infected sex workers form a bridge population to the general public. This thesis focuses on HIV acquisition and immune function among a long-standing cohort of FSWs located in Nairobi, the capital of Kenya.

1.2 HIV Identification, Transmission and Prevention

1.2.1 Identification of HIV

The discovery of the human immunodeficiency virus was preceded by the description of a cluster of infections of the fungus *Pneumocystis carinii* (now *Pneumocystis jiroveci*) in the United States in 1981 (3). This rare infection, and, additionally, Kaposi's sarcoma, was reported among previously healthy, young, gay men who exhibited signs of severe immunodeficiency (4). As more cases of the newly-named Acquired Immunodeficiency Syndrome (AIDS) were reported, risk factors were determined to include homosexuality, intravenous drug use (IDU), Haitian ethnicity and hemophilia A (5). By 1983, several groups identified the etiological agent of AIDS, a retrovirus similar to the human T cell leukemia virus (HTLV) group that was later named the Human Immunodeficiency Virus (HIV) (6-9).

Subsequent research has led to a detailed understanding of the origins and diversity of HIV throughout the world. The original HIV isolates described above belong to the type HIV-1, which is responsible for the vast majority of the worldwide HIV pandemic. A second type, HIV-2, is genetically distinct from HIV-1 and results in slower disease progression and, in some cases, lack of progression to AIDS (reviewed in (10)). HIV-1 (referred to herein as HIV) is phylogenetically divided into groups M, N, O, and, most recently, P (11, 12), all of which originated from zoonotic transmission of simian immunodeficiency virus (SIV) from chimpanzees or gorillas to humans (reviewed in (13)). HIV strains are further subdivided into clades, which exhibit regional variation in prevalence (14), with clade B predominating in North America, and clades A, C and D in

Africa.

1.2.2 HIV Transmission

HIV is transmitted via contact with infected blood or mucosal secretions, and is most

commonly acquired by unprotected sexual intercourse, injection drug use, blood

transfusion or vertical transmission from mother to infant. In contrast to the risk factors

identified in the 1980s, heterosexual intercourse is now a major driver of transmission in

many parts of the world, including sub-Saharan Africa (15). The risk of transmission via

sexual intercourse is low, but transmission from male to female is more likely than from

female to male (16, 17). Mechanisms of HIV transmission across the mucosal barrier at

the female genital tract are reviewed in Section 1.9, but factors that increase the risk of

sexual HIV transmission include the presence of other sexually transmitted infections

(STIs) (17-19) and transmitter viral load (17, 20).

Although mother to child transmission (MTCT) is infrequent among developed countries

due to the use of antiretroviral (ARV) drugs (21), it remains an important mode of

transmission in sub-Saharan Africa (22). MTCT can occur *in utero*, intrapartum (during

delivery) or postpartum (via breastfeeding) and is more likely among women with high

viral loads. Current WHO guidelines for the prevention of MTCT include prophylactic

ARV therapy (ART) and exclusive breastfeeding for the first six months of life (23).

1.2.3 HIV Treatment and Prevention

Since the beginning of the HIV epidemic, the discovery of successful treatment and prevention interventions has remained a top research priority. The development of ARV drugs that control viral load and prevent/delay disease progression remains one of the most important breakthroughs in HIV research; only 47% of eligible individuals in low- and middle-income countries, however, currently receive treatment (24). In addition to delaying disease progression and extending life expectancy, early initiation of ART during infection and use of pre-exposure prophylaxis (PrEP) are now being considered as prevention tools with the potential to eliminate sexual HIV transmission (25-30). Indeed, implementation of the WHO guidelines for ARV initiation is projected to have a profound impact on HIV prevalence in the most highly affected regions of sub-Saharan Africa (31). Despite this, the logistical challenges of implementing ART scale-up in resource-poor settings, the difficulty in identifying cases of acute infection, the costs of treatment and testing, and increasing rates of viral resistance remain significant barriers to the use of ARVs as prevention tools (28, 32, 33).

In addition to the promotion of condom use, several biomedical interventions have shown promise in preventing HIV infection. Male circumcision is now recognized to reduce HIV acquisition by 38-66%, and can safely be implemented even in resource-limited settings (34, 35). Despite initially disappointing clinical trials, microbicides also represent a promising tool for preventing HIV acquisition among women (36). Recently, adherent application of an ARV-based gel was shown to reduce HIV incidence by 54%, representing a significant advancement in HIV prevention for women unable to negotiate

condom use (37). Finally, the development of a successful HIV vaccine, either to induce protective immunity or to reduce viral load and slow disease progression following infection, has been elusive thus far (reviewed in (38)). The most successful vaccine candidate tested to date, RV144, demonstrated a modest 31% efficacy (39) with immune correlates of protection involving plasma IgG titres against the HIV gp120 protein (40). A more successful vaccine candidate will, therefore, likely need to elicit both B cell and T cell responses (41, 42).

1.3 HIV structure and replication

HIV is a single-stranded RNA retrovirus of the family *Retroviridae* and genus *Lentiviridae*. The 9.5 kilobase positive-sense genome contains 9 open reading frames that encode 15 proteins (43), including the 3 structural polyproteins Gag, Pol and Env, the 3 accessory proteins Vif, Vpr and Vpu, and the 3 regulatory proteins Nef, Tat and Rev. The Gag polyprotein is cleaved to form the matrix (MA), capsid (CA) and two nucleocapsid (NC) proteins. The env gene encodes the surface glycoproteins gp120 and gp41, required for host cell attachment and entry. The pol protein produces the protease (PR), reverse transcriptase (RT) and integrase (IN) enzymes.

HIV entry into host cells occurs via interaction of the viral gp120-gp41 trimer with the target cell receptor CD4 (44, 45), expressed primarily on macrophages and CD4+ T cells. Conformational changes then allow gp120 to bind to a G protein-coupled receptor (GPCR), commonly C-C chemokine receptor 5 (CCR5) or C-X-C chemokine receptor 4 (CXCR4), although other chemokine receptor usage has been documented *in vivo*. A

detailed description of gp120-GPCR binding and signal transduction is discussed in Section 1.4. This interaction mediates membrane fusion or endocytosis and allows the virus to enter the cell and become uncoated (46). Reverse transcription of the RNA genome involves host cellular factors and the error-prone RT enzyme, which promotes HIV genetic diversity through the large number of mutations introduced into the genome during replication ($3x10^5$ per replication cycle) (46). The newly-formed dsDNA genome associates with IN, MA, Vpr and a number of host proteins to form the pre-integration complex (PIC). This complex travels to the nucleus where IN catalyses the integration of linear HIV DNA into the host chromosome. The 5' long terminal repeat (LTR) acts as a promoter and enhancer for HIV genomic transcription, which is initially mediated by host cellular machinery until sufficient Tat is translated to drive viral transcription. Production of Rev stabilizes gag, pol and env RNA transcripts and allows full translation of viral proteins in the cytoplasm. Assembly of the viral particle at the cell membrane is directed by Gag. During or after viral budding from the host cell, the viral protease cleaves the Gag and Gag/Pol polyproteins and allows for complete viral maturation.

1.4 Heterotrimeric G protein signaling and HIV replication

Following the identification of CD4 as the primary receptor for HIV, it became apparent that the CD4 molecule was necessary, but not sufficient, to mediate viral infection of human cells. Expression of CD4 on non-human and hybrid cells suggested that a permissibility factor expressed on human cells facilitated viral entry. Studies of viral isolates also demonstrated differences in tropism for macrophages and T cell lines, leading to the classification of isolates as either macrophage (M)-tropic, T cell-line (T)-tropic or dual-tropic, possibly due to differing affinities for cellular co-receptors. The

chemokine receptor CXCR4 (fusin) was the first HIV co-receptor to be identified, and was shown to mediate the entry of T-tropic (now X4-tropic) viruses (47); the M-tropic (now R5-tropic) viral co-receptor CCR5 was identified soon after (48-52). While the vast majority of viral isolates utilize either CXCR4 or CCR5 as the viral co-receptor, other chemokine receptors including CCR1, CCR3 and CXCR6 can be utilized (53, 54).

Chemokine receptors belong to the seven transmembrane domain G protein-coupled receptor (GPCR) superfamily, a large receptor family that initiates intracellular signaling events mediated by heterotrimeric G proteins. Heterotrimeric G proteins (referred to herein as G proteins) form a trimer comprised of one each of an α, β and γ subunit. The β and γ subunits form a constitutive dimer that binds an α subunit- guanosine 5'-diphosphate (GDP) complex. Activation of the GPCR recruits the G protein complex and results in the exchange of guanosine 5'-triphosphate (GTP) for GDP, inducing the dissociation of the βγ dimer from the α subunit and initiating downstream signalling pathways from all subunits. The intrinsic guanosine triphosphatase activity of the α subunit cleaves the GTP into GDP and promotes the reformation of the G protein trimeric complex (Fig. 2A). Signaling specificity is partially achieved by combinations of subunit isoforms with varying properties (Table 1). Currently, 16 α subunit, 5 β subunit, and 12 γ subunit genes have been identified. Notably, the majority of lymphocyte G protein signalling is mediated by the Gαi family of α subunits.

Table 1.1. G protein subunit isoforms and characteristics.

Subunit Type	Families/ Isoforms	Characteristics
Gα	Gαs	Stimulates adenylyl cyclase (AC)
	Gαi/o	Inhibits AC, most common Gα subunit coupled to chemokine receptors
	Gαq/11	Can couple to CXCR4 receptor and mediate T cell receptor activation (55); activates phospholipase C-β
	Gα12/13	Interaction with RhoGEFs; mediate T cell adhesion/motility (in mice (56))
Gβ	Gβ1	Similar to Gβ2 and Gβ4 subunits
	Gβ2	
	Gβ3	GNB3 C825T SNP associated with multiple diseases (see section 1.7.1)
	Gβ4	
	Gβ5	Associates with regulator of G protein signalling (RGS) domains; localized to multiple intracellular membranes
Gγ	Gγ1-12	More overall sequence diversity between γ subunits than between β subunits

There are several major effectors of G protein subunits in lymphocytes (Fig. 2B). The Gα

effectors include adenylyl cyclase (AC), phosphodiesterase (PDE), phospholipase C

(PLC) and Rho guanine exchange factors (RhoGEF) (described in detail in (57)). The βγ

dimer is capable of regulating a variety of effectors, including AC, PLCβ and PLCε, class

IB phosphatidylinositol-3-kinase γ (PI3Kγ), G protein-regulated kinases (GRK) and ion

channels (58). Activation of PI3Kγ produces the second messenger phosphatidylinositol

(3,4,5)-triphosphate (PIP3), which binds pleckstrin homology domain-containing proteins

such as Akt/protein kinase B, ultimately promoting cell survival (reviewed by (59)). PLC

activation promotes Ca^{2+} release via second messengers as well as protein kinase C

(PKC) activation, leading to the induction of the mitogen-activated protein kinase

(MAPK) pathway (Erk, JNK, p38 MAPK) and activation of focal adhesion kinase Pyk2.

Given the ability of gp120 to bind CCR5 and CXCR4 and, given that many of these G

protein signaling pathways ultimately lead to transcription factor activation (including

HIV transcriptional regulators NFκB and AP-1), many studies have attempted to

determine the capacity of gp120 to elicit intracellular signaling responses and to assess

the requirement for those signal transduction events in the HIV lifecycle.

1.4.1 G protein signaling and HIV entry

Controversy over the precise role of, and requirement for, G protein signalling during the

viral life cycle has persisted, with conflicting reports of the capacity of gp120 to elicit G

protein-mediated signals during entry and the effect of those signalling cascades

(reviewed in (60, 61)). gp120-GPCR binding is sufficient to activate G protein signaling

in primary peripheral blood mononuclear cells (PBMC), causing Ca^{2+} fluxes,

phosphorylation of Erk1/2 and Akt, and activation of PI3K in CD4+ T cells (62). After

identification of the chemokine co-receptors, early studies investigated whether this G

protein signalling activity is required for co-receptor function, but all initial studies

concluded that G protein signalling was dispensable (63-68). These studies, however,

only focused on dissociating receptor activation from Gαi signalling pathways. More

recently, Harmon and Ratner (69) demonstrated a requirement for Gαq signalling

through CCR5 for viral entry. This signalling pathway is dependent on PLCβ, PKC, Pyk2

and Ras, and is required for Rac-1 mediated actin reorganization that facilitates HIV

membrane fusion, demonstrating the importance of G protein signalling in HIV entry.

1.4.2 G protein signaling and HIV replication

Similarly, detailed studies now suggest that G protein signalling through both CCR5 and

CXCR4 promotes HIV replication following entry. Pre-incubation of primary monocytes

and monocyte-derived macrophages with CCR5 ligands suggest that G protein-mediated

signals promote a cellular environment that is highly permissive to viral replication (70).

Specific inhibition of G protein-mediated chemotaxis pathways (71, 72) blocked R5-

tropic HIV replication (73), consistent with a study showing that gp120 binding to CCR5

results in activation of Erk1/2 and phospholipase D (PLD), and promotes transactivation

of Tat and the HIV LTR (74). Others have shown that gp120-induced G protein-mediated

Ca^{2+} release and PI3K/Akt activation removes a block to viral replication (75). Evidence

points to a similar role for G protein signalling in CD4+ T cells, where high surface
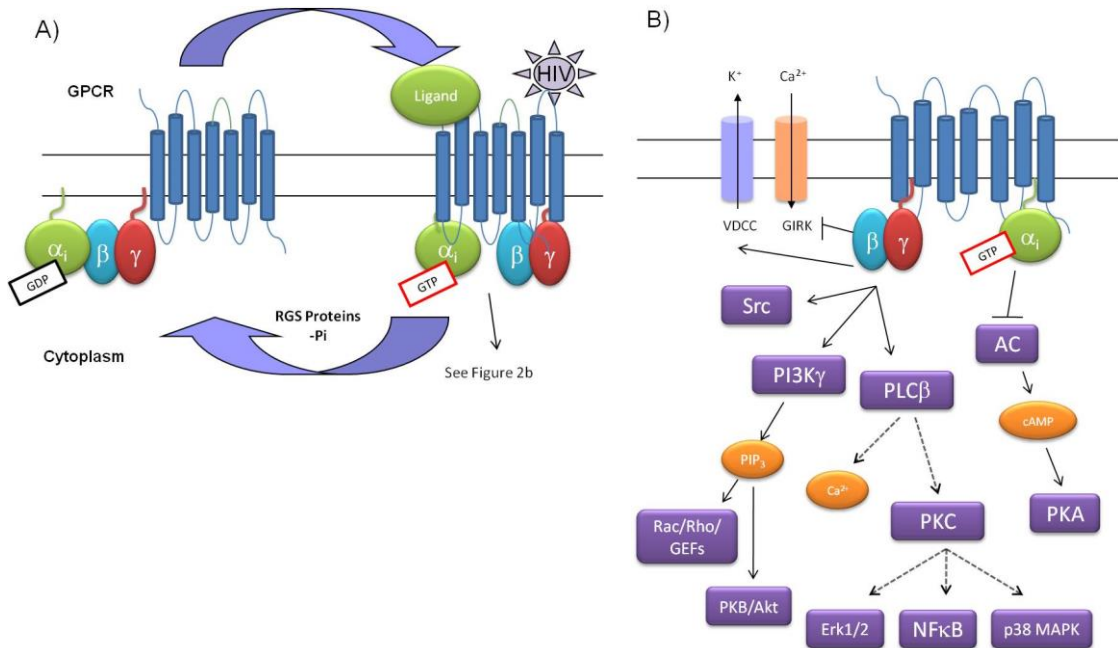
Figure 1.1. G protein activation following G protein-coupled receptor stimulation by ligand or HIV. **(A)** Activation of the receptor results in G protein recruitment, exchange of guanosine 5'-triphosphate for guanosine 5'-diphosphate at the α subunit, dissociation of the α subunit from the βγ dimer and initiation of downstream signaling pathways. Regulators of G protein signaling (RGS) and the guanosine triphosphatase activity of the α subunit results in re-association of the trimeric G protein complex. **(B)** Schematic of major signaling pathways initiated by Gαi protein signaling in response to endogenous ligand. Purple represents effector proteins, orange represents second messengers. Dashed lines indicate pathways with multiple intermediate effectors. GPCR: G protein-coupled receptor; PI3K: phosphatidylinositol-3-kinase; PLC: phospholipase C; AC: adenylyl cyclase; GEF: guanine exchange factor; PKB: protein kinase B; PKC: protein kinase C; PKA: protein kinase A.

density of CCR5 correlates with an increased level of HIV replication while CCR5-Gαi

signaling mutants poorly support HIV replication (76).

Both R5- and X4-tropic viruses are capable of inducing MAPK/Erk activation in

unstimulated PBMC, which is dependent on Gαi signals and is required for the late

stages of reverse transcription (77, 78). Most recently, CXCR4-mediated Gαi signals

have been shown to overcome actin-based restriction of HIV infection in resting T cells

(79). Gαi pathways activate cofilin, an actin filament severing protein, to allow viral

nuclear import. Inhibition of this pathway strongly inhibits latent infection of resting T

cells. This work was subsequently extended to include activation of cofilin by chemokine

ligands of CCR7, CXCR3 and CCR6, which can promote HIV latency through viral

integration into the genomes of resting cells (80, 81). Viral budding also appears to

require Gαi signaling and phosphorylation of Arp2/3 proteins (82), implicating G protein

signaling events in almost every stage of the viral lifecycle.

Additionally, gp120 has been repeatedly shown to induce T-cell chemotaxis through

activation of both CCR5 and CXCR4 (62, 83-86). The inappropriate activation of

chemotaxis by viral gp120 may play an important role in recruiting uninfected cells to

sites of viral replication, thus facilitating the spread of the virus (84, 85). These signals

may also lead to dysregulation of cellular function in lymphatic organs, as well as

activation of T cells. Interestingly, defects in lymphocyte chemotaxis, particularly those

observed during HIV-mediated destruction of the gut lymphoid tissue, were partially

attributed to Nef-mediated degradation of Gαi2 subunits (87). Chandrasekaran *et al*

speculate that this degradation could result in increased free Gβγ dimers and promote signaling cascades that promote viral replication. Viral infection, therefore, has the potential to alter both immune activation and cell behaviour through G protein signaling, especially in late-stage HIV infection.

1.5 HIV disease course and stages of infection

Acquisition of HIV through sexual exposure results in viral infection of mucosal CD4+ T cells and Langerhans cells (88); while macrophages are targets of systemic viral infection, they are poorly infected by transmitted virus (89). Dissemination of the virus to the draining lymph nodes by dendritic cells (DCs) (approximately 6 days post infection) allows for robust viral replication within the gut-associated lymphoid tissue (GALT). Infection targets CD4+ T cells expressing the mucosal-homing receptor α4β7, which is bound by gp120 (90). Widespread viral replication results in extensive depletion of gut CD4+ T cells, an effect that is not reversed even following ART. A widespread systemic infection is then initiated, with viral replication targeting and irreversibly depleting the CD4+ T effector memory cell pool. Like other lentiviruses, HIV is capable of infecting both dividing and non-dividing cells, but activated cells favour infection and viral replication (91-93). Infection of resting or quiescent T cells, or differentiation of activated infected cells to quiescent memory cells, establishes a latent viral reservoir in peripheral and lymph node memory T cells (94); this persistent reservoir prevents eradication of the virus even during successful ARV therapy (95).

The period of time following HIV acquisition but prior to the development of an antibody response to the virus is known as the 'window period' and generally lasts for 3 – 4 weeks post infection. Symptoms of acute infection are non-specific and include flu-like symptoms such as fever, rash and lymphadenopathy (96). Following an initial spike in viral load and depletion of systemic CD4+ T cells, the activation of the adaptive immune response corresponds to a decrease in viral load to a maintained 'set-point' and a partial rebound of CD4+ T cell count. Set-point viral load is a useful predictor of future disease progression (97). Between 3 weeks and 3 months post-infection, the induction of the humoral antibody response results in detectible HIV-specific systemic antibodies, allowing for diagnosis of HIV infection and denoting the time of seroconversion.

The control of viral replication by the host immune response leads to the asymptomatic chronic phase of HIV infection. During chronic infection, loss of CD4+ T cells is believed to be a primary cause of immunodeficiency and correlates with disease progression, allowing CD4 count to be used as a clinical measure of disease stage (98). CD4+ T cell counts and viral load are relatively stable during chronic infection, and may remain so for 2-10 years. The gradual decline in CD4 count results in immune dysregulation and eventual spikes in viral replication. The Centres for Disease Control (CDC) classify HIV disease progression through three CD4 count categories (>500 cells/μL, 200 – 499 cells/μL and <200 cells/μL) and three clinical disease categories (acute/asymptomatic, symptomatic and symptomatic with AIDS-defining illness) (99). AIDS is defined as the point at which the CD4 count declines below 200 cells/μL. Due to the destruction and dysregulation of the host immune system, viral replication increases

and the host becomes susceptible to a range of opportunistic infections (AIDS-defining illnesses). Without successful ARV therapy, AIDS leads to death.

1.6 Altered disease progression and susceptibility

1.6.1 Altered Disease Progression

While a 'typical' course of HIV disease progression is often described, there is significant variation in the rate of progression between both individuals and populations (see also Section 1.7). While some discrepancies exist over whether disease progression in Africa is more rapid than in North America (100), vulnerable subpopulations such as female sex workers (FSWs) can exhibit more rapid progression than the rest of the population (101). Groups of individuals exhibiting particularly rapid progression or natural control of infection have been intensely studied in order to identify immune responses desirable for an HIV vaccine (102).

Compared to normal progressors, who reach CD4 counts of <350 cells/µL in 8 - 10 years, rapid progressors (RP) may do so in less than 2 years. In some populations, progression to AIDS within a year of seroconversion has been documented in an extreme phenotype of rapid progression (Keynan, personal communication). Conversely, approximately 5-10% of individuals are able to maintain natural immunological control of HIV infection (103). Long term non-progressors (LTNP) maintain high CD4 counts (often >500 cells/µL) for long durations (>14 years in some cases), while the rarer group of elite controllers/elite suppressors (EC/ES; <1% of HIV-positive subjects) exhibit low or undetectable viral loads (<50 copies/mL) in the absence of ARV therapy (reviewed in

(102)). Although some cases of LTNPs and ECs have been attributed to infections with low fitness viruses (104), most arise from environmental effects or genetic polymorphisms associated with viral control (discussed further in Section 1.7) (105-107).

1.6.2 Natural Immunity to HIV infection

Just as natural variation in HIV progression produces a spectrum of disease progression patterns, not all individuals are equally susceptible to HIV infection. It is now recognized that despite repeated exposure to HIV, some individuals remain uninfected. This group is termed HIV-exposed seronegative (HESN) (108-110) and includes uninfected recipients of HIV-infected blood products, seronegative partners of discordant couples, children born to HIV-infected mothers, seronegative injection drug users and uninfected individuals with high-risk sexual practices such as men who have sex with men (MSM) and HIV-resistant FSWs (111). While the mechanisms underpinning the protection of HESNs likely differ between subgroups (112), extensive research has focused on an extreme HESN phenotype: highly exposed FSWs in Nairobi, Kenya who remain HIV negative for more than 7 years of follow-up and are described as relatively resistant to HIV infection (HIV-R) (113).

The HIV-R women of the Pumwani FSW cohort do not differ in their sociodemographics or sexual practices from HIV-susceptible cohort members, and are not resistant to other STIs. Attempts to define the correlates of protection in these women has led to the proposal of the role of immune quiescence (IQ), a phenotype characterized by low baseline immune activation (114) and gene expression (115, 116), increased levels of

regulatory T cells (114) and increased levels of genital tract anti-inflammatory anti-proteases (117) coupled with decreased expression of inflammatory chemokines (118). The state of IQ is proposed to decrease HIV target cell availability and reduce favourable conditions for viral replication, although the mechanisms underpinning these correlates of protection have yet to be determined. Causal factors are likely to be both environmental and genetic, as evidenced by the familial relationships of many HIV-R women (119).

1.7 Genetic correlates of HIV susceptibility and control

As with many human diseases, genetic variation plays a major role in shaping an individual's susceptibility to HIV infection and the quality of the subsequent immune response (reviewed in (120)). The most consistent, and arguably the strongest, associations between HIV susceptibility/disease progression and host genetics involve the *human leukocyte antigen* (*HLA*) genes (107, 121, 122), which are the most polymorphic genes in the human genome. An individual's *HLA* alleles determine what viral epitopes will be presented to CD8+ T cells, thereby shaping the quality and effectiveness of the adaptive immune response. The *HLA B*57* allele is consistently associated with slow disease progression in both Caucasian and African populations (107), and has been identified in three genome-wide association studies of markers of HIV control (123-125), while *HLA B*27* and *HLA C* alleles have similarly been associated with delayed progression (107, 126, 127). HLA molecules not only present peptides to CD8+ T cells, but also act as ligands for killer cell immunoglobulin-like receptors (KIRs) expressed on natural killer (NK) cells. Perhaps unsurprisingly, a number of *KIR-HLA* allele combinations also affect HIV susceptibility, viral load set point and disease progression

(128, 129) (reviewed in (130)). Aside from *HLA*-related allelic variation, the majority of host genetic polymorphisms that are repeatedly associated with HIV acquisition or disease progression are related to the expression and function of the GPCR HIV co-receptors.

The earliest identified genetic correlate of resistance to HIV infection is the *CCR5Δ32* deletion, in which a 32bp deletion in the *CCR5* co-receptor gene prevents surface expression of functional CCR5 (131). Homozygous *CCR5Δ32* individuals are relatively resistant to HIV acquisition, and heterozygotes exhibit delayed disease progression (132-134). Additional *CCR5* promoter polymorphisms have been associated with accelerated disease progression, possibly due to increased CCR5 expression (135); other *CCR5* SNPs identified in South African populations are known to affect CCR5 expression and chemokine binding, but their role in HIV susceptibility is unknown (136). A single nucleotide polymorphism (SNP) in the *CCR2* gene (*CCR2 V64I*), which is located near the *CCR5* locus on chromosome 3, is associated with delayed disease progression (137), reduced viral load, and reduced vertical transmission (138), either due to linkage disequilibrium with *CCR5* promoter polymorphisms (139) or the expression of *CCR2* splice variants that alter CCR5/CXCR4 expression (140) (141). Recently, our lab identified a SNP in the *CD4* gene associated with increased risk of seroconversion and accelerated disease progression in a Nairobi-based FSW cohort, likely via a mechanism involving increased signal transduction through lck-initiated pathways (142) (Oyugi unpublished).

The importance of the co-receptor binding pathway in HIV infection is further underscored by the identification of polymorphisms in CCR5/CXCR4 ligands that alter HIV acquisition and progression. Increased expression of these ligands can compete with gp120 for co-receptor binding and also induce receptor internalization upon binding, thereby inhibiting HIV infection. *MIP-1α* (CCL3) (143), *MIP-1β* (CCL4 and CCL4L1) (144), *SDF-1α* (CXCL12) (145), *MCP-1* (CCL2), *MCP-3* (CCL7), *eotaxin* (CCL11) (146) and *RANTES* SNPs (147, 148) have been associated with rate of progression in some, but not all, cohorts tested (149, 150), (reviewed in (151)). It is important to note that in some cases, associations are observed only within specific ethnic populations (152). *CCL3L1* (MIP-1α) copy number was widely believed to affect HIV susceptibility and progression, with individuals with greater than average gene copy numbers within an ethnic population being less susceptible and progressing more slowly to AIDS (153), although this association has recently been questioned (154-156).

1.7.1 G Protein Gene Polymorphisms - GNB3 C825T

Despite the numerous examples of co-receptor/chemokine ligand SNPs that regulate HIV immunity, relatively few studies have examined the impact of variation in downstream G protein signalling pathway components on HIV susceptibility or progression. Given that G protein-mediated signal transduction initiated by gp120-co-receptor binding is required for viral replication (as reviewed in Section 1.4), enhancement or reduction of G protein signaling activity could substantially impact the likelihood of productive T cell infection. Many polymorphisms in G protein subunit genes result in tissue-specific disorders (for a review, see (157)), but several have been documented to have wide-ranging pleiotropic

effects. Gain- and loss-of-function mutations in the *GNAS* locus (the complex genetic locus encoding Gαs proteins) have been associated with a more severe course of malarial infection, and a silent SNP in *GNAS* exon 5 is associated with lymphocytic cancer progression and survival (158, 159). To date, no published studies have tested any associations between *GNAS* polymorphisms and HIV susceptibility or progression.

In contrast, a well described SNP in the *guanine nucleotide binding protein beta polypeptide 3* (*GNB3*) gene (C825T; rs5443) has been associated with several disease outcomes including differing rates of HIV progression and responses to ART (160-162). *GNB3* encodes the Gβ3 protein, one of the five isoforms of G protein β subunits. The T allele of the 825 SNP is a silent mutation that does not alter the Gβ3 amino acid sequence but is instead associated with the production of two mRNA splice variants, Gb3s and Gb3s2, that contain deletions of 123bp and 129bp, respectively (160, 163). *In vitro* expression of Gβ3s/s2 proteins suggests that they are biologically active, dimerize with Gγ subunits and result in increased G protein signaling activity (160, 163). These results are consistent with observations of increased lymphocyte chemotaxis in response to GPCR ligands in *GNB3 825TT* individuals (164, 165). Despite this data, controversy exists over the biological relevance of the *GNB3* splice variants and the mechanism of action of the 825T allele (166). While Siffert *et al* (160) suggest that Gβ3s/s2 expression results in decreased affinity of the Gβγ dimer for Gα, which therefore more readily dissociates upon activation, other groups that have found no impact of Gβ3s on signal transduction have suggested that the splice variants are non-functional and result in a

decrease in viable Gβ3 protein (167). Evaluation of these claims is difficult given the lack of data demonstrating Gβ3s/s2 expression at the protein level *in vivo* (160, 168).

Despite the conflicting reports of *GNB3* splice variant activity, *GNB3* genotype is reported to modulate multiple aspects of the immune system. Some authors have suggested that the 825T allele is predictive of immunocompetence (164, 169), as 825T allele carriers exhibit improved cellular responses to hepatitis B virus (HBV) vaccination compared to CC/CT allele carriers (169), who, in contrast, show poor responses to hepatitis C virus (HCV) therapy (170) and increased risk of infant death due to infection (171). Functional effects of the *GNB3 825T* allele on immune cells include increased chemotaxis of T cells (164, 165), increased CD4 T cell counts, greater proliferative responses to recall antigens and decreased lymphocyte apoptosis (164, 169, 172).

Together, these data suggest intriguing ways in which the 825TT genotype could affect HIV acquisition and/or disease progression, either by altering the activation of G protein signaling pathways required for HIV replication or through the modulation of chemotaxis, immune activation and antigen-specific cellular immune responses. Indeed, a study of HIV disease progression among a Caucasian cohort reported a significant impact of *GNB3 825* genotype on rate of progression, with 825TT individuals progressing to AIDS more than twice as fast as 825CC subjects (162). Somewhat paradoxically, a small study of CD4 count rebound and viral load suppression following initiation of ART reported improved responses to therapy among 825TT participants compared to 825CC/CT genotypes (161). Although intriguing, these observations have not been

replicated in any additional cohorts. Given the potential for linkage disequilibrium (LD) between genetic markers and the risk of false positives among candidate gene association studies (173), it is important to confirm the effects of the *GNB3 825* SNP in additional cohorts, particularly those of different ethnic backgrounds (151).

GNB3 825T allele frequency is moderate (~20%) within Caucasian populations such as the cohort involved in the HIV progression study (162). Within African populations where worldwide HIV burden is highest, however, an effect of *GNB3 825* genotype on HIV disease progression could have a dramatic impact, as the 825T allele frequency is extremely high (~80%) (174). Genetic association studies of *GNB3* genotype in African populations are generally lacking in the literature and represent a significant gap in knowledge (175), but reports tend to suggest that the epidemiological impact of *GNB3* in Africans differs from the associations reported in Caucasian and Asian populations (175-177). In many cases, genetic association studies have not been followed up with functional experiments designed to directly assess the impact of the *GNB3 C825T* SNP on immune function.

Epidemiological analysis of the impact of *GNB3 825* genotype on HIV susceptibility and disease progression among multiple African cohorts is presented in Section 3. Assessment of *GNB3 825TT* genotype and mRNA splicing is presented in Section 4.

1.8 Introduction to the human immune system

1.8.1 Innate Immunity

The human innate immune system is responsible for the rapid recognition of invading pathogens, which results both in the induction of non-specific immune responses and the activation and biasing of the adaptive immune response. The initiation of the innate immune response relies primarily on the activation of pattern recognition receptors (PRRs) that bind common pathogen-associated molecular patterns (PAMPs) to activate signaling pathways that initiate interferon (IFN) and cytokine secretion. The main classes of human PRRs include toll-like receptors (TLRs), nod-like receptors (NLRs), RIG-I-like receptors (RLRs), C-type lectin receptors (CLRs) and hematopoietic interferon-inducible nuclear protein (HIN)-200 proteins. TLRs are well characterized membrane-bound and intracellular PRRs that recognize a variety of PAMPs, including flagellin, lipopolysaccharide (LPS), and double stranded (ds)RNA (reviewed in (178)). NLRs and RLRs are localized in the cytoplasm and recognize bacterial peptidoglycan-derived peptides and dsRNA, respectively (reviewed in (179)). CLRs and HIN-200 are not universally recognized as PRR families, but bind carbohydrate moieties and dsDNA, respectively, and can induce antiviral signaling pathways (180, 181).

Immune cell subsets involved in innate immunity include professional antigen presenting cells (APCs) and natural killer (NK) cells. APCs include dendritic cells (DCs), macrophages and B cells (discussed in Section 1.8.2). APCs express a variety of PRRs and are primarily involved in pathogen recognition and uptake, resulting in the production of IFN/cytokines/chemokines (including IL-12, IL-15 and IL-18) and the

presentation of antigens to T lymphocytes via MHC class I and II molecules in the lymph node (182). NK cells play important roles in antiviral immunity by recognizing and lysing pathogen-infected cells and by modulating the adaptive immune response (183, 184). NK cell activation occurs in response to downregulation of inhibitory killer immunoglobin-like receptor (KIR) ligands (MHC I molecules) or through upregulation of activating KIR ligands (reviewed in (185)). Peripheral blood NK cells are typically defined as either $CD56^{dim}CD16^{+}$ or $CD56^{hi}CD16^{-}$. The $CD56^{dim}CD16^{+}$ subset represents approximately 90% of circulating peripheral NK cells and is predominately cytotoxic in nature. In contrast, the $CD56^{hi}CD16^{-}$ subset is capable of secreting large amounts of cytokines and is referred to as the immunoregulatory NK subset (184).

1.8.2 Adaptive Immunity

The adaptive immune system includes both B and T lymphocytes and can be broadly divided into humoral and cell-mediated arms. Adaptive immunity involves antigen-specific responses (mediated by the B cell or T cell receptor) and includes the generation of a long-lasting memory response.

B lymphocytes orchestrate humoral immunity by producing antibodies in response to invading pathogens (186). Recognition of an antigen by the B cell receptor (BCR) results in proliferation and affinity maturation, whereby antibody genes are mutated to increase antibody-antigen affinity. Antibodies are responsible for numerous functions including phagocytosis, opsonization, neutralization and antibody-dependent cellular cytotoxicity (ADCC).

Cell-mediated immunity involves the activation of CD4+ and CD8+ T lymphocytes. CD4+ T cells, also known as T helper (Th) cells, are crucial orchestrators of the adaptive immune response, and provide co-stimulation signals to B cells and CD8+ T cells to promote an effective antigen-specific response. CD4+ T cell responses are restricted by MHC class II proteins. CD4+ T cell subsets were originally described as either Th1 or Th2 based on cytokine production patterns, but are now recognized to include an array of phenotypically and functionally distinct groups (187) including Th17/Th22 cells, regulatory T cells (Tregs), Th9 cells and T follicular helper cells (Tfh) (188). Tregs play a particularly important role in modulating immune activation and maintaining peripheral tolerance. Tregs can be phenotypically defined by expression of CD25 (IL-2Rα) and the transcription factor FOXP3 and negatively regulate the immune response through inhibitory cytokine production (IL-10, TGF-β, IL-35), cytolysis, metabolic disruption and inhibitory receptor expression (CTLA-4, LAG-3, discussed further in Section 1.11.7.1) (189, 190).

CD8+ T lymphocytes are MHC class I-restricted cells that can differentiate into effector (cytotoxic T lymphocyte, CTL) or memory subsets during infection (reviewed in (191)) and play a crucial role in eliminating infected cells. Antigen-specific CTLs commonly express perforin and granzyme to mediate cytolysis, while effector memory cells can produce a number of cytokines including IFNγ, TNFα, MIP-1β and IL-2. During chronic viral infection, persistent exposure to antigen and an inflammatory environment can induce immune exhaustion, a phenotype whereby CTLs lose their effector functions and proliferative capacity (described in detail in Section 1.11.7).

1.8.3 Double Negative T (DNT) cells

The double negative T (DNT) cell population, defined as CD3+CD4-CD8- lymphocytes, represents a heterogeneous population with recently described immunoregulatory properties. Based on expression of CD3, CD4 and CD8 alone, DNT cells can include αβ T cells, γδ T cells and NKT cells, all of which exhibit differing antigen specificities and functions. The phenotype and function of iNKT cells (including DN iNKTs) is discussed below in section 1.8.4.

γδ T cells, defined by their expression of the alternative γδ TCR chains instead of a typical αβ TCR, recognize pyrophosphate antigens expressed by both prokaryotic and eukaryotic cells. Numerous functions have been ascribed to γδ T cells, including acquisition of antigen presentation capabilities, pro-inflammatory cytokine production and regulatory/suppressive activity (reviewed in (192)). The functions of αβ DNT cells are similarly diverse and include cytotoxicity, IL-17 production, Th activity and immunoregulation through a contact-dependent mechanism (193, 194) (reviewed in (195)). αβ DNT cells are detected at frequencies of 3-8% in peripheral blood, and may reach the periphery through several mechanisms. Some speculate that CD4 downregulation on CD4+ T cells in peripheral blood may produce αβ DNT cells; conversely, immature double negative thymocytes may migrate directly to the periphery after acquisition of the αβ TCR or during negative selection. In contrast to the relatively low frequency of DNT cells in peripheral blood, mucosal sites such as the foreskin can contain elevated DNT frequencies, as high as 15% - 30% of CD3+ T cells (196).

1.8.4 Invariant NKT Cells

A small subset of T lymphocytes expressing surface markers characteristic of both T cells (T cell receptor, CD4/CD8) and NK cells (CD161) are now appreciated to form an important link between the innate and adaptive immune responses. These 'NKT' cells can be activated in both antigen-dependent and -independent manners and respond with robust Th1 and Th2 cytokine production, allowing them to exhibit remarkable functional plasticity with both pro-inflammatory and immunoregulatory characteristics (197). NKT cells can be grouped into several subsets (Table 1), but the most commonly described group is the Type 1 or invariant NKT (iNKT) subset. iNKTs are so named due to the expression of a highly restricted TCR comprised of α-chain variable region 24 (Vα24) and α-chain joining region 18 (or Q; Jα18 or JaQ) paired with Vβ chain 11 (Vβ11) (reviewed in (198)).

iNKT cells are restricted not by MHC molecules but by CD1d, an atypical antigen-presenting transmembrane protein that associates with β2-microglobulin and binds lipid antigens (198). While the natural ligand of CD1d has not been conclusively identified, it binds with high affinity to the marine sponge-derived lipid α-galactosylceramide (αGalCer, discussed below) (199). CD1d is expressed on all human lymphocytes, but is enriched on APCs (200). Despite the low frequency of the iNKT population in the periphery (0.01 – 1% of CD3+ lymphocytes in humans), iNKT activity is now appreciated to play an important role in immunity to infectious diseases (201).

1.8.4.1 iNKT activation:

The earliest known and best described CD1d-restricted iNKT cell ligand is αGalCer, a glycosphingolipid derived from the marine sponge Agelas mauritinius (199). While αGalCer does not represent a natural ligand for iNKT activation, its ability to strongly and specifically activate iNKT cells has made it a gold standard in iNKT stimulation experiments. Both endogenous iNKT ligands (including the controversial ligand iGb3 (202-205) and lysophospholipids (206)) and bacterial-derived iNKT ligands are increasingly being described (207-218) (reviewed in (219)), although no viral-encoded iNKT lipid ligands are known to exist. A recent breakthrough in iNKT ligand identification has demonstrated that the endogenous lipid β-D-glucopyranosylceramide (β-GlcCer) accumulates *in vivo* after bacterial infection/LPS treatment and is a potent activator of both murine and human iNKT cells (220, 221).

iNKT activation by APC-mediated antigen presentation involves IL-12 production and is strongly dependent on CD40/CD40L interactions (222-224), with low levels of CD40L being detectible *ex vivo* on the surface of iNKT cells (225, 226) and intracellular, pre-formed CD40L mobilized upon activation (227). Activation of iNKT cells in the absence of a pathogen-derived lipid antigen can occur in a CD1d-dependent or independent manner (reviewed in (228-230)). Both gram negative and gram positive bacteria are capable of activating iNKT cells via TLR stimulation of, and IL-12/IFNα/β production by, APCs (210, 231-234). This mechanism appears to require CD1d-restricted presentation of endogenous lipid (210, 235). Virus-induced alteration of endogenous lipid presentation can also contribute to iNKT activation, as in the case of *in vitro* HBV

Table 1.2. Human CD1d-restricted NKT cell types

Type I	TCR	Vα24-Ja18; Vβ11
	Subsets	CD4+, CD8+, double negative
	Ligand	αGalCer, βGlcCer
	Restriction	CD1d
	NK Receptors	CD161+/-
Type II	TCR	Diverse
	Subsets	CD4+, CD8+
	Ligand	Sulfatide, Lysosulfatide, Lysophosphatidylcholine
	Restriction	CD1d
	NK Receptors	CD161+

infection (236). CD1d-independent iNKT activation can also occur in the context of LPS-induced APC production of IL-12 and IL-18 or CpG-induced TLR9 signaling and IL-12 production (237, 238).

1.8.4.2 iNKT subsets and functional capacity

While many studies simply characterize human iNKTs as CD4+ or CD4-, a proportion of human iNKTs express CD8α (239, 240), allowing human iNKT subsets to be defined as CD4+, CD4-CD8- (DN) or CD8+. Subset-specific differences in surface marker expression have been described, with CD4+ iNKTs exhibiting lower expression of CCR5 compared to the CD4- subset, which characteristically expresses CCR1, CCR6, CXCR6, 2B4, CD161 and NKG2D (225, 241)(reviewed in (242)). All iNKTs express high levels of CXCR3 and CXCR4, express CD69 upon activation (225, 243) and typically exhibit an effector/memory phenotype (244, 245).

A hallmark of iNKT activation is the rapid production of a vast array of cytokines and chemokines (200, 246, 247) including IFNγ, TNFα, TGFβ, GM-CSF, IL-2, IL-4, IL-5, IL-6, IL-10, IL-13, IL-17, IL-21, RANTES, Eotaxin, MIP-1α and MIP-1β (reviewed in (200, 228)). CD4+, DN and CD8+ subsets differ in their cytokine production patterns (239, 248-250), as CD4+ iNKTs produce both Th1 and Th2 cytokines (251) while CD4- iNKTs generally produce only Th1 cytokines (248, 250) (reviewed in (242)). Other iNKT effector functions include perforin/granzyme release associated with NKG2D engagement (228, 249, 250, 252, 253), and Fas/FasL-mediated cytotoxicity (200, 228).

In addition to direct cytolytic function and cytokine secretion, iNKTs play an important role in the activation and regulation of other immune cell subsets. iNKT activation reciprocally modulates DC function (254-256) and quickly leads to NK cell activation in an IFNγ-dependent manner, followed by T and B cell activation (257). Stimulation of iNKT cells in conjunction with soluble T cell antigen enhances both CD4+ and CD8+ antigen-specific responses in a DC-derived CD1d-dependent manner (258, 259) via a mechanism involving CD40 signaling (254), and the use of αGalCer and iNKT ligands as vaccine adjuvants is receiving considerable attention (260-262). The capacity to modulate multiple aspects of the immune response through iNKT activation has led to interest in the use of synthetic CD1d-presented antigens as adjuvants in influenza, HIV and tuberculosis vaccine candidates (263-268)reviewed in (261, 269, 270)).

1.8.4.3 iNKT cell tissue distribution

Peripheral blood iNKT cells account for a very small proportion of CD3+ lymphocytes (generally 0.01%-1% (271)), and the expression of surface markers including CD62L and CD11a suggests both lymph node homing and tissue infiltrating capabilities. The combination of chemokine receptor markers expressed on this subset resembles that of 'Th1 inflammatory homing cells' and suggests that iNKT cells may traffic to peripheral tissues rather than lymphoid tissues (272). A majority of iNKT cells also express the mucosal-homing marker α4β7 (241). Given that memory T cells expressing α4β7 and CXCR3 are recruited to the female genital tract following bacterial infection (273), it seems likely that iNKT cells would be similarly recruited to vaginal or endocervical tissues. At this time, no reports of human iNKT cell frequency or phenotype at the female

genital tract have been published, but CD1d is expressed by vaginal (274) and cervical

epithelium (275). Recruitment of iNKT cells to mucosal tissues has been demonstrated in

studies of inflammatory bowel disease and the gastrointestinal mucosa (276, 277). In

mice, iNKT activation by αGalCer is protective against genital tract *Chlamydia*

muridarum infection (278), demonstrating a role for iNKT activation in mucosal

immunity that has yet to be confirmed in humans.

1.9 Immunity to HIV infection at the female genital tract (FGT)

In order to develop preventative strategies to reduce sexual transmission of HIV to

women, we must improve our understanding of mucosal immunity at the FGT. Numerous

innate immune defense mechanisms exist at the FGT, including the intact genital

epithelium, a thick layer of mucous (279) containing antiviral proteins such as defensins

and serpins, and the low pH of the vagina (280). These natural defense mechanisms are

extremely effective, with a sexual HIV transmission rate of <1% (281). HIV transmission

can occur, however, by several mechanisms: breaches in the epithelial layer that allow

viral access to target cells (particularly in the epithelial monolayer of the cervix (282)),

binding of HIV to Dendritic Cell-Specific Intercellular adhesion molecule-3-Grabbing

Non-integrin (DC-SIGN) on DCs resulting in presentation to CD4+ T cells (283) (which

can both promote and inhibit viral transmission (284)), and internalization of HIV in

Langerhans cells and subsequent presentation to CD4+ T cells (88) (285). A major

determinant of successful establishment of infection involves the availability of target

cells in the submucosal epithelium (286). In most cases, the initial infection is caused by

only one or a few viral variants (287) which are almost exclusively R5-tropic viruses

(287-289). Interestingly, founder virus gp120 tends to demonstrate high affinity for $\alpha4\beta7$ (290), making both CCR5+ and $\alpha4\beta7+$ CD4+ T cells, but not macrophages, major targets of early infection (280, 286, 290-293). Unfortunately, cervical $\alpha4\beta7+$ CD4+ T cells tend to co-express CCR5 and the activation marker CD69, making this T cell population highly susceptible to infection (294).

After establishment of a small founder population of infected cells, most commonly at the endocervix or transformation zone (295), the infection must expand to the lymphatic system in order to propagate systemically. Based on evidence from studies of SIV transmission, exposure to virus results in MIP3-α expression in the cervical epithelium that recruits plasmacytoid DCs (pDCs), which, in turn, secrete MIP1-β to recruit activated T cells and macrophages to the site of infection (289). Thus, the innate inflammatory response to viral exposure actually promotes target cell availability and infection propagation. This model is further supported by a study of the use of glycerol monolaurate (GML), a fatty acid that blocks immune activation, as a microbicide to prevent SIV transmission. GML application reduced FGT MIP-3α levels and provided protection from vaginal SIV challenge in non-human primates (NHPs), highlighting the impact of successful immune activation downregulation during viral exposure (296). Establishment and expansion of the founder population is believed to occur during the first week of infection (282), after which the virus disseminates to the draining lymph nodes and subsequently spreads systemically (289).

1.10 Innate Immunity to HIV

Innate immunity can counteract HIV infection in several ways: through innate restriction factors expressed in both innate and adaptive immune cells, and through the antiviral activity of innate cell subsets such as NK cells. Numerous antiviral innate restriction factors, and the viral components that overcome them, have now been identified (reviewed in (297)). Most recently, the interferon-stimulated gene Schlafen 11 was identified as an innate restriction factor that inhibits HIV protein expression by exploiting viral codon usage bias (298). HIV replication in DCs, macrophages and resting CD4+ T cells is restricted by the activity of SAM- and HD-domain containing protein 1 (SAMHD1), a dNTP phosphohydrolase protein whose activity is countered by the HIV-2/SIV protein Vpx (299-303). The apoplipoprotein B mRNA-editing, enzyme-catalytic, polypeptide-like 3G (APOBEC3G) protein is expressed in T cells, causes viral genome hypermutation through cytosine deaminase activity and is inhibited by the viral protein Vif in conjunction with host core binding factor β (304-306). Virion budding can be inhibited by the host protein tetherin (bone marrow stromal antigen 2/BST-2) which is expressed on the cell membrane and is countered by Vpu (307). Finally, NHP Tripartite motif-containing protein 5-alpha (TRIM5α) inhibits HIV replication by interfering with uncoating of the capsid protein, an inhibitory effect which is modest for human TRIM5α (308).

During early infection, HIV both subverts and activates the innate immune response. As most innate restriction factors are IFN-stimulated genes, HIV employs strategies to block IFN production by infected cells, including the sequestration of cytoplasmic RIG-I RNA

sensors (309) and disruption of IRF-3 activation (310). IFN production by uninfected DCs, however, may be advantageous in driving inflammation and recruiting target CD4+ T cells to sites of infection (311, 312). Infection also results in innate cell functional defects. Despite widespread activation of DCs during acute infection, myeloid and plasmacytoid DCs (mDC and pDC, respectively) display defects in antigen presentation and cytokine secretion (313) as well as altered responses to TLR stimulation (314). NK cell function is also perturbed during infection, with reduced production of IL-12, IL-15 and several chemokines (315). Notably, chronic infection is associated with a progressive decline in CD56^{dim}CD16+ NKs and an accumulation of anergic CD56-CD16+ NKs that express high levels of inhibitory receptors (316).

1.11 Adaptive Immunity to HIV

1.11.1 Humoral

Although antibody responses to HIV develop over the course of infection, they are not associated with viral control or rate of disease progression (317, 318). Despite this, several potent, broadly neutralizing antibodies have been isolated from infected patients (b12, 4E10, PG9) and are the targets of rational vaccine design. Given that plasma levels of IgG targeting HIV env were inversely correlated with risk of infection in the recent RV144 HIV vaccine trial, it is conceivable that antibody responses could contribute to protection from infection (40).

1.11.2 CD8+ T Lymphocytes

The generation of HIV-specific CD8+ T cell responses coincides with the decrease in early viremia, and much evidence points to a crucial role for CTL responses in viral control. Patterns of CTL responses, both *ex vivo* and *in viro*, correlate with viral load setpoint and rate of CD4 decline (319, 320), while depletion of CD8+ T cells during SIV infection of NHPs results in rapid disease progression (321). Characterization of CTL responses among long term non-progressor (LTNP) and elite controller (EC) cohorts suggests that the maintenance of a proliferative, polyfunctional HIV-specific response (cells producing >1 cytokine/chemokine) is associated with viral control (322-325). During progressive disease, however, HIV-specific CD8+ T cells begin to lose cytokine production and proliferative capacity in a phenomenon termed immune exhaustion, described in detail in section 1.11.7. Although the CD8+ T cell response is insufficient to control viral replication after infection, the elicitation of CD8+ responses at the genital mucosa remains a focus of vaccine design (326).

1.11.3 CD4+ T Lymphocytes

As the major target of HIV infection, CD4+ T cells are depleted during chronic infection, with preferential infection and depletion of HIV-specific memory cells contributing to the loss of viral control during late stages of disease (327). Indeed, the low level of CCR5 expression on Sooty Mangabey central memory T cells is thought to protect the memory pool from infection and contribute to the lack of progression during SIV infection in this species (328). Recent evidence now suggests that, similar to CD8+ T cell responses, HIV-specific CD4+ T cell responses during early infection play a large role in controlling

viral replication and determining the rate of disease progression. The early emergence of cytolytic CD4+ T cell responses was predictive of slow disease progression in a cohort of HIV+ subjects (329), and depletion of CD4+ T cells during SIV infection in rhesus macaques ablated the post-peak decline of viremia and resulted in rapid disease progression (330).

1.11.4 Double Negative T Lymphocytes

While relatively little is known about the role of double negative T cells (DNT cells) in control of HIV infection or progression, some data suggests that DNT frequency may influence immune activation during infection. In a small study of primary HIV infection, baseline DNT frequency was negatively correlated with CD8+ T cell activation and proliferation, both at baseline and at immune activation setpoint. In this study, DNT cells produced immunoregulatory cytokines TGFβ and IL-10 upon stimulation, and were composed of approximately 50% γδ TCR+ cells. In NHP models of non-pathogenic SIV infection, DNT cells can provide Th-like functions and SIV-specific responses (331). In both species, the maintenance of DNT frequency may help to control immune activation and contribute to HIV/SIV T cell responses.

1.11.5 iNKT regulation and responses during HIV infection

1.11.5.1 CD4+ iNKT depletion

iNKT cells, particularly the CD4+ subset, are depleted during HIV infection, with significant loss during the first year post seroconversion (332, 333). Multiple mechanisms may account for the loss of iNKT cells, as van der Vliet *et al* attributed the majority of

the iNKT loss to apoptosis mediated by the high expression levels of Fas (CD95) on iNKTs from HIV+ individuals, while subsequent studies have shown high expression of CCR5 on both CD4- and CD4+ iNKTs (244, 333, 334), iNKT susceptibility to R5-tropic, X4-tropic and primary isolate viruses (244, 333, 334) and preferential depletion of CD4+ iNKT cells following *in vitro* infection (333). Similar studies in a number of cohorts has largely confirmed these observations (263, 335-337), although the impact of ART on iNKT cell reconstitution remains controversial. Some cohorts report full recovery of both CD4+ and CD4- iNKT subsets following ART (335) while other report no effect of therapy (332, 338), and the kinetics of CD4+ iNKT reconstitution appear to be slower than that of conventional CD4+ T cells (337, 339). Interestingly, initiation of ART during acute infection (3-4 months post seroconversion) prevented further iNKT depletion within the first year of treatment (336).

Little data is available to clarify the impact of this depletion on disease progression and viral pathogenesis. It is unknown whether iNKT activation could control HIV replication and immune activation, or what role the iNKT subset might play in anti-tumor responses and prevention of opportunistic infections in immunocompromised hosts (340). Only one study to date has demonstrated anti-HIV activity of iNKT cell culture supernatant, which was shown to be IFNγ-dependent (336). In a study of risk factors involved in developing cancer among HIV+ women, NKT cell frequency was associated with a reduced risk of cancer (341). Recently, gut-resident CD4+ iNKT cells were reported to be depleted following HIV infection, with the degree of depletion correlating with systemic immune activation (342). In non-human primates, pre-infection peripheral blood iNKT frequency

correlated with retention of CD4 T cell counts following SIV infection (343). Together, these data do suggest the possibility that iNKT cells could contribute to the regulation of immune activation and the delay of disease progression during HIV/SIV infection.

1.11.5.2 iNKT dysfunction

Regardless of the extent of iNKT depletion during HIV infection, the iNKT subset displays functional impairment (243, 336, 338, 344), with both CD4+ and, especially, CD4- iNKTs exhibiting reduced proliferation and IL-4, TNFα and IFNγ production. Functional restoration during ART is controversial (336). In one study, iNKT cytokine production inversely correlated with bulk iNKT CD161 expression, but the cell-specific relationship between CD161 and IFNγ/TNFα production was not assessed (344). Increased iNKT PD-1 expression has been reported among HIV-1 positive subjects but does not correlate with IFNγ production or proliferative capacity (338). Blockade of the PD-1/PD-L1 or PD-L2 pathway also did not restore proliferative or IFNγ responses. These results are particularly interesting given that PD-1 expression has been shown to regulate iNKT activation and anergy in mice (345-347). While Moll *et al* suggest that the failure of PD-1 blockade to reverse iNKT dysfunction implies an irreversibly exhausted phenotype, the expression and functional impact of other inhibitory receptors such as 2B4, Tim3 and LAG-3 on the iNKT subset during HIV-1 infection remains unknown (discussed further in section 11.7.1).

1.11.5.3 Non-human primates and SIV infection:

Studies of NHP iNKT function during SIV infection further imply an important role for iNKT function during chronic infection (348). Non-natural hosts of SIV infection, such as the Rhesus Macaque (RM), have SIV-susceptible iNKT cells that are depleted during infection just as in humans (349, 350). RMs also exhibit the emergence of an IL-17 producing iNKT subset during acute infection that is associated with pathogenic chronic infection (351). In contrast, natural hosts of SIV infection such as Sooty Mangabeys (SM), which control immune activation and do not exhibit progressive immunodeficiency (reviewed in (352)), have qualitatively distinct iNKT cells. SM iNKTs express neither CD4 nor CCR5 (353), do not become dysfunctional during chronic infection, and do not exhibit the increased IL-17 production observed in RM (351). Rout *et al* speculate that iNKT IL-10 production may promote Treg proliferation and may, therefore, play a role in controlling immune activation in this model of natural infection (353).

1.11.5.4 CD1d downregulation

While iNKT cells are depleted and exhausted during HIV infection, CD1d expression is also modulated by the virus itself. The HIV-1 protein Nef, responsible for the downregulation of MHC-I A and B alleles (354), also downregulates CD1d via a common tyrosine-based motif (355, 356). This downregulation was shown *in vitro* to reduce NKT activation and IFNγ secretion after αGalCer stimulation (355, 356).

During the course of HIV infection, chronic immune activation is believed to be a major determinant of disease progression. CD4+ T cell decline and viral replication are strongly associated with levels of T cell activation (measured by surface expression of chronic activation markers such as HLA DR and CD38) (357), T cell apoptosis, B cell hyperactivation and proinflammatory cytokine levels (reviewed in (358)). Given the relatively small proportion of CD4+ T cells that are productively infected at any time, the majority of activated T cells during HIV infection are uninfected, non-HIV-specific bystander cells (359, 360). Successful control of viral replication with ARV therapy often reduces T cell immune activation, while persistent activation during therapy is associated with poor CD4+ T cell reconstitution (361).

In addition to HIV-specific antigenic stimulation, microbial translocation is believed to be a major cause of immune activation during chronic infection (362). The massive depletion of gut mucosa CD4+ T cells and the pathogenic effect of HIV gp120 on mucosal epithelial integrity (363) allows the translocation of microbial products such as LPS, flagellin and other PAMPs into systemic circulation. As a result, elevated plasma levels of LPS and sCD14 have been described among HIV+ subjects and correlate with disease progression and mortality in multiple studies (364-366).

The importance of controlling immune activation during HIV infection is underscored by comparisons between pathogenic and non-pathogenic models of SIV infection. Despite similar induction of the innate immune response during acute SIV infection, Sooty

Mangabeys rapidly downregulate the interferon response, maintain low levels of immune

activation and do not exhibit progressive immunodeficiency (367, 368). In contrast,

pathogenic SIV infection among macaques results in high levels of immune activation

similar to HIV infection. Detrimental consequences of chronic T cell activation include

an increased pool of activated CD4+ T cells that are permissive to viral infection and

replication, as well as the induction of immune exhaustion, as discussed below.

1.11.7 Immune exhaustion during Chronic HIV Infection

The continual increase in immune activation throughout the course of HIV infection has a

particularly detrimental effect on T cell function, resulting in the phenomenon of immune

exhaustion. Immune exhaustion refers to a dysfunctional state characterized by the loss of

T cell proliferative and effector functions and increased expression of a number of

inhibitory cell surface receptors (369). Immune exhaustion is not unique to HIV

infection; a variety of chronic infections and carcinomas result in T cell exhaustion in

both humans and mice (370). Clinical trials have demonstrated the utility of blocking

inhibitory receptor signaling as a cancer treatment (371), demonstrating proof-of-concept

for reversing immune exhaustion as a treatment for chronic disease. It is important to

note that most descriptions of immune exhaustion focus on the loss of CD8+ effector

function, although CD4+ T cells also exhibit exhausted phenotypes. Immune exhaustion

occurs progressively, with IL-2 production, proliferation and cytotoxicity lost early,

TNFα production lost at an intermediate stage and IFNγ production lost during severe

exhaustion (372). Progression through these stages tends to coincide with high viral load,

duration of infection and/or loss of CD4+ T cell help, as occurs during HIV infection.

Immune exhaustion can be mediated by three major families of effectors: expression of

inhibitory cell surface molecules, binding of soluble inhibitory factors or through

interactions with immunoregulatory cell subsets (370). Much work has recently focused

on the patterns of inhibitory surface receptor expression during HIV infection (373).

Many of these inhibitory receptors are normally expressed following T cell activation in

order to prevent rampant immune activation. During chronic viral infection, however,

expression of multiple inhibitory receptors due to ongoing activation leads to exhaustion

and T cell dysfunction. It has been known for some time that expression of programmed

death (PD)-1 (CD279) is increased during HIV infection and that blocking the PD-1/PD-

L pathway restores antigen-specific CD8+ T cell function (374, 375).

Following that discovery, other exhaustion molecules upregulated among HIV-infected

subjects were identified: cytoxic T lymphocyte antigen (CTLA)-4 (CD152) (376), T cell

immunoglobulin and mucin domain-containing molecule (Tim)-3 (377), lymphocyte

activation gene (LAG)-3 (CD223) (378, 379), 2B4 (CD244) (380) and CD160 (380).

Expression of combinations of these receptors results in varying degrees of dysfunction,

as PD-1 and LAG-3 appear to be expressed earlier in progressive exhaustion than 2B4

and CD160 (370). Following initiation of suppressive ART, expression of PD-1 and Tim-

3 are reduced, correlating with an improvement in T cell function. In some models,

blockade of multiple inhibitory receptor pathways results in synergistic improvements in

T cell function (381), and administration of anti-PD-1 antibody to SIV-infected rhesus

macaques and humanized HIV-infected mice has had promising results (382, 383). The

mechanisms by which these surface receptors inhibit T cell function are varied and

include competition for co-stimulatory/MHC molecules, recruitment of inhibitory intracellular signaling proteins or induction of inhibitory gene expression. This thesis focuses on the expression and function of LAG-3 during chronic HIV infection.

1.11.7.1 Lymphocyte activation gene 3 (LAG-3)

LAG-3 is a single transmembrane domain-containing cell surface receptor of the immunoglobulin (Ig) supergamily with high structural homology to the CD4 molecule (384). The *LAG-3* gene is located on chromosome 12 approximately 10Kb from *CD4* and is believed to have arisen from a gene duplication event. Some evidence suggests that *LAG-3* transcription may be controlled by regulatory elements that also bind the *CD4* promoter (385). Although the *LAG-3* gene contains intronic, missense and frameshift polymorphisms, there are no reliable associations between *LAG-3* SNPs and human diseases. Several *LAG-3* polymorphisms were implicated in susceptibility to multiple sclerosis (386), but a follow-up study failed to confirm this association(387).

Like CD4, LAG-3 binds to MHC class II molecules, but with 100-fold greater affinity and can, therefore, compete with CD4 for MHCII engagement (388, 389). Despite its structural similarity to CD4, LAG-3 does not bind HIV gp120 (388). A soluble form of LAG-3 (sLAG-3) consisting of the extracellular domains of full-length LAG-3 is detectible in human plasma and has been associated with differential disease outcomes in tuberculosis and cancer (390-392), despite a lack of understanding of the function or significance of sLAG-3 production. In humans, sLAG-3 is generated by the expression of multiple splice variants of LAG-3 mRNA (393, 394), while in mice, a single RNA

transcript is produced (395) and sLAG-3 occurs as a non-functional byproduct of metalloprotease cleavage of surface LAG-3 (396).

LAG-3 expression is negligible in both human and murine resting PBMC, and is generally reported to be expressed as a weak dimer on the surface of activated T and NK cells (384, 397). Recent evidence suggests that murine LAG-3 is also expressed by plasmacytoid DCs (pDCs) (398), some B cells (399), NKT cells (400) and γδT cells (384, 395). In humans, some CD25^{high}Foxp3+ Tregs (401, 402) express low levels of LAG-3, as do iNKT cells (271). Recently, expression of human LAG-3 has been extended to a subset of lymphocytes called T regulatory type 1 (Tr1) cells (403), as well as some pDCs (404). LAG-3 surface expression is induced on naïve T cells by IL-12 in an IFNγ-dependent manner (405).

LAG-3 engagement regulates T cell homeostasis (406, 407) and results in inhibition of T cell proliferation and cytokine secretion (408, 409). While disruption of MHCII-CD4 interactions does not contribute significantly to LAG-3-mediated T cell functional inhibition in *in vitro* systems (410), LAG-3 cross-linking inhibits Ca^{2+} flux, T cell proliferation and IFNγ, TNFα and IL-2 (but not Th2 cytokine) production following TCR re-stimulation (411, 412). This inhibitory activity largely depends on the presence of the LAG-3 intracellular cytoplasmic tail, which contains a KIEELE motif critical for inhibitory function and an EP repeat motif that binds the intracellular LAG-3-associated protein (LAP) (410, 413). LAG-3 activity is, however, cell type- and species-specific. In mice, LAG-3 contributes to regulatory T cell (Treg) and NK cell function (414-417),

while in humans, LAG-3 expression does not alter NK (or CD8+ T cell) cytotoxicity

(418, 419) and less is known about its role in Treg function (409). Similarly, LAG-3 is

upregulated on murine iNKT cells following αGalCer stimulation (420) and can inhibit

proliferation (400), but the regulation and consequences of LAG-3 expression on human

iNKT cells are unknown.

LAG-3 is somewhat unique among exhaustion markers in that its ligand is MHC class II

molecules. Not only does MHCII-LAG-3 engagement initiate intracellular signaling

through LAG-3, it also initiates unique MHCII signaling pathways affecting the MHCII-

expressing cell (417, 421, 422). LAG-3 ligation of APC MHCII results in expression of

co-stimulatory molecules and chemokine receptors, morphological changes and secretion

of IL-12 and TNFα in peripheral blood (423-427), while limiting monocyte

differentiation into macrophages and DCs during inflammation (428).

1.11.7.2 LAG-3 in Chronic Infections

While the basic details of human LAG-3 function are known, data regarding its role in

immune exhaustion and dysfunction during chronic infection are largely derived from

murine studies. Significant evidence has accumulated to suggest that, in mice, LAG-3

and PD-1 are upregulated during (373, 429), and appear to be important determinants of,

T cell exhaustion during lymphocytic choriomeningitis virus (LCMV) and *Plasmodium*

infection (430, 431). In humans, however, the regulation and effect of LAG-3 expression

is often either not tested (431) or appears to be of lesser consequence than in murine

models (380, 418, 432).

While the expression and functional impact of PD-1 and Tim-3 during HIV infection has been the subject of much research (433, 434), less is known about the role of LAG-3. With the exception of one report (378), early studies have suggested that LAG-3 is expressed at extremely low levels and is not upregulated on bulk T cells during HIV infection (435). Recent characterization of HIV-specific T cells found that the major populations of exhausted HIV-specific CD8+ and CD4+ T cells are LAG-3- (380, 436), with similar expression levels on both subsets (436). These observations stand in contrast to the expression patterns of CD160, 2B4 and PD-1, which are highly upregulated on HIV-specific CD8+ T cells and are differentially expressed between CD4+ and CD8+ subsets (436). Indeed, it is unclear whether LAG-3 expression denotes exhausted or, conversely, highly activated T cells, given the observation that LAG-3 is expressed on pathogenic CD4+PD-1+ T cells from immune reconstitution inflammatory syndrome (IRIS) patients (379). Although a recent study reported on a population of LAG-3+ HIV-specific CD8+ T cells associated with low viral loads, the authors actually found no evidence of LAG-3 expression on HIV-specific T cells using traditional methods; rather, an extended stimulation protocol with no control for bystander T cell activation was used to induce LAG-3 upregulation over the course of 30 hours of stimulation (437).

Despite the lack of *ex vivo* T cell LAG-3 expression during chronic HIV infection, microarray studies of gene expression during multiple stages of infection in both human and NHP models of SIV control indicate modulation of LAG-3 expression (438, 439). Specifically, LAG-3 transcript levels positively correlated with viral load set point and were significantly higher among rapid progressors compared to viremic non-progressors

(440). *In vitro,* HIV-pulsed DCs can induce the expression of a number of exhaustion markers including LAG-3 on T cells (441). This study did not, however, assess the impact of individual markers on T cell cytokine/effector function following DC co-culture, and the simultaneous increase in T cell Foxp3 expression makes it difficult to assess whether the upregulation of inhibitory surface molecules reflects a transient state of activation, induction of exhaustion, or an artifact of the *in vitro* system.

A comparison of LAG-3 expression on lymphocyte subsets among HIV-, HIV+ and HIV+ ART-experienced subjects will be presented in Section 5. A comparison of LAG-3 expression between peripheral blood and mucosal-derived lymphocytes will be presented in Section 6. Analysis of LAG-3 function on invariant NKT cells will be presented in Section 7.

Study Rationale, Hypotheses and Objectives

<u>**Study Rationale**</u>

Numerous reports have demonstrated the impact of genetic polymorphisms and variation in gene expression on HIV acquisition and disease progression. Our lab has previously demonstrated that a single nucleotide polymorphism (SNP) in the *CD4* gene is associated with increased risk of HIV acquisition and, subsequently, accelerated disease progression. The *CD4* gene is located on chromosome 12 in a gene-rich cluster that includes several additional immune-related genes: most notably *GNB3* and *LAG-3*. While the expression and biological function of G protein signaling gene *GNB3* are well known, the *GNB3 C825T* SNP has been reported to alter immune function and was associated

with rapid HIV progression in a single, cross-sectional, Caucasian cohort study. Given the high frequency of the 825T allele in African populations, the lack of data surrounding the functional impact of the SNP among Africans and the possibility of *GNB3* genotype contributing to the effects on HIV acquisition and disease progression associated with the *CD4* SNP, we were interested in assessing the impact of *GNB3 825* genotype on HIV acquisition, disease progression and immune activation in two Kenyan cohorts of high- and low-risk women.

In contrast to GNB3, less is known about the regulation of LAG-3 RNA and protein expression, especially during HIV infection. Given the similar inhibitory capacity of LAG-3 to well described exhaustion markers such as PD-1 and Tim-3, we wondered whether increased LAG-3 expression during chronic HIV infection could contribute to immune exhaustion or rate of disease progression. We therefore sought to determine the expression of LAG-3 on lymphocyte subsets during chronic HIV infection and ARV therapy, and the impact of blocking LAG-3 activity on immune function.

Hypotheses

This thesis includes two major hypotheses:

1) *GNB3 825TT* genotype is associated with increased risk of HIV acquisition and rapid disease progression compared to the *GNB3 825CC/CT* genotypes. This is associated with Gb3s RNA splicing and increased expression of immune activation markers among *GNB3 825TT* subjects.

2) LAG-3 protein expression is increased on CD4+ and CD8+ T cells, NK cells and iNKT cells during chronic HIV infection compared to healthy individuals, and is decreased among participants receiving ARV therapy. LAG-3 expression correlates with loss of T cell function and disease progression.

Objectives

1a: To determine the impact of *GNB3 825* genotype on risk of HIV acquisition and disease progression among two Kenyan cohorts: high-risk commercial sex workers and a low-risk perinatal transmission cohort.

1b: To quantify expression of immune activation markers on T lymphocytes of HIV-negative (HIV-N) and HIV-infected (HIV+) subjects of differing *GNB3 825* genotypes.

1c: To confirm the differential expression of GNB3 splice variants associated with the *GNB3 825T* genotype.

2a: To quantify the expression of LAG-3 on T cell, NK cell and iNKT cell subsets in both the peripheral blood and genital mucosa among HIV-N, HIV+ and ARV-treated (HIV+ ART) subjects.

2b: To determine the functional impact of LAG-3 expression on lymphocyte cytokine production and proliferation.

2. Materials and Methods

2.1 General reagents

2.1.1 Solutions

Phosphate-buffered saline (PBS): 9.55g PBS Powder (137.93mM NaCl, 2.67mM KCl, 8.1mM Na_2HPO_4, 1.47mM KH_2PO_4; Gibco) dissolved in ddH_2O to a final volume of 1L, pH 7.0

FACS Wash: PBS + 2% Fetal Calf Serum (FCS; inactivated at 56ºC for 1hr; Hyclone)

R-10 Cell Culture Media: RPMI-1640 (Hyclone) + 10% FCS + 1% Penicillin/Streptomycin/Fungizone (PSF) (Gibco)

R-30 Cell Culture Media: RPMI-1640 (Hyclone) + 30% FCS + 1% Penicillin/Streptomycin/Fungizone (PSF)

Freezing Media: 10% dimethyl sulfide (DMSO, tissue culture grade, Sigma) + 90% FCS

ELISA Coating buffer: 1.59g Na2CO3 + 2.93g NaHCO3 dissolved in ddH_2O to a final volume of 1L

ELISA Blocking buffer: PBS, 10% Bovine Serum Albumin (BSA, Sigma)

ELISA Dilution buffer: PBS, 2% BSA, 0.1% Tween 20

ELISA Wash Buffer: COBAS Amplicor Wash Buffer (90mL + 910mL ddH2O) <2% phosphate buffer; <9% NaCl, EDTA, <2% detergent, 0.5% ProClin 300

2.1.2 Antigens and Mitogens

α-Galactosylceramide (KRN7000): Purchased from Enzo Life Sciences. Used to stimulate iNKT cytokine production and proliferation.

Phorbol 12-myristate 13-acetate (PMA) and Ionomycine (Io): Purchased from Sigma. Used to stimulate cytokine production by PBMC.

HIV Gag peptide pools: Purchased from Sigma. A series of 15-mer peptides (overlapping by 10 amino acids) were generated using a consensus sequence from HIV isolates of the Majengo cohort and the clade A ancestral sequence. A total of 112 Gag peptides were divided into 2 pools, each containing 56 peptides (Gag A and Gag B). The Gag peptides used are listed in the appendix (Section 10.2).

2.2 Biological Samples

2.2.1 Source of human peripheral blood and cervical samples

2.2.1.1 Pumwani female sex worker (FSW) cohort

The Pumwani FSW cohort was established in 1984 (442) and is an open cohort based in the Pumwani slum of Nairobi, Kenya. The FSW cohort follows both HIV-negative and HIV-positive women with bi-annual visits at which HIV status, CD4 count and antiretroviral therapy (ART) status are determined.

2.2.1.2 Perinatal HIV transmission (PHT) cohort

This cohort recruited HIV+ pregnant women from antenatal clinics in Nairobi, Kenya to investigate factors affecting in utero, postpartum and breastmilk HIV transmission. Participants were enrolled at 32 weeks gestation and began taking zidovudine twice a day from 34-46 weeks of pregnancy and following through delivery, as per Kenyan guidelines [29]. Women visited the clinic antenatally, at delivery, 2 weeks after birth and

monthly for 12 to 24 months. Blood specimens were collected at months 1, 3, 6, 9, 12, 18 and 24 following delivery for CD4+ T cell count and HIV viral load (VL) determination.

2.2.1.3 Ethical Approval

The studies reported in this thesis received ethical approval from all sites involved. Approval was given from the University of Manitoba research ethics board for all studies, and the University of Nairobi/Kenyatta National Hospital and the University of Washington ethics boards gave approval where appropriate. All study participants gave free and informed consent for each protocol.

2.2.2 Biological sample processing

2.2.2.1 Peripheral blood collection and processing

Peripheral blood samples were collected in heparin vacutainers and processed for plasma and peripheral blood mononuclear cell (PBMC) collection. Plasma was collected from whole blood by centrifugation at 600xg for 7 minutes, cleared of precipitate by centrifugation at 514xg for 7 minutes, aliquoted and stored at -70ºC.

PBMC were isolated by density gradient centrifugation. The remaining whole blood samples were diluted in PBS+2% FCS, layered over Ficoll (Lymphoprep, MJS BioLynx Inc.) and centrifuged at 400rpm for 25 minutes. The PBMC layer was collected, washed with PBS+2% FCS, centrifuged at 600xg for 10 minutes, resuspended and washed with R-10 media. Following centrifugation at 400xg for 10 minutes, PBMC were again resuspended in R-10 media and counted by trypan blue (HyClone) dye exclusion. Where

indicated, PBMC were assayed either "fresh" (immediately following isolation) or following thawing of cryopreserved samples (resuspended at 10×10^6/mL in freezing media and cryopreserved in liquid nitrogen).

Cryopreserved samples were thawed in a 37ºC water bath, added drop-wise into a total volume of cold 10mL of R-30 media, centrifuged, washed again with R-10 media and rested overnight in R-10 media at 2×10^6 cells/mL prior to assay. Cell viability as determined by trypan blue exclusion was required to be >80% for sample use (but was typically >95% both immediately after thawing and after overnight resting). Typical recovery was approximately 85%.

2.2.2.2 Cervical cell and lavage collection and processing

Cervical mononuclear cells (CMC) were collected by cervical cytobrush and speculum scraping. Both cytobrush and scraper were collected in 5mL of PBS kept on ice. The PBS, brush and scraper were vortexed vigorously for 30 seconds to dislodge CMCs into suspension. Mucus and cells remaining on the cytobrush were manually dissociated from the brush. The cell suspension was filtered through a 100uM nylon cell strainer. Both the collection tube and filter were washed with PBS. The filtrate was centrifuged at 600xg for 10 minutes, resuspended, washed with PBS and centrifuged again at 600xg for 10 minutes. The CMCs were resuspended in PBS for immediate assay by flow cytometry.

Cervicovaginal lavage (CVL) samples were collected by washing the ectocervix with 2mL of PBS. Lavages were transferred to 15mL conical tubes and kept on ice during

transport. Samples cleared of debris by centrifugation at 400xg for 7 minutes and were frozen at -70ºC for future analysis.

2.2.2.3 HIV Testing and Confirmation

Plasma samples from the Pumwani FSW cohort were tested for HIV serostatus using the Recombigen (Trinity Biotech) ELISA. All positive samples were confirmed using the Detect HIV1/2 immunoassay (Adaltis). Samples testing positive in both assays were considered to be HIV-positive.

2.2.2.4 CD4 count enumeration

CD4+ T cell counts were collected for HIV-positive FSW cohort participants using the Tritest CD3/CD4/CD8 flow cytometry assay (BD Biosciences). Lymphocyte counts were multiplied by the percentage of CD4+ T cells to generate the CD4 count.

2.2.2.5 Plasma viral load determination

Plasma viral loads were determined for HIV-positive mothers in the PHT cohort. HIV-1 RNA VL was quantified in plasma using the Gen-Probe Transcription Mediated Amplification assay, which is sensitive for detection of Kenyan HIV-1 subtypes A, C, and D (Gen-Probe Incorporated, San Diego, CA).

2.3 General Methods

2.3.1 Flow Cytometry

2.3.1.1 Surface Staining

PBMC were stained in 96 well V bottom plates, with $1 \times 10^6 – 2 \times 10^6$ cells/well. Cells were pelleted by centrifugation at 514xg for 7 minutes and washed with PBS+2% FCS. Following centrifugation (514xg for 7 minutes) and resuspension, surface marker antibody cocktail was added to the well and incubated for 30 minutes at 4ºC in the dark. Cells were washed with PBS+2% FCS and resuspended in 1% paraformaldehyde fixation buffer (BD Biosciences) or permeabilized for intracellular staining (as in Section 2.3.1.2). The cell suspension was transferred to 5mL FACS tubes in a volume of 300μL for acquisition on the LSRII flow cytometer. Surface staining of CMC samples was similar but carried out in 5mL FACS tubes due to increased pellet size. Samples were resuspended in a final volume of 800μL for acquisition.

2.3.1.2 Intracellular cytokine staining

Surface-stained cells were washed with PBS+2% FCS, centrifuged at 600xg for 10 minutes, resuspended in Fixation/Permeabilization buffer (CytoFix/CytoPerm, BD Biosciences) and incubated at 4ºC in the dark for 20 minutes. Cells were washed in a 1X solution of Fixation/Permeabilization wash buffer (BD Biosciences) and centrifuged at 600xg for 10 minutes. Resuspended cells were then incubated with intracellular antibody cocktail prepared in a final volume of 50μL of Fixation/Permeabilization wash buffer at 4ºC in the dark for 30 minutes. Cells were washed in Fixation/Permeabilization wash buffer, pelleted, resuspended and transferred to 5mL FACS tubes for acquisition on the LSRII flow cytometer.

2.3.1.3 Viability Assay

To restrict analysis of flow cytometry data to viable cells (particularly in the case of stimulations and CMCs), a viability dye was included in some panels. The Live/Dead viability dye (Invitrogen) is an amine-reactive fluorescent dye that binds free amines on the cell surface (in the case of viable cells) as well as the cell interior of cells with compromised membrane integrity (in the case of dead cells). Dead cells therefore stain brightly in the Live/Dead dye channel and can be excluded from analysis. Lyophilized Live/Dead Red dye was resuspended in 50μL DMSO for use. Staining was performed in in 96 well V-bottom plates (PBMC) or 5mL FACS tubes (CMCs). Reconstituted Live/Dead dye was added at 1μL/test, incubated for 30 minutes at 4ºC and removed by washing.

2.3.1.4 Compensation

The use of multiple fluorochromes in multiparameter flow cytometry results in overlap of the emission spectra between some fluorescently conjugated antibodies. To account for this spillover and remove it from data analysis, the BD FACS Diva software uses an algorithm to calculate and compensate for the overlap. This requires the analysis of singly stained populations for each fluorescent marker. Surface and intracellular antibody compensation were performed using CompBeads (BD Biosciences) that bind either mouse or rat antibodies. Compensation samples were prepared in 5mL FACS tubes, where 1 drop of mouse/rat CompBead mix and 1 drop of negative control CompBead mix were added to up to 400μL of PBS+2% FCS. 100μL of bead mix was aliquoted per single stained sample, to which 1μL of a single antibody was added. Following

incubation, the samples were diluted with PBS+2% FCS and acquired on the LSRII flow cytometer.

Live/Dead viability dye single stained compensation samples were prepared with the use of ArC Beads (Invitrogen). To prepare ArC bead compensation tubes, 1 drop of ArC amine bead suspension was aliquoted into a FACS tube. 1μL of Live/Dead Red reagent was added to the bead drop and incubated at room temperature for 30 minutes. After washing twice with 3mL FACS wash, the beads were resuspended in 300μL FACS wash to which 1 drop of ArC negative beads were added.

2.3.1.5 Data acquisition and analysis

Samples were acquired on the LSRII flow cytometer (BD Biosciences). For T cell and NK cell phenotyping experiments (Section 5), a minimum of 100,000 lymphocyte gate events were collected. For iNKT phenotyping and stimulation experiments (Section 7), a minimum of 200,000 (and maximum of 400,000) lymphocyte gate events were collected. In the case of CMC samples (Section 6), the entire tube was acquired.

Gating of cell populations was determined by fluorescence minus one (FMO) controls, in which a sample labelled with all antibodies except the antibody of interest is used to determine the background fluorescence in that channel. Data was acquired and compensated using BD FACS Diva software (v6.1.2, BD Biosiences) and was analysed with FlowJo software (v7.5, Tree Star Inc.).

Concentrations of cytokines and chemokines in plasma, cervicalvaginal lavage (CVL)

and cell culture supernatant samples were quantified using Milliplex MAP bead array kits

(Millipore). Analytes are described in detail in chapter specific method sections. Samples

were processed according to manufacturer instructions, as described below.

Lyophilized human cytokine standard (containing standards of all analytes of interest)

was prepared by reconstituting with 250μL ddH2O, vortexing and incubating for 10

minutes. Five-fold serial dilutions were prepared in assay buffer. High and low

concentration quality control samples were reconstituted in 250μL ddH2O, vortexed and

incubated for 10 minutes. 60μL of individual, antibody-immobilized beads were

combined and brought to a total volume of 3mL with bead diluent.

200μL of 1X wash buffer was added to each well of the 96-well plate and incubated for

10 minutes at room temperature on a plate shaker. Wash buffer was decanted. 25μL of

standard, quality control or assay buffer (background) were added to appropriate wells.

An additional 25μL of matrix solution (human serum matrix, PBS or cell culture media,

depending on the sample type) was added to these wells. 25μL of sample was added to

sample wells in addition to 25μL of assay buffer, for a total volume of 50μL in all wells.

Finally, 25μL of mixed beads was added to each well, and the plate was incubated on a

plate shaker at room temperature for 2 hours (plasma or cell culture supernatant samples)

or overnight at 4ºC (CVL samples).

The plate was washed twice with wash buffer using the ELx405 (Biotek) plate washer.

25µL of detection antibodies were added to each well, and the plate was incubated on a

plate shaker for 1 hour at room temperature. 25µL of streptavidin-phycoerythrin was

added to each well, and the plate was incubated for 30 minutes at room temperature on a

plate shaker. The plate was washed twice and wells were resuspended in 150µL of sheath

fluid on a plate shaker for 5 minutes.

Data were acquired on a Bio-Plex 200 (Bio-Rad) and analysed with Bioplex Manager

software (version 5.0, Bio-Rad). Standard curves for each analyte were generated using 5

parameter logistic regressions. Sensitivities for each analyte are listed in section specific

methods. Wells were excluded if fewer than 40 bead events were collected.

2.3.3 Soluble LAG-3 ELISA

Soluble LAG-3 (sLAG-3) concentrations were quantified in plasma samples by an

optimized sandwich ELISA assay. 96-well, flat bottom, polystyrene ELISA plates

(Corning, 25805-96, NY) were coated with 100µL of 5µg/mL anti-human LAG-3

antibody 11E3 (Enzo Life Sciences) diluted in ELISA coating buffer. Plates were

incubated overnight at 4ºC in a humid container.

Plates were then washed six times with 300µL ELISA wash buffer using a microplate

washer (ELx405, Biotek). Wells were blocked with 300µL ELISA blocking buffer for 2

hours at room temperature in a humid container. After six washes, samples and standards

were added to the plate. 100µL of undiluted plasma was added in duplicate for each

sample. A 10-point standard curve was generated using doubling dilutions of recombinant human LAG-3-Fc (Enzo Life Sciences) from 8ng/mL to 15.6pg/mL. Samples and standards were incubated overnight at 4ºC in a humid container.

Plates were washed six times. 100μL of 0.5μg/mL anti-human LAG-3 17B4-biotin detection antibody was added to each well. Plates were incubated for 1 hour at room temperature and washed six times. 100μL of a 1:5000 dilution of Streptavidin-HRP (Invitrogen) was added to each well and incubated for 30 minutes. After washing six times, 100μL of super sensitive tetramethyl benzidine (TMB) was added to each well. Colour development was monitored visually and by a SpectraMax Plus spectrophotometer (Molecular Devices) at 650nm at 5, 8, 15, 20 and 30 minutes. To stop the development reaction, 50μL of a 3% HCL solution was added to each well. The optical density (OD) was then measured at 450nm (usually after 30 minutes of development).

Data was analysed with SoftMax Pro software (version 3.1.2, molecular devices). All optical densities were background-subtracted based on the average OD of blank wells. The standard curve was generated using 4 point logistic regression, and fit of the regression curve to the data points was required to have an r value of >0.995. The concentration of sLAG-3 in sample wells was determined by interpolation from the standard curve.

2.4 Association of *GNB3 825* Genotype with HIV Acquisition and Disease

Progression

2.4.1 DNA Extraction

Template DNA for PCR amplification and genotyping was extracted from biological

samples using the QIAmp DNA Mini kit (Qiagen) according to manufacturer's protocols.

DNA was extracted from maternal serum samples from the PHT cohort (Body Fluids

protocol) and children's dried bloodspots (Bloodspot Protocol).

Portions of dried bloodspots on filter paper were placed in 1.5mL eppendorf tubes and

incubated with 180μL of Buffer ATL (kit) at 85ºC for 10 minutes, then briefly pulse

centrifuged. 20μL of Proteinase K (Qiagen) was added to each tube. Tubes were vortexed

and incubated at 56ºC for 1 hour. 200μL of Buffer AL (kit) was then added to each tube,

mixed by vortexing and incubated for 10 minutes at 70ºC. Serum samples were prepared

by adding 200μL of sample/5x10^6 lymphocytes to a 1.5mL eppendorf tube containing

20μL of Proteinase K. 200μL of Buffer AL was added to each tube, vortexed for 15

seconds and incubated at 56ºC for 10 minutes.

For both sample types, 200μL of ethanol was added to the sample and mixed by

vortexing. The samples were then transferred to a QIAmp Spin Column and centrifuged

at 6000xg for 1 minute. The column was then transferred to a fresh collection tube and

the filtrate discarded. 500μL of Buffer AW1 was added to each column. The columns

were spun at 6000xg for 1 minute, and the filtrate again discarded. 500μL of Buffer AW2

was added to each column, which was then spun at 20,000xg for 3 minutes. After

discarding the filtrate, 200μL of Buffer AE was added to the column. The samples were

incubated for 1 minute at room temperature, then spun at 6,000xg for 1 minute. The

eluted solution of template DNA was frozen at <-20ºC for PCR amplification.

2.4.2 Genotyping and PCR

Genotyping of the GNB3 C825T SNP (rs5443, Gene ID 2784, accession NC_000012.11,

6949375 - 6956564) was performed by PCR amplification and Sanger sequencing. The

PCR reaction consisted of ddH_20, $MgCl_2$, equal concentrations of dATP, dGTP, dCTP,

dTTP (Invitrogen), forward and reverse primers (Invitrogen) (Table 3), Taq polymerase

(Invitrogen) and template DNA. Following the first round of amplification, 2μL of

product was used as template for the second round of amplification.

Table 2.1. Primers used to amplify and sequence the GNB3 825 locus

Primer	Sequence (5'-3')	Annealing Temperature (T_a)
Outer – Forward	GCTGCCCAGGTCTGATCCCT	60ºC
Outer – Reverse	CCAGTGACAAGGGACAGCAGTAAG	60ºC
Inner – Forward	TGACCCACTTGCCACCCGTGC	60ºC
Inner – Reverse	GCAGCAGCCAGGGCTGGC	60ºC
Sequencing – Forward	CAGTTCTTCCCCAATGGAGAGG	55ºC
Sequencing - Reverse	GGCTGGCCCTTACCCACACG	55ºC

PCR products were purified using Montage PCR filter units (EMD Millipore). The entire

volume of the PCR reaction was added to the filter unit containing 450μL of TE (pH 8.0)

buffer. The columns were spun at 3300rpm for 15 minutes (or until dry). To elute the

DNA, ddH_20 was added, the column inverted and placed in a fresh 1.5mL eppendorf tube

and centrifuged at 3300rpm for 2 minutes.

Purified products were sequenced in both directions by Sanger sequencing. Template DNA was incubated with BigDye terminator mix v3.1 (Invitrogen) and either the forward or reverse sequencing primer (Table 3). PCR products were precipitated by adding NaOAC and EtOH to each sample for 3 hours in the dark. Tubes or plates were then spun at 4000rpm for 1 hour, the supernatant discarded, and 70% EtOH added to each well. Samples were spun at 4000rpm for 10 minutes, supernatants discarded and the EtOH wash repeated. Excess EtOH was removed by incubating the samples on a thermocycler at 90ºC. Samples were resuspended in HiDi formamide, vortexed and spun down prior to sequencing. Sequencing products were resolved on an ABI3100 sequencer and data was analysed in Sequencher (Gene Codes Corporation). Genotypes were only assigned when both the forward and reverse sequences were identical.

2.4.3 Cytokine/Chemokine Bead Array Analytes

Concentrations of cytokines and chemokines in plasma samples were quantified using Milliplex MAP bead array kits (Millipore) as described in Section 2.3.2. The Human Cytokine/Chemokine bead panel included the following analytes (with given sensitivities): MIP-1β (4.8pg/mL), SDF-1α (55.8pg/mL) and TRAIL (3.5pg/mL).

2.4.3 Statistical Analysis

Comparison of GNB3 genotype frequency by HIV infection status and assessment of Hardy-Weinberg equilibrium were performed by chi-square analysis. Comparison of HIV acquisition rate and disease progression rate between *GNB3* genotypes was performed by Cox Proportional Hazard regression. In both cases, the survival analysis was also

performed with adjustment for *CD4 868* genotype. To assess the rate of disease progression among all HIV+ cohort participants, progression rate was adjusted for baseline CD4 count. Determination of CD4 decline and viral load increase over time in PHT cohort mothers was performed by linear mixed modeling. Expression of immune activation markers was analysed by Kruskal-Wallis test (non-parametric) and ANCOVA (parametric). The ANCOVA test is similar to the ANOVA, but includes a single co-variate in the analysis to remove the impact of one confounding variable. In this case, CD4 count was used as a covariant to compare immune activation levels in HIV-infected women while controlling for disease progression. Results were analysed in GraphPad Prism (version 4), SPSS (version 16), SAS and STATA (version 11). Differences in all cases were considered to be statistically significant at a p value <0.05.

2.5 Impact of *GNB3 825* Genotype on RNA splicing and immune activation

2.5.1 RNA extraction, purification and concentration

RNA was extracted from whole PBMC samples that were previously cryopreserved. PBMC were thawed as described in Section 2.2.2.1. The PBMC were spun down for 4 minutes, resuspended in 1mL of Trizol (Invitrogen) and incubated for 5 minutes at room temperature. 0.2mL chloroform was added and samples were shaken vigorously for 15 seconds. After incubating at room temperature for 2 minutes, samples were spun for 15 minutes at 4ºC at 12,000xg. The upper aqueous phase containing the RNA was removed and transferred to a fresh eppendorf tube. 0.5mL isopropyl alcohol and 20ug glycogen was added to each sample, which was then incubated for 10 minutes at room temperature. Tubes were spun at 12,000xg for 10 minutes at 4ºC. The supernatant was removed and

75% EtOH added to wash the RNA pellet. Tubes were vortexed, spun at 7,500xg for 5 minutes at 4ºC and the pellet air dried. The sample was resuspended in 75uL RNAse-free ddH$_2$O by incubating at 55ºC for 10 minutes and was cooled at 4ºC for 5 minutes.

RNA samples were purified using the RNeasy MinElute kit (Qiagen) according to manufacturer's protocols. Briefly, RNA samples were incubated with DNAseI and RDD buffer for 10 minutes at room temperature to remove contaminating DNA prior to RNA clean up protocol. 100% EtOH was then added to each sample and mixed. The mixture was transferred to an RNeasy MinElute spin column and centrifuged at 8,000xg for 15 seconds. The column was transferred to a fresh eppendorf tube and RPE buffer was added prior to spinning at 8,000xg for 15 seconds. 80% EtOH was added to each tube, which was then spun at 8,000xg for 2 minutes. The column was transferred to a new eppendorf tube, the lid opened, and the column spun at full speed for 5 minutes. The column was then transferred to a fresh eppendorf tube, 14μL of RNase-free ddH2O added to the column, and the sample spun at full speed for 1 minute to collect the eluted RNA.

2.5.2 RNA Exon Microarrays

RNA isolated as described in section 2.5.1 was used as the sample for the Affymetrix Human ST 1.0 exon microarray assay. RNA concentration in each sample was determined by Nanodrop (Thermo Scientific). Samples with RNA concentrations greater than 350μg/μL were diluted to a final concentration of 350μg/μL in ddH$_2$O. RNA samples were applied to the Affymetrix Human ST 1.0 exon array chips and processed on

the GeneChip Fluidics Station at the DNA Core facility of the National Microbiology

Laboratory according to Affymetrix protocols. Expression data was exported, normalized

and analysed using the Partek Genomics Suite software.

2.5.3 cDNA preparation

RNA samples prepared in section 2.5.1 were utilized as templates for cDNA generation

using the QantiTect RT kit (Qiagen) according to manufacturer's protocol. Briefly, RNA

template was incubated with gDNA Wipeout buffer and RNase-free ddH$_2$O for 5 minutes

at 42ºC to degrade genomic DNA. The entire volume of the RNA sample was then

incubated with QuantiScript Reverse Transcriptase enzyme, RT buffer and RT primer

mix for 20 minutes at 42ºC. Enzyme activity was halted by incubated the sample for 3

minutes at 95ºC. Samples were then either frozen at -80ºC or used for qRT-PCR

reactions.

2.5.4 Quantitative Real-Time PCR (qRT-PCR)

LAG-3 (Gene ID 3902, accession NC_000012.11, 6881670 - 6887621) cDNA abundance

was quantified by qRT-PCR compared to the expression of 18S rRNA, which is

commonly used as a housekeeping gene known to be consistent between samples from

the FSW cohort. Specificity of the primers and generation of the appropriately sized PCR

product was confirmed by gel electrophoresis.

A standard curve of cDNA was generated in order to quantify the relative abundance of

LAG-3 and 18S rRNA expression. PBMC isolated from healthy local donors was

stimulated overnight with PHA, RNA extracted as in Section 2.5.1, and cDNA generated

as in Section 2.5.3. 2µg of cDNA was generated, and then serially 10-fold diluted. cDNA

samples/standards were incubated with forward and reverse primers (Table 4), ddH$_2$O

and QuantiTect SYBR Green PCR master mix containing HotStarTaq DNA polymerase,

QuantiTect SYBR Green PCR buffer, dNTP mix (including dUTP), SYBR Green I, ROX

passive reference dye and MgCl$_2$ (Qiagen). Reactions were performed using the Roche

LightCycler System 1.5 (Roche). Samples were run in duplicate with negative controls

(no RNA template). Transcript abundance was expressed as a concentration derived from

the standard curve, and LAG-3 expression was normalized to 18S rRNA expression for

each sample.

Table 2.2. Primers used to amplify LAG-3 cDNA.

Primer	Sequence (5' – 3')
Exon 2/3 Forward	TGGCAGCATCAGCCAGAC
Exon 2/3 Reverse	GCAGCCATAGCGAGAACTCC
Exon 6 Forward	GCTTTGTGAGGTGACTCCAG
Exon 6 Reverse	GGGCTAGACAGCTCTGTGAAC

2.5.5 Statistical Analysis

The Partek Analysis Suite provides p values describing differences in expression and

splicing of RNA transcripts between specified groups. These uncorrected p values,

however, are not adjusted for the extremely large number of comparisons generated in a

whole transcriptome, exon-by-exon microarray, and are, as such, subject to a high degree

of type I error. While there are numerous sophisticated statistical methods that can be

used to properly weight and adjust p values generated by microarray experiments, the use

of the exon array in this thesis was primarily as a hypothesis-generating tool, with any

results requiring independent confirmation at the RNA and protein level. As such, no p

values are presented for the Partek splicing/expression analysis. LAG-3 expression

quantified by qRT-PCR was analysed by Mann-Whitney test in GraphPad prism version

4.0 (GraphPad software). P values of <0.05 were considered to be statistically significant.

2.6 Expression of LAG-3 during HIV infection

2.6.1 Flow cytometry panels

Freshly isolated PBMC were surface stained to determine the expression of LAG-3,

activation and exhaustion markers *ex vivo*. $1x10^6$ cells were stained and fixed, and

100,000 lymphocyte events were collected on the BD LSRII flow cytometer. The panels

used to identify and phenotype lymphocyte subsets are shown in Table 5.

Table 2.3. Flow cytometry panels used to phenotype fresh PBMC for LAG-3 expression and immune activation/exhaustion.

Fluorochrome	Lymphocyte Subset Panel			Activation/Exhaustion Panel		
	Marker	Clone	Source	Marker	Clone	Source
FITC	LAG-3	17B4	Enzo Life Science	LAG-3	17B4	Enzo Life Science
PE	iNKT	6B11	BD	PD-1	MIH4	BD
PE-Cy5	CD69	FN50	BD	CD69	FN50	BD
Pacific Blue	CD3	UCHT1	BD	CD3	UCHT1	BD
V500	CD8	SK1	BD	CD8	SK1	BD
APC	CD56	B159	BD	Tim-3	344823	R&D
Alexa700	CD4	RPA-T4	BD	CD4	RPA-T4	BD
APC-H7	CD16	3G8	BD	HLA DR	L243	BD

2.6.2 Cytokine/Chemokine Bead Array Analytes

Concentrations of cytokines and chemokines in plasma samples were quantified using

Milliplex MAP bead array kits (Millipore). The Human Cytokine/Chemokine bead panel

included the following analytes (with given limits of detection): IFNα2 (7.2pg/mL), IFNγ (2.4pg/mL), IL-4 (0.6pg/mL), IL-6 (0.4pg/mL), IL-10 (0.5pg/mL), MIP-1β (4.8pg/mL), sCD40L (9.9pg/mL) and TNFα (1.6pg/mL). The standard curve for the Human Cytokine/Chemokine panel analytes was composed of six 5-fold dilutions ranging from 10,000pg/mL to 3.2pg/mL. For the analysis of plasma samples, the standard curve, background and quality control wells were incubated with human serum matrix (Millipore), which was prepared by reconstitution in 1mL ddH2O and incubation for 10 minutes.

2.6.3 Antigen-specific stimulations

To compare LAG-3 expression on bulk and antigen-specific T cells, PBMC were stimulated with 2 HIV Gag peptide pools. PBMC samples were cryopreserved and later thawed, as described in Section 2.2.2.1. PBMC were cultured at $2x10^6$/mL in 24-well tissue culture plates at 1mL/well. T cells were stimulated with HIV Gag A and/or HIV Gag B peptide pools at a concentration of 2ug/peptide/mL for 10 hours. Detection of cytokine production following stimulation requires the inhibition of golgi transport through the addition of GolgiPlug (containing brefeldin A) and GolgiStop (containing monensin) (BD Biosciences), which were added to culture at 1uL/mL and 0.66uL/mL, respectively, 2 hours post-stimulation. Unstimulated control wells were used to calculate background cytokine production.

2.6.4 Statistical Analysis

Comparisons of flow cytometry and cytokine bead array data were performed by Mann-Whitney or Kruskal-Wallis test (non-parametric, continuous variables). Where appropriate, Dunn's post-test was used to determine inter-group differences following a significant Kruskal-Wallis test. Correlations between continuous variables were performed using Spearman correlation. Trend lines displayed on graphs with significant correlations were derived by linear regression. All statistical analyses were performed in GraphPad Prism, version 4.0 (GraphPad Software). P values of <0.05 were considered to be statistically significant. Correlations were described as 'weak' if the rho value was less than 0.5.

2.7 Expression of LAG-3 at the genital mucosa

2.7.1 Flow Cytometry Panels

Freshly isolated PBMC and CMC were surface stained to phenotype LAG-3+ iNKT and T cells *ex vivo* (Table 6). $2x10^6$ PBMC were stained and fixed, and 400,000 lymphocyte events (for PBMC, all events for CMC) were collected on the BD LSRII flow cytometer. CMCs were processed as described in Section 2.2.2.2. All cells isolated were surface stained, and the entire tube was acquired on the LSRII flow cytometer.

Table 2.4. CMC *ex vivo* flow cytometry panel.

Fluorochrome	*Ex vivo* iNKT Phenotype Panel		
	Marker	**Clone**	**Source**
FITC	LAG-3	17B4	Enzo Life Sciences
PE	iNKT	6B11	BD
ECD	Live/Dead	--	Invitrogen
PE-Cy5	CD40L	TRAP1	BD
PE-Cy7	CCR5	2D7/CCR5	BD
Brilliant Violet 421	PD-1	EH12.2H7	Biolegend
V500	CD8	RPA-T8	BD
APC	CD69	FN50	BD
Alexa700	CD3	UCHT1	BD
APC-H7	CD4	RPA-T4	BD

2.7.2 Cytokine/Chemokine Bead Array Analytes

Concentrations of cytokines and chemokines in plasma samples were quantified using

Milliplex MAP bead array kits (Millipore). The Human Cytokine/Chemokine magnetic

bead panel included the following analytes (with given limits of detection): interferon

(IFN)-α2 (4.8pg/mL), interleukin (IL)-15 (1.7 pg/mL), IL-1α (12.6 pg/mL), IL-8 (0.7

pg/mL), IFNγ-induced protein (IP)-10 (14.0 pg/mL), monocyte chemotactic protein

(MCP)-1 (3.4 pg/mL), macrophage inflammatory protein (MIP)-1α (6.2 pg/mL), MIP-

1β (4.8 pg/mL) and sCD40L (9.9 pg/mL). The Human Th17 magnetic bead panel

included the following analytes: IL-1β (3.6 pg/mL), IL-2 (9 pg/mL), IL-6 (2.9 pg/mL),

IL-10 (0.5 pg/mL), IL-12p70 (2.2 pg/mL), IFNγ (2.4 pg/mL), tumor necrosis factor

(TNF)α (1.7 pg/mL), IL-23 (169 pg/mL), MIP3α (3.4 pg/mL), IL-17A (2.8 pg/mL), IL-

17F (16 pg/mL), IL-17E (186 pg/mL) and IL-22 (32 pg/mL).

The standard curve for the Human Cytokine/Chemokine panel analytes was composed of six 5-fold dilutions ranging from 10,000pg/mL to 3.2pg/mL. The standard curve for the Th17 panel analytes was composed of six 4-fold dilutions as follows: 100ng/mL to 20pg/mL (IL-17F), 40,000 pg/mL to 10pg/mL (IFNγ), 5,000pg/mL to 1 pg/mL (IL-10), 20,000pg/mL to 5pg/mL (MIP3α, IL-12p70, IL-1β), 50,000pg/mL to 12pg/mL (IL-17A, IL-2), 150ng/mL to 40pg/mL (IL-22), 1500ng/mL to 300pg/mL (IL-23), 10,000pg/mL to 2.5pg/mL (IL-6, TNFα), 2,000ng/mL to 480pg/mL (IL-17E).

Identical kits were used for both plasma and CVL samples. For the analysis of plasma samples, the standard curve, background and quality control wells were incubated with human serum matrix (Millipore), which was prepared by reconstitution in 1mL ddH2O and incubation for 10 minutes. For the analysis of CVL samples, the standard curve, background and quality control wells were incubated with PBS to reflect the composition of the CVL sample. CVL samples were run in duplicate and plates were incubated overnight at 4ºC.

2.7.3 Statistical Analysis

Comparisons of flow cytometry and cytokine bead array data were performed by Wilcoxon Rank Sum test/Friedman test (non-parametric, paired, continuous variables) or Chi square/Fisher's exact test (dichotomous variables). Where appropriate, Dunn's post-test was used to determine inter-group differences following a significant Friedman test. Correlations between continuous variables were performed using Spearman correlation. Trend lines displayed on graphs with significant correlations were derived by linear

regression. All statistical analysis was performed in GraphPad Prism, version 6.0 (GraphPad Software). P values of <0.05 were considered to be statistically significant. Correlations were described as 'weak' if the rho value was less than 0.5.

2.8 Function of LAG-3 expression on iNKT cells

2.8.1 Stimulations

PBMC samples were cryopreserved and later thawed, as described in 2.2.2.1. To assess iNKT cytokine production, PBMC were stimulated with lipid antigen (αGalCer) or the positive control PMA/Io. PBMC were cultured at $2x10^6$/mL in 24-well tissue culture plates at 1mL/well. To quantify cytokine secretion, PBMC were stimulated for 6 hours (with 25ng/mL PMA and 500ng/mL Io) or 10 hours (with 100ng/mL αGalCer). Detection of cytokine production following stimulation requires the inhibition of golgi transport through the addition of GolgiPlug (containing brefeldin A) and GolgiStop (containing monensin) (BD Biosciences), which are added to culture at 1uL/mL and 0.66uL/mL, respectively, 2 hours post-stimulation. TCR-mediated activation of iNKT cells results in rapid and sustained TCR downregulation. As the iNKT population is identified using a TCR-specific antibody (6B11-PE), TCR downregulation prevents identification of the entire activated iNKT population. To limit this issue, the 6B11-PE antibody was added to all culture wells at the time of stimulation, similarly to the protocols used for tetramer-based identification of antigen-specific T cells.

Due to limitations in the number of channels available for multicolour flow cytometry, analysis of iNKT cytokine production by flow cytometry was limited to IFNγ and TNFα.

To quantify the production of other iNKT cytokines and chemokines, cell culture supernatants were harvested for Milliplex bead array analysis. PBMC were cultured as above and stimulated with 100ng/mL αGalCer (or unstimulated control) for 24 hours, at which point supernatants were harvested and stored at -80ºC. Additionally, supernatants were collected from the 5 day unstimulated and αGalCer-stimulated proliferation cultures, and stored at -80ºC.

2.8.2 Flow cytometry panels

$2x10^6$ PBMC were surface stained with an iNKT phenotype panel, as shown in Table 7. The remaining PBMC were stimulated as described in 2.8.4. Following stimulation, $2x10^6$ PBMC were stained for surface expression of LAG-3 and PD-1 and intracellular cytokine production or proliferation. The panel for ICS is shown in Table 8. In all cases, between $2x10^5$ and $4x10^5$ lymphocyte events were collected per sample on the BD LSRII flow cytometer. Samples with fewer than 30 iNKT gate events were excluded from analysis.

Table 2.5. Flow cytometry panel for iNKT phenotyping of PBMC.

Fluorochrome	*Ex vivo* iNKT Phenotype Panel		
	Marker	**Clone**	**Source**
FITC	LAG-3	17B4	Enzo Life Science
PE	iNKT	6B11	BD
ECD	Live/Dead	--	Invitrogen
PE-Cy5	CD40L	TRAP1	BD
PE-Cy7	CCR5	2D7/CCR5	BD
Brilliant Violet 421	PD-1	EH12.2H7	Biolegend
V500	CD8	RPA-T8	BD
APC	CD69	FN50	BD
Alexa700	CD3	UCHT1	BD
APC-H7	CD4	RPA-T4	BD

Table 2.6. Flow cytometry panel for ICS quantification following iNKT stimulation.

Fluorochrome	ICS Panel		
	Marker	**Clone**	**Source**
FITC	LAG-3	17B4	Enzo Life Science
PE	iNKT	6B11	BD
ECD	Live/Dead	--	Invitrogen
PE-Cy5	CD3	UCHT1	BD
PE-Cy7	TNFα	MAb11	BD
Brilliant Violet 421	PD-1	EH12.2H7	Biolegend
V500	CD8	RPA-T8	BD
APC	CD69	FN50	BD
Alexa700	IFNγ	B27	BD
APC-H7	CD4	RPA-T4	BD

2.8.3 Cytokine/Chemokine Bead Array Analytes

Plasma samples were analysed with the kits described in section 2.7.2.

Cell culture supernatants from the iNKT αGalCer stimulations were analysed for

expression of the following analytes (with corresponding sensitivities): IFNγ (0.8pg/mL),

IL-4 (4.5pg/mL), IL-10 (1.1pg/mL), IL-13 (1.3pg/mL), IL-17 (0.7pg/mL), IP-10

(8.6pg/mL), IL-12p70 (0.6pg/mL), MIP-1α (2.9pg/mL), MIP-1β (3.0pg/mL) and TNFα

(0.7pg/mL). Plates quantifying cytokines in cell culture supernatants used R10 media as

the matrix for standard, control and background wells. Culture supernatant samples were

run in duplicate and plates were incubated at room temperature for 2 hours.

2.8.4 Soluble LAG-3 ELISA

Soluble LAG-3 was quantified in cell culture supernatant samples as in section 2.3.3,

with minor modifications. As the culture supernatants are composed primarily of RPMI

media with FCS, the recombinant LAG-3 standard was diluted in R10 media, rather than

PBS. In all other respects, the ELISA protocol and data analysis followed that described for the detection of sLAG-3 in plasma samples.

2.8.5 Statistical Analysis

Comparisons of flow cytometry, ELISA and cytokine bead array data were performed by Kruskal-Wallis test (non-parametric, continuous variables) or Chi square/Fisher's exact test (dichotomous variables). Where appropriate, Dunn's post-test was used to determine inter-group differences following a significant Friedman test. Correlations between continuous variables were performed using Spearman correlation. Trend lines displayed on graphs with significant correlations were derived by linear regression. All statistical analysis was performed in GraphPad Prism, version 6.0 (GraphPad Software). p values of <0.05 were considered to be statistically significant. Correlations were described as 'weak' if the rho value was less than 0.5.

3. Association of *GNB3 825* Genotype with HIV Acquisition and Disease Progression

3.1 Rationale

The *GNB3 825* SNP has previously been associated with differential rates of HIV progression and response to highly active antiretroviral therapy (HAART) in Caucasian cohorts (161, 162). The impact of *GNB3* genotype on HIV acquisition and progression among African cohorts has not been assessed, and is of interest for several reasons. First, the frequency of the *GNB3 825T* allele in African populations is extremely high (~80%) (174) and could, therefore, have a substantial impact on HIV progression based on the hazard ratios for progression to AIDS reported in the Caucasian cohort. Although the effect of genetic variability is often population-dependent (151), the associations between *GNB3 825* genotype and disease susceptibility are particularly disparate among Caucasian, Asian and African populations (175), with detailed study of *GNB3* genotypes in African populations representing an important gap in knowledge.

Second, the *GNB3* gene is located near the *CD4 C868T* SNP that we have previously reported to be associated with HIV acquisition and disease progression in a high-risk Kenyan cohort (142). It is therefore conceivable that linkage between *GNB3* and *CD4* SNPs could contribute to the observed epidemiological effect of *CD4 868T* genotype. Therefore, we assessed the impact of *GNB3* genotype on HIV acquisition, rate of disease progression and response to ART in two Kenyan cohorts: high-risk commercial sex workers (FSW cohort) and HIV+ mothers and children (perinatal HIV transmission (PHT) cohort). The results of this study are also reported in the publication by Juno *et al*, Retrovirology, 2012 (443).

3.2 <u>Hypothesis</u>

The *GNB3 825TT* genotype is associated with an elevated risk of HIV acquisition and disease progression, but more rapid response to ART, compared to the *GNB3 825CC/CT* genotype due to elevated peripheral blood T cell activation.

3.3 <u>Objectives</u>

1) Genotype participants in the FSW and PHT cohorts for *GNB3 825* allele and compare risk of HIV acquisition, rate of disease progression and response to ART between participants with the *GNB3 825TT* and *825CC/CT* genotypes.

2) Quantify the expression of T cell activation markers and plasma levels of CCR5 and CXCR4 ligands among participants with *GNB3 825TT* and *825CC/CT* genotypes.

3.4 <u>Results</u>

3.4.1 Study Populations

GNB3 825 genotyping was performed among participants enrolled in two Kenyan cohorts. 1031 participants from the Majengo commercial sex worker cohort (FSW cohort), including both HIV-N and HIV+ high-risk women, were genotyped at the *GNB3 825*, and in some cases, the *CD4 868*, locus (Table 3.1). In the low-risk perinatal HIV transmission cohort (PHT cohort), 395 HIV+ women and 395 HIV-N or HIV+ infants were genotyped at the *GNB3 825* locus. Events of mother-to-child HIV transmission (whether *in utero*, intrapartum or postpartum) were recorded, in addition to monitoring of maternal viral load and CD4 count (Table 3.2).

Table 3.1 *GNB3 C825T* genotype frequency for HIV-1 negative and HIV-1 positive individuals in the FSW cohort.

GNB3 825 Genotype	HIV-N (n=349)	HIV+ (n=682)
CC (homozygous wildtype)	15 (4.3%)[*]	27 (4.0%)[*]
CT (heterozygous)	124 (35.5%)[*]	206 (30.2%)[*]
TT (homozygous variant)	210 (60.2%)[*]	449 (65.8%)[*]
CT Frequency	0.355	0.302
p for HWE	0.904	0.942
C allele frequency	0.22	0.19
T allele frequency	0.78	0.81

[*]Data are no. (%) of subjects

For the comparison of genotype frequency between HIV-N and HIV+ subjects, p=0.19 (chi squared test). HWE, Hardy-Weinberg equilibrium.

Table 3.2 Characteristics of mothers and transmission events in the PHT cohort.

Parameter	Median (IQR) or Number (%)	N, data available
Age	25 (22-28)	390
Deaths	14 (4%)	395
CD4 Count, Month 1	555 (387-745)	329
Plasma HIV Viral Load, Month 1 ($\log_{10}$ copies/mL)	4.79 (4.17-5.35)	376
GNB3 825 genotype frequency	CC 98 (24.9%); CT 94 (23.9%); TT 201 (51.1%)	393
Total number of HIV-infected infants [a]	79 (20%)	393
In utero transmission events [b]	24 (31%)[e]	79
Peripartum transmission events [c]	39 (49%)[e]	79
Breastmilk transmission events [d]	16 (20%)[e]	79

IQR, Inter-quartile range; [a] percentage of HIV-infected infants with mothers with genotype data; [b] transmission occurring within 48hrs of birth; [c] transmission occurring more than 48hrs after birth but prior to 1 month of age; [d] transmission occurring between 1 month of age and 1 year of age; [e] percentage of all HIV-infected infants

GNB3 825 genotype frequency was compared between HIV-N (n=349) and HIV+

(n=682) FSW cohort participants. There was no significant difference between

825CC/CT and *825TT* genotype frequency based on serostatus (p=0.19, Chi squared)

(Table 3.1). Among all participants, *GNB3 825* genotypes were in Hardy-Weinberg

equilibrium (HIV-N subjects p=0.904, HIV+ subjects p=0.942, Chi squared) (Table 3.1).

Cox regression survival analysis of the time to seroconversion among 277 HIV-N

participants with known dates of seroconversion (n=99 *GNB3 825CC/CT*, n=178 *GNB3*

825TT) demonstrated no significant impact of *GNB3 825* genotype on risk of HIV

acquisition (Hazard Ratio (HR) 1.313, 95% CI 0.910, 1.895, p=0.15, Cox proportional

hazard analysis) (Figure 3.1). Despite the proximity of the *GNB3* gene to the *CD4 C868T*

SNP on chromosome 12, analysis of linkage disequilibrium using LOD score (logarithm

of odds) between the *GNB3 825* and *CD4 868* SNPs demonstrated no significant linkage

between genotypes (LOD = 1.14, D' = 0.338, r^2 =0.0060). Accordingly, inclusion of *CD4*

868 genotype in the survival analysis of seroconversion did not affect the relative risk of

seroconversion between *GNB3 825* genotype groups.
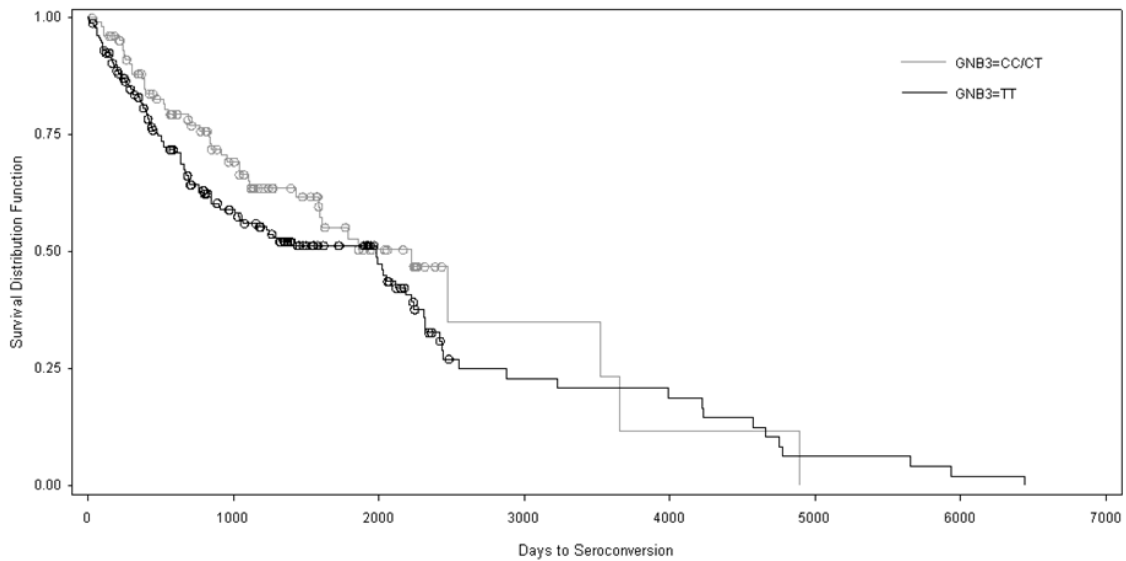
Figure 3.1 Kaplan-Meier survival analysis of time from enrolment to seroconversion in FSW cohort participants. 277 individuals with a known date of seroconversion were included in this analysis: 99 *GNB3 825CC/CT* and 178 *GNB3 825TT*. There was no difference in time to seroconversion as determined by Cox proportional hazard regression (Hazard Ratio (HR) 1.313, 95% CI 0.910, 1.895, p=0.15). Icons between drops in the lines represent the end of an individual's data set (censoring event).

3.4.3 HIV Acquisition in the Perinatal HIV transmission cohort

We also analysed *GNB3 825* genotype with respect to maternal HIV-1 transmission rates either *in utero*, peripartum or via breastmilk in a low-risk Kenyan perinatal HIV transmission cohort (PHT) for which both viral load and CD4 count data were available. The overall risk of mother-to-child transmission was not associated with infant *GNB3* genotype in an unadjusted model (HR 1.23, 95% CI: 0.76, 1.98, p=0.40) or following adjustment for maternal viral load (p=0.51). Subgroup analysis of *in utero,* peripartum and breastmilk transmission events revealed no effect of 825 genotype on *in utero* transmission (Odds ratio (OR) 0.89, 95% CI: 0.38, 2.07, p=0.78 unadjusted; OR 1.00, 95% CI 0.41, 2.44, p=1.00 adjusted for maternal viral load) or peripartum transmission (OR 0.94, 95% CI 0.47, 1.87, p=0.85 unadjusted; OR 0.84, 95% CI 0.40, 1.73, p=0.63 adjusted), but did show a trend toward an increased risk of breastmilk transmission in the TT genotype group (OR 8.35, 95% CI 1.09, 64.13, p=0.04 unadjusted; OR 7.41, 95% CI 0.94, 58.2, p=0.06 adjusted). This was not accompanied by a significant difference in maternal breastmilk viral load (p=0.54), plasma viral load at delivery (p=0.22) or cervicovaginal viral load (p=0.46) between CC/CT and TT mothers.

3.4.4 HIV Progression in the FSW cohort

Given that Caucasian HIV-positive patients with the *GNB3 825TT* genotype were reported to exhibit accelerated disease progression and to respond more favourably to ART than CC or CT genotypes [7, 8], we assessed HIV disease progression in both the FSW and PHT cohorts. Within the FSW cohort, 73 genotyped participants seroconverted after their enrolment and returned for at least one follow-up visit (n=21 *GNB3*

825CC/CT, n=52 *GNB3 825TT*). Among those participants, survival analysis of time to CD4 counts of <350 cells/μL did not show any significant effect of the *GNB3 825* genotype, nor was there any interaction with the *CD4 868* genotype (HR 0.665, 95% CI 0.369, 1.198, p=0.1742, Cox proportional hazard analysis) (Figure 3.2A). Given the relatively small sample size of seroconverter patients, we also analysed disease progression among 146 women who were HIV+ with CD4 counts >500 cells/μL at the time of recruitment (n=48 *GNB3 825CC/CT,* n=98 *GNB3 825TT*). Because the seroconversion dates for these women were not known, the time to CD4 <350 cells/μL and CD4 <250 cells/μL was adjusted for baseline CD4 count. After adjustment, there was no significant difference in time to progression in 825 CC/CT patients compared to 825 TT patients, nor was there any interaction with *CD4* genotype (CD4<350: HR=0.956, 95% CI 0.619, 1.477, p=0.8397; CD4<250: HR=0.966, 95% CI 0.594, 1.570, p=0.8879, Cox proportional hazard analysis) (Figure 3.2B).

3.4.5 HIV Progression in the PHT cohort

Although infant HIV progression data were not available for the transmission events in the PHT cohort, maternal data regarding progression to CD4 <350 cells/μL, monthly rate of CD4 decline, death and viral load were available. CD4 decline to <350 cells/μL among 262 subjects (n=125 *GNB3 825CC/CT*, n=137 *GNB3 825TT*) did not significantly differ between 825TT and 825CC/CT genotypes before or after adjustment for baseline CD4 count (HR=0.75, 95% CI 0.47, 1.19, p=0.22 adjusted) (Figure 3.3). Overall risk of death was not affected by GNB3 genotype (HR=1.94, 95% CI 0.46, 8.18, p=0.36).
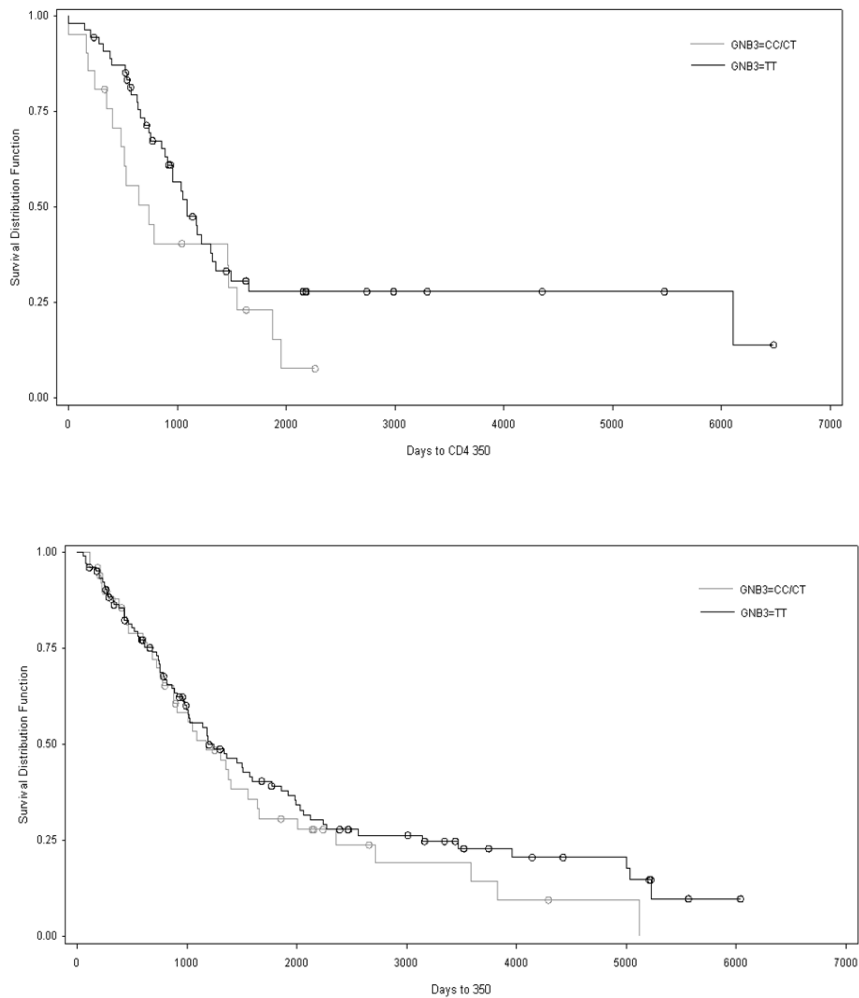
Figure 3.2 Kaplan-Meier survival analysis of HIV disease progression to CD4 count <350 cells/μL across *GNB3* genotypes. **(A)** Survival analysis for 73 FSW cohort participants who seroconverted during follow-up: 21 *GNB3 825CC/CT* subjects and 52 *GNB3 825TT* subjects. There were no significant differences in time to CD4 <350 cells/μL as determined by Cox proportional hazard analysis (HR 0.665, 95% CI 0.369, 1.198, p=0.1742). **(B)** Survival analysis for 146 HIV-1-positive FSW cohort subjects: 48 *GNB3 825CC/CT* subjects and 98 *GNB3 825TT* subjects. Following adjustment for baseline CD4 count, there were no significant differences in time to CD4 <350 cells/μL as determined by Cox proportional hazard analysis (HR=0.956, 95% CI 0.619, 1.477, p=0.8397).
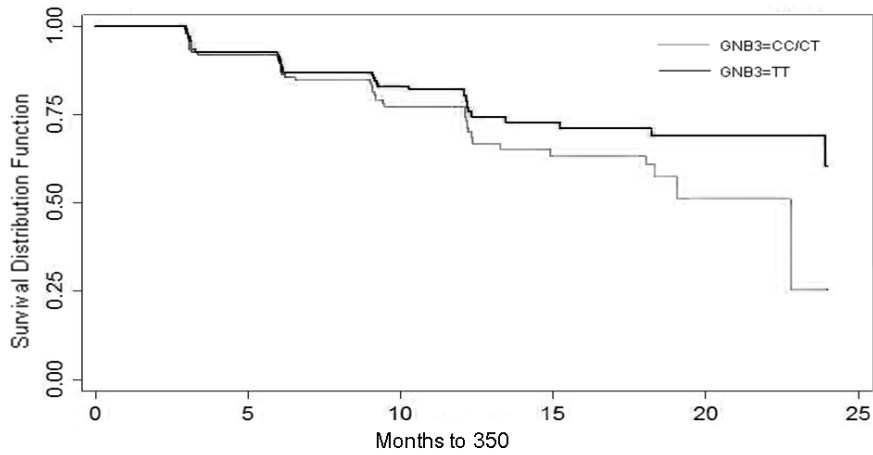
Figure 3.3 Kaplan-Meier survival analysis of HIV disease progression to CD4 count <350 cells/μL among 262 PHT cohort HIV-1-positive mothers. 125 *GNB3 825CC/CT* subjects and 137 *GNB3 825TT* subjects. Following adjustment for baseline CD4 count, there were no significant differences in time to CD4 <350 as determined by Cox proportional hazard analysis (HR=0.75, 95% CI 0.47, 1.19, p=0.22).

Linear mixed modeling (LMM) analysis of CD4 loss over two years of follow-up demonstrated a trend toward slower CD4 decline among 825TT genotype mothers, although the difference was only an average of 2.82 cells per month (9.46 cells/month among 825 CC/CT versus 6.64 cells/month among 825TT) (p=0.08, LMM). Similar modeling of viral load change over time did not reveal any significant effect of GNB3 genotype on viral load increase (p=0.5, LMM).

3.4.6 Response to ARV therapy in the FSW cohort

A number of HIV+ FSW cohort participants with available *GNB3* genotypes initiated antiretroviral therapy between January 2005 and January 2012. Because *GNB3* genotype was previously reported to influence CD4 recovery following ART initiation (161), we compared the CD4 count at time of ARV initiation and CD4 recovery 1 year after post-initiation between *GNB3* genotype groups.

CD4 counts at ART initiation and 1 year post-initiation were available for 30 *CC/CT* and 64 *TT* genotype participants. CD4 counts at the time of ARV initiation did not differ significantly between *GNB3 CC/CT* (median=192.5 cells/µL) and *TT* (median=198.5 cells/µL) genotype groups (Figure 3.4A) (p=0.925, Mann-Whitney test). Among all participants, CD4 counts increased significantly between baseline (median=196 cells/µL) and one year of ART (median=302 cells/µL) (p<0.0001, Wilcoxon test), and 75 of 94 participants demonstrated an increase in CD4 count over 1 year of follow-up. Absolute CD4 counts following 1 year of ART did not differ between *GNB3* genotype groups (*CC/CT* median=317.5 cells/µL, *TT* median=299 cells/µL, p=0.668, Mann-

Whitney test) (Figure 3.4B). The change in CD4 count from baseline (baseline subtracted values) was also similar between *CC/CT* and *TT* groups (*CC/CT* median=94 cells/mL, *TT* median=93.5 cells/µL, p=0.879, Mann-Whitney test) (Figure 3.4C), as was the percent change in CD4 count from baseline (*CC/CT* median=33.58%, *TT* median=44.39%, p=0.624, Mann-Whitney test) (Figure 3.4D). A comparison of the proportion of individuals exhibiting an increase in CD4 count following ART revealed no significant differences between genotype groups (p=0.594, Fisher's exact test) (Figure 3.4E).

3.4.7 Immune activation among HIV-N subjects

The potential for *GNB3* genotype to influence lymphocyte chemotaxis, cellular activation, apoptotic pathways and CD4 counts [18] could have important implications for HIV-1 disease progression, which can be driven by increasing immune activation and apoptosis [4]. The only data available describing T cell immune activation in subjects with varying *GNB3* genotypes is reported in an assessment of healthy Caucasian individuals [20]. No differences in HLA DR expression on T cells was observed, and although bulk CD4 counts were shown to be increased in Caucasian subjects, the study did not measure any CD4+ T cell subsets such as regulatory T cells (Tregs).

Cross-sectional measurements of *ex vivo* T cell expression of CD69, HLA-DR and CD38, and Treg proportion in GNB3-genotyped women from the FSW cohort were available from several previously published studies (114, 444). We therefore compared immune activation between GNB3 genotypes groups in both HIV-N and HIV+ participants.
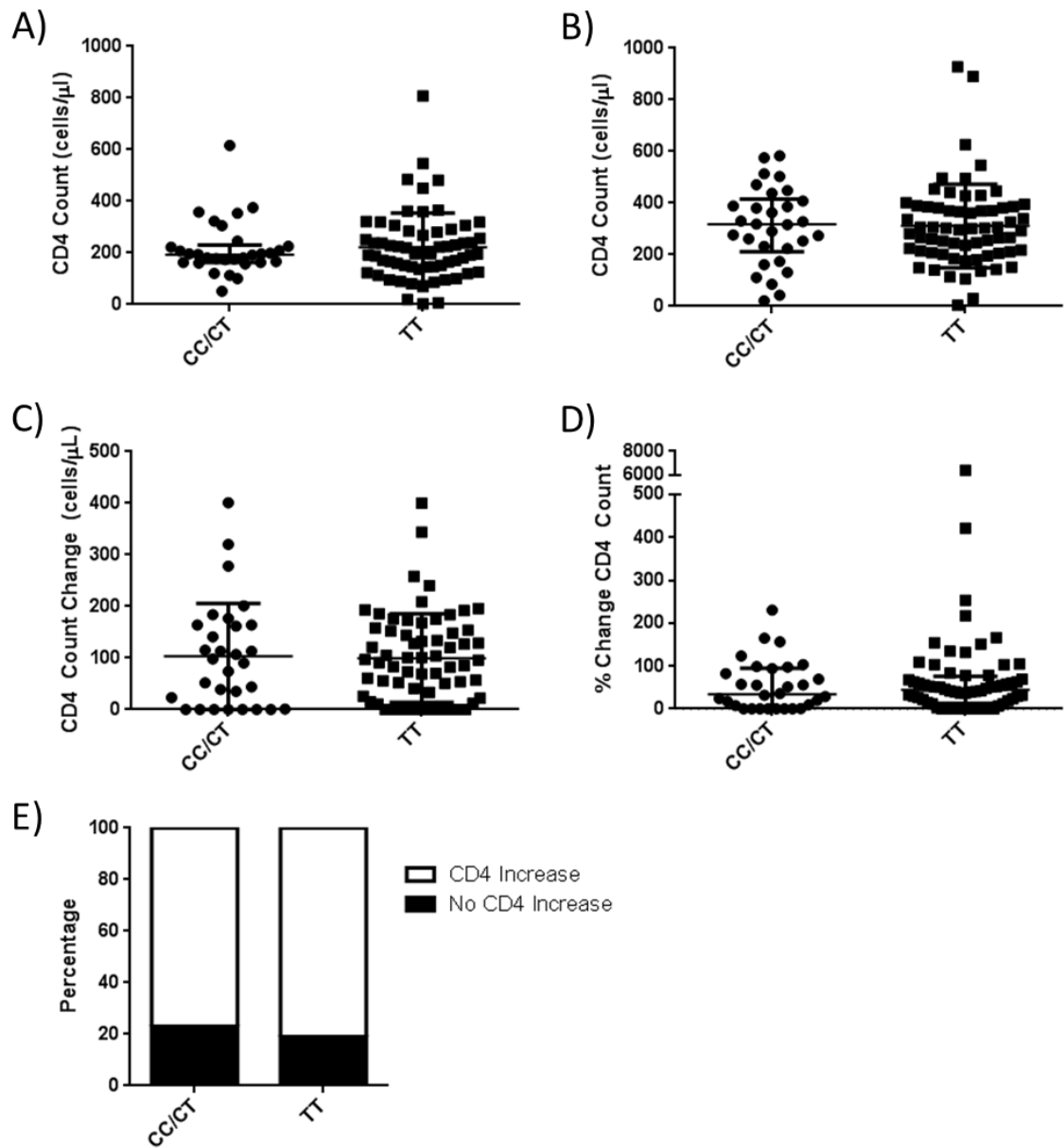
Figure 3.4 CD4 recovery following ART initiation among *GNB3 825* CC/CT and TT FSW cohort participants. (**A**) CD4 counts at time of ART initiation were similar between *GNB3 825* CC/CT (n=30) and TT (n=64) groups. (**B**) CD4 counts 1 year post-ART initiation were similar between genotype groups. (**C**) The change in CD4 count over one year of ART did not differ between genotype groups. (**D**) The change in CD4 count over one year of ART, expressed as a percentage of baseline CD4 count, did not differ between genotype groups. (**E**) The proportion of participants exhibiting an increase in CD4 count during one year of ART was similar between genotype groups. In (A) through (D), median and interquartile range are indicated.

In healthy women, no differences in expression of CD69 (acute activation), HLA-DR or CD38 (chronic activation) were observed between CC/CT and TT genotypes on either CD4+ or CD8+ T cells (p>0.1 for all, Mann-Whitney) (Figure 3.5A, B). Expression patterns of HLA-DR and CD38 were confirmed to be similar in a second cross-sectional study (p>0.1 for all, Mann-Whitney). There were also no differences in Treg frequency, expressed as a percentage of CD4+ T cells (p=0.96, Mann-Whitney) (Figure 3.5A, B).

Although activated CD4+ T cells are generally considered to be prime targets for HIV-1 infection and replication, cellular susceptibility to HIV-1 infection requires the expression of either the CCR5 (in early infection) or CXCR4 (in late infection) co-receptor. To more specifically characterize T cell susceptibility to infection, we compared the percentage of cells expressing either CXCR4 or CCR5 between *GNB3* genotypes, but found no differences between 825 CC/CT and TT groups (p>0.1 for both, Mann-Whitney) (Figure 3.5C). As most infecting viruses utilize the CCR5 co-receptor, we also compared the density of CCR5 expression on CD4+ T cells (as measured by median fluorescence intensity) (Figure 3.5C) and the activation state of CD4+CCR5+ cells (as measured by CD69 and HLA DR expression) (Figure 3.5D). No differences in any of these parameters were observed between genotype groups (p>0.1 for all, Mann-Whitney).

3.4.8 Immune activation among HIV+ subjects

In HIV+ women, expression of CD69, HLA-DR and CD38 did not differ between *GNB3* genotype groups on either CD4+ or CD8+ T cells, before or after adjustment for CD4

count (p>0.1 for all, Mann-Whitny; p>0.1 for all, ANCOVA (Analysis of Co-Variance) with CD4 count as covariate) (Figure 3.6A, B). Comparison of HLA-DR expression between genotypes was replicated in 4 cross-sectional studies, and CD38 expression was assessed in 3 replicate studies. Additionally, we compared the expression of IL-7Rα (CD127) and Fas (CD95), both known correlates of HIV-1 disease progression [21, 22], between genotype groups. Expression of both markers did not differ between GNB3 genotypes, either before or after adjustment for CD4 count (p>0.1 for all, Mann-Whitney and ANCOVA) (Figure 3.6A, B). Finally, the proportion of Tregs expressed as a percentage of CD3+ cells was also similar between genotype groups (p=0.91, Mann-Whitney) (Figure 3.6A).

3.4.9 Plasma chemokine expression

To complement the cell surface marker data, we assessed plasma concentrations of three cytokines/chemokines of interest: SDF-1α, MIP-1β and TRAIL. Given that 825TT patients are known to exhibit enhanced SDF-1α-mediated chemotaxis, we wondered whether plasma chemokine levels might vary between *GNB3* genotype during infection. Additionally, some evidence points to lower levels of lymphocyte apoptosis in 825TT patients, leading us to assess plasma levels of the cleaved form of TNF-related apoptosis-inducing ligand (TRAIL, CD253). There were no significant differences in plasma TRAIL, SDF-1α or MIP-1β levels between CC/CT and TT genotypes (Mann-Whitney, p=0.31, p=0.14 and p=0.88 respectively, Mann-Whitney) (Figure 3.7). Subgroup analysis based on ARV treatment status did not reveal any further differences in protein concentration between genotypes.
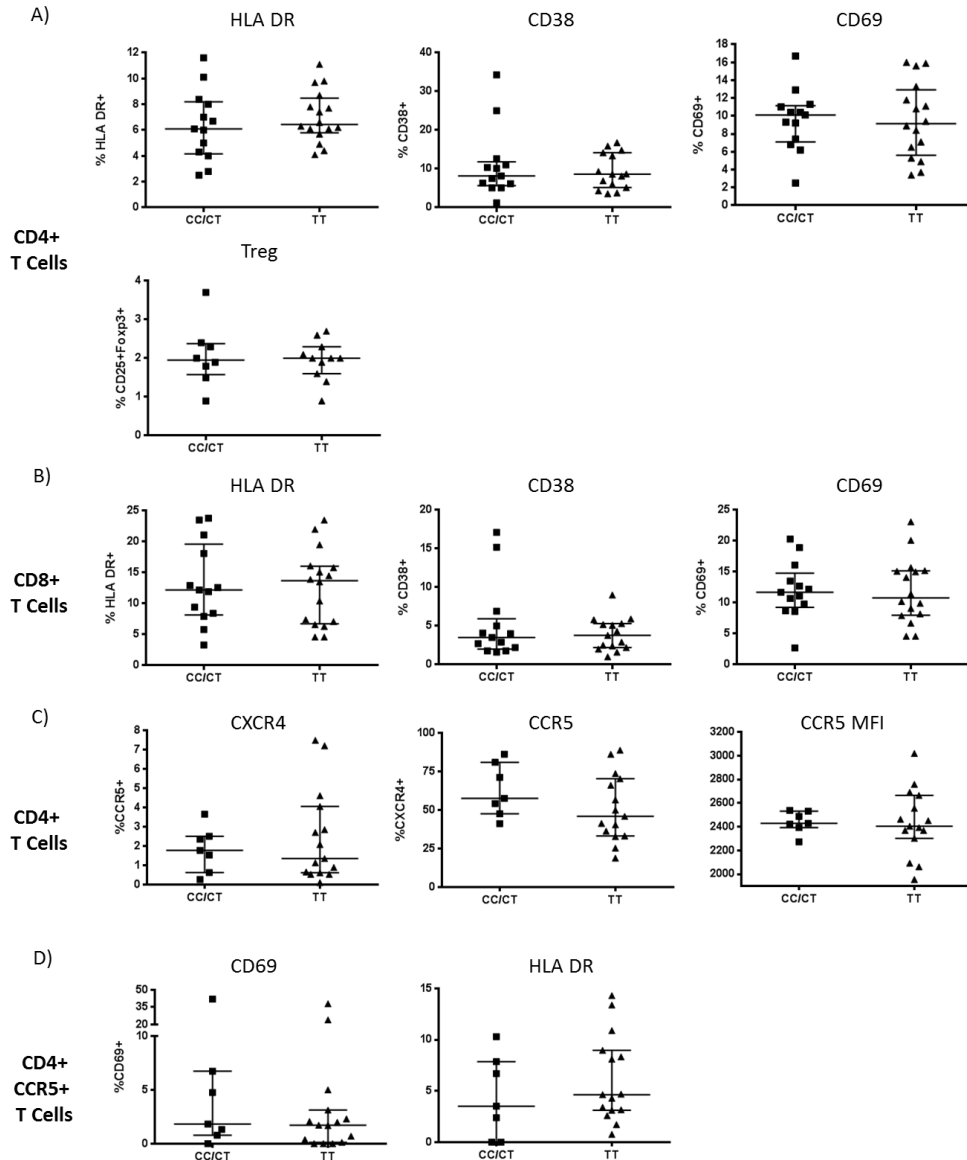
Figure 3.5 Expression of *ex vivo* cell surface markers measured by flow cytometry among HIV-1-negative subjects. (A) Expression of CD69, HLA-DR, CD38 and regulatory T cells (Tregs; defined as CD3+CD4+CD25+FOXP3+) among HIV-1-negative FSW cohort subjects. Values are expressed as a percentage of the parental CD4+ or CD8+ T cell population. CD38 and HLA-DR plots are representative of two distinct studies. There were no significant differences in expression levels between *GNB3 825CC/CT* and *825TT* groups. **(B)** Expression of HIV-1 co-receptors CCR5 and CXCR4 expressed as a percentage of the parental CD4+ T cell population. There were no significant differences in expression levels or CCR5 median fluorescence intensity (MFI) between *GNB3 825CC/CT* and *825TT* groups. **(C)** Expression of activation markers CD69 and HLA DR on CD4+CCR5+ T cells. There were no significant differences in expression levels between *GNB3 825CC/CT* and *825TT* groups. Median and interquartile range are shown for all plots.
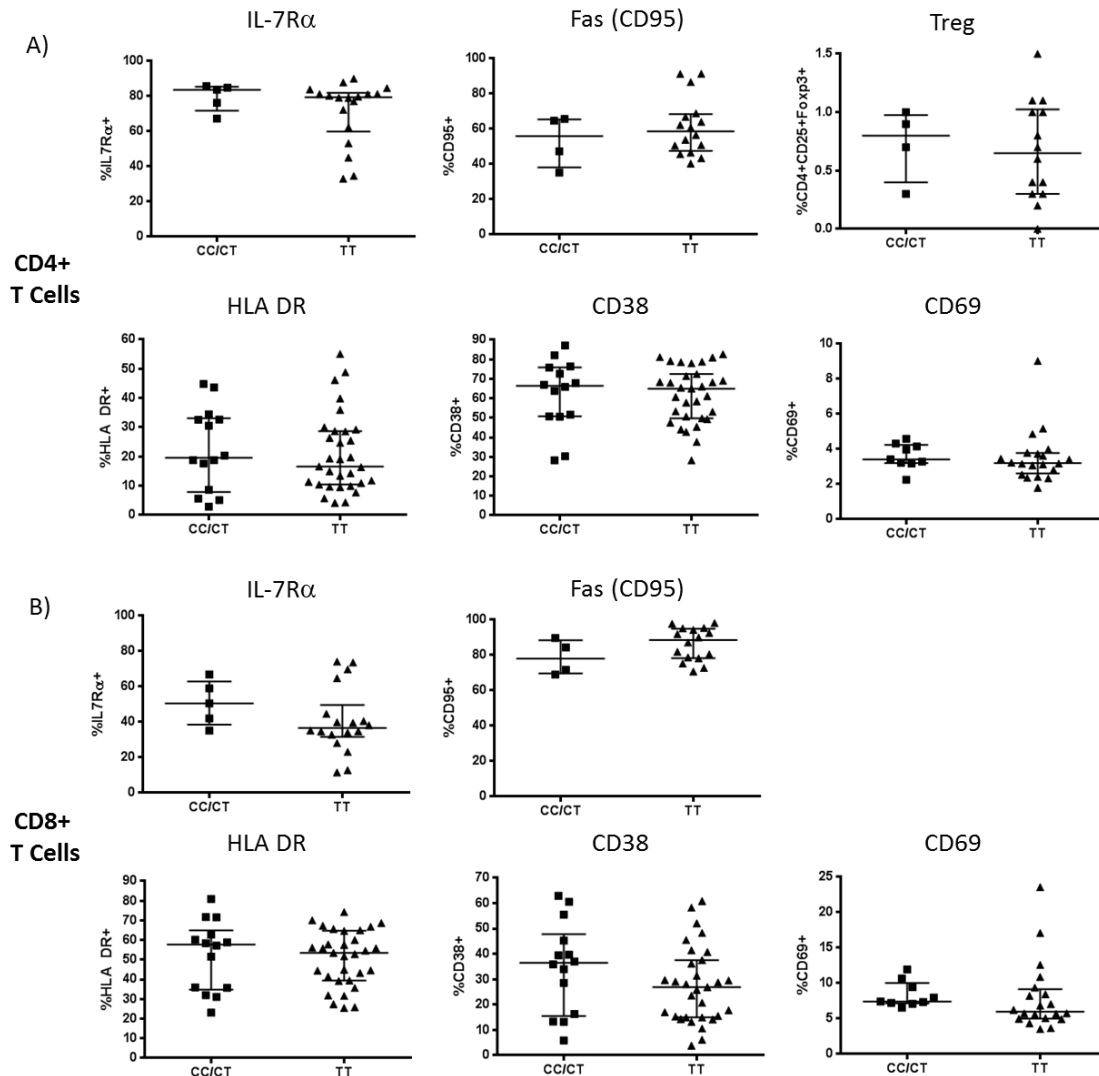
Figure 3.6 Expression of *ex vivo* cell surface markers among HIV+ subjects.
Expression of IL-7Rα (n=5 CC/CT, 18 TT), Fas (n=5 CC/CT, 18 TT), Treg (n=5 CC/CT, 18 TT), CD69 (n=9 CC/CT, 20 TT), HLA-DR (n=14 CC/CT, 31 TT), and CD38 (n=14 CC/CT, 31 TT) was among HIV+ FSW cohort participants. Values are expressed as a percentage of the parental **(A)** CD4+ or **(B)** CD8+ T cell population, as indicated, except Tregs, which are presented as % of CD3+ cells. Median and interquartile range are shown. There were no significant differences in expression levels between *GNB3 825CC/CT* and *825TT* groups.

93
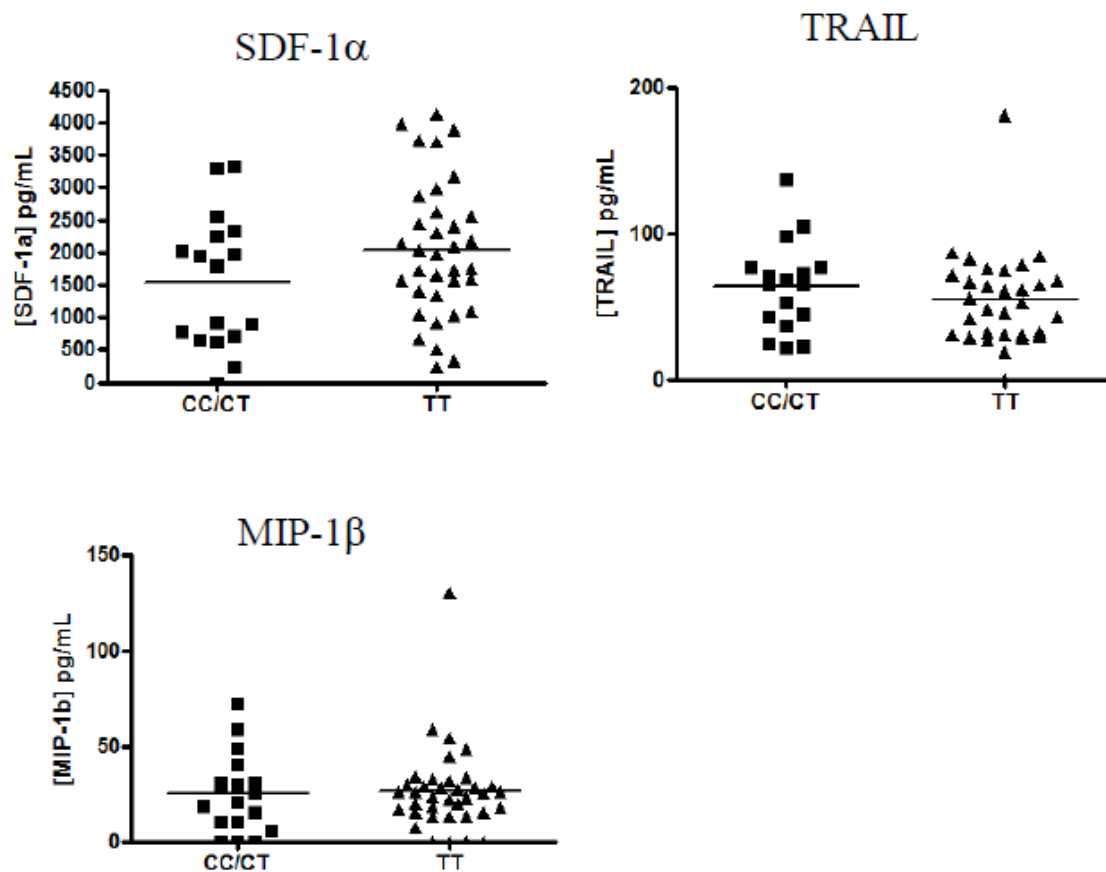
Figure 3.7 Quantification of plasma cytokine/chemokine levels between HIV+ participants with differing *GNB3* genotypes. Plasma SDF-1α, MIP-1β and TRAIL concentrations were quantified by Milliplex bead assay among HIV+ women of the FSW cohort. No significant differences in concentration between *GNB3 825CC/CT* and *825TT* groups.

3.5 Summary

This study aimed to determine whether *GNB3 825* genotype is associated with altered risk of HIV acquisition/disease progression, response to ART or peripheral blood immune activation in two Kenyan cohorts. *GNB3* genotype had no impact on the risk of HIV acquisition in either cohort, nor did it affect the rate of disease progression. CD4 recovery following initiation of ART was similar between genotype groups. Immune activation levels did not differ based on *GNB3* genotype. Overall, there was no significant impact of *GNB3* genotype on any of the epidemiological or biological parameters analysed, thereby refuting the hypothesis.

4. Impact of *GNB3 825* Genotype on RNA splicing and immune activation

4.1 Rationale

Despite the numerous studies reporting epidemiological associations between *GNB3 825* genotype and disease susceptibility and immune function, the mechanism of action of the *825T* allele remains controversial (166). Although the *C825T* SNP is a silent mutation, it is found in strong linkage disequilibrium with additional intronic *GNB3* SNPs that, together, are predicted to promote alternative mRNA splicing and the generation of two splice variants, Gb3s and Gb3s2 (160, 163). Given the lack of evidence demonstrating Gβ3s and Gβ3s2 protein expression (168), assessment of the functional impact of the *825T* allele is generally determined at the mRNA level. To confirm that the *GNB3 825TT* genotype is associated with splice variant production, we aimed to confirm GNB3 RNA splicing at previously described loci in PBMC from FSW cohort participants.

4.2 Hypothesis

Cohort participants with the *GNB3 825TT* genotype exhibit *GNB3* RNA splicing characteristic of the Gb3s and Gb3s2 transcripts, but exhibit normal expression of other genes at the *GNB3* locus.

4.3 Objectives

1. Quantify exon-by-exon RNA expression of *GNB3* and neighbouring genes (*LAG-3, CD4, etc.*) using RNA exon microarrays and compare between *GNB3* genotypes.

4.4 Results

4.4.1 GNB3 exon array mRNA expression

To confirm whether the presence of the *GNB3 825TT* genotype was associated with

mRNA splicing as described by Siffert *et al* (163, 164) in the FSW cohort, we took

advantage of exon microarray technology. Unlike conventional RNA microarrays, which

use probesets targeting the 3' end of RNA transcripts to detect total transcript levels,

exon microarrays contain probesets targeting multiple intronic and exonic sequences

within each RNA transcript. The Affymetrix GeneChip Human Exon 1.0 ST Array

included probesets located within the deletions described for both Gb3s and Gb3s2, and

should, therefore, be able to detect splicing events in *GNB3 825TT* individuals.

It is important to note that the extremely large number of statistical comparisons

performed when comparing the expression of multiple probes for thousands of genes

requires sophisticated statistical analysis to adjust the p values appropriately for inflated

type I error. Because the analysis of the exon array samples for this study was a sub-study

nested within the design of the main array analysis, p values are not presented for the

exon array data. Instead, p values unaffected by multiple comparisons are presented for

the qRT-PCR confirmation of specific RNA expression patterns for individual genes.

PBMC RNA was isolated from 46 FSW cohort participants, including 23 HIV-N (2

825CC, 3 825CT and 18 TT) and 23 HIV+ (5 825CC, 7 CT and 11 TT) women. *GNB3*

transcript expression levels were similar between 825CC and 825TT genotype groups

(Figure 4.1). In particular, RNA expression detected by probesets located in the Gb3s/s2

deletion sequences was virtually identical between *GNB3* genotypes (Figure 4.1, indicated by arrows). Based on the exon array results, there was no evidence to suggest the occurrence of Gb3s/s2 splicing among *GNB3 825TT* participant PBMCs.

4.4.2 Expression of genes at the GNB3-CD4 locus

Because the exon microarray data also contained expression data for genes surrounding the *CD4-GNB3* genetic locus, we investigated whether *GNB3* genotype was associated with differential expression or splicing of any other neighbouring genes. Genes located on chromosome 12p13 near *GNB3/CD4* include *G protein coupled receptor 162 (GPR162), leprecan-like 2 (LEPREL2), cell division cycle associated 3 (CDCA3), parathymosin (PTMS), lymphocyte activation gene 3 (LAG-3, CD223)* and *myeloid leukemia factor 2 (MLF2)* (Figure 4.2A). There were no consistent differences in expression and splicing of *CDCA3, LEPREL2, GPR162, PTMS* or *MLF2* in probesets covering known splicing regions (Figure 4.2B-D, Figure 4.3A-C).
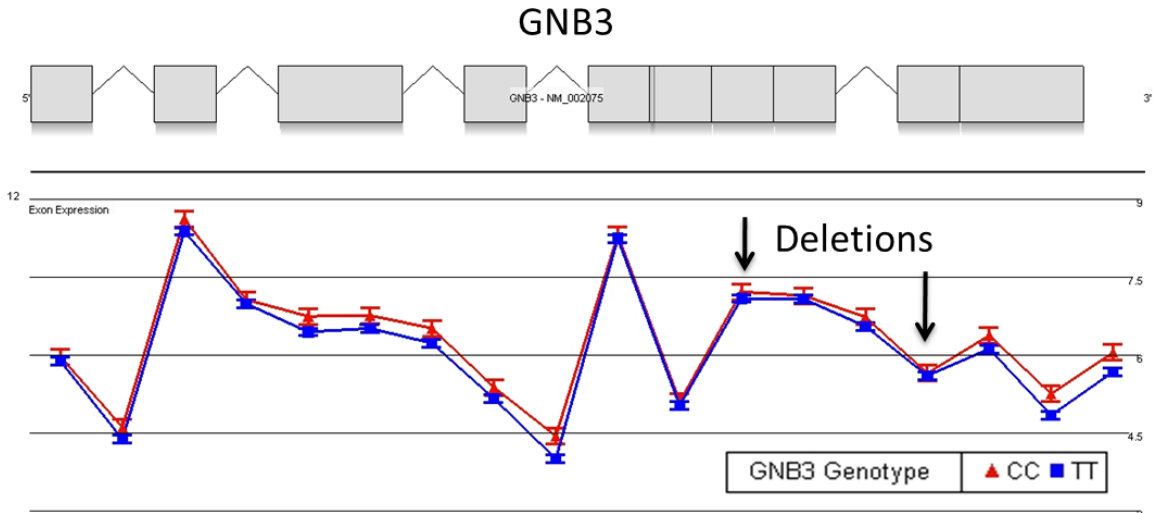
Figure 4.1 GNB3 RNA transcript expression in FSW cohort participants. GNB3 expression levels were similar between *GNB3 825CC* (n=7) and *85TT* (n=29) genotype groups. Probesets located within sequences previously reported to be deleted during Gb3s/s2 splicing are indicated by arrows.
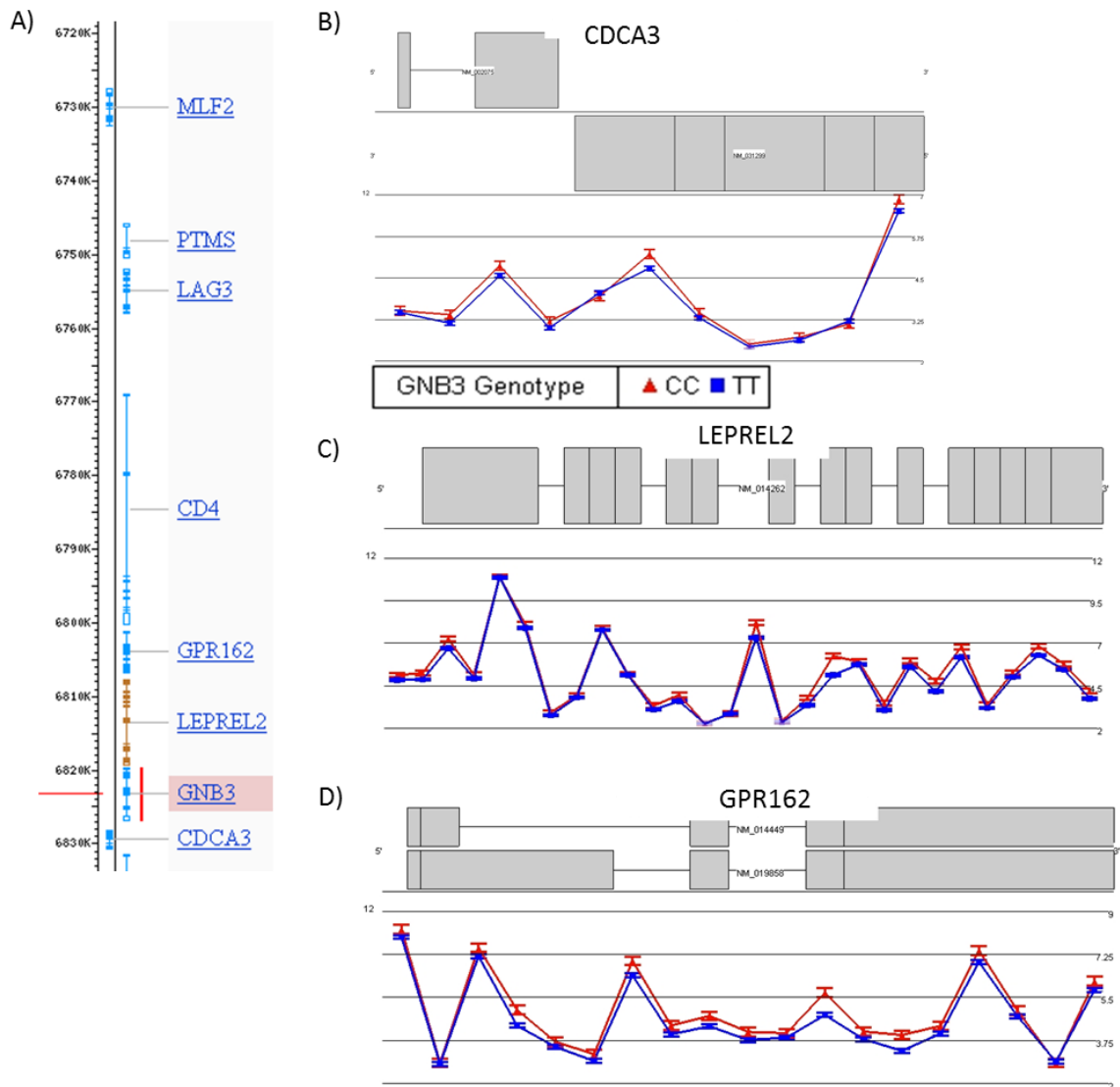
Figure 4.2 RNA expression of genes at the CD4/GNB3 locus. (A) Genes located near GNB3 and CD4 on chromosome 12p13 include cell division cycle associated 3 (CDCA3), leprecan-like 2 (LEPREL2), G protein coupled receptor 162 (GPR162), lymphocyte activation gene 3 (LAG-3, CD223), parathymosin (PTMS), and myeloid leukemia factor 2 (MLF2). Map obtained from NCBI gene database Map Viewer (http://www.ncbi.nlm.nih.gov/gene). Expression of **(B)** CDCA3, **(C)** LEPREL2, and **(D)** GPR162 were similar between GNB3 825CC (n=7, red) and 825TT (n=29, blue) groups. Exons are depicted as grey blocks, while introns are contained in the intervening spaces.

100
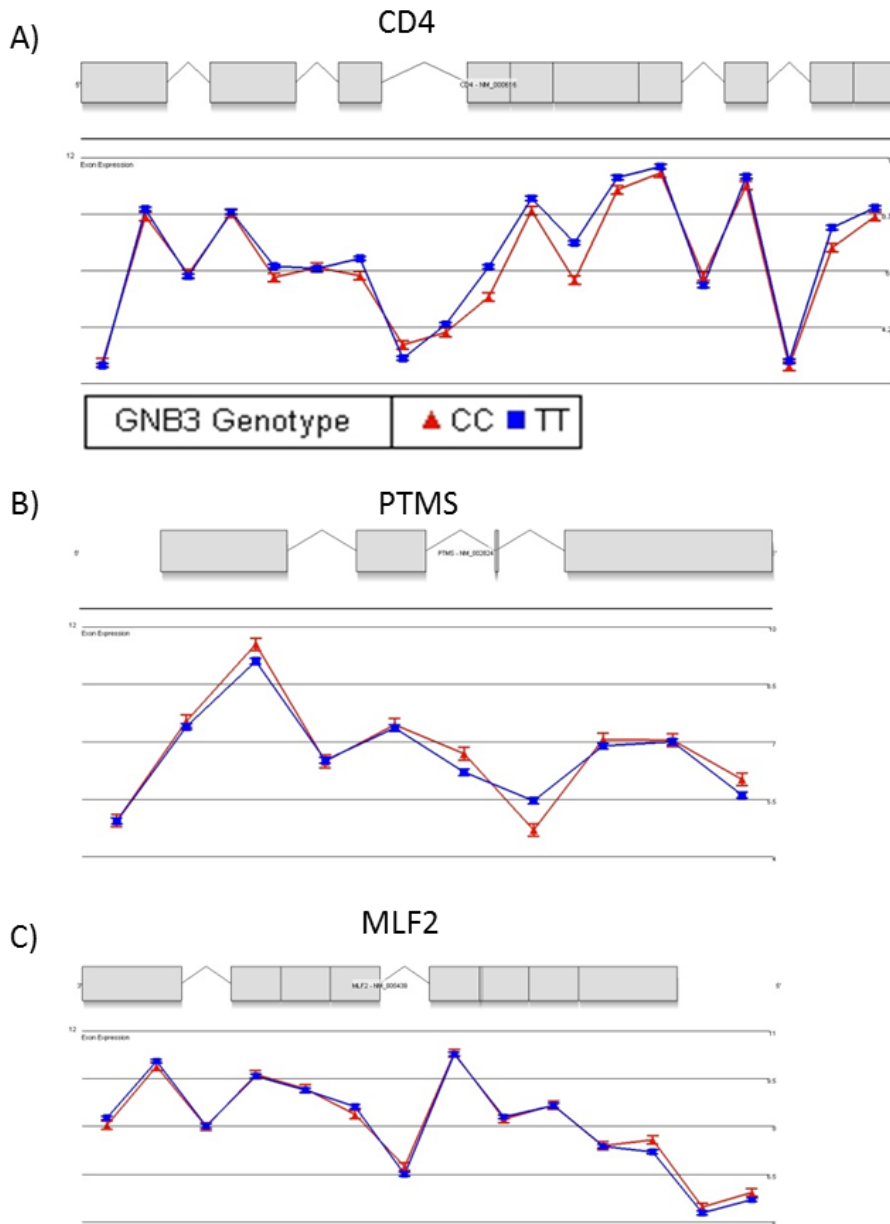
Figure 4.3 RNA expression of genes at the *CD4/GNB3* locus. Expression of **(A)** *CD4*, **(B)** *parathymosin (PTMS)*, and **(C)** *myeloid leukemia factor 2 (MLF2)* were similar between *GNB3 825CC* (n=7, red) and *825TT* (n=29, blue) groups.

4.4.3 LAG-3 exon array mRNA expression

Unlike other genes at the _GNB3/CD4_ locus, _LAG-3_ 3' exon expression appeared to differ

between _GNB3 825CC_ and _825TT_ groups (Figure 4.4A). Indeed, when the probesets

were restricted to exonic sequences and all 3 _GNB3_ genotype groups included, there

appeared to be a dose-dependent effect of the _825T_ allele on 3' LAG-3 exon expression

(Figure 4.4B).

This expression pattern was maintained when analysis was restricted to HIV+

participants only (Figure 4.5A), and, furthermore, 3' LAG-3 exon expression appeared to

be higher among HIV+ participants compared to HIV-N participants (Figure 4.5B).

Differential expression of the 3' portion of the LAG-3 transcript is biologically plausible,

as LAG-3 is known to be expressed in both a full-length cell surface bound form, as well

as several truncated, soluble forms (Figure 4.6). Furthermore, linkage between the _GNB3_

_825_ SNP and polymorphisms in _LAG-3_ that could regulate LAG-3 splicing are possible.

According to the NCBI SNP database for _LAG-3_, the intron between exons 4 and 5

contains 12 SNPs, and the intron between exons 3 and 4 contains 24 SNPs and

insertions/deletions. There are no nonsense mutations currently identified in exons 3 or 4

that would result in a truncated protein product. To confirm the exon array results, the

expression of LAG-3 exon 2/3 and exon 6 was compared between genotype groups

relative to 18S RNA expression by qRT-PCR. While exon 2/3 expression was similar

between _GNB3 825CC_ (n=5) and _825TT_ (n=6) groups (p=0.424, Mann-Whitney), exon 6

expression was significantly higher among _825CC_ individuals (p=0.030, Mann-Whitney)

(Figure 4.6).
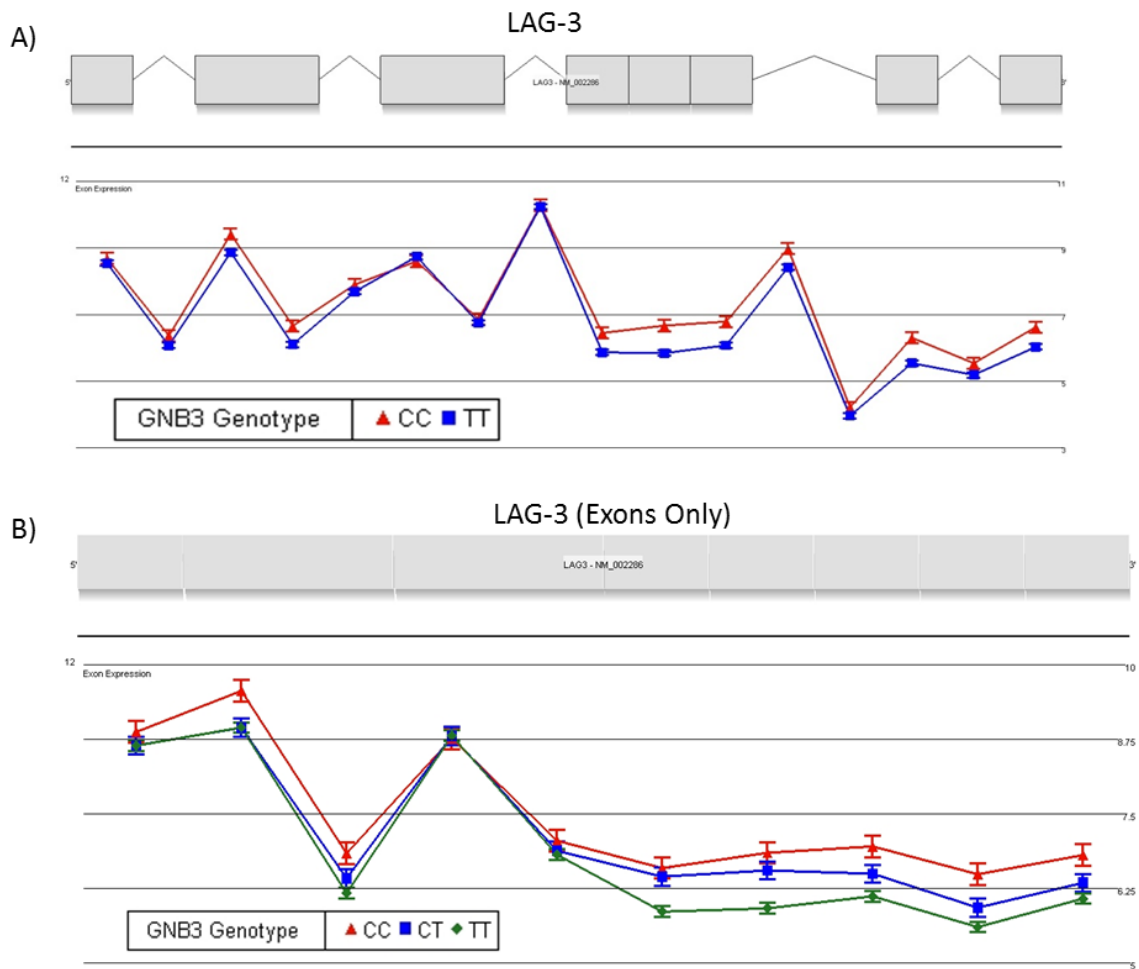
Figure 4.4 Expression of lymphocyte activation gene 3 (LAG-3) RNA between *GNB3* genotype groups. (A) *GNB3* genotype appeared to influence the expression of the 3' end of the LAG-3 RNA transcript (n=7 *GNB3 825CC*, red; n=29 *GNB3 825TT,* blue). **(B)** Restricting analysis to the probsets specific to exonic sequences of the LAG-3 transcript revealed differential expression of the 3' exons across *GNB3 825CC* (n=7, red), *GNB3 825CT* (n=10, blue) and *GNB3 825TT* (n=29, green) groups.
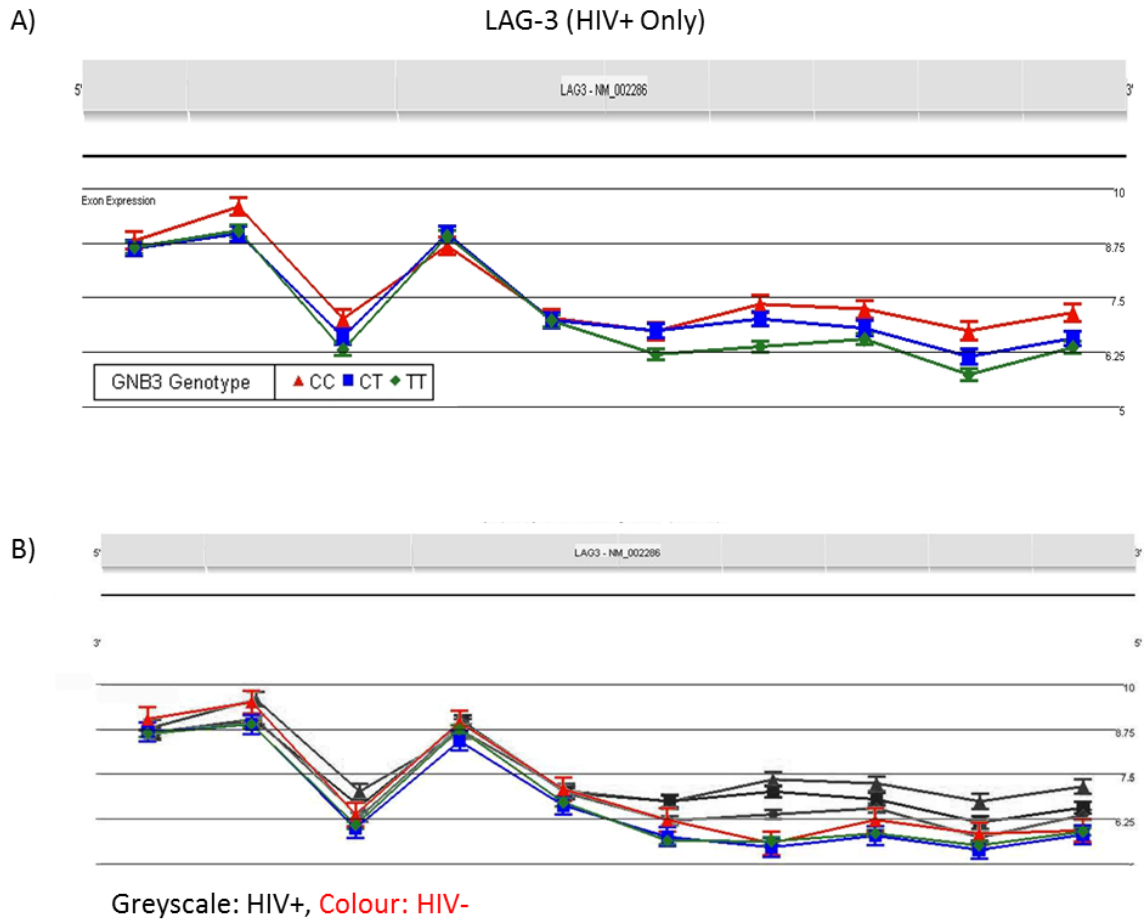
Figure 4.5 LAG-3 transcript expression and HIV status. (**A**) Among only HIV+ participants, differences remained in LAG-3 transcript expression between *GNB3* genotype groups (n=5 *GNB3 825CC*, red; n=7 *GNB3 825CT*, blue; n=11 *GNB3 825TT*, green). (**B**) Compared to HIV-N participants (red, blue and green lines, n=23), HIV+ participants (greyscale lines, n=23) generally exhibited increased expression of 3' LAG-3 exons.
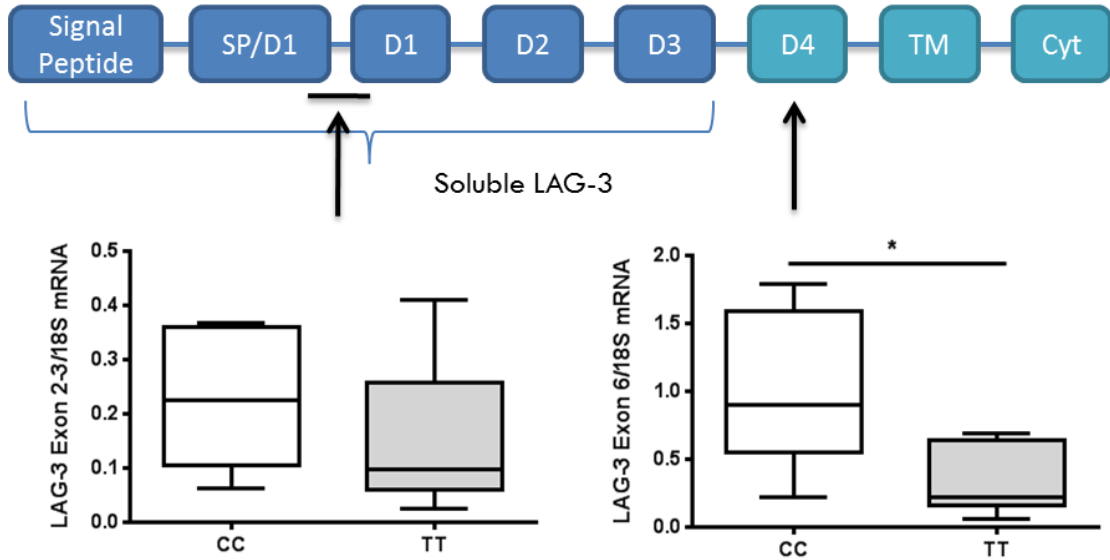
Figure 4.6 qRT-PCR validation of LAG-3 transcript expression. qRT-PCR quantification of LAG-3 mRNA expression revealed similar levels of exon 2/3 expression between *GNB3 825CC* (n=5) and *GNB3 825TT* (n=6) groups (p=0.424, Mann-Whitney), but significantly higher expression of exon 6 among *GNB3 825CC* participants (p=0.030, Mann-Whitney). LAG-3 mRNA expression for each individual was normalized to 18S mRNA levels.

4.5 Summary

Contrary to the hypothesis, splicing events in the regions corresponding to Gb3s and Gb3s2 were not detected among *GNB3 825TT* genotype participants. This observation is consistent with the lack of epidemiological association between *GNB3* genotype and HIV acquisition and progression described in Section 3. Although the splicing and expression of the majority of genes surrounding the *GNB3* locus were similar between *GNB3* genotype groups, LAG-3 splicing differed between *GNB3 825CC, CT* and *TT* individuals, as well as between HIV serostatus groups. The differences in LAG-3 splicing were confirmed by qRT-PCR. Given the potential modulation of LAG-3 expression during HIV infection, assessment of LAG-3 expression on lymphocyte subsets was carried out in Chapter 5. Overall, there was no evidence to suggest that the *GNB3 825T* allele is associated with the production of Gb3s and Gb3s2 splice variants previously reported by Siffert *et al*.

5. Expression of LAG-3 during HIV infection

5.1 Rationale

Given that LAG-3 mRNA was found to be differentially expressed between HIV-N and

HIV+ participants of the FSW cohort, we aimed to confirm whether LAG-3 protein

expression was similarly increased during chronic HIV infection. Although very little

published data was available describing the expression of LAG-3 during HIV infection,

LAG-3 has previously been shown to be expressed on activated T cells and NK cells, as

well as invariant NKT subsets. Furthermore, the extracellular domains of LAG-3 can be

secreted as soluble LAG-3 (sLAG-3) and quantified in human plasma. As LAG-3 was

reported to play an important role in mediating immune exhaustion during chronic

LCMV infection in mice, it was possible that LAG-3 was upregulated during chronic

HIV infection in a manner similar to that reported for the T cell exhaustion markers PD-1

and Tim-3. We therefore sought to determine the relative expression of sLAG-3 in

plasma and surface LAG-3 on T cell, NK cell and iNKT cell subsets among healthy and

HIV-infected FSW cohort participants.

5.2 Hypothesis

HIV infection is associated with elevated lymphocyte LAG-3 expression due to chronic

immune activation, and decreased sLAG-3 expression due to loss of CD4+ T cells. ART

restores total LAG-3 expression to levels characteristic of HIV-uninfected women.

5.3 Objectives

1. Quantify LAG-3 expression on CD4+ and CD8+ T cells, CD56^{hi}CD16$^-$, CD56^{dim}CD16$^+$ and CD56$^-$CD16$^+$ NK cells, and CD4+, CD8+ and double negative (CD4-CD8-) iNKT cells of HIV+ and healthy participants of the FSW cohort.

2. Quantify sLAG-3 expression in plasma among HIV+ and healthy cohort participants.

3. Correlate surface LAG-3 and sLAG-3 expression with CD4 count, T cell activation and plasma cytokine/chemokine expression among HIV+ participants.

5.4 Results

5.4.1 Study Populations

To broadly determine which lymphocyte subsets expressed LAG-3 among healthy and HIV-infected individuals, PBMC samples were collected from 90 participants of the FSW cohort for *ex vivo* phenotyping. 10 HIV-N, 40 HIV+ ART naïve and 40 HIV+ ART-experienced women were recruited for this study (Table 5.1). A subsequent, smaller study recruited 35 women to follow up on the observations of the first screening study and to investigate the function of LAG-3 on iNKT cells during HIV infection (iNKT function study). PBMC samples were collected from 17 HIV-N, 9 HIV+ ART naïve and 17 HIV+ ART-experienced women (Table 5.2). Analysis of a subset of these data is described in this chapter (sections 5.4.3.3 – 5.4.3.5), while the bulk of the assays performed on these samples are described in Chapters 6 and 7.

Table 5.1 Characteristics of subjects included in the *ex vivo* LAG-3 screening study.

	HIV-N	HIV+ ART Naïve	HIV+ ART Experienced	p Value[**]
Age, years[*]	31.5 (28.75, 41)	37 (32.5, 41)	40 (34, 45.25)	0.164
Duration of sex work, years[*]	9 (5.25, 13.5)	7 (5, 14)	11.5 (5, 19)	0.552
CD4 Count[*]	--	428 (369.3, 632.3)	354 (245, 481)	**0.011**
Duration of ART, years[*]	--	--	2.14 (1.16, 3.64)	--

[*]Data are presented as median (IQR)
[**] Groups were compared by Kruskal-Wallis test (age, duration of sex work) or Mann-Whitney test (CD4 count)

Table 5.2 Characteristics of subjects included in the iNKT function study.

	HIV-N	HIV+ ART Naïve	HIV+ ART Experienced	p Value[**]
Age, years[*]	40 (34, 44.5)	35 (29, 41)	40 (34.5, 44)	0.522
Duration of sex work, years[*]	10 (6.5, 12)	9 (5, 14)	11 (8, 20)	0.324
CD4 Count[*]	--	475.5 (321, 618)	526.5 (407, 698)	0.297
Duration of ART, years[*]	--	--	3 (3, 5.5)	--

[*]Data are presented as median (IQR)
[**] Groups were compared by Kruskal-Wallis test (age, duration of sex work) or Mann-Whitney test (CD4 count)

5.4.2 Quantification of surface LAG-3 expression

LAG-3 expression was assessed simultaneously on multiple lymphocyte subsets including conventional T cells (CD4+ and CD8+), iNKT cells (CD3+6B11+) and NK cells (CD56^{hi}CD16^{-}, CD56^{dim}CD16^{+} and CD56^{-}CD16^{+}). The gating strategy for each subset is shown in Figure 5.1. The monoclonal antibody 17B4 was used throughout this thesis for the detection of surface LAG-3 expression. The generation and specificity of this antibody has been described in the literature (388, 445), and this clone is the most widely used antibody in studies of LAG-3 expression by flow cytometry. For the remainder of the thesis, cell surface-associated LAG-3 expression will be referred to as LAG-3, and soluble LAG-3 will be referred to exclusively as sLAG-3.

5.4.3 Ex vivo LAG-3 expression on T lymphocytes

5.4.3.1 LAG-3 expression on CD4+ and CD8+ T cells

LAG-3 was expressed at very low levels on both CD4+ and CD8+ T cells among all participants in the study (Figure 5.2A) (n=10 HIV-N, 35 HIV+, 36 HIV+ ART). Despite the low levels of expression, HIV+ ART experienced participants demonstrated significantly higher levels of LAG-3 expression compared to healthy controls (p=0.0170 for CD4, Kruskal-Wallis, Dunn's post-test p<0.05 for HIV+ ART versus HIV-N; p=0.0183 for CD8, post-test p<0.05 for HIV+ ART versus HIV-) (Figure 5.2B, Table 5.3). Analysis of CD4+ and CD8+ T cell LAG-3 expression within each individual revealed significantly greater LAG-3 expression on the CD8+ T cell subset (p=0.0195 for HIV-N, p<0.0001 for HIV+, p<0.0001 for HIV+ ART, Wilcoxon test) (Figure 5.2C).

Viral load determination is not performed as the standard of care in Kenya. Instead, CD4 count and CD8+ T cell activation (measured by HLA DR expression) were used as surrogates of disease progression. LAG-3 expression on CD4+ T cells did not correlate with CD4 count among either group of HIV+ participants (r=-0.0809, p=0.5058 for all HIV+; r=0.0647, p=0.7163 for HIV+ ART naïve; r=-0.0434, p=0.8015 for HIV+ ART experienced, Spearman) (Figure 5.3A). Similarly, CD8+ T cell LAG-3 expression was unrelated to CD4 count (r=0.0302, p=0.8043 for all HIV+; r=0.1728, p=0.3284 for HIV+ ART naïve; r=0.0177, p=0.9183 for HIV+ ART experienced, Spearman) (Figure 5.3A).

In addition to CD8+ T cell activation being an indicator of disease progression, LAG-3 is reported to be expressed primarily on activated T cells. We therefore assessed the correlation between LAG-3 expression and CD4+ and CD8+ T cell activation (Table 5.4). LAG-3 expression did not correlate with HLA DR expression on any cell subset among any HIV+ groups (p>0.1 for all, Spearman). Notably, LAG-3 expression on both CD4+ and CD8+ T cells significantly correlated with CD69 expression on each subset, respectively (r=0.5598, p=0.0029 for CD4+ T cells; r=0.4016, p=0.0420 for CD8+ T cells, Spearman) (Figure 5.3B).

Table 5.3 Summary of *ex vivo* LAG-3 expression on lymphocyte subsets among HIV-N and HIV+ participants.

Lymphocyte Subset	Median % LAG-3+ (fold change vs HIV-N)			p value[*]	Post-test differences[**]
	HIV-N	HIV+	HIV+ ART		
CD3+CD4+	0.14	0.16 (1.1)	0.225 (1.6)	**0.017**	**HIV-N vs ART**
CD3+CD8+	0.165	0.24 (1.5)	0.34 (2.1)	**0.0183**	**HIV-N vs ART**
CD3-CD56^{hi}CD16-	0.565	1.32 (2.3)	1.695 (3.0)	**0.0134**	**HIV-N vs ART**
CD3-CD56^{dim}CD16+	1.085	1.27 (1.2)	1.79 (1.6)	**0.0368**	**HIV-N vs ART (Mann-Whitney)**
CD3-CD56-CD16+	2.45	2.72 (1.1)	3.32 (1.4)	0.1474	--
CD3+6B11+ (iNKT)	4.195	9.835 (2.3)	11.16 (2.7)	**0.0274**	**HIV-N vs ART**

[*]Groups compared by Kruskal-Wallis test
[**]Post-test p<0.05 by Dunn's post-test, or Mann-Whitney in the event that no Dunn's post-tests were significant, following a significant Kruskal-Wallis test
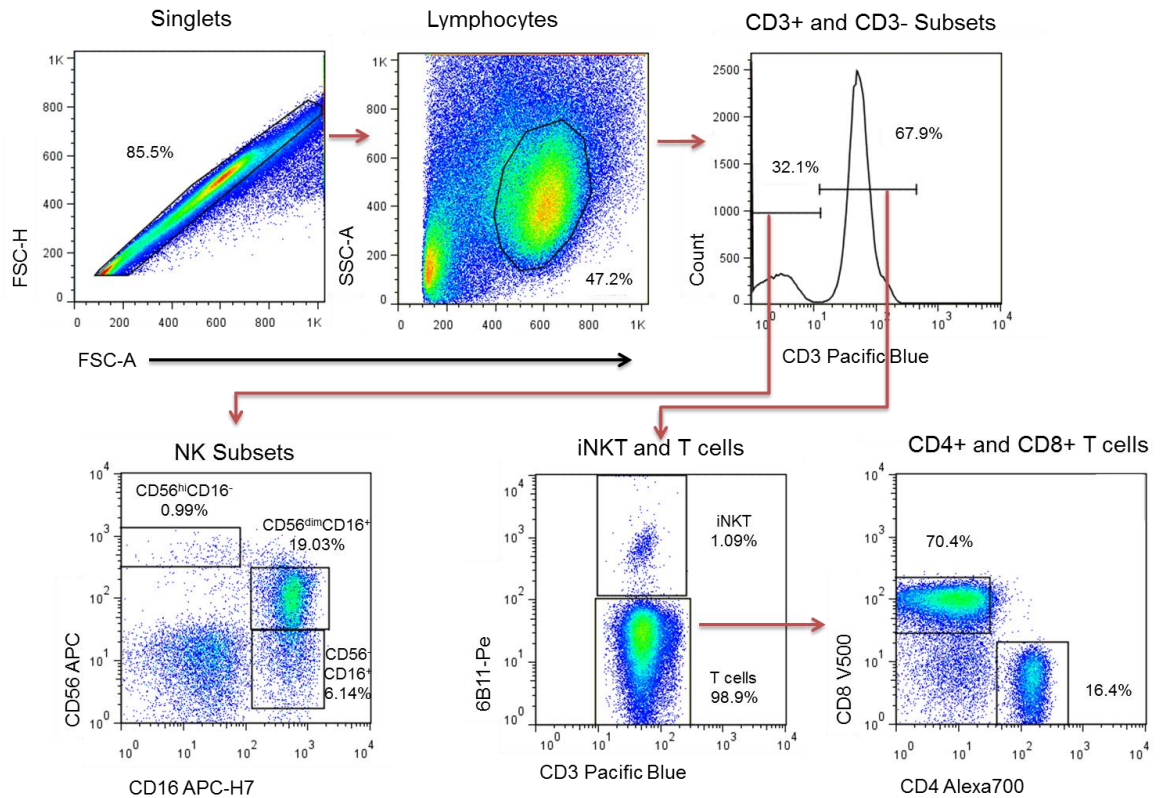
Figure 5.1 Representative ex vivo staining of PBMC samples to identify lymphocyte populations. Singlets were identified by FSC-area (FSC-A) versus FSC-height (FSC-H) gating, followed by lymphocyte gating based on forward and side scatter. CD3+ and CD3- subsets were identified by histogram gating. iNKT cells were identified as CD3+6B11+, while conventional T cells were identified as CD3+6B11- and further subgated based on CD4 and CD8 expression. NK cells were gated as CD56^hiCD16^-, CD56^dimCD16^+ or CD56^-CD16^+ within the CD3- population. Data from ML3290 (HIV+ ART experienced) are shown.
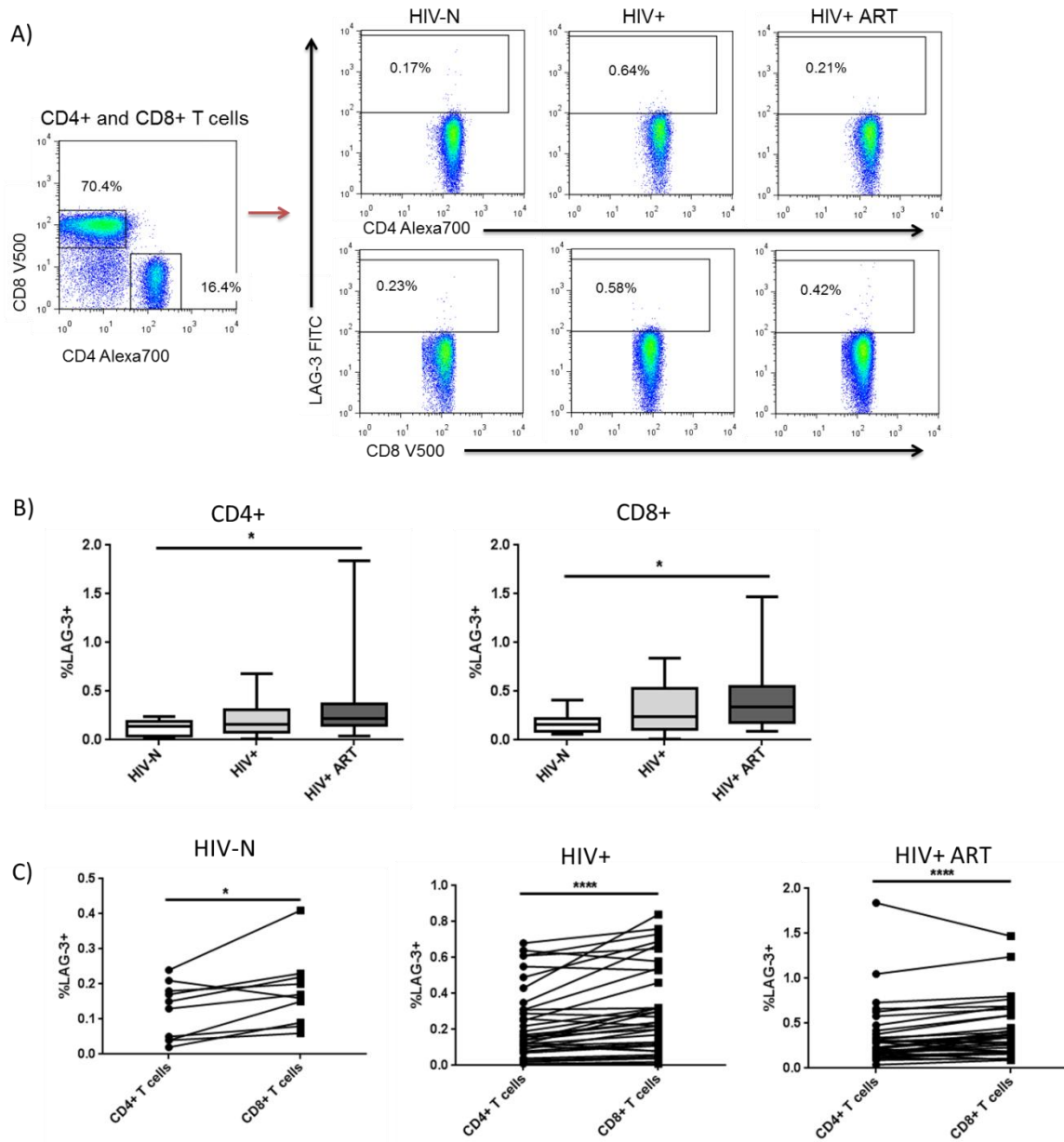
Figure 5.2 Ex vivo LAG-3 expression on CD4+ and CD8+ T cell subsets. (A) Representative staining of LAG-3 on CD4+ and CD8+ T cells from HIV-N (ML3501) , HIV+ (ML2732) and HIV+ ART experienced (ML2680) participants. **(B)** LAG-3 expression was significantly higher on both CD4+ and CD8+ T cells among HIV+ ART participants compared to healthy controls. **(C)** When compared within each individual, LAG-3 expression was significantly higher on CD8+ T cells compared to CD4+ T cells among all participant groups. *p<0.05, ****p<0.0001
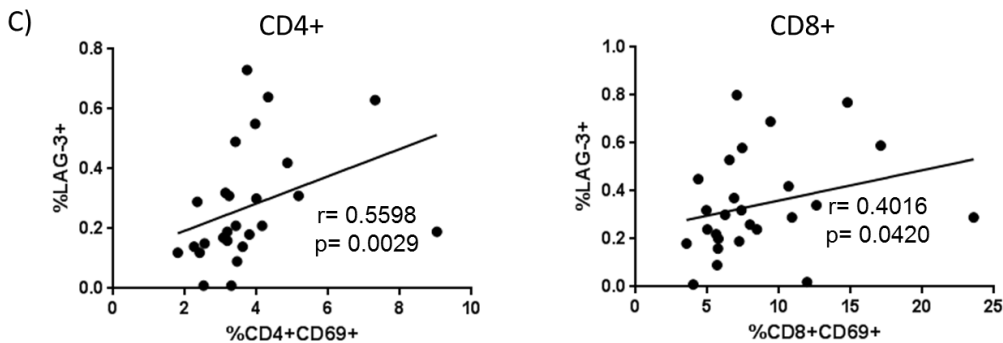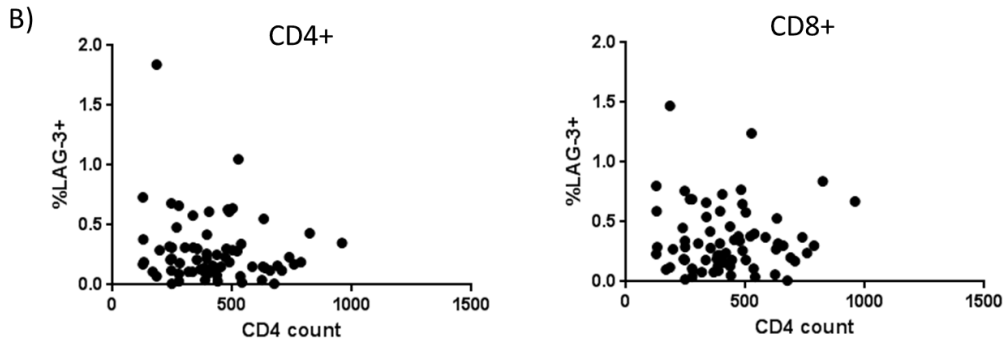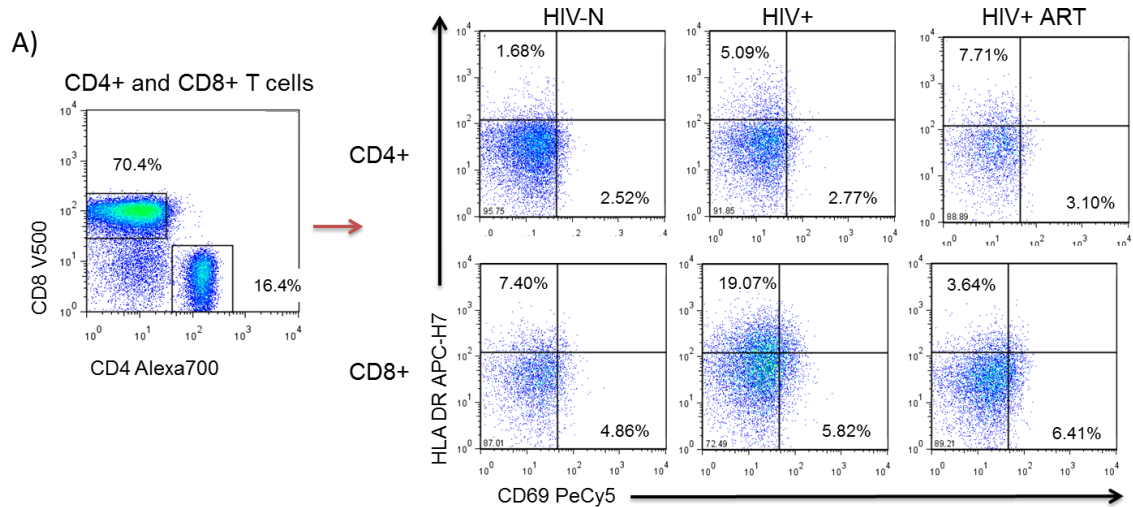
Figure 5.3 Correlates of LAG-3 expression on CD4+ and CD8+ T cells. (A) Representative staining of T cell activation markers HLA DR and CD69 on CD4+ and CD8+ T cell populations. Data are shown from HIV-N (ML3512), HIV+ (ML3215) and HIV+ ART (ML3356) individuals. **(B)** LAG-3 expression on CD4+ and CD8+ T cell subsets did not correlate with CD4 count among HIV+ participants (n=70). **(C)** On both CD4+ and CD8+ T cells, LAG-3 expression significantly correlated with CD69 expression among all HIV+ participants (n=26). Trend line derived from linear regression is shown.

Table 5.4 Correlations between LAG-3 expression and CD4+ and CD8+ T cell activation.

Subset 1	Subset 2	Population	n	Spearman r	p value
%CD4+ LAG-3+	%CD4+HLA DR+	All HIV+	70	0.0631	0.6010
		HIV+	34	-0.0246	0.8882
		HIV+ ART	36	0.1615	0.3466
	%CD8+HLA DR+	All HIV+	70	-0.0962	0.4245
		HIV+	34	-0.0433	0.8049
		HIV+ ART	36	-0.0732	0.6712
	%CD4+CD69+	All HIV+	26	**0.5598**	**0.0029**
		HIV+	12	**0.4982**	**0.1016**
		HIV+ ART	14	0.3789	0.1811
%CD8+ LAG-3+	%CD8+HLA DR+	All HIV+	70	-0.1124	0.3507
		HIV+	34	-0.1006	0.5651
		HIV+ ART	36	-0.0310	0.8576
	%CD8+CD69+	All HIV+	26	**0.4016**	**0.0420**
		HIV+	12	0.3404	0.2770
		HIV+ ART	14	0.4026	0.1535

p values≤0.1 (trend) are indicated in bold.

As described above, the strongest differences in LAG-3 expression on both T cell subsets were observed between healthy controls and HIV+ ART experienced participants. Although viral load data was unavailable to demonstrate viral suppression among the ART group, CD8+ HLA DR expression was significantly decreased among ART recipients compared to the ART naïve group, suggesting a control of immune activation among this population (p=0.0058, post-test p<0.05 for HIV-N versus HIV+, p<0.05 for HIV+ versus HIV+ ART, Kruskal-Wallis) (Figure 5.4A). Despite this, LAG-3 expression did not correlate with duration of ART (r=-0.0348, p=0.8404 for CD4+ LAG-3; r=-0.0043, p=0.9801 for CD8+ LAG-3, Spearman) (Figure 5.4B) nor did it differ among participants with CD4 reconstitution to CD4 counts above or below 350 cells/µL (p=0.5887 for CD4+ LAG-3; p=0.9688 for CD8+ LAG-3, Mann-Whitney) (Figure 5.4C). Finally, LAG-3 was similar between groups when participants were stratified based on CD8+ HLA DR expression above or below the median expression level of the entire ART experienced group (p=0.7815 for CD4+ LAG-3; p=0.8305 for CD8+ LAG-3 expression, Mann-Whitney) (Figure 5.4D).

In summary, LAG-3 was poorly expressed on CD4+ and CD8+ T cells among all participants, despite a statistically significant elevation during HIV infection. LAG-3 expression did not correlate with any measures of disease progression or ART.
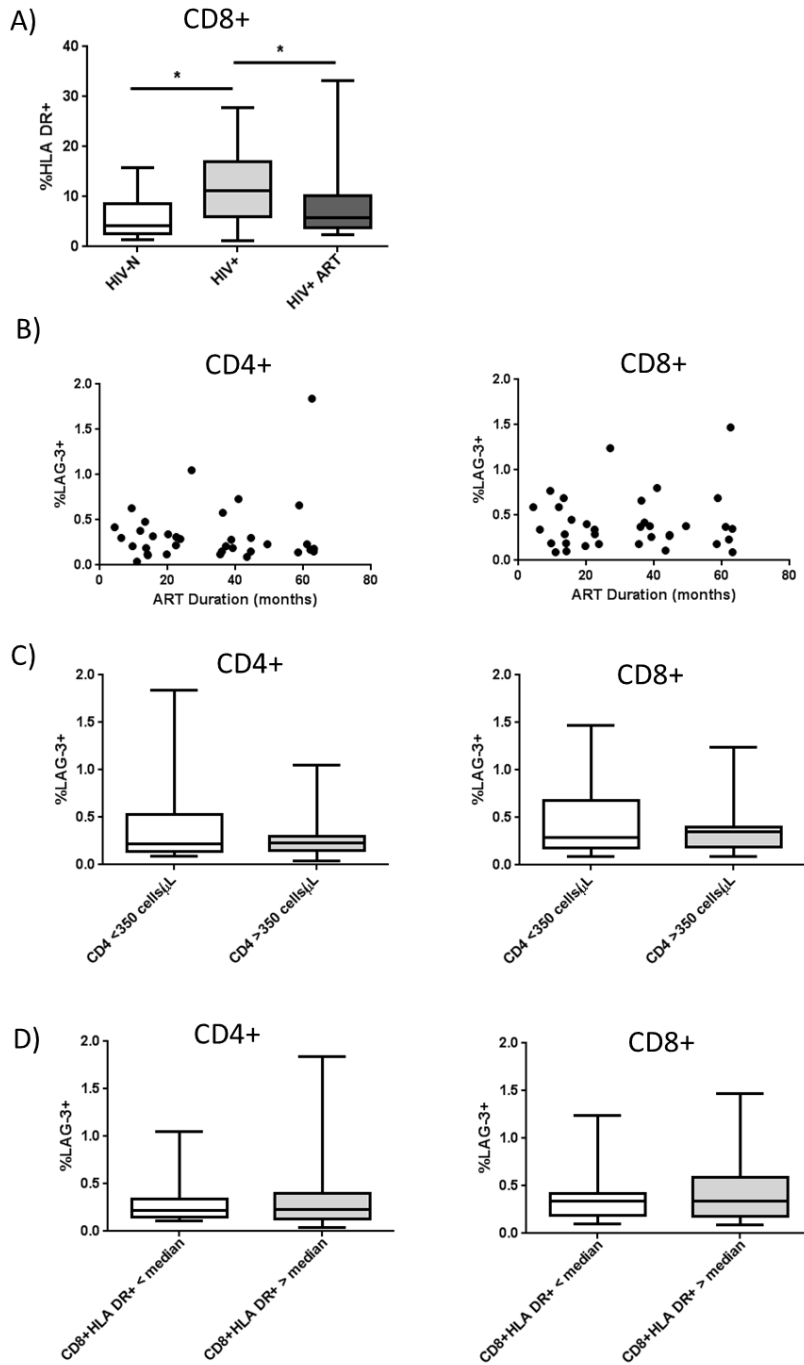
Figure 5.4 Relationship between LAG-3 expression and ART duration and CD4 reconstitution. (**A**) ARV therapy was associated with a significant reduction in CD8+ HLA DR expression compared to HIV+ ART naïve participants. (**B**) ART duration did not correlate with LAG-3 expression on either CD4+ or CD8+ T cells. (**C**) LAG-3 expression among HIV+ ART subjects did not differ when stratified by CD4 count above (n=17) or below (n=19) 350 cells/μL. (**D**) LAG-3 expression was similar between HIV+ ART participants who exhibited higher (n=15) or lower (n=21) than the median %CD8+ HLA DR+. *p<0.05

118

5.4.3.2 Comparison of LAG-3 and PD-1 expression

The PD-1 antibody used in the LAG-3 screening study produced poor signal and was therefore not included in data analysis. Excellent PD-1 staining was generated, however, in the surface panel of the iNKT function study. We therefore compared PD-1 and LAG-3 expression on CD8+ T cells from the 15 HIV-N, 8 HIV+ and 17 HIV+ ART participants of that study. Representative PD-1 staining is shown in Figure 5.5A.

Due to the relatively small sample size, the HIV+ and HIV+ ART groups were combined for most analyses. Both PD-1 and LAG-3 were expressed at higher levels on CD8+ T cells among HIV+ participants compared to healthy controls (p=0.0425 for PD-1, p=0.0475 for LAG-3, Mann-Whitney) (Figure 5.5B, C). LAG-3 expression did not correlate with PD-1 expression on CD8+ T cells (r=0.0077, p=0.9709, Spearman) (Figure 5.5D). CD8+LAG-3+ T cells, however, expressed significantly more PD-1 than the bulk CD8+ T cell population (p<0.0001, Wilcoxon test) (Figure 5.5E, F), indicating that LAG-3 tends to be co-expressed with PD-1 during HIV infection.

5.4.3.3 LAG-3 expression on antigen-specific T cells

Although studies published following the FSW cohort LAG-3 screening study also found low levels of T cell LAG-3 expression during chronic infection on both bulk and HIV-specific T cells (380, 436), we could not rule out an enrichment of LAG-3 expression on HIV-specific CTLs among the FSW cohort. Samples from 7 HIV+ ART-experienced enrollees in the iNKT function study had sufficient cells to perform stimulations with HIV gag peptide pools to identify gag-specific CD8+ T cell responses. Although ARV

119

therapy can suppress antigen-specific responses, robust IFNγ and TNFα responses (>2-fold above background) were detected after 10 hours of stimulation in these participants (Figure 5.6). 5 participants responded to only one of the two gag peptide pools, while 2 participants responded to both pools.

Consistent with the current literature, PD-1 expression on Gag-specific CD8+ T cells (CD8+IFNγ+) was significantly elevated compared to the bulk CD8+ T cell population (p=0.0039, Wilcoxon test) (Figure 5.7A). In contrast, there was no significant difference between LAG-3 expression on CD8+IFNγ+ T cells and bulk CD8+ T cells (p=0.2031, Wilcoxon test) (Figure 5.7B) among the same participants. Furthermore, the simultaneous measurement of both IFNγ and TNFα following peptide stimulation allows for the identification of both dual-positive and single-positive cytokine-expressing cells. When comparing the expression of PD-1 and LAG-3 on double-positive (CD8+IFNγ+TNFα+) versus single-positive (CD8+IFNγ+TNFα-) cells, PD-1 expression was significantly elevated on the CD8+IFNγ+TNFα- subset (p=0.0273, Wilcoxon test) (Figure 5.7C). LAG-3 expression, however, did not significantly differ between single- and double-positive antigen-specific cells (p>0.999, Wilcoxon test) (Figure 5.7D).

In summary, there was no evidence to suggest that LAG-3 expression was enriched on HIV-specific T cells among participants of this cohort. LAG-3 was co-expressed, however, with PD-1 on CD8+ T cells.
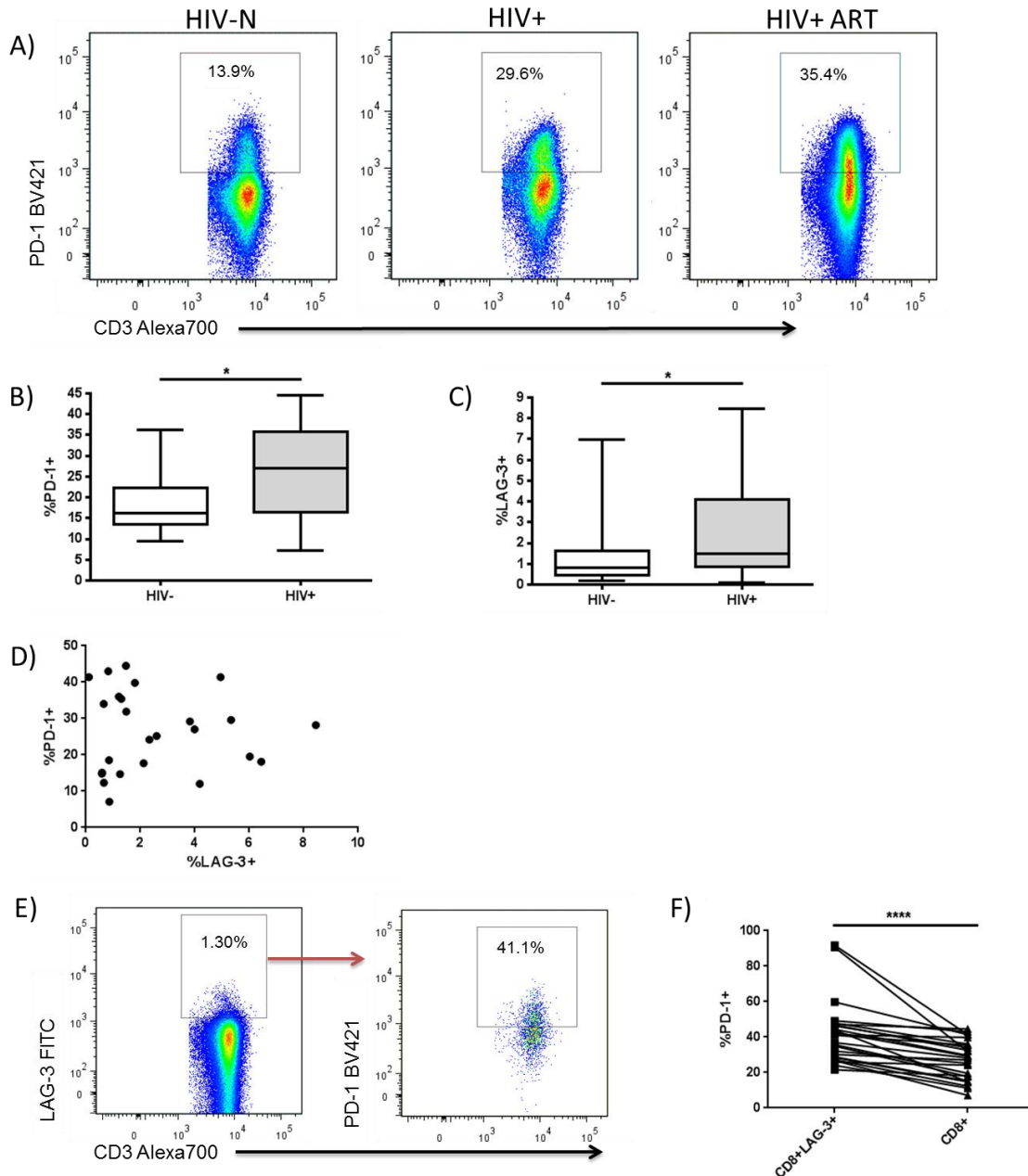
Figure 5.5 Relationship between LAG-3 and PD-1 expression on CD8+ T cells. (A)
Representative staining of PD-1 on CD8+ T cells among HIV-N (ML2505), HIV+
(ML3013) and HIV+ ART (ML2169) participants. **(B)** PD-1 expression is significantly
increased among HIV+ participants compared to healthy controls. **(C)** LAG-3 expression
on CD8+ T cells is significantly increased among HIV+ subjects compared to healthy
controls. **(D)** PD-1 expression does not correlate with LAG-3 expression on CD8+ T
cells. **(E)** Representative staining of LAG-3 on CD8+ T cells, and PD-1 expression on
CD8+LAG-3+ T cells (data shown from ML2169). **(F)** PD-1 expression is significantly
higher among CD8+LAG-3+ T cells compared to bulk CD8+ T cells. *p<0.05,
****p<0.0001
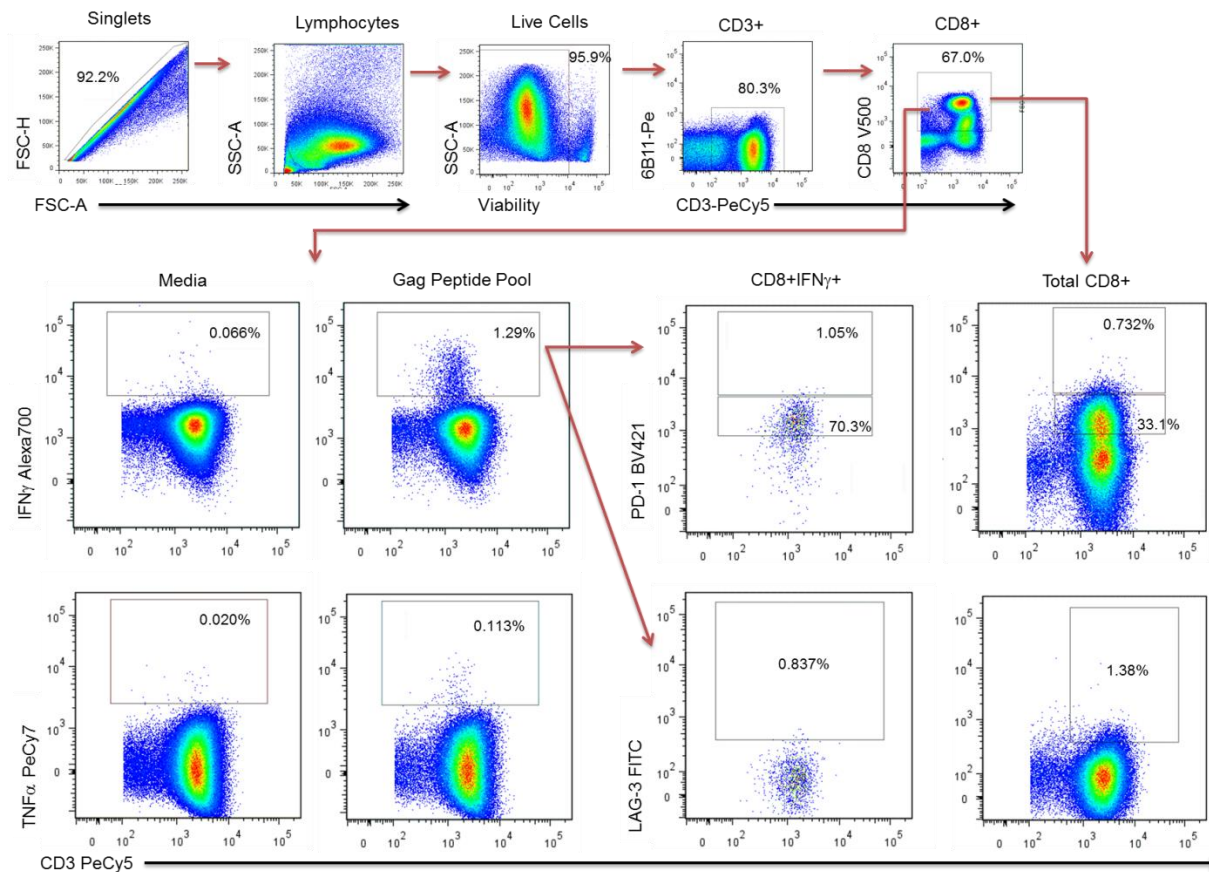
Figure 5.6 Representative staining of HIV gag-specific CD8+ T cell responses. Singlets were identified by FSC-area (FSC-A) versus FSC-height (FSC-H) gating, followed by lymphocyte gating based on forward and side scatter. Live cells were identified by Live/Dead Red staining. T cells were gated as CD3+CD8+ (hi or lo). The CD3 gate was expanded to include some antigen-specific populations which were CD3^{lo} compared to bulk T cells. Expression of IFNγ and TNFα was measured by intracellular staining, and PD-1 and LAG-3 by surface staining. Plots from both media control and gag peptide pool stimulation are shown. Data from ML1932 (HIV+, ART experienced) are shown.
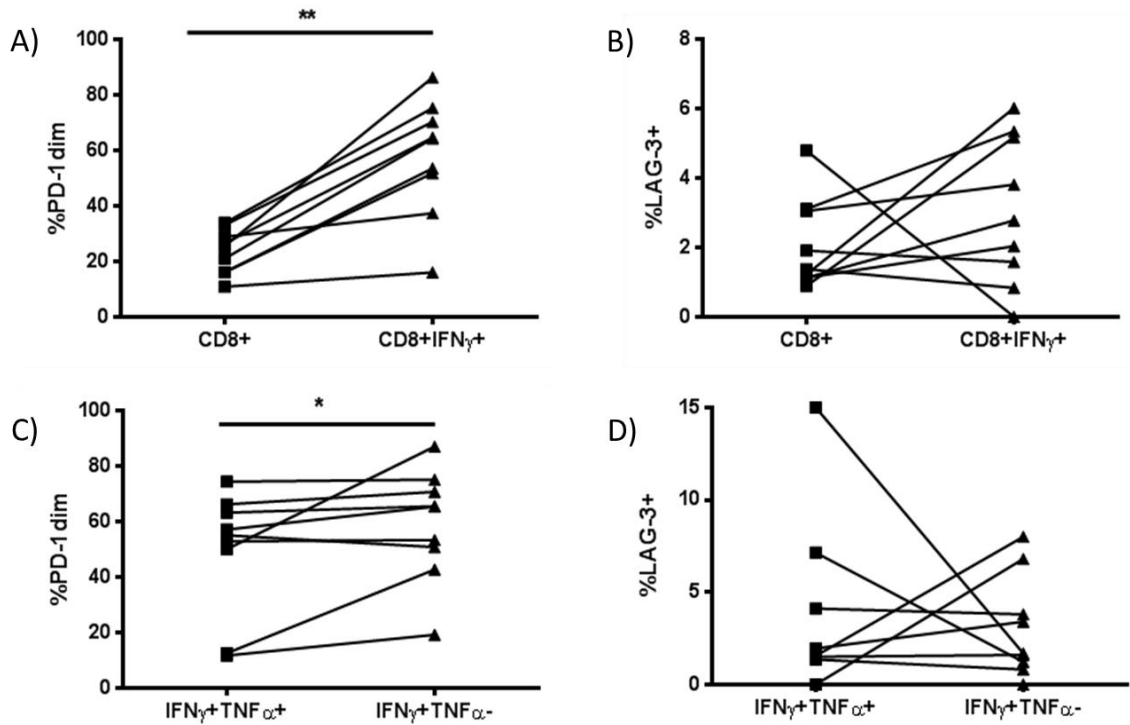
Figure 5.7 Expression of LAG-3 and PD-1 on antigen-specific T cell populations. (A) PD-1 expression is significantly enriched on HIV gag-specific CD8+ T cells (measured by IFNγ expression) compared to the bulk CD8+ population. **(B)** LAG-3 expression is similar between bulk CD8+ and gag-specific CD8+ populations. **(C)** PD-1 expression is preferentially associated with IFNγ+TNFα- gag-specific CD8 responses compared to dual-positive cells. **(D)** LAG-3 expression is similar between single- and dual-positive gag-specific T cells. $*p<0.05$, $**p<0.01$

5.4.3.4 LAG-3 expression and GNB3 825 genotype

The exon array analysis of *GNB3* and *LAG-3* RNA splicing described in section 4.4

suggested that LAG-3 mRNA was differentially spliced between *GNB3* genotype groups.

The differences in expression were observed at the 3' end of the transcript, which

encodes the transmembrane domain and cytoplasmic tail present in cell surface LAG-3.

We therefore compared T lymphocyte surface LAG-3 expression between *GNB3* 825

genotype groups in an attempt to confirm the exon array results. Due to significant

differences in LAG-3 expression during HIV infection, analysis was restricted to HIV+

participants (n=17 CC/CT, 35 TT). There were no significant differences in LAG-3

expression between *GNB3* genotype groups for any lymphocyte subset analysed (CD4+,

CD8+, iNKT, $CD56^{dim}CD16^+$, $CD56^{hi}CD16^-$) (p>0.1 for all, Mann-Whitney) (Figure

5.8A-E).

5.4.4 LAG-3 expression on NK cells

Human NK cell subsets are commonly defined as $CD56^{hi}CD16^-$ and $CD56^{dim}CD16^+$, with

a dysfunctional $CD56^-CD16^+$ population accumulating during chronic HIV infection

(446) (Figure 5.9A). In this study, there was no statistically significant change in the

frequency of any NK subset as a percentage of total CD3- lymphocytes, including the

$CD56^-CD16^+$ population, between any disease status groups (n=10 HIV-, 35 HIV+, 36

HIV+ ART) (p>0.1 for all, Kruskal-Wallis test) (Figure 5.9B). Furthermore, the CD56-

CD16+ NK population was not expanded as a relative proportion of the total NK

population in either HIV-infected group (p=0.51, Kruskal-Wallis test) (Figure 5.9C).
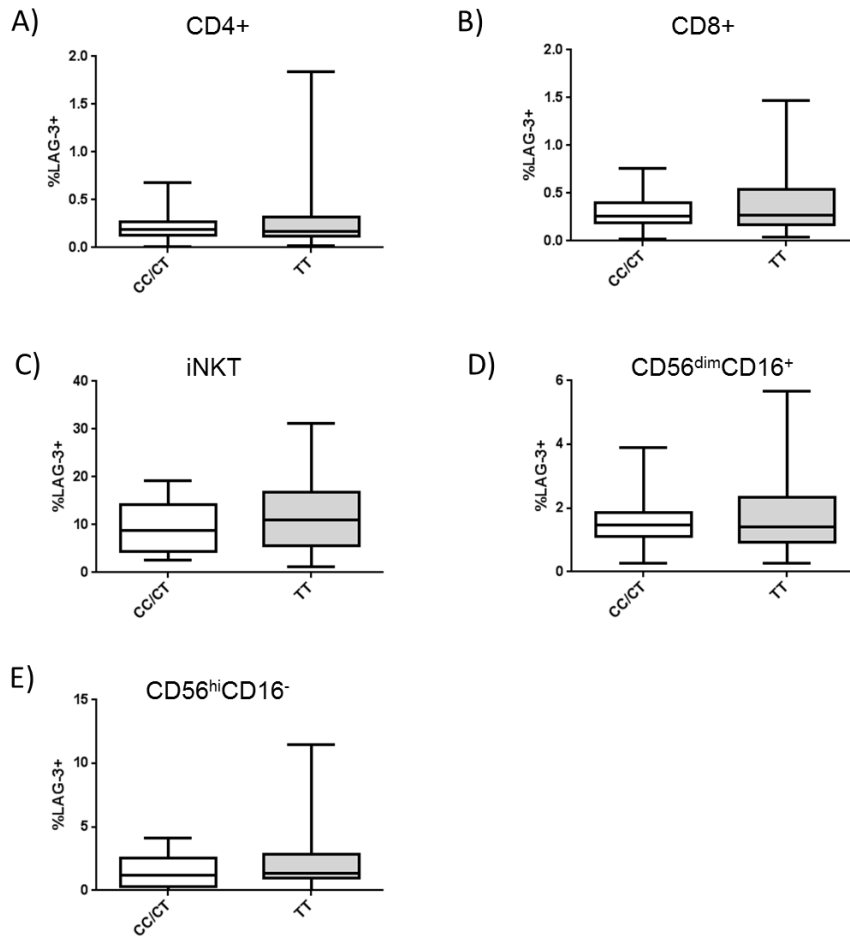
Figure 5.8. Comparison of surface LAG-3 expression between *GNB3 825* genotypes. Among HIV+ participants (n=17 CC/CT, 35 TT), there was no difference in LAG-3 expression between *GNB3* genotype groups on (**A**) CD4+ T cells, (**B**) CD8+ T cells, (**C**) iNKT cells, (**D**) CD56^{dim}CD16^{+} NK cells, or (**E**) CD56^{hi}CD16^{-} NK cells.

LAG-3 expression was detected at low levels on all NK subsets (Figure 5.10A).

Expression was significantly higher on the CD56^{dim}CD16$^+$ and CD56^{hi}CD16$^-$ NK subsets among HIV+ ART experienced women compared to healthy controls (CD56^{dim}CD16$^+$: p=0.0368, Kruskal-Wallis test, post-test p=0.0151 for HIV+ ART versus HIV-N (Mann-Whitney), p=0.799 for HIV+ versus HIV-N (Mann-Whitney); CD56^{hi}CD16$^-$: p=0.0134, Kruskal-Wallis test, post-test p<0.05 for HIV+ ART versus HIV-N) (Figure 5.10B, Table 5.3). There was no difference in LAG-3 expression across groups on the CD56$^-$CD16$^+$ subset (p=0.1474, Kruskal-Wallis).

Intra-participant comparison of LAG-3 expression across NK subsets revealed significantly higher LAG-3 expression on the CD56-CD16+ NK subset compared to either the CD56dim or CD16hi populations. The differences remained significant for both healthy (p=0.0004, post-test p<0.05 for CD56- versus CD56dim, p<0.01 for CD56- versus CD56hi, Friedman) and HIV+/ART participants (p<0.0001, post-test p<0.0001 for CD56- versus both CD56^{dim} and CD56^{hi}, Friedman) (Figure 5.10C). A parametric ANOVA test for linear trend demonstrated a significant decline in LAG-3 expression across NK cell subsets with increasing CD56 expression (CD56- > CD56dim > CD56hi) (p<0.0001, ANOVA test for linear trend).

CD4 count did not correlate with LAG-3 expression on any NK cell subset, regardless of whether all HIV+ participants were grouped together or stratified based on ARV treatment (p>0.1 for all, Spearman correlation) (Table 5.5, Figure 5.11A). Similarly, LAG-3 expression among ART experienced participants did not vary according to

duration of therapy for any NK subset (r=-0.0904, p=0.6002 for CD56^{dim}CD16$^+$; r=-0.2105, p=0.2178 for CD56^{hi}CD16$^-$; r=-0.0810, p=0.6387 for CD56$^-$CD16$^+$, Spearman) (Figure 5.11B). When stratified based on recovery of CD4 count to greater or less than 350 cells/µL, ART-experienced participants exhibited similar levels of LAG-3 on all NK subsets (p=0.7013 for CD56^{dim}CD16$^+$; p=0.7845 for CD56^{hi}CD16$^-$; p=0.9563 for CD56$^-$CD16$^+$, Mann-Whitney) (Figure 5.11C).

Due to limitations in the number of channels available for a single flow cytometry panel, the only phenotypic marker assessed on NK cells was the acute activation marker CD69. Among all HIV+ participants, LAG-3 expression significantly correlated with CD69 expression on CD56^{dim}CD16$^+$ NK cells, but not CD56^{hi}CD16$^-$ or CD56$^-$CD16$^+$ NK subsets (n= 21 HIV+, 7 HIV+ ART) (r=0.4155, p=0.0311 for CD56^{dim}CD16$^+$; r=-0.1512, p=0.4426 for CD56^{hi}CD16$^-$; r=0.1402, p=0.4946 for CD56$^-$CD16$^+$, Spearman) (Figure 5.12A). Although LAG-3 and CD69 expression were positively correlated on the CD56^{dim}CD16$^+$ subset, the two surface markers were not co-expressed; LAG-3+CD69- cells were significantly more frequent than LAG-3-CD69+ cells, which formed only a minor population in HIV+ individuals (p<0.0001, Wilcoxon) (Figure 5.12B). These results may indicate differences in the temporal expression of LAG-3 and CD69, whereby LAG-3 may be upregulated following peak CD69 expression.

In summary, LAG-3 expression was elevated on both CD56^{dim} and C56^{hi} NK cell subsets during HIV infection. Like its expression on T cells, NK LAG-3 expression did not correlate with disease progression or ART duration. Interestingly, LAG-3 expression was highest on CD56- anergic NK cells among healthy women.
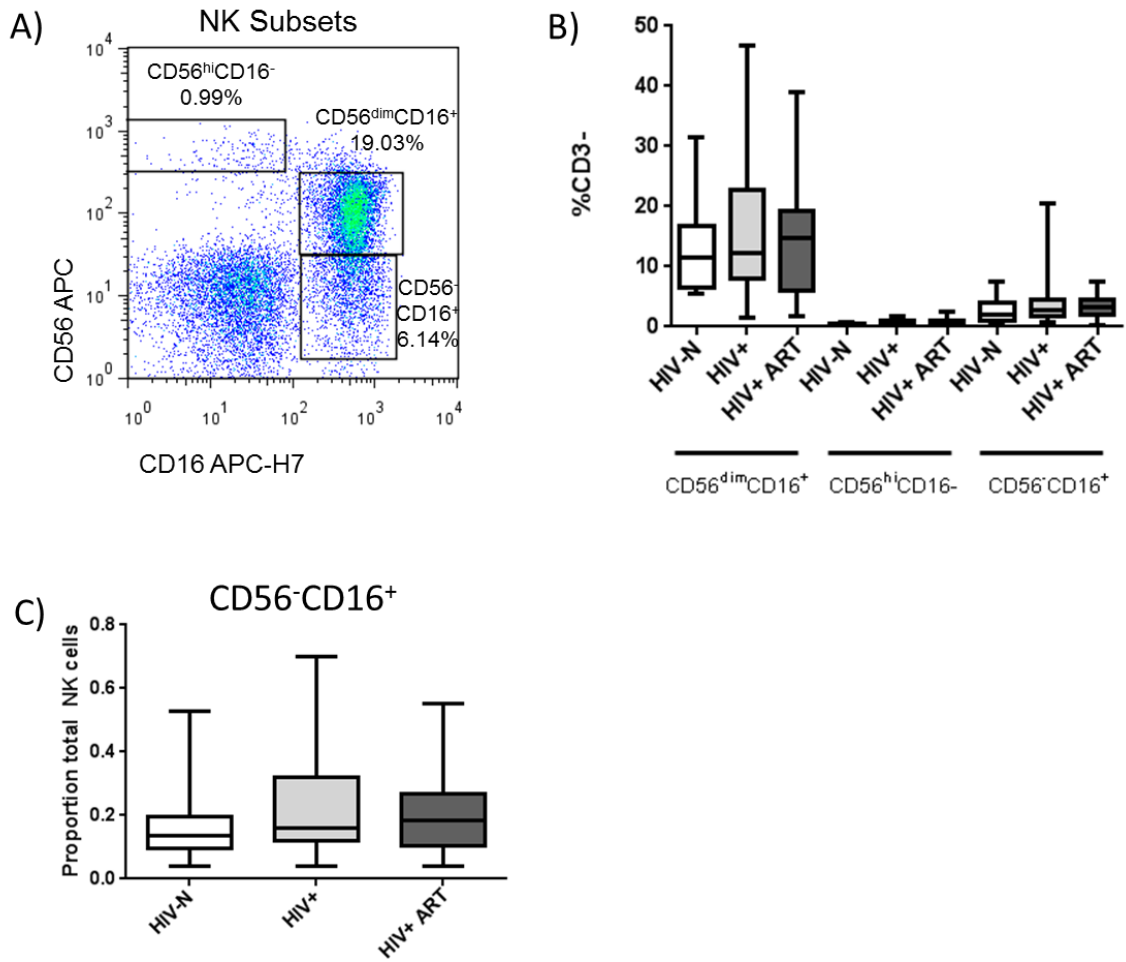
Figure 5.9. NK cell populations among HIV+ participants. (A) Representative staining of NK cell subpopulations (ML3290, HIV+ ART experienced). **(B)** NK subset frequencies were unchanged by HIV infection status. **(C)** The CD56⁻CD16⁺ population was not significantly expanded as a proportion of the total NK population among HIV+ participants.
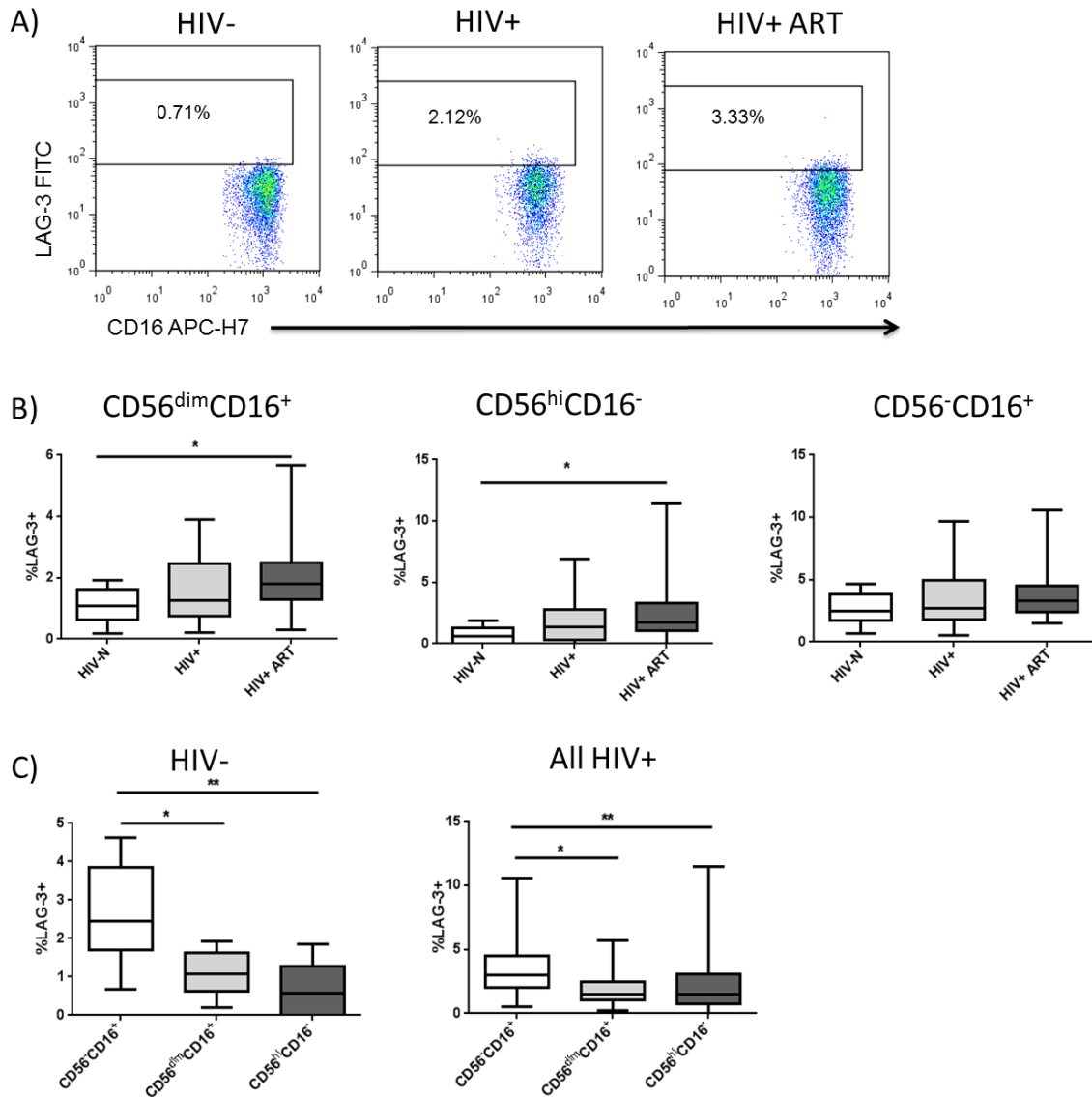
Figure 5.10 LAG-3 expression on NK cell subsets. (A) Representative staining of LAG-3 expression on CD56dimCD16+ NK cells among HIV-N (ML2971), HIV+ (ML3013) and HIV+ ART (ML2585) participants. **(B)** LAG-3 expression is significantly increased among HIV+ ART participants on both the CD56dimCD16+ and CD56hiCD16- NK subsets. **(C)** LAG-3 expression was significantly higher on CD56-CD16+ NK cells compared to either the CD56dim or CD56hi populations, regardless of HIV serostatus. *p<0.05, **p<0.01 ****p<0.0001

Table 5.5. Correlations between NK subset LAG-3 expression and CD4 count among HIV+ participants.

NK Subset	Population	Spearman r	p value
CD56^{dim}CD16$^+$	All HIV+	-0.0496	0.6837
	HIV+ ART Naïve	0.1163	0.5125
	HIV+ ART experienced	-0.0294	0.8648
CD56^{hi}CD16$^-$	All HIV+	-0.1266	0.2965
	HIV+ ART Naïve	0.0797	0.6542
	HIV+ ART experienced	-0.2208	0.1956
CD56$^-$CD16$^+$	All HIV+	-0.0180	0.8822
	HIV+ ART Naïve	0.1612	0.3624
	HIV+ ART experienced	-0.0393	0.8201
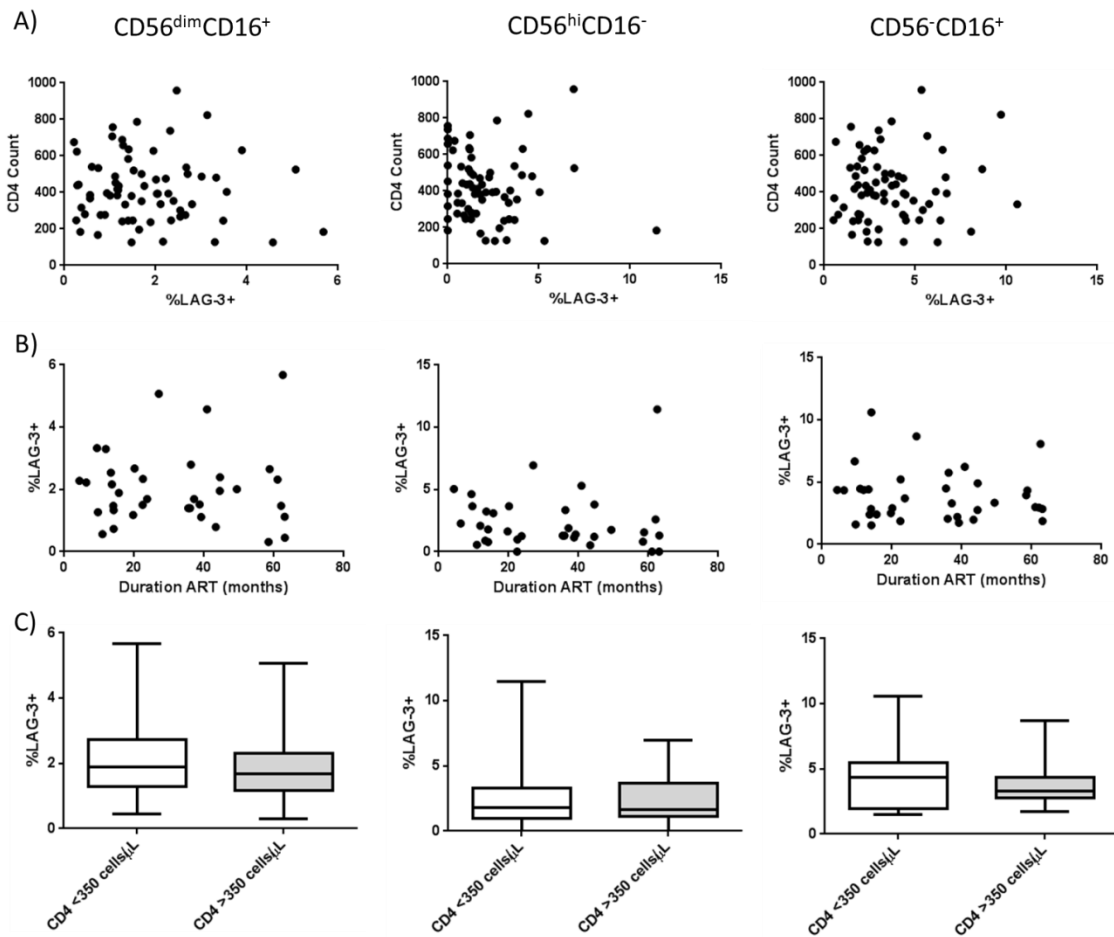
Figure 5.11. Relationship between NK LAG-3 expression and CD4 count and ARV therapy. (A) Among all HIV+ participants, CD4 count did not correlate with LAG-3 expression on any NK subset (n=70). **(B)** Among participants on ART, LAG-3 expression did not correlate with duration of ARV therapy on any NK subset (n=36). **(C)** LAG-3 expression on NK subsets did not differ between participants on ART with CD4 counts above or below 350 cells/μL (n=17 <350 cells/μL, 19 >350 cells/μL).
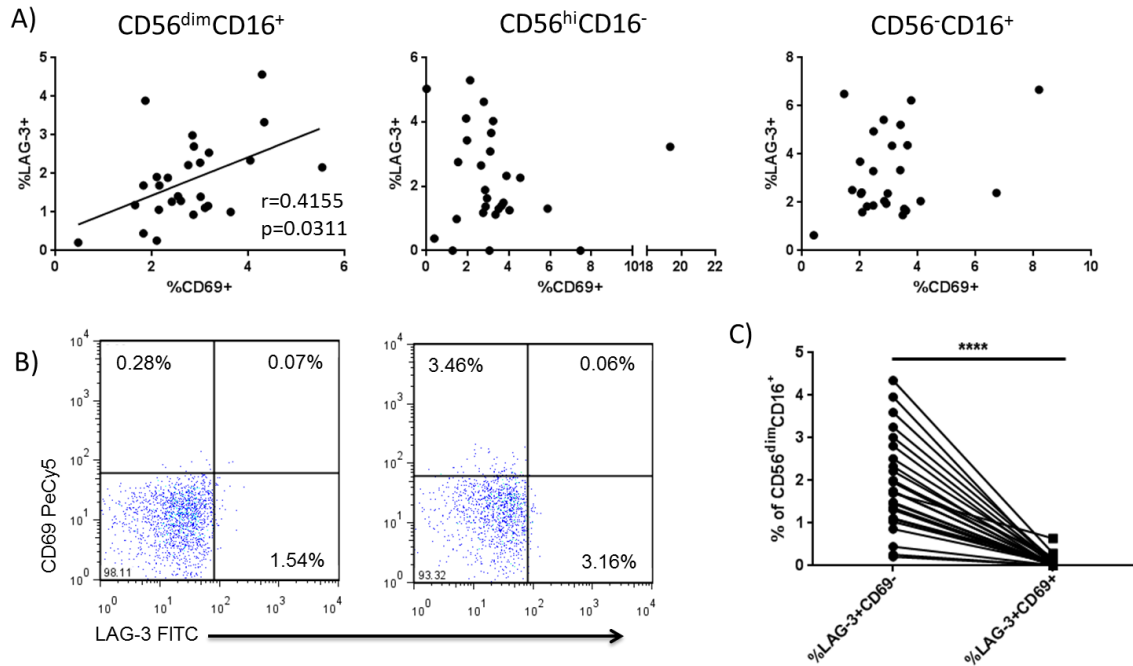
Figure 5.12. Relationship between LAG-3 and CD69 expression on NK subsets. (A) LAG-3 expression significantly correlated with CD69 expression on only the CD56^{dim}CD16^{+} NK subset among all HIV+ participants. Trend line derived from linear regression. **(B)** Representative staining of LAG-3 and CD69 co-expression on CD56^{dim}CD16^{+} NK cells. **(C)** LAG-3 and CD69 were not co-expressed on CD56^{dim}CD16^{+} NK cells, with LAG-3+ cells being significantly more likely to be CD69- than CD69+. ****p<0.0001

Human iNKT population frequencies are highly variable, ranging from <0.01% of CD3+

T cells to >1% in published reports (271, 447). An iNKT population was detected using

the 6B11 antibody specific to the iNKT TCR (Figure 5.13A). These frequencies are

comparable to those observed in the FSW cohort in this study (Figure 5.13B). Overall,

iNKT frequencies were similar between HIV-, HIV+ and HIV+ ART experienced

participants (p=0.914, Kruskal-Wallis test) (Figure 5.13B).

Similar to the depletion of conventional CD4+ T cells during chronic HIV infection, the

proportion of CD4+ iNKT cells was reduced in both HIV+ and HIV+ ART experienced

participants compared to healthy controls (n=8 HIV-, 34 HV+, 34 HIV+ ART) (Figure

5.13C) (p=0.0012, Kruskal-Wallis test, post-test p<0.01 for healthy vs. HIV+, p<0.001

for healthy vs. HIV+ ART experienced). There was no significant difference in the

frequency of CD4+ iNKTs between ART naïve and experienced participants, suggesting

a lack of iNKT reconstitution following ARV therapy. The proportionate decrease in

CD4+ iNKT cells was associated with an inflated proportion of CD8+ iNKT cells, while

the frequency of DN iNKTs remained similar across groups (Figure 5.13C) (p=0.0005 for

CD8+ iNKT frequency, Kruskal-Wallis test, post-test p<0.01 for healthy vs. HIV+,

p<0.001 for healthy vs. HIV+ ART experienced). There was no difference in the

frequency of double negative (CD4-CD8-. DN) iNKT cells between groups (p=0.9247,

Kruskal-Wallis).

LAG-3 expression was detected at low levels on iNKTs among healthy women, and was significantly elevated during chronic HIV infection among ART experienced participants (p=0.0274, post-test p<0.05 for HIV-N versus HIV+ ART, Kruskal-Wallis) (Figure 5.14A,B, Table 5.3). LAG-3 median fluorescence intensity (MFI) was similar across groups, but exhibited a trend of increasing intensity between HIV-, HIV+ and HIV+ ART groups (p=0.085, Kruskal-Wallis) (Figure 5.14C).

Analysis of iNKT subset phenotypes is limited by the low number of iNKT cells acquired by flow cytometry. Quantification of LAG-3 expression on CD4+, CD8+ and DN iNKT subsets was therefore restricted to samples with >20 events collected in each subset gate, and should be interpreted with caution. Analysis did suggest, however, that LAG-3 expression was primarily increased on the CD4+ iNKT subset among HIV+ ART experienced individuals rather than the CD8+ or DN subsets (CD4+ iNKT n=8 HIV-N, 26 HIV+, 25 HIV+ ART; CD8+ iNKT n=4 HIV-N, 28 HIV+, 27 HIV+ ART; DN iNKT n=7 HIV-N, 27 HIV+, 28 HIV+ ART) (CD4+ iNKT p=0.029, post-test p<0.05 HIV-N versus HIV+ ART; CD8+ iNKT p=0.978; DN iNKT p=0.099, Kruskal-Wallis) (Figure 5.14D).
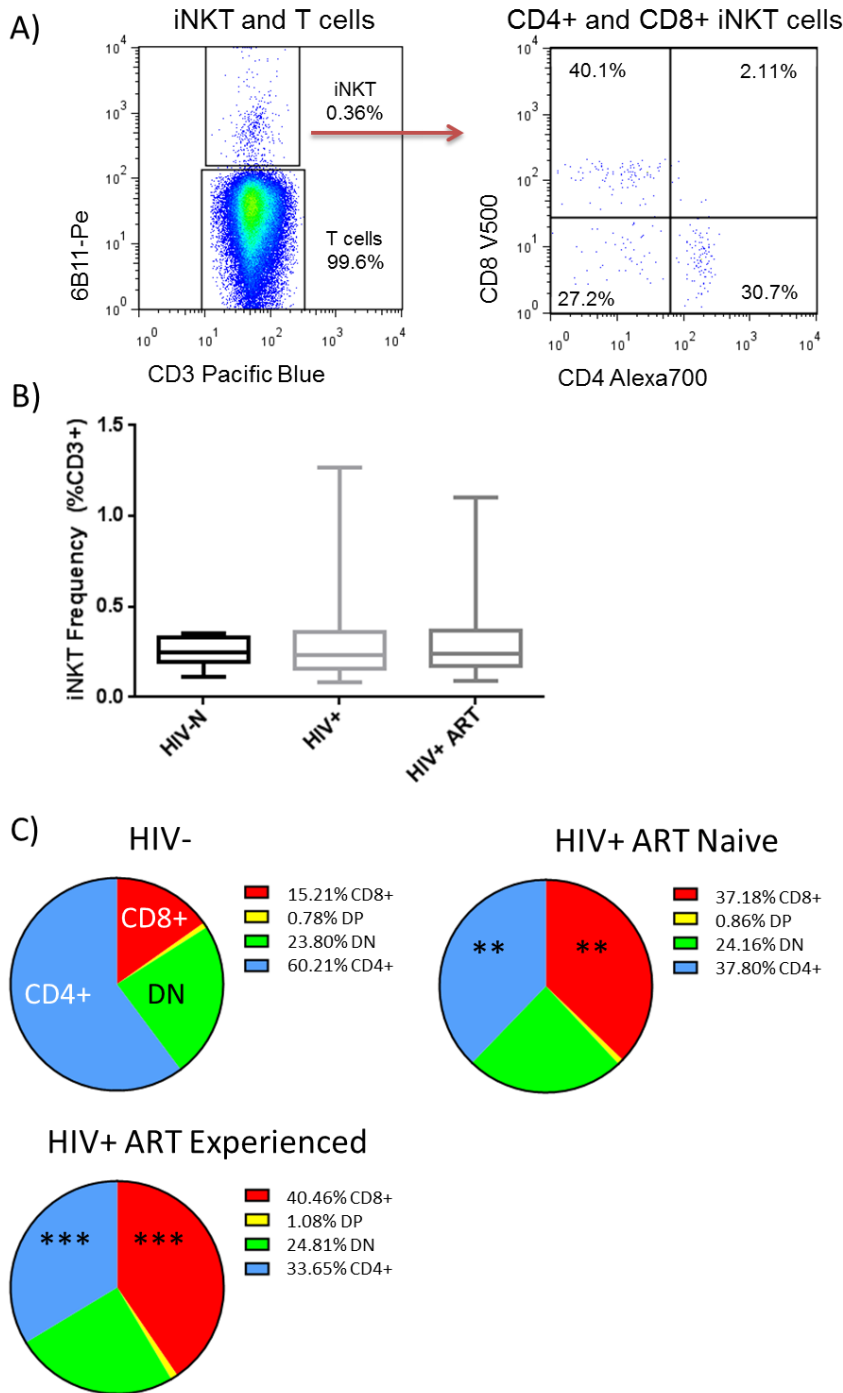
Figure 5.13. iNKT population frequency and subset proportions. (A) Representative staining of iNKT cells (CD3+6B11+) and subgating into CD4+, CD8+ and double negative (DN) subsets. Data are shown from ML2197 (HIV+ ART). **(B)** iNKT population frequency was similar across HIV-, HIV+ and HIV+ ART groups. **(C)** Both HIV+ groups exhibited significantly decreased proportions of CD4+ iNKTs and increased proportions of CD8+ iNKTs compared to healthy controls. **p<0.01, ***p<0.001.
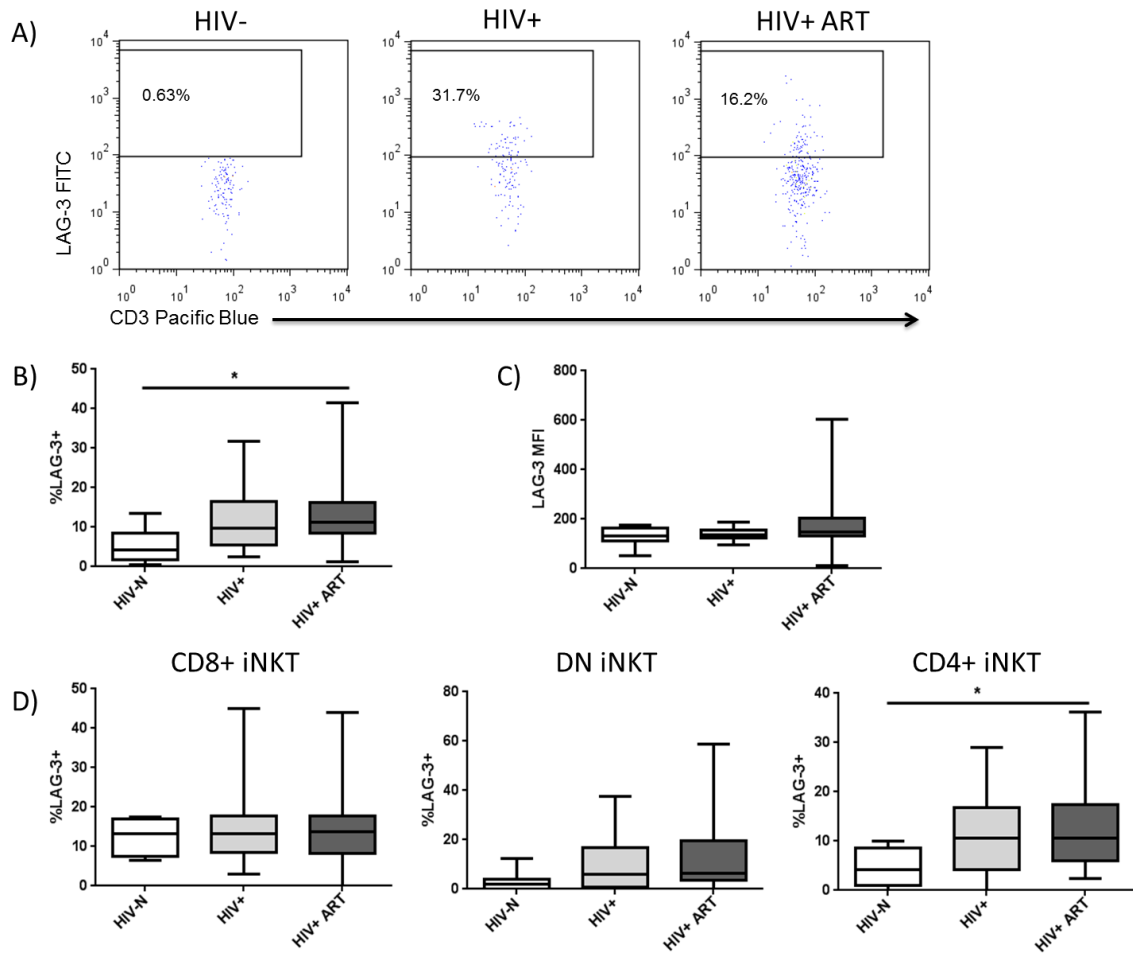
Figure 5.14. LAG-3 expression on iNKT subsets. (A) Representative staining of LAG-3 on CD3+6B11+ iNKT cells among HIV-N (ML2644), HIV+ (ML2312) and HIV+ ART (ML2197) participants. **(B)** LAG-3 expression is significantly increased on iNKT cells among the HIV+ ART group compared to healthy controls. **(C)** LAG-3 MFI was similar across all groups, regardless of HIV status. **(D)** Increased LAG-3 expression among HIV+ ART participants was primarily restricted to the CD4+ iNKT subset, which exhibited significantly greater LAG-3 expression compared to healthy controls. *$p<0.05$.

LAG-3 expression on the bulk iNKT subset did not correlate with CD4 count among

HIV+ participants, whether grouped together or stratified by ART use (r=0.0255,

p=0.8374 for all HIV+; r=0.1035, p=0.5667 for HIV+ ART naïve; r=0.0396, p=0.8241

for HIV+ ART experienced, Spearman) (Figure 5.15A). ART duration did not correlate

with LAG-3 expression (r=-0.0076, p=0.9658, Spearman) (Figure 5.15B), nor did LAG-3

expression differ between individuals with CD4 reconstitution above 350 cells/μL

(p=0.7139, Mann-Whitney) (Figure 5.15C). Among all HIV+ participants, iNKT LAG-3

expression significantly correlated with iNKT activation measured by CD69 expression

(n=11 HIV+, 11 HIV+ ART) (r=0.4507, p=0.0353, Spearman) (Figure 5.15D).

In summary, CD4+ iNKT cells were depleted during HIV infection and not restored

by ART. LAG-3 expression was elevated on iNKT cells among HIV+ women, but

did not correlate with measures of disease progression.
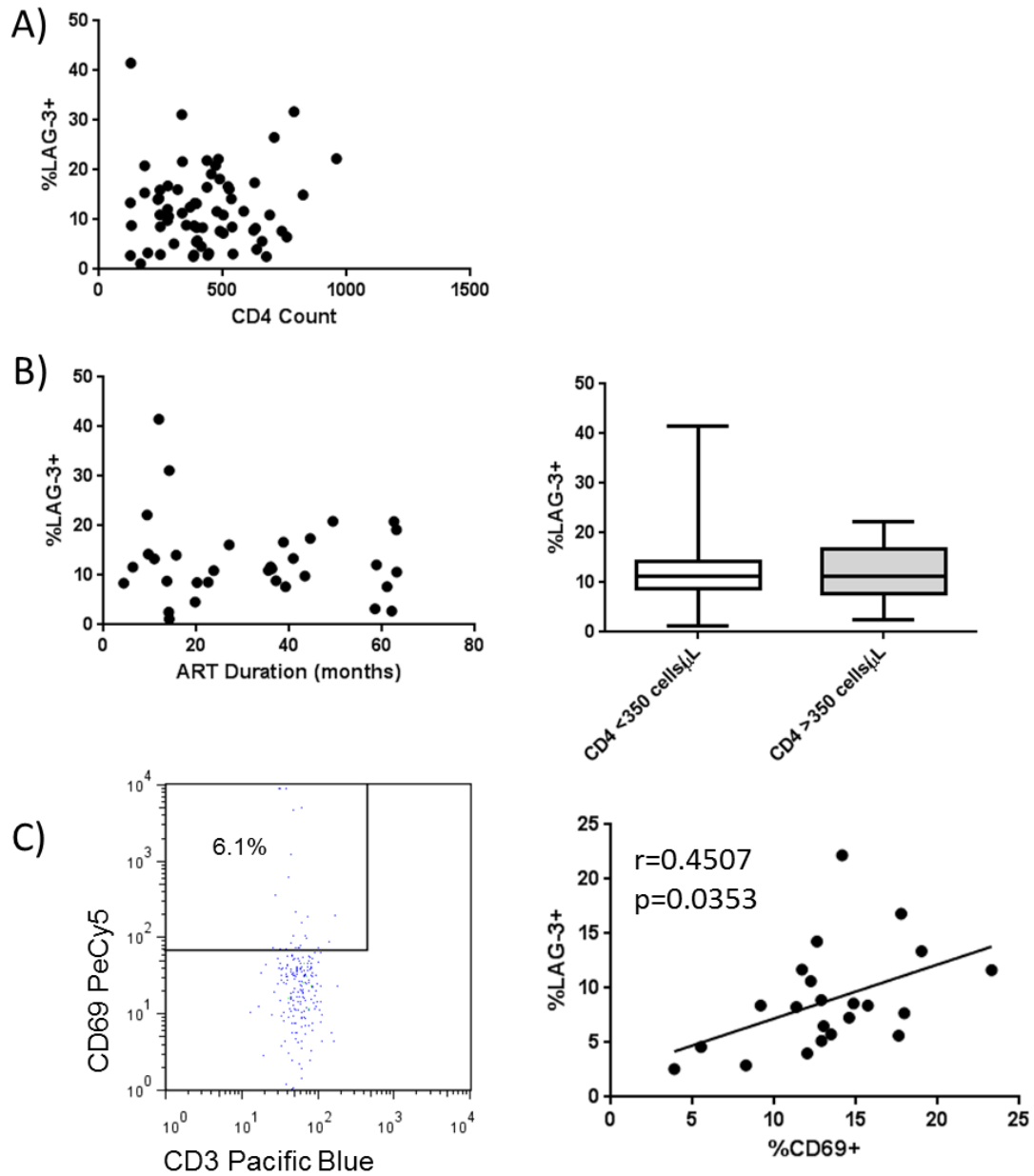
Figure 5.15. Correlates of iNKT LAG-3 expression. (A) LAG-3 expression did not correlate with CD4 count among HIV+ participants. **(B)** ART duration did not correlate with LAG-3 expression, nor did LAG-3 expression differ when participants were stratified based on CD4 reconstitution above or below 350 cells/μL. **(C)** Representative staining of CD69 on iNKT cells (ML2197 is shown). CD69 expression significantly correlated with LAG-3 expression on iNKT cells among HIV+ participants. Trend line derived from linear regression.

5.4.6 LAG-3 expression and plasma cytokine/chemokine expression

The lack of correlation between LAG-3 expression and any correlates of disease

progression or treatment (chronic T cell activation, CD4 count, duration of ART) was

unexpected, and notably distinct from the expression patterns of other exhaustion markers

during HIV infection. We therefore wondered whether LAG-3 expression might instead

be regulated by specific cytokines/chemokines, or be specifically associated with levels

of Th1 or Th2-like cytokines. Some published data indicates that LAG-3 expression is

IFNγ dependent (405), while murine data strongly associates LAG-3 expression with

Treg cells that produce IL-10 (402). To determine whether LAG-3 expression was

associated with a proinflammatory (IL-6, TNFα), Th2 (IL-4) or regulatory (IL-10)

plasma cytokine environment, cytokine bead arrays were used to measure 8 plasma

cytokines/chemokines (IFNα2, IFNγ, IL-4, IL-6, IL-10, MIP-1β, sCD40L, and TNFα) in

7 HIV-, 31 HIV+ and 30 HIV+ ART participants. IFNα2 was included as an output of

innate immune activation, while sCD40L is commonly associated with immune

activation. IL-4 and IL-6 were detected in only 5 and 3 samples, respectively, and were

therefore excluded from further analysis. Median concentrations of each analyte and the

number of participants with detectable levels of each cytokine/chemokine are given in

Table 5.6.

LAG-3 expression on CD4+ and CD8+ T cells, all three NK cell subsets and iNKT cells

was correlated with the concentration of each cytokine/chemokine among all HIV+

participants, as well as ART naïve and ART experienced subjects separately. No

significant correlations were found (p>0.05 for all, Spearman). Because IFNγ and IL-10

139

were detectable in less than half of HIV+ participants, correlations were also performed

including only participants with plasma concentrations above the limit of detection.

Among all HIV+ participants with detectable levels of cytokine, CD8+ T cell LAG-3

expression trended toward a positive correlation with plasma IFNγ (n=22, r=0.4113,

p=0.0572, Spearman) (Table 5.7, Figure 5.16A). iNKT LAG-3 expression exhibited a

weak negative correlation with plasma IL-10 concentrations (n=22) among all HIV+

participants, as well as ART experienced participants (r=-0.4291, p=0.0463 for all HIV+;

r=-0.6210, p=0.0438 for HIV+ ART) (Table 5.7, Figure 5.16B,C).

In summary, plasma cytokines/chemokines appeared to be poor predictors of LAG-3 expression on all lymphocyte subsets studied.

Table 5.6. Concentrations of plasma cytokines and chemokines in HIV-N and HIV+ participants.

Analyte	HIV-		HIV+		HIV+ ART	
	Median (pg/mL)	N Detected	Median (pg/mL)	N Detected	Median (pg/mL)	N Detected
IFNα2	20.10	5	36.04	27	38.15	28
IFNγ	1.20*	3	1.20*	12	1.20*	10
IL-10	0.25*	1	0.25*	12	0.25*	11
MIP-1β	7.50	5	23.66	26	23.83	27
sCD40L	4045	7	3873	31	3185	30
TNFα	6.43	6	9.44	26	7.05	28

*indicates value midway between limit of detection and 0pg/mL.

Table 5.7. Correlations between plasma cytokines/chemokines and CD8+ T cell LAG-3 expression among participants with detectable cytokine/chemokine expression.

Analyte	Lymphocyte Subset	All HIV+		HIV+		HIV+ ART	
		Spearman rho	p value	Spearman rho	p value	Spearman rho	p value
IFNγ (n=22)	CD3+CD8+	**0.4113**	**0.0572**	0.4445	0.1482	0.2884	0.4196
	CD3+CD4+	0.3257	0.1390	0.2008	0.5279	0.3697	0.2957
	CD56^{dim}CD16$^+$	0.3420	0.1193	0.3937	0.2049	0.2614	0.4622
	CD56^{hi}CD16$^-$	0.3320	0.1312	0.3908	0.2084	0.2121	0.5603
	iNKT	-0.1644	0.4647	-0.3722	0.2010	-0.1515	0.6821
IL-10 (n=23)	CD3+CD8+	-0.0565	0.8028	-0.2968	0.3258	-0.2673	0.3986
	CD3+CD4+	0.0043	0.9849	-0.3506	0.2486	-0.0961	0.7610
	CD56^{dim}CD16$^+$	-0.0408	0.8571	-0.1119	0.6809	-0.2494	0.4376
	CD56^{hi}CD16$^-$	0.1172	0.6036	-0.0561	0.8034	0.0776	0.8218
	iNKT	**-0.4291**	**0.0463**	-0.1819	0.5337	**-0.6210**	**0.0438**

Correlations with p≤0.1 are highlighted in bold.
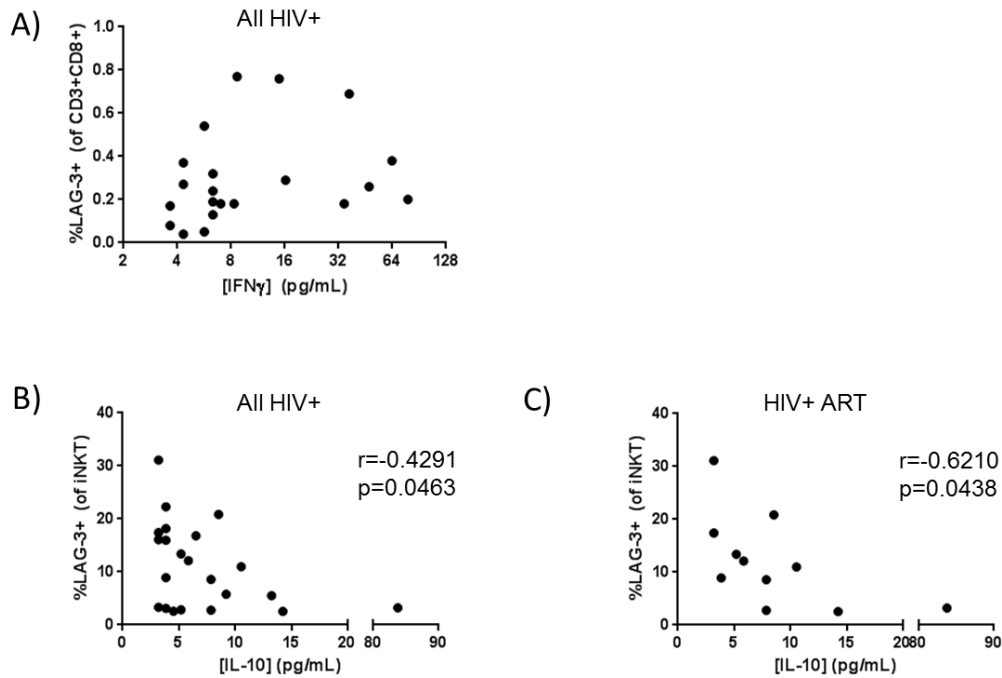
Figure 5.16. Correlations between lymphocyte LAG-3 expression and plasma cytokine/chemokine concentrations. (A) LAG-3 expression on CD8+ T cells trended toward positively correlating with plasma IFNγ concentrations among HIV+ participants with detectable IFNγ (n=22). **(B)** Among HIV+ participants with detectable IL-10, LAG-3 expression on iNKTs negatively correlated with plasma IL-10 (n=22). **(C)** The correlation between iNKT LAG-3 and plasma IL-10 remained significant among HIV+ ART participants (n=11).

5.4.7 Soluble LAG-3 expression in plasma

Plasma samples with sufficient volume to quantify sLAG-3 by in-house ELISA were available from participants of the iNKT function study. sLAG-3 was detected in all plasma samples (n=17 HIV-, 9 HIV+, 17 HIV+ ART). One sample read above the upper limit of detection of the assay, and was assigned an arbitrary value for the purpose of statistical analysis (because non-parametric statistics rank all values, the highest value receives the same rank regardless of the actual concentration). sLAG-3 concentrations were highly variable between individuals, and only trended toward exhibiting differences based on HIV status (p=0.1077, Kruskal-Wallis) (Figure 5.17A).

Interestingly, sLAG-3 significantly inversely correlated with CD4 count among the 17 HIV+ participants for whom CD4 counts were available (r=-0.5735, p=0.0179, Spearman) (Figure 5.17B). Plasma cytokine/chemokine concentrations were also available for these participants. Because the conditions under which sLAG-3 is generated are unknown, the relationship between sLAG-3 concentration and other soluble immune mediators (cytokines/chemokines) was assessed. Analytes included IL-8, IL-15, sCD40L, IP-10, MCP-1, MIP-1α, MIP-1β, IL-1α, IFNα2, IL-17F, IFNγ, IL-10, MIP-3α, IL-12p70, IL-17A, IL-22, IL-1β, IL-2, IL-23, IL-6, IL-17E, and TNFα. IL-1β, IL-2, IL-17E, IL-1a, IL-10, MIP-1a and IL-15 were not detectable in the samples, and were not included in future analyses (median concentrations are reported in Appendix 10.3).

 Among all HIV+ participants, sLAG-3 correlated with IP-10 (r=0.8353, p<0.0001, Spearman) and IL-23 (r=-0.5438, p=0.0168) (Figure 5.17C). When sub-grouped based on

ART status, no significant relationship remained with IL-23, but the correlation between

sLAG-3 and IP-10 remained significant in both groups (r=0.9048, p=0.0046 for HIV+

ART naïve; r=0.8407, p=0.0006 for HIV+ ART, Spearman) (Figure 5.18A).

Interestingly, although IP-10 concentration was significantly elevated in the HIV+ ART

naïve group compared to healthy controls (p=0.0243, Kruskal-Wallis, post-test p<0.05)

(Figure 5.18B), CD4 count only trended toward an inversely correlation with IP-10 levels

(r=-0.4289, p=0.0873, Spearman) (Figure 5.18C). **Plasma sLAG-3 was therefore a**

stronger correlate of CD4 decline than IP-10 concentration in this study.
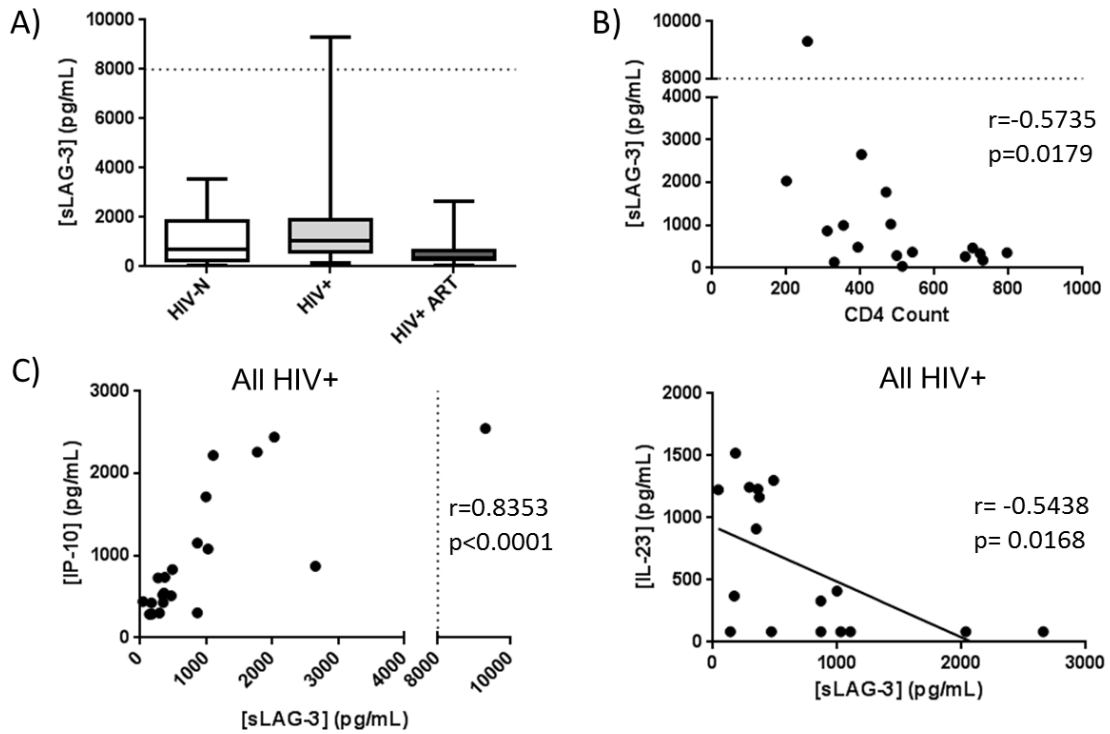
Figure 5.17. Quantification of plasma sLAG-3 in healthy and HIV+ participants of the iNKT function study. (A) Plasma sLAG-3 concentrations trended toward an increase among HIV+ ART naïve participants compared to healthy controls. **(B)** sLAG-3 inversely correlated with CD4 count among all HIV+ participants (n=17). **(C)** Plasma sLAG-3 significantly correlated with plasma IP-10 (n=21) and IL-23 (n=17) concentration among all HIV+ participants.
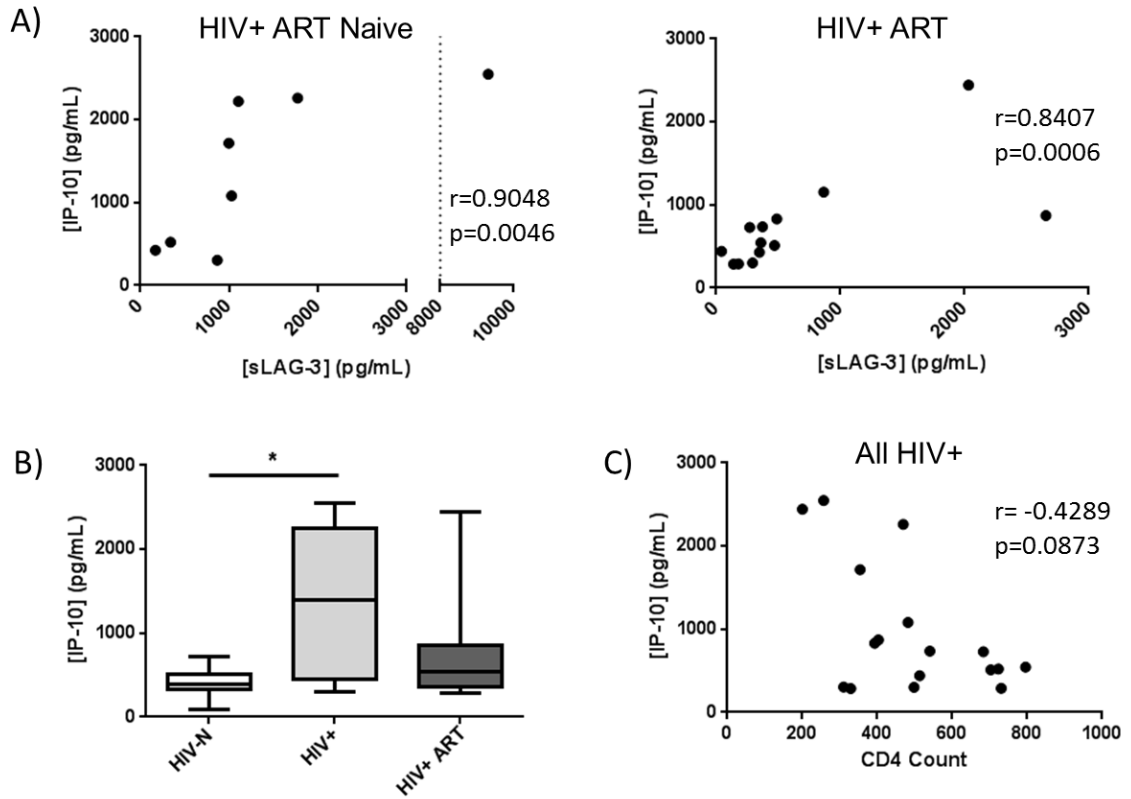
Figure 5.18. Relationship between sLAG-3, plasma IP-10 and CD4 count among HIV+ women. (A) The correlation between IP-10 and sLAG-3 was maintained among HIV+ ART naïve (n=8) and HIV+ ART experienced (n=13) participants. Dashed line indicates upper limit of sLAG-3 ELISA. **(B)** Plasma IP-10 concentrations were significantly elevated among HIV+ ART naïve women compared to healthy controls. **(C)** CD4 count trended toward an inverse correlation with plasma IP-10 concentration among all HIV+ participants. *p<0.05

5.5 Summary

The aim of this study was to identify lymphocyte subsets expressing high levels of LAG-3 during chronic HIV infection. LAG-3 expression was significantly increased among HIV+ participants on CD4+ and CD8+ T cells, $CD56^{dim}CD16^{+}$ and $CD56^{hi}CD16^{-}$ NK cells and iNKT cells. LAG-3 expression did not correlate with CD4 count or chronic immune activation on any cell subsets examined, nor was it decreased among participants receiving ART. On both NK and iNKT cells, LAG-3 expression correlated with acute activation marker CD69. The largest differences in LAG-3 expression between healthy and HIV-infected participants, as well as the highest proportion of LAG-3-expressing cells were observed on the iNKT subset. Overall, these results suggest that LAG-3 expression is increased on iNKT cells during chronic HIV infection, where it could contribute to iNKT exhaustion. Although LAG-3 expression did not correlate with plasma cytokines/chemokines, sLAG-3 concentration was related to both CD4 count and plasma IP-10 concentration. Surprisingly, sLAG-3 was a stronger correlate of CD4 decline during HIV infection than IP-10, which was a previously identified predictor of HIV disease progression.

6. Expression of LAG-3 at the genital mucosa

6.1 Rationale

Although LAG-3 is poorly expressed by the majority of resting PBMC in healthy individuals, it is known to be expressed following T cell and NK cell activation. Lymphocytes isolated from the female genital tract are typically more activated than those derived from peripheral blood, but the expression of exhaustion/activation markers such as LAG-3 and PD-1 at the genital mucosa have not been extensively described in either healthy or HIV+ individuals. Similarly, whether sLAG-3 is detectable in cervical vaginal lavage (CVL) is unknown. Given our lab's recent data suggesting that induction of an immunoregulatory environment at the genital tract may protect against HIV infection and that activated T cell subsets are depleted at the FGT following HIV infection, we assessed the expression of cell surface and soluble LAG-3 at the female genital mucosa in healthy and HIV+ participants.

6.2 Hypothesis

LAG-3 expression at the female genital mucosa is associated with lymphocyte activation and a pro-inflammatory cytokine environment. Due to increased activation of cervical T cells, LAG-3 expression is therefore elevated at the genital mucosa compared to the systemic compartment.

6.3 Objectives

1. Quantify T cell surface expression of LAG-3 and markers of immune activation (CD69) and exhaustion (PD-1) in PBMC and CMC samples and compare between healthy and HIV+ individuals.

2. Quantify expression of sLAG-3 and cytokines/chemokines in plasma and CVL samples from healthy and HIV+ individuals.

6.4 Results

6.4.1 Study Population

Mucosal LAG-3 expression was assessed in cervical scrapings collected from participants of the FSW cohort. A total of 37 women were recruited. Phenotypic analysis of cervical mononuclear cells derived from cytobrush samples is notoriously difficult, and samples often contain poor lymphocyte populations not suitable for flow cytometry. Samples were only included in this study if a viable, CD3+ lymphocyte population could be identified upon gating (see Figure 6.1) and therefore a total of 6 HIV-negative and 5 HIV+ participants (1 of whom was receiving ART) were included in the final analysis. The characteristics of these individuals, including age, duration of follow-up, CD4 count and presence of sexually transmitted infections are described in Table 6.1.

Table 6.1. Demographics of participants in the mucosal phenotyping study.

	HIV-Negative (n=6)	HIV+ ART Naïve (n=4)	HIV+ ART Experienced (n=1)	p Value [***]
Age, years[*]	37.5	34.0	42	0.567
Duration of Sex Work, years[*]	11.0	8.0	8.0	0.357
CD4 Count[*]	--	481.5	658	--
Duration of ART, years	--	--	3	--
Chlamydia/Gonorrhea	0	0	0	--
Syphillis Serology	0	0	0	--
Contraceptive Use[**]				
None	0	1	0	--
Condom	2	1	1	--
Depo-Provera	3	0	0	--
Other	1	2	0	--

[*]Data are presented as the median
[**]Data are presented as the number of participants in each category
[***]p value from Mann-Whitney test comparing HIV-N with all HIV+
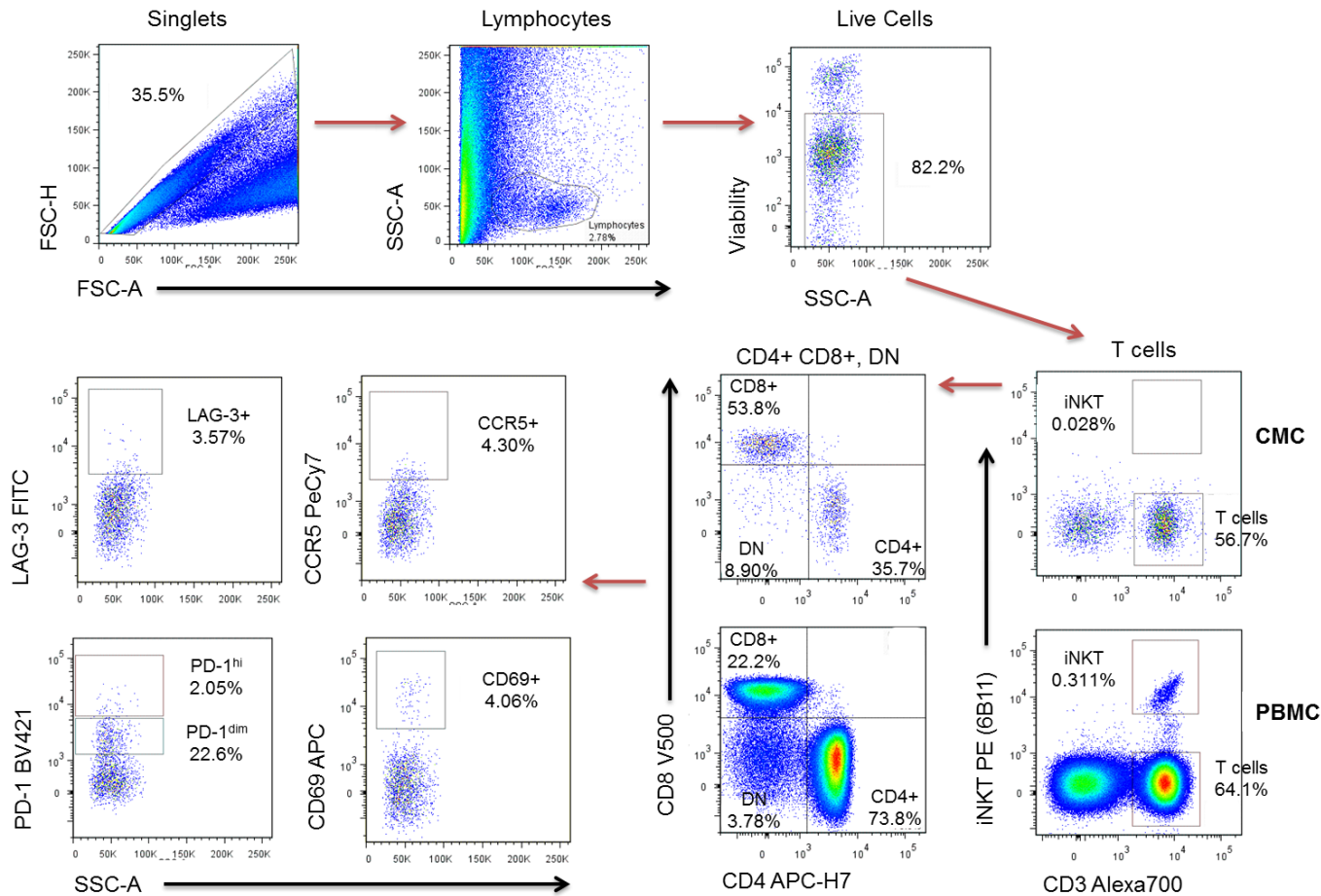
Figure 6.1. Representative staining of T cell subsets in CMC and PBMC samples. Singlets were identified by FSC-area (FSC-A) versus FSC-height (FSC-H) gating, followed by lymphocyte gating based on forward and side scatter. Live cells were identified by Live/Dead Red staining. T cells were gated as CD3+6B11(iNKT)- lymphocytes. CD4+, CD8+ and DN CD3+ subsets were identified and subsequently evaluated for expression of PD-1, LAG-3, CD69 and CCR5. Data from ML2002 (HIV-N) are shown.

6.4.2 T cell LAG-3 expression – PBMC versus CMC

Consistent with previous evaluation of T cell LAG-3 expression (Section 5.4.3), *ex vivo* LAG-3 expression was negligible on PBMC-derived CD4+ and CD8+ T cells. In contrast to PBMC, LAG-3 was significantly more likely to be expressed on both CD4+ and CD8+ T cells derived from the FGT (p=0.0273 for CD4+, p=0.0039 for CD8+, Wilcoxon) (Figure 6.2A,B). LAG-3 MFI was also significantly greater on the CMC CD8+ T cell population compared to PBMC, and trended toward a higher MFI on the CD4+ CMC subset (p=0.0645 for CD4+, p=0.0039 for CD8+, Wilcoxon) (Figure 6.2A,B), indicating greater per-cell expression of LAG-3 at the FGT. The increased expression of LAG-3 was generally consistent across all participants, regardless of HIV status.

While PBMC CD4+:CD8+ T cell ratios are largely consistent between healthy individuals, the T cell composition among CMCs can vary greatly between participants, with some samples containing the presence of a large double negative (DN) T cell population (Figure 6.1). Similar to the CD4+ and CD8+ populations, LAG-3 expression was significantly higher on mucosal DN T cells compared to systemic DN T cells (p=0.0020 for proportion, p=0.0098 for MFI, Wilcoxon) (Figure 6.2C). Surprisingly, LAG-3 expression was significantly higher on the DNT subset compared to the CD4+ T cell subset in both CMCs and PBMCs (Friedman p=0.0112, post-test p<0.01 for CMC, Friedman p=0.0002, post-test p<0.001 for PBMC) (Figure 6.2D).
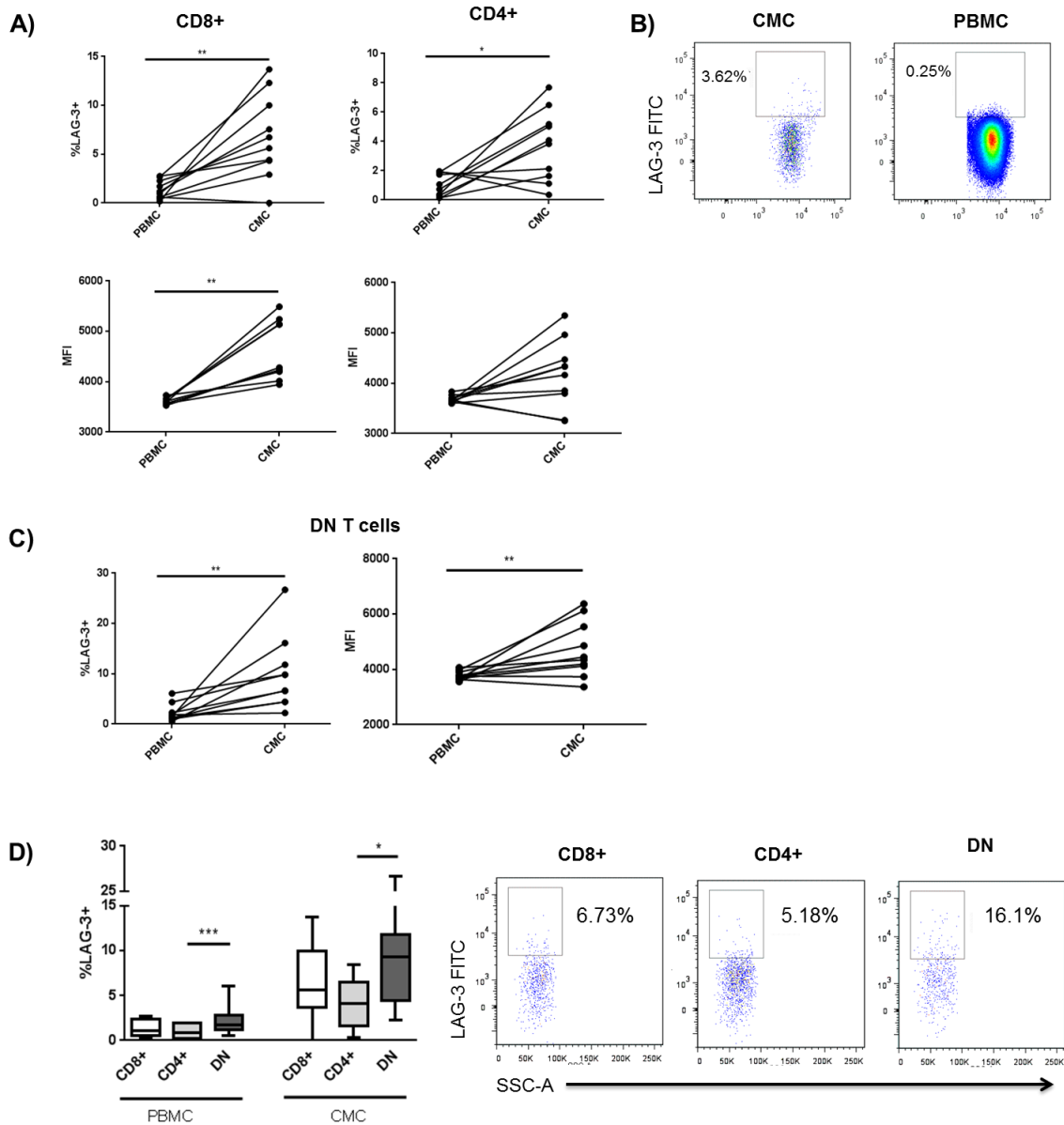
Figure 6.2. LAG-3 expression on mucosal and systemic T lymphocyte subsets. (A) The proportion of LAG-3+ cells on both CD8+ and CD4+ subsets and LAG-3 MFI on CD8+ T cells were significantly increased among CMC compared to PBMC (n=10). LAG-3 MFI on CD4+ T cells trended toward increased levels on CMC compared to PBMC. **(B)** Representative differences in expression of LAG-3 on mucosal and systemic CD3+ T lymphocytes. Data from ML2002 is shown. **(C)** LAG-3 is expressed on double negative (DN) T cells in both PBMC and CMC and is expressed at a significantly higher proportion and MFI in CMCs compared to PBMCs. **(D)** When contrasted across T lymphocyte subsets, LAG-3 expression is significantly enriched on DN T cells compared to CD4+ T cells at both the systemic and genital mucosal compartments. *p<0.05, **p<0.01, ***p<0.001.

6.4.3 CVL cytokine/chemokine expression and LAG-3

The cytokine/chemokine milieu at the FGT impacts the recruitment of T cells to the genital mucosa and can provide important information about HIV susceptibility (118). To determine whether mucosal LAG-3 expression was associated with a pro-inflammatory or Th17-biased immune environment, CVL levels of cytokines/chemokines were quantified by cytokine bead array. The elevation of LAG-3 expression at the FGT could be associated with chemokine-induced T cell migration, or elevated immune activation due to a pro-inflammatory cytokine environment. As previously described, T cell LAG-3 expression may be induced by IL-12 and IFNγ. Additionally, Th17 responses at the FGT are known to be related to susceptibility to HIV infection (294), so IL-17, IL-22 and IL-23 were included in the panel. Pro-inflammatory cytokines measured included IL-8, MCP-1, MIP-3α, IL-1β, IL-6 and TNFα. Chemokines included MIP-1α and MIP-1β. NK, and to some extent NKT, cells can be regulated by IL-15. Analytes measured therefore included IL-8, IL-15, sCD40L, IP-10, MCP-1, MIP-1α, MIP-1β, IL-1α, IFNα2, IL-17F, IFNγ, IL-10, MIP-3α, IL-12p70, IL-17A, IL-22, IL-1β, IL-2, IL-23, IL-6, IL-17E, and TNFα. IL-15, IL-17F, IFNγ, IL-10, IL-12p70, IL-17A, IL-22, IL-2, IL-23, and IL-17E were not detectable in CVL, and were not included in future analyses.

CVL cytokines and chemokines did not appear to be major predictors of LAG-3 expression at the genital mucosa. Only IL-8, IP-10, MCP-1 and IL-1α were detected above the limit of detection in more than half of the samples, and of those, none

155

correlated with LAG-3 expression on bulk CD3+ T cells, CD4+ T cells, CD8+ T cells or DN T cells (Table 6.2).

6.4.4 Double Negative T cell phenotypes at the FGT

The DN T cell population at the genital mucosa is not well characterized. Notably, the frequency of DN T cells at the genital tract was significantly higher than in matched peripheral blood samples (p=0.0098, Wilcoxon) (Figure 6.3A). Among the participants of this study, DN T cells trended toward increased expression of activation marker CD69 (p=0.0576, Friedman) and CCR5 (p=0.0867, Friedman) compared to the conventional T cell subsets (Figure 6.3B). To assess whether DN T cell recruitment to, or activation at, the genital mucosa is related to a proinflammatory or regulatory cytokine environment, we correlated DN T cell frequency and activation with cytokine/chemokine concentrations in the CVL. DN T cell frequency, which is highly variable between individuals, did not correlate with any CVL cytokines or chemokines (Figure 6.3C). DN T cell activation (as measured by CD69 expression) did not correlate with most CVL cytokines or chemokines – only a correlation with IL-1α concentration was detected (p=0.0456, r=-0.646) (Figure 6.3D).

6.4.5 T cell PD-1 expression – PBMC versus CMC

Use of the Brilliant Violet 421 fluorochrome allows for the discrimination of PD-1^{dim} and PD-1^{hi} populations in both CMC and PBMC samples (Figure 6.1). The relative proportion of PD-1 dim versus high cells varies according to CD8+ T cell memory subset (448). In contrast to LAG-3, the PD-1^{dim} population was significantly elevated only on

the CD8+ CMC T cell subset compared to PBMC (p=0.0195, Wilcoxon), although there

was also a trend toward increased PD-1 expression on the mucosal CD4+ subset

(p=0.0645, Wilcoxon) (Figure 6.4A,B). The PD-1^{hi} population was significantly enriched

both CD4+ and CD8+ mucosal T cells compared to the periphery (p=0.0137 for CD8+,

p=0.0488 for CD4+, Wilcoxon) (Figure 6.4A). Interestingly, PD-1 expression was not

elevated on FGT-derived DN T cells compared to the systemic DN T population

(p=0.7695 for PD-1^{dim}, p=0.1602 for PD-1^{hi}, Wilcoxon) (Figure 6.4C). A comparison of

the PD-1dim population between T lymphocyte subsets demonstrated no differences

among PBMC subsets and significantly decreased expression on DN T cells compared to

CD8+ T cells at the mucosa (Friedman p=0.3159 for PBMC, Friedman p=0.0112, post-

test p<0.01 for CMC) (Figure 6.4D).

Similarly, the PD-1^{hi} population was significantly lower among DN T cells compared to

CD4+ T cells within CMCs (Friedman p=0.0008, post-test p<0.01), while PD-1^{hi}

expression differed only between CD4+ and CD8+ T cells in the periphery (Friedman

p=0.0034, post-test p<0.01) (Figure 6.5A,B). The decreased PD-1 expression on DN T

cells at the FGT compared to other T cell subsets stands in direct contrast to the

enrichment of LAG-3 on this lymphocyte population.

Due to its relatively low expression on *ex vivo* PBMC, LAG-3 exhibited the highest fold

change in expression between CMCs and PBMCs compared to PD-1^{hi} and PD-1^{dim}

populations (Figure 6.5C). On DN T cells, the fold change in LAG-3 expression was

significantly greater than the PD-1^{dim} population (Friedman p=0.0179, post-test p<0.05),

but a similar trend was observed for both CD8+ and CD4+ T cell subsets (Friedman

p=0.0665 for CD8+, p=0.0781 for CD4+).

Table 6.2. Correlations between cervical vaginal lavage cytokines/chemokines and T lymphocyte LAG-3 expression. IQR, inter-quartile range.

Cytokine/ Chemokine	N Detectible (Total n=11)	Median [IQR] (pg/mL)	Spearman p value			
			CD3+	CD4+	CD8+	DN
IL-8	6	400.1 [213.2, 1089]	0.297	0.242	0.919	0.419
sCD40L	3	4.95 [4.95, 12.5]	-	-	-	-
IP-10	8	120.5 [60.71, 285.3]	0.272	0.380	0.613	0.407
MCP-1	9	12.73 [4.499, 34.08]	0.707	0.133	0.537	0.235
MIP-1α	4	3.10 [3.10, 10.06]	-	-	-	-
MIP-1β	4	2.4 [2.4, 9.141]	-	-	-	-
IL-1α	8	58.34 [10.95, 137.0]	0.299	0.506	0.110	0.204
IFNα2	3	2.4 [2.4, 7.255]	-	-	-	-
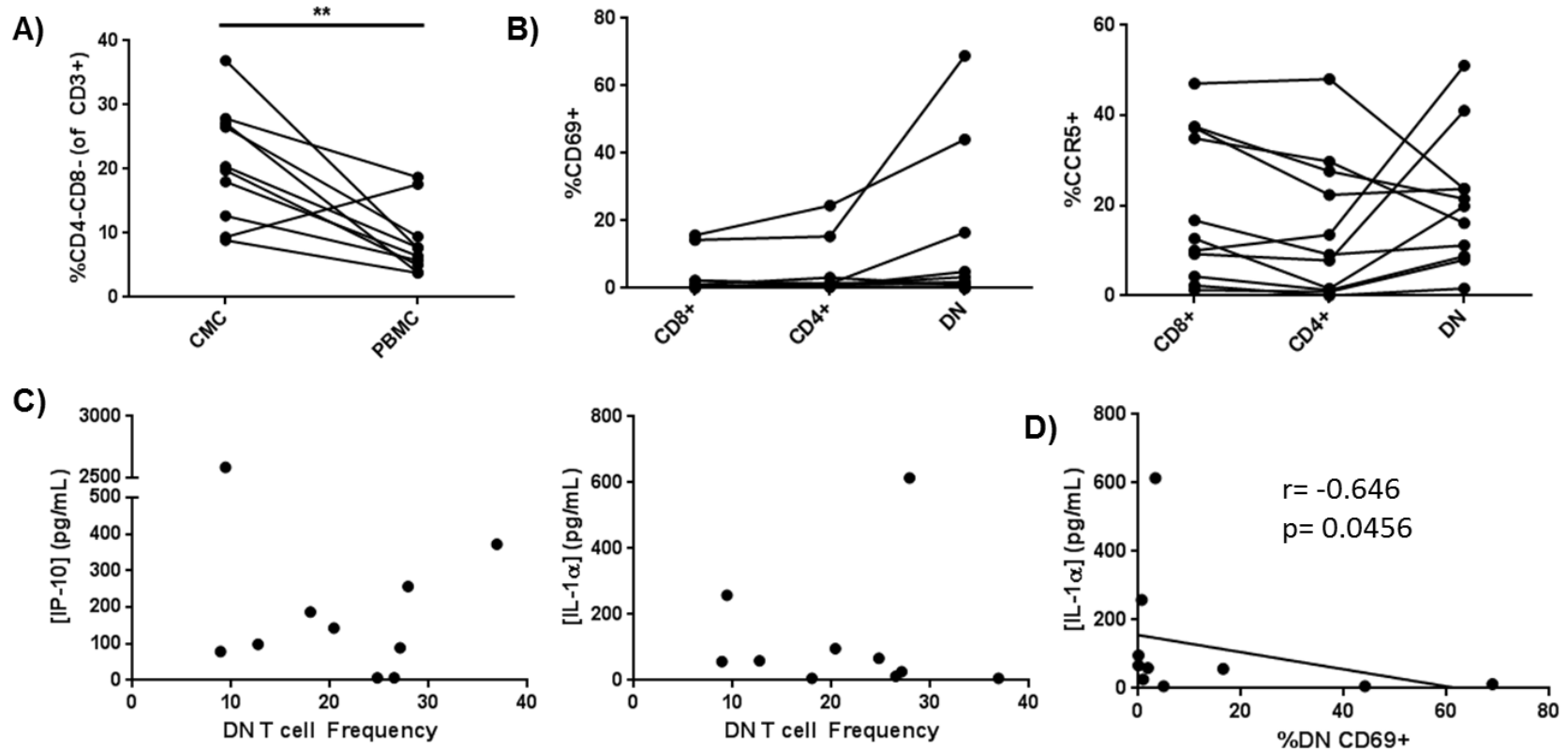
Figure 6.3. Characteristics of mucosal double negative (DN) T cells. (A) DN T cell frequency was significantly higher among CMC samples compared to matched PBMC samples. **(B)** DN T cells exhibited a trend toward increased expression of activation marker CD69 compared to CD4+ and CD8+ T lymphocyte subsets. CCR5 expression was similar across lymphocyte subsets. **(C)** DN T cell frequency at the genital mucosa did not correlate with CVL cytokines or chemokines. Representative plots for IP-10 and IL-1α are shown. **(D)** DN T cell activation (CD69 expression) only weakly correlated with CVL IL-1α concentration.

6.4.6 T cell LAG-3 expression – HIV+ vs HIV-N CMC

The number of participants with suitable CMC lymphocyte populations was underpowered to rigorously assess differences in LAG-3 or PD-1 expression between HIV-N and HIV+ participants, but we performed a preliminary comparison of LAG-3 expression on CD4+, CD8+ and DNT cells between these groups. HIV status did not significantly affect LAG-3 or PD-1 expression on any subset (Figure 6.6).

6.4.7 Co-expression of LAG-3 and phenotypic markers

Given that LAG-3 is known to be expressed on activated T cells in the periphery, we assessed the relationship between LAG-3 expression and T cell activation and HIV susceptibility using the markers CD69 and CCR5, as well as PD-1. Overall, there was no correlation between LAG-3 expression and CD69 or CCR5 expression (p=0.2483 for CD69, p=0.1142 for CCR5, Spearman) (Figure 6.7A), regardless of whether bulk CD3+ T cells were analysed or the CD4+, CD8+ or DN T cell subsets analysed separately.

On a per-cell basis, however, CD3+LAG-3+ T cells were more likely co-express CD69 and CCR5 than CD3+LAG-3- T cells (p=0.0186 for CD69, p=0.0020 for CCR5, Wilcoxon) (Figure 6.7B,C). Due to low cell numbers when CMC samples are sub-gated into CD3+CD4+LAG-3+CD69+ populations, analysis of the CD4+ T cell population should be interpreted with caution. Within the CD4+ T cells, however, LAG-3+ cells trended toward being more likely to co-express both CD69 and CCR5 (p=0.0645 for CD69, p=0.0840 for CCR5, Wilcoxon) (Figure 6.7D).
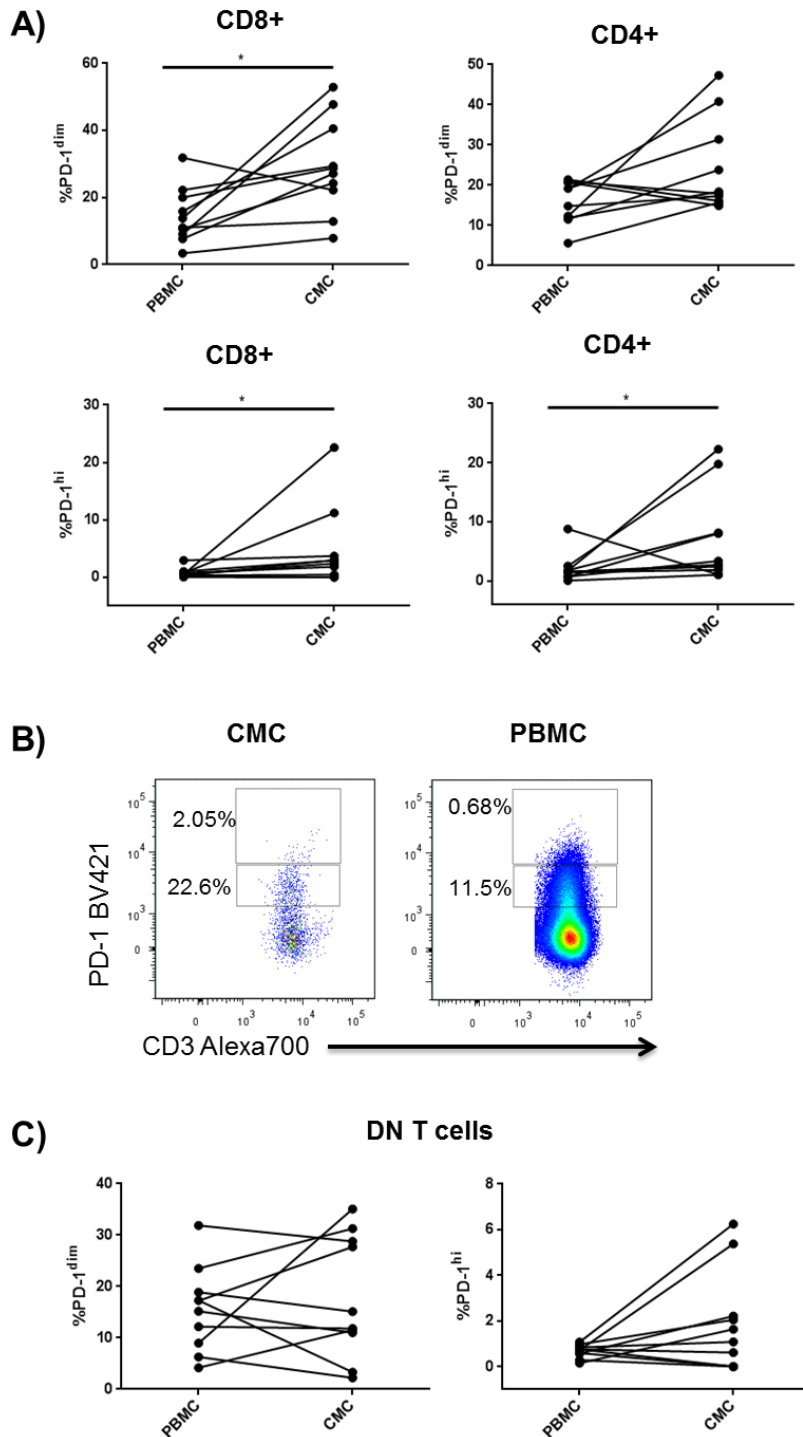
Figure 6.4. PD-1 expression on mucosal T lymphocyte subsets. (A) The proportions of CD8+ PD-1^{dim}, CD8+ PD-1^{hi} and CD4+ PD-1^{hi} cells were significantly increased at the genital mucosa compared to PBMC (n=10). **(B)** Representative differences in expression of PD-1 on mucosal and systemic CD3+ T lymphocytes. **(C)** PD-1 is expressed on double negative (DN) T cells but did not differ between systemic and mucosal compartments. *p<0.05
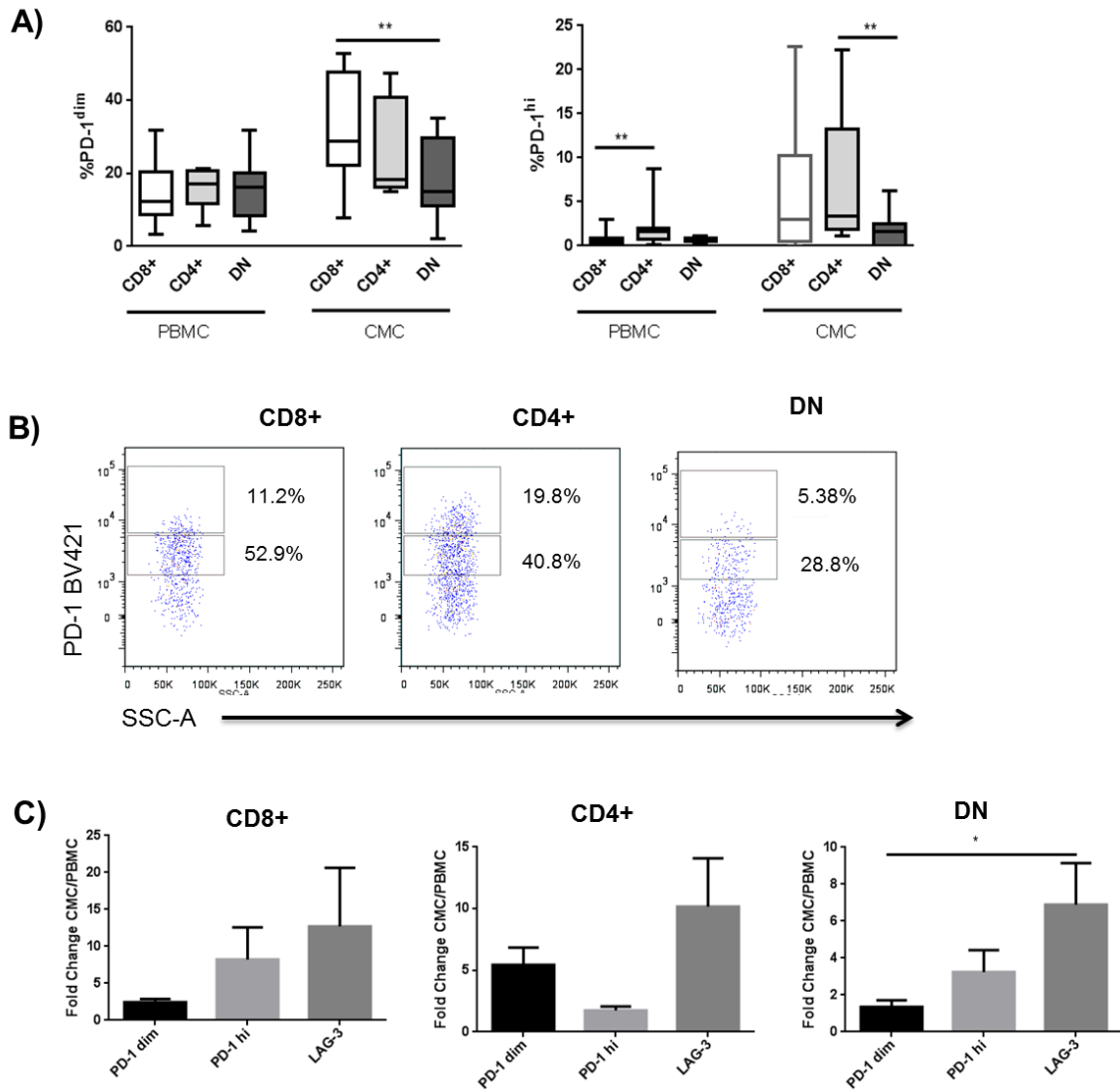
Figure 6.5 PD-1 expression across mucosal and systemic T lymphocyte subsets.
(A) When contrasted across T lymphocyte subsets, PD-1 expression is significantly reduced on DN T cells compared to CD8+ or CD4+ T cells at the systemic and genital mucosal compartments. **(B)** Representative differences in expression of PD-1 across lymphocyte subsets. **(C)** LAG-3 exhibits the greatest fold change in expression between CMCs and PBMCs on all three T cell subsets. Staining data shown is from ML2002. *p<0.05, **p<0.01.
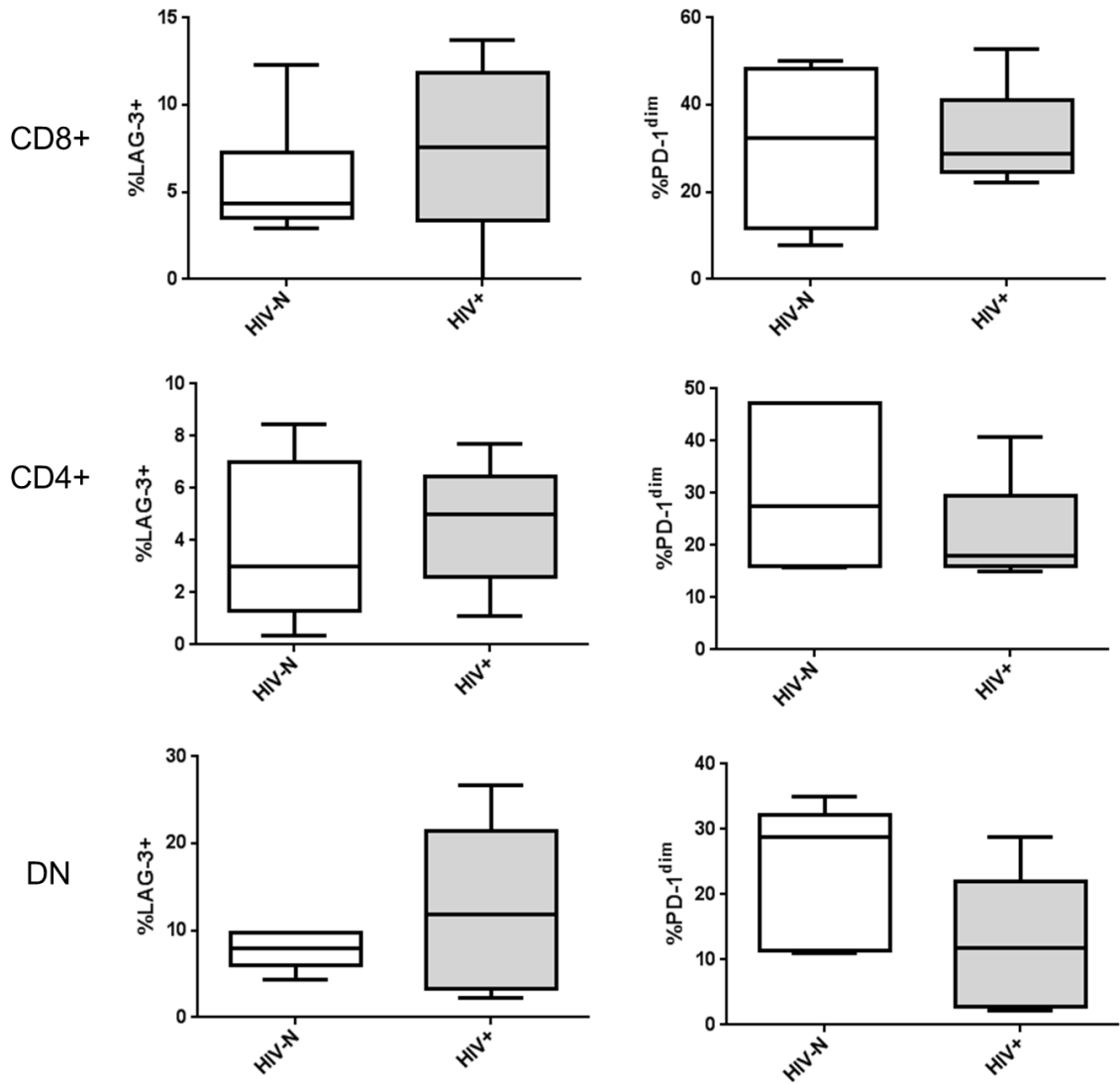
Figure 6.6. LAG-3 and PD-1 expression among HIV+ participants. There were no significant differences in either LAG-3 or PD-1 expression on either the CD8+, CD4+ or DN T cell subsets between HIV-N (n=6) or HIV-infected (n=5) women.

Unlike CD69 and CCR5, LAG-3 expression was not associated with PD-1 expression on any T lymphocyte subsets. LAG-3 did not correlate with the frequency of the PD-1^{dim} or PD-1^{hi} populations on bulk CD3+ T cells (p=0.4854 for PD-1^{dim}, p=0.3713 for PD-1^{hi}, Spearman) (Figure 6.8A) or on CD8+, CD4+ or DN T cell subsets, nor was there any significant difference in PD-1 expression between LAG-3+ and LAG-3- CD3+ T cell populations (Figure 6.8B). Indeed, co-expression of LAG-3 and PD-1 was highly variable between individuals (Figure 6.8C). While LAG-3 expression was often preferentially associated with the PD-1^{hi}, PD-1^{dim} or PD-1- subset across different individuals, it was rarely distributed evenly across all three (Figure 6.8C).

6.4.8 iNKT cells in CMC

Given the relatively high expression of LAG-3 on iNKT cells compared conventional T cells in the periphery, as well as the tissue-homing phenotype of peripheral blood iNKT cells and the recent description of gut-resident iNKT subsets, we aimed to identify an iNKT population among CMCs. Although strong and consistent iNKT 6B11 antibody staining was observed among PMBCs, no 6B11+ lymphocyte population was observed among CMCs from any participant in this study (Figure 6.9).
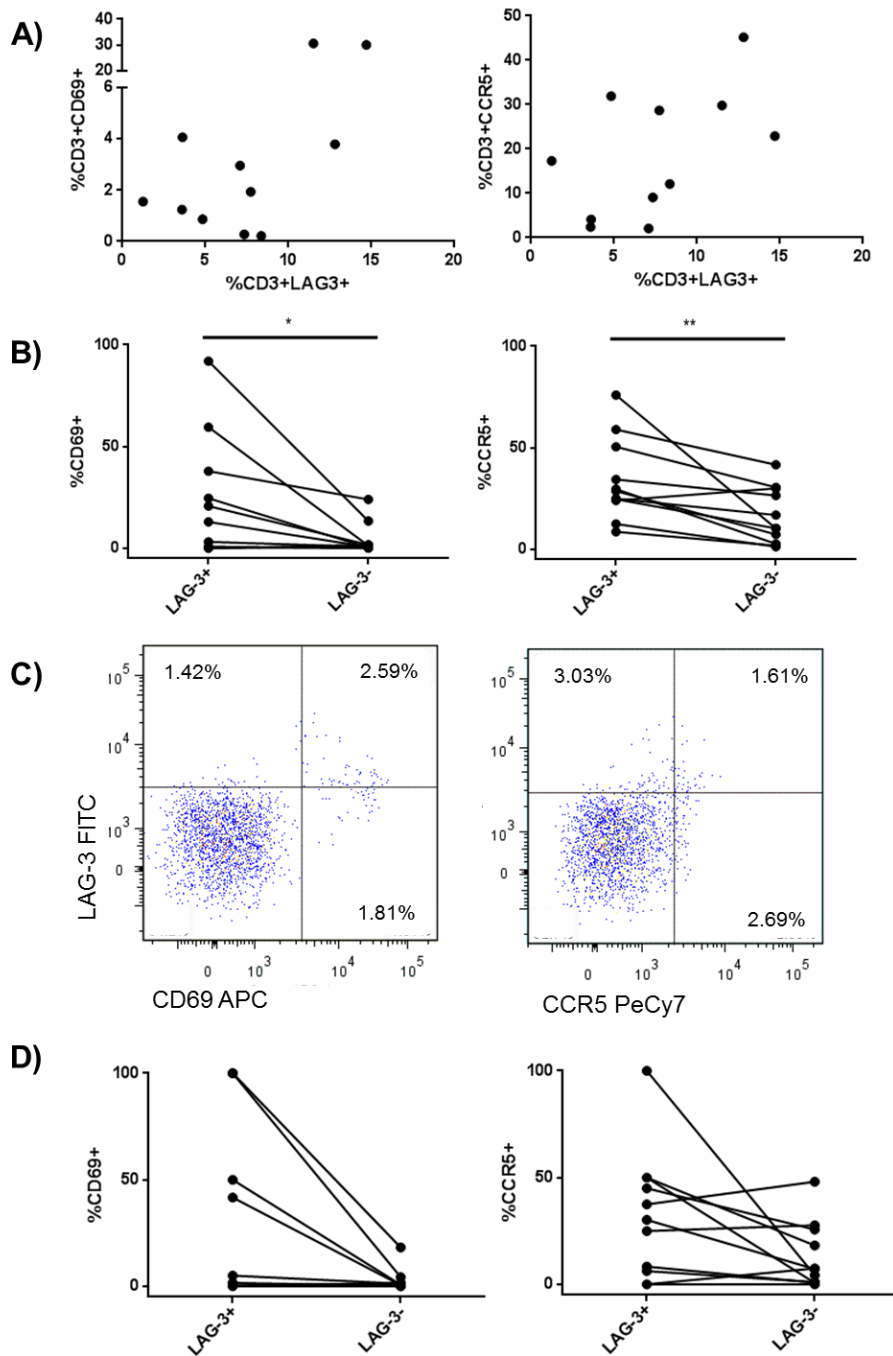
Figure 6.7. Co-expression of LAG-3, CD69 and CCR5. (A) CD3+ T cell LAG-3 expression was not correlated with either CD69 or CCR5 expression on mucosal T cells. **(B)** CD3+LAG-3+ mucosal T cells are significantly more likely to express CD69 and CCR5 compared to CD3+LAG-3- T cells. **(C)** Representative staining of LAG-3, CD69 and CCR5 co-expression. Data from ML2002 are shown. **(D)** When restricted to the CD4+ T cell subset, LAG-3+ cells trended toward being more likely to co-express CD69 and CCR5 compared to LAG-3- cells. *p<0.05, **p<0.01.
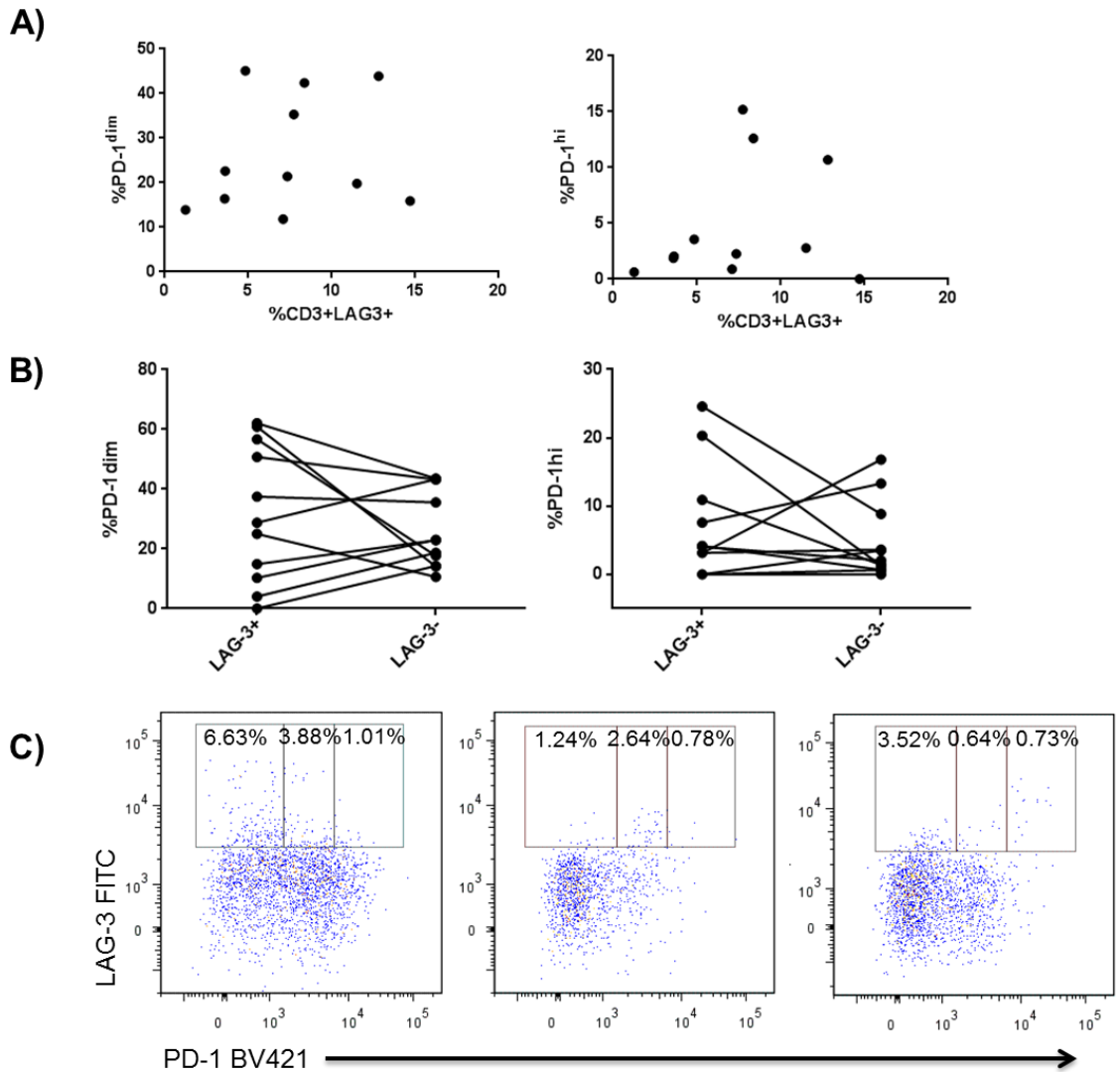
Figure 6.8. Co-expression of PD-1 and LAG-3 on mucosal T lymphocytes. (A) LAG-3 expression on CD3+ lymphocytes did not correlate with proportion of either the PD-1^{dim} or PD-1^{hi} populations. **(B)** CD3+LAG-3+ T cells were no more or less likely to be PD-1^{dim} or PD-1^{hi} than CD3+LAG-3- T cells at the genital mucosa. **(C)** Co-expression of LAG-3 and PD-1 exhibited highly variable patterns between individuals. Data from ML2002, 2540 and 4029 are shown.
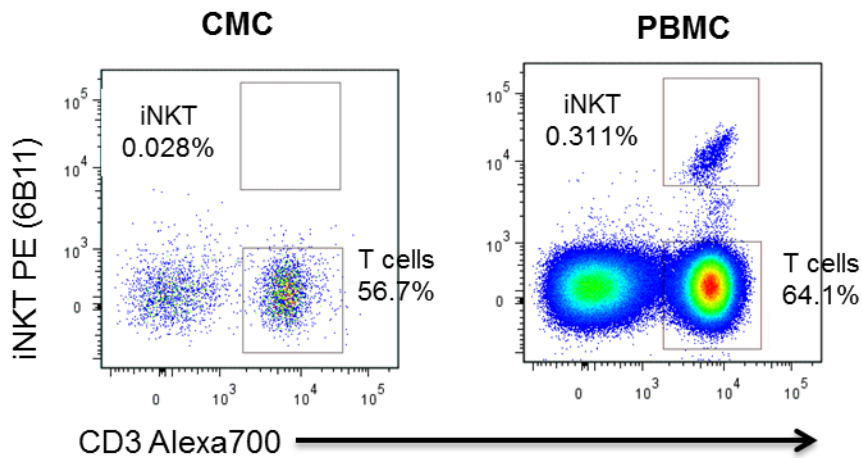
Figure 6.9. Lack of iNKT TCR among CMCs. Staining of PBMCs for the iNKT TCR (antibody 6B11) reveals a distinct CD3+6B11+ iNKT population. No such population was observed in any CMC sample from the study participants. Representative data from ML2002 (HIV-N) are shown.

6.4.9 Soluble LAG-3 expression in CVL

Concentrations of cytokines/chemokines at the FGT as measured in cervical vaginal lavage (CVL) can be important markers of mucosal inflammation and HIV susceptibility. Detection of sLAG-3 in serum/plasma has been described in several cohorts as well as elsewhere in this thesis, but quantification of sLAG-3 protein in CVL has never been reported. Using the in-house ELISA that detects sLAG-3 in plasma and cell culture supernatant, we assessed sLAG-3 secretion in CVL from 35 women recruited for the study described in chapter 7. The in-house ELISA was optimized to use a 10-point standard curve with doubling dilutions from 8ng/mL to 16pg/mL.

While plasma and culture supernatant samples routinely read on the linear portion of the standard curve, 33/35 (94%) CVL samples read below the 16pg/mL standard. The two samples with detectible readings read at the low end of the standard curve (ML3373, 38pg/mL and ML3531, 44pg/mL). Although ML3373 is HIV+, ML3531 is uninfected, making a link between HIV infection and sLAG-3 detection unlikely.

6.5 Summary

The aim of this study was to determine whether LAG-3 expression was enriched at the female genital mucosa compared to peripheral blood. LAG-3 expression was indeed significantly higher among CD4+, CD8+ and DN T cells derived from CMC samples compared to PBMC lymphocytes. In both the mucosal and systemic compartments, LAG-3 expression was highest on DN T cells, in contrast to PD-1. Although LAG-3 and PD-1 were not consistently co-expressed on mucosal T cells, LAG-3+ cells were

significantly more likely to express CD69 and CCR5 compared to LAG-3- cells. This suggests that LAG-3 may be a marker of HIV-susceptible cells at the genital tract. Soluble LAG-3 was not detectible in most CVL samples collected, and was not associated with the presence of HIV infection. Overall, these data support a role for LAG-3 in regulating mucosal immunity in healthy and HIV+ women.

7. Association of LAG-3 expression with iNKT cytokine production

7.1 Rationale

The most striking impact of HIV infection on peripheral blood lymphocyte LAG-3 expression was observed on the iNKT subset (as demonstrated in 5.4.5). Although the inhibitory activity of LAG-3 following expression on activated T cells has been previously described, the function of other inhibitory receptors such as Tim-3 on T cells and NK cells is not always consistent. Given the positive association between LAG-3 expression and iNKT activation as measured by CD69 expression, it remained unclear whether LAG-3 upregulation could contribute to the dysfunction of the iNKT subset reported during chronic infection. A previous study reported increased expression of PD-1 on iNKT cells among HIV+ individuals, but found that PD-1 expression was not associated with iNKT cytokine production, and blockade of PD-1 signaling failed to reverse defects in iNKT cytokine production or proliferation (338). We therefore sought to clarify the expression kinetics of LAG-3 following iNKT activation and the impact of LAG-3 and PD-1 expression on iNKT cytokine production and proliferation.

7.2 Hypothesis

Both LAG-3 and PD-1 are elevated on iNKT cells derived from HIV-infected women, but only LAG-3 regulates iNKT cytokine production. ART does not restore the phenotype or function of iNKT cells to that of HIV-uninfected participants.

7.3 Objectives

1. Quantify iNKT phenotype and cytokine secretion following αGalCer and PMA/Ionomycin stimulation.

2. Correlate surface LAG-3 expression with αGalCer-induced expression of IFNγ and TNFα among healthy and HIV+ individuals.

3. Correlate surface LAG-3 expression with αGalCer-induced cytokine/chemokine secretion in 5 day PBMC cultures

7.4 Results

7.4.1 Study Population

iNKT phenotype and function was assessed in participants from the FSW cohort. A total of 17 HIV-uninfected, 9 HIV+ ART naïve, and 17 HIV+ ART experienced women were recruited. The characteristics of these groups, including age, duration of sex work, CD4 count and duration of ART are described in Table 7.1.

Table 7.1. Characteristics of subjects included in the iNKT function study.

Variable[*]	HIV- Negative	HIV+ ART Naïve	HIV+ ART Experienced	p Value[**]
Age, years	40 (34, 44.5)	35 (29, 41)	40 (34.5, 44)	0.522
Duration of sex work	10 (6.5, 12)	9 (5, 14)	11 (8, 20)	0.324
CD4 Count	--	475.5 (321, 618)	526.5 (407, 698)	0.297
Duration of ART	--	--	3 (3, 5.5)	--

[*]Data are presented as median (IQR)
[**]Groups were compared by Kruskal-Wallis test (age, duration of sex work) or Mann-Whitney test (CD4 count)

7.4.2 Ex vivo iNKT LAG-3 and PD-1 expression

Ex vivo iNKT expression of LAG-3 and PD-1 were determined by flow cytometry

(Figure 7.1). Consistent with previous observations, LAG-3 expression was elevated on

the iNKT subset during HIV infection (p=0.008, Kruskal-Wallis), with post-tests

revealing significant differences between the HIV-N and HIV+ ART experienced groups

(p<0.01) (Figure 7.2A). In contrast, PD-1 expression was similar across groups, with only

a trend toward decreased PD-1 expression in the HIV+ ART experienced group that did

not reach statistical significance (p=0.085) (Figure 7.2A). Among all participants, iNKT

LAG-3 expression inversely correlated with PD-1 expression (p=0.017, r=-0.3815,

Spearman's), a relationship that persisted as a trend among HIV-infected women

(p=0.098, Spearman's) (Figure 7.2B).

The relationship between PD-1 and LAG-3 expression, and even PD-1 expression itself,

on iNKT cells was distinct from the conventional CD8+ T cell subset. PD-1 expression

on the iNKT subset was significantly higher than on CD8+ T cells among all participants

(p<0.0001, Wilcoxon) or when stratified by HIV status (p<0.0001 for both HIV-N and all

HIV+, Wilcoxon) (Figure 7.2C). Unlike the iNKT subset, PD-1 expression was

significantly elevated on CD8+ T cells among HIV+ ART naïve participants compared to

healthy controls (p=0.016, Mann Whitney) and no correlation between CD8+ T cell

LAG-3 and PD-1 expression was observed among HIV+ participants (p=0.971,

Spearman's) (Figure 7.2D).

Among HIV+ participants, iNKT LAG-3 expression did not correlate with CD4 count (p=0.9148, Spearman's), while iNKT PD-1 expression trended toward an inverse correlation with CD4 count (p=0.059, Spearman's) (Figure 7.2E).

7.4.3 Correlations between plasma cytokine/chemokine milieu, soluble LAG-3 and iNKT surface LAG-3 and PD-1 expression

To determine whether iNKT phenotype reflected pro-inflammatory or Th17-biased immune environments, plasma levels of cytokines/chemokines were quantified by cytokine bead array. Analytes measured included IL-8, IL-15, sCD40L, IP-10, MCP-1, MIP-1α, MIP-1β, IL-1α, IFNα2, IL-17F, IFNγ, IL-10, MIP-3α, IL-12p70, IL-17A, IL-22, IL-1β, IL-2, IL-23, IL-6, IL-17E, and TNFα. IL-1β, IL-2, IL-17E, IL-10, IL-1α, MIP-1α and IL-15 were not detectible in the samples, and were not included in future analyses (median concentrations are reported in Appendix 10.3)

Plasma cytokines and chemokines did not appear to be major predictors of LAG-3 or PD-1 expression on the iNKT subset. Among all participants, *ex vivo* iNKT LAG-3 expression only weakly negatively correlated with IL-8 concentration (r=-0.429, p=0.009) (Figure 7.3A). Among all HIV-infected participants, no correlations reached significance; when restricted to HIV+ ART experienced subjects, iNKT LAG-3 correlated with sCD40L concentration (r=0.593, p=0.036) (Figure 7.3B). PD-1 did not correlate with any of the analytes, regardless of whether analysis included all participants, HIV+ participants, or HIV+ ART experienced participants only.
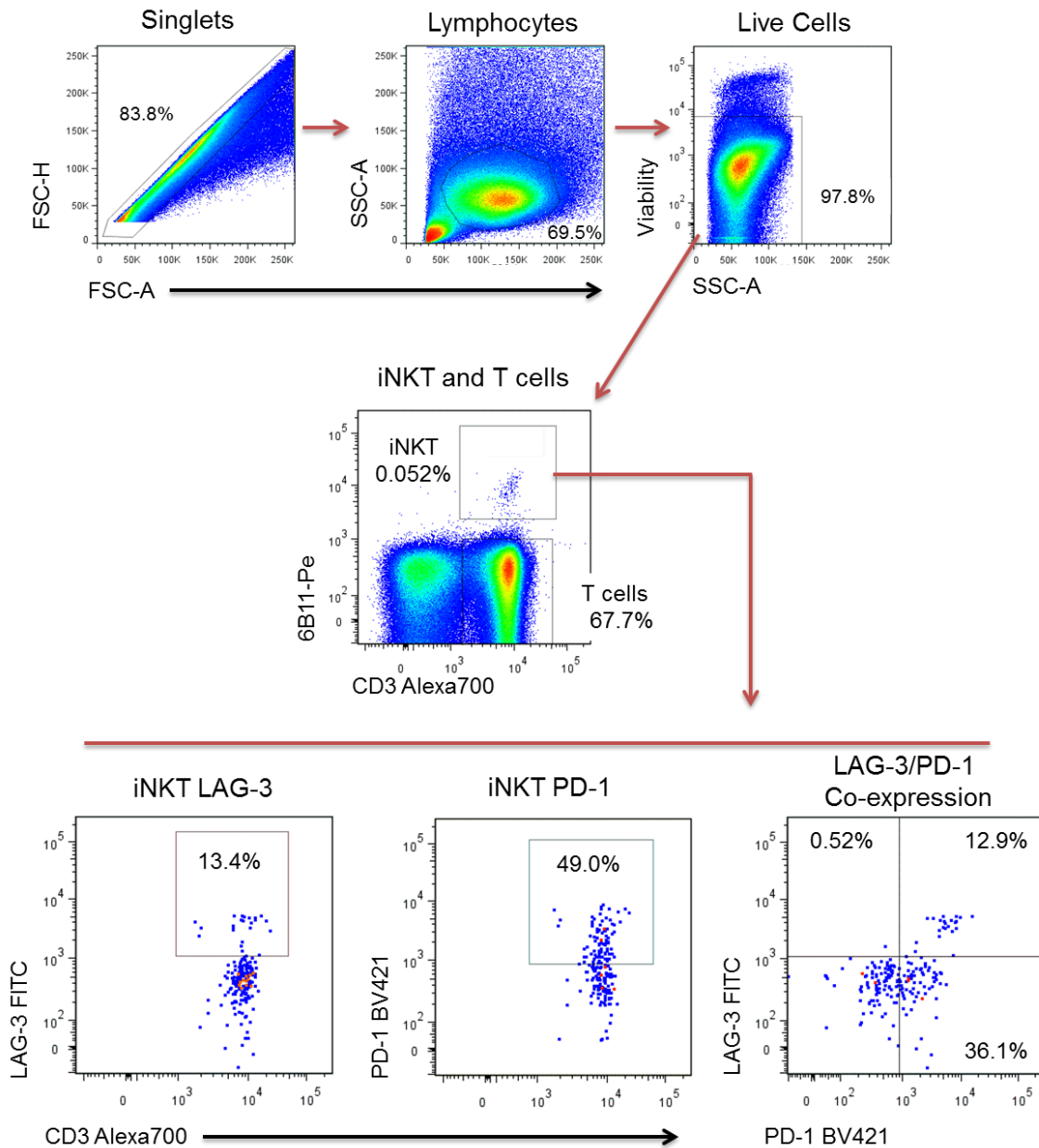
Figure 7.1. Representative staining of LAG-3 and PD-1 on iNKT cells of thawed PBMC samples. Singlets were identified by FSC-A versus FCS-H gating, followed by gating on the lymphocyte population. Dead cells were excluded by Live/Dead viability staining. iNKT cells were gated as CD3+6B11+. iNKT cells were phenotyped for LAG-3 and PD-1 expression. Data from ML2041 (HIV+ ART experienced) are shown.
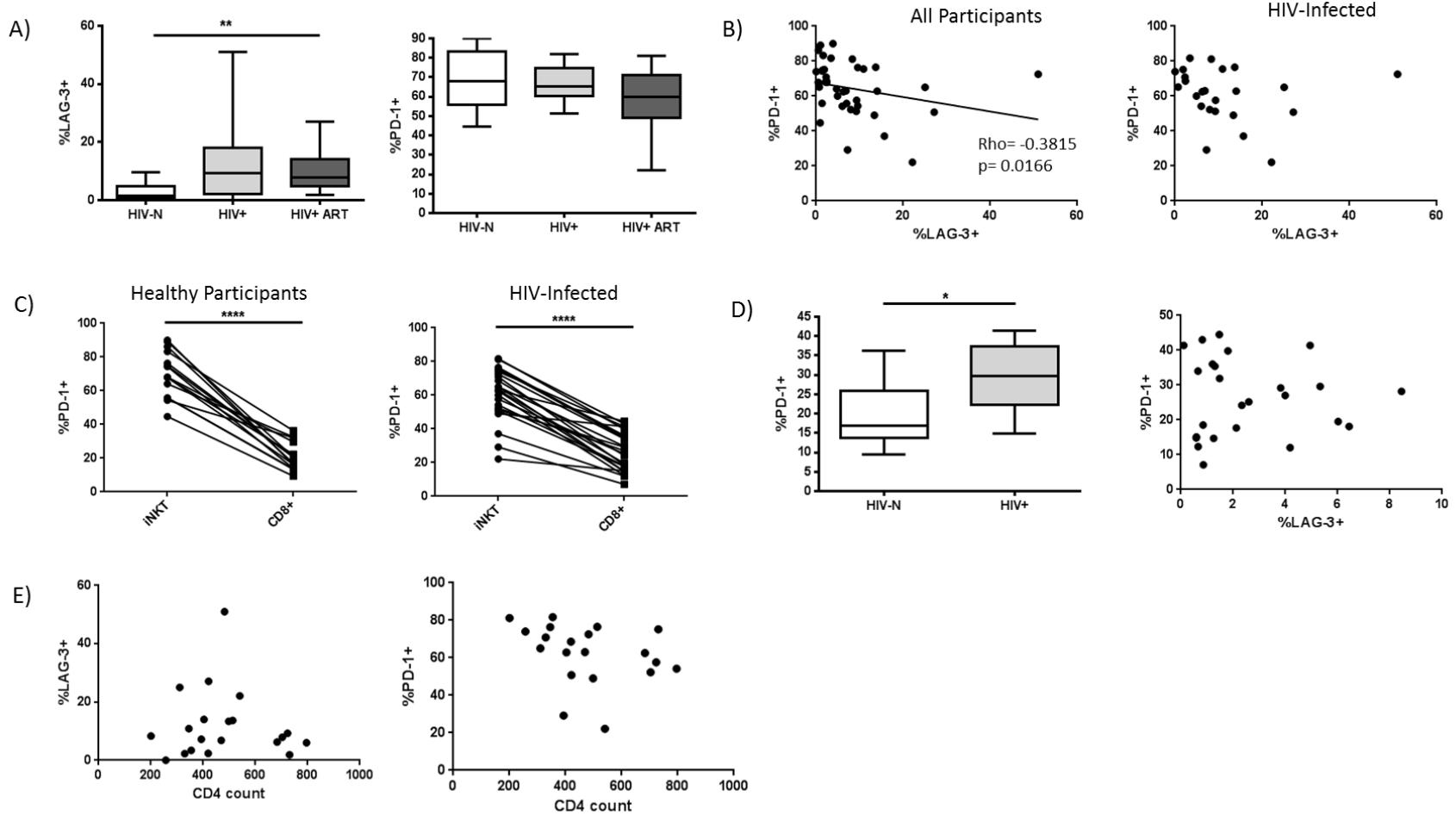
Figure 7.2. iNKT LAG-3 and PD-1 expression. (**A**) iNKT LAG-3 expression was significantly elevated among HIV+ ART participants compared to healthy controls (n=15 HIV-, 9 HIV+, 15 HIV+ ART). PD-1 expression was similar across groups, but trended toward decreased expression among HIV+ ART women. (**B**) LAG-3 expression inversely correlated with PD-1 expression on iNKT cells among all participants (n=39), and exhibited a similar trend among HIV-infected women (n=24). (**C**) PD-1 expression was

significantly elevated on iNKTs compared to conventional CD8+ T cells among both healthy (n=15) and HIV-infected (n=24) women. **(D)** Unlike the iNKT subset, PD-1 expression on CD8+ T cells was significantly elevated among HIV+ ART naïve women (n=9) compared to healthy controls (n=17), and did not correlate with LAG-3 expression. **(E)** iNKT LAG-3 expression did not correlate with CD4 count among HIV infected women (n=20), while PD-1 expression trended toward an inverse correlation with CD4 count.

sLAG-3 in plasma was quantified by in-house ELISA, and comparisons between groups were presented in section 5.4.7. Among HIV+ participants, plasma sLAG-3 did not correlate with iNKT LAG-3 or PD-1 expression (p=0.2949 and 0.8423, respectively, Spearman) (Figure 7.3C), nor did it correlate with iNKT frequency (0.4362, Spearman), suggesting that iNKT cells are not a significant source of plasma sLAG-3 during infection. Among HIV-N participants, however, sLAG-3 showed a trend toward correlation with iNKT LAG-3 expression that did not reach statistical significance (p=0.081, r=0.4679) (Figure 7.3D).

In summary, participants in this study demonstrated elevated levels of LAG-3, but not PD-1, during HIV infection and treatment. iNKT PD-1 expression was not associated with any plasma cytokines or chemokines, although iNKT LAG-3 expression did correlate with sCD40L concentrations among ART participants.

7.4.3 iNKT stimulations – Intracellular cytokine staining

To assess iNKT cytokine production, PBMC from HIV-, HIV+ and HIV+ ART experienced participants were stimulated with the iNKT lipid antigen αGalCer or PMA/Io. IFNγ and TNFα were measured by intracellular flow cytometry (Figure 7.4).

Following stimulation with αGalCer, HIV status significantly affected IFNγ production by iNKT cells (p=0.029, Kruskal-Wallis) (Figure 7.5A), with HIV+ ART naïve participants producing significantly less IFNγ compared to healthy controls (p<0.05, Dunn's post-test). IFNγ production was only partially restored among the HIV+ ART

group, as the median %IFNγ+ cells remained lower than that of healthy controls (2.43% for HIV+ ART compared to 6.82% for HIV-N and 2.06% for HIV+). TNFα production was more similar across subject groups, with only a trend toward differences in cytokine production based on HIV status (p=0.052, Kruskal-Wallis) (Figure 7.5B). Similar to the results observed for IFNγ, the HIV+ ART naïve group exhibited the lowest median cytokine production (1.29% TNFα+ for HIV+ ART naïve compared to 4.79% for HIV-N and 5.62% for HIV+ ART).

Inclusion of both TNFα and IFNγ in the same flow cytometry panel allows for the identification of single- and double-positive cytokine expressing cells. While the frequency of TNFα+IFNγ- cells was similar across all groups, HIV+ ART naïve participants responded to stimulation with significantly fewer double positive TNFα+IFNγ+ cells than healthy controls (p=0.035, Kruskal-Wallis, post-test p<0.05) (Figure 7.5C). Similarly, the HIV+ ART group exhibited significantly fewer TNFα-IFNγ+ cells in response to lipid stimulation compared to uninfected women (p=0.040 Kruskal-Wallis, Mann Whitney post-test p=0.020). HIV+ women also trended toward reduced single-positive IFNγ-producing cells (p=0.091, Mann Whitney post-test) (Figure 7.5C).
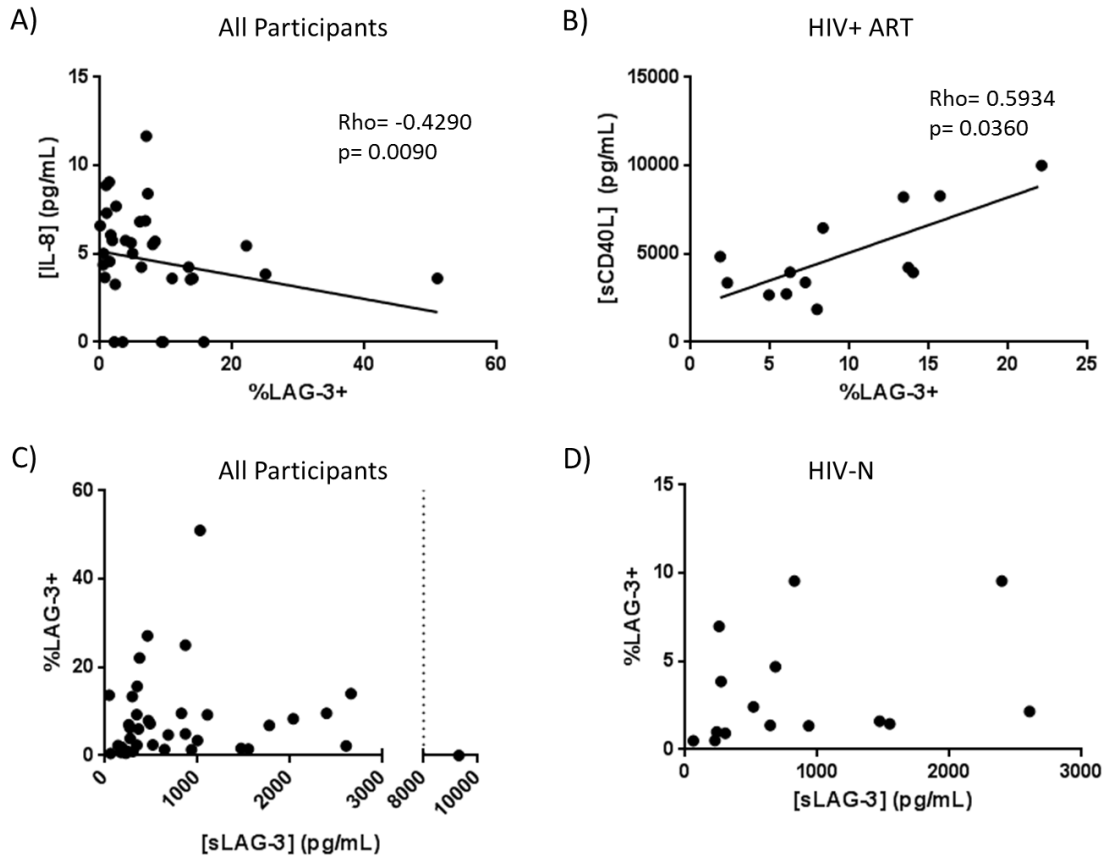
Figure 7.3. Relationship between iNKT phenotype and plasma protein concentrations. (A) *Ex vivo* iNKT LAG-3 expression inversely correlated with plasma IL-8 concentrations among all participants (n=36). **(B)** Among HIV+ ART women, iNKT LAG-3 expression positively correlated with plasma sCD40L concentration (n=13). **(C)** Among all participants, plasma sLAG-3 concentration did not correlate with iNKT LAG-3 expression (n=38). The upper limit of the sLAG-3 ELISA is denoted by a dashed line. **(D)** Among HIV-N women, plasma sLAG-3 concentration trended toward a positive correlation with iNKT LAG-3 expression (n=15).
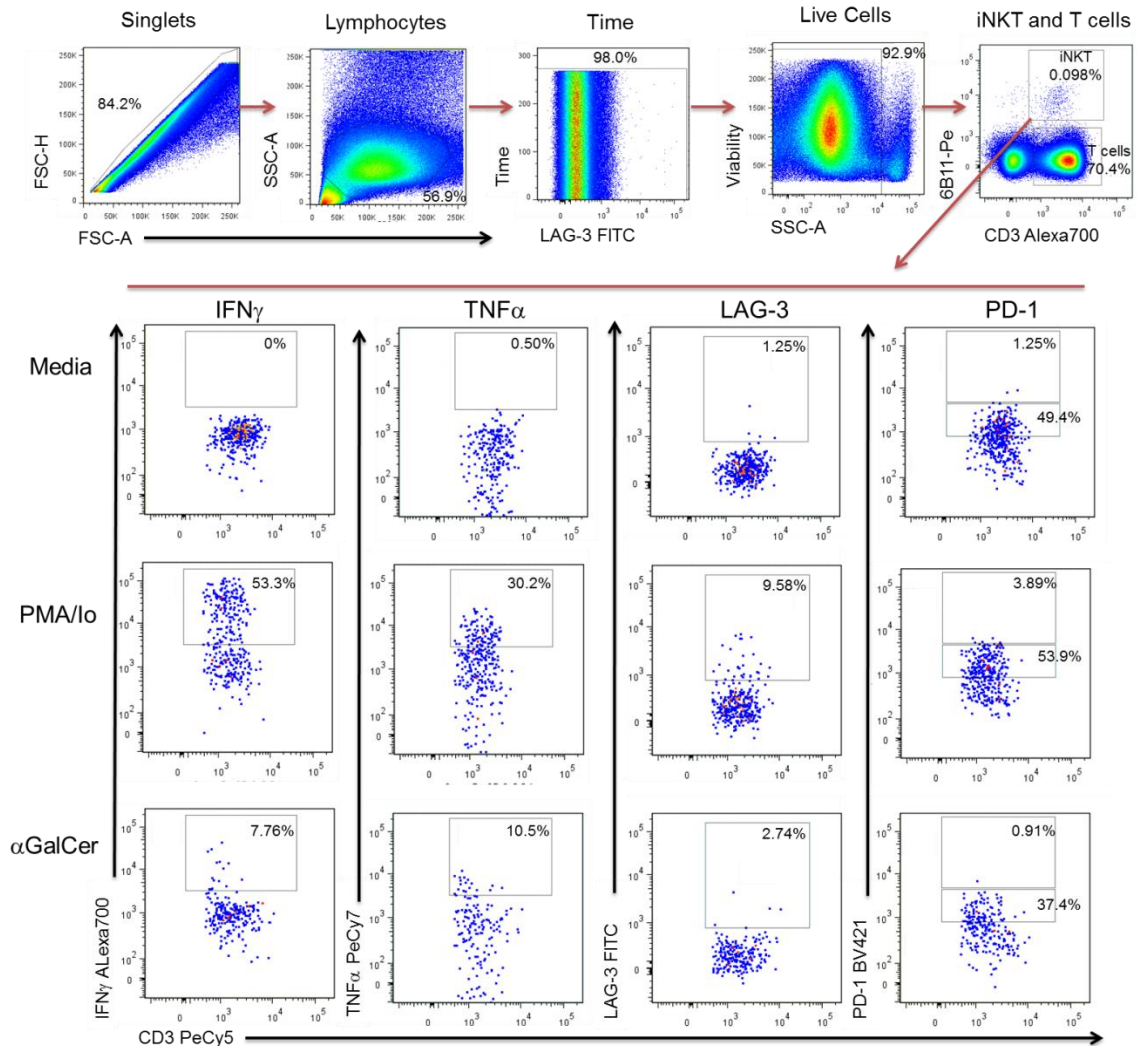
Figure 7.4. Representative surface and cytokine staining of iNKT stimulations.
Singlets were identified by FSC-A versus FCS-H gating, followed by gating on the
lymphocyte population. Aberrant fluorescence signals were excluded by gating on FITC
fluorescence over time. Dead cells were excluded by Live/Dead viability staining. iNKT
cells were gated as CD3+6B11+. Intracellular staining of IFNγ and TNFα and surface
staining of LAG-3 and PD-1 is shown for media (negative control), PMA/ionomycin and
αGalCer stimulations. Data from ML2296 (HIV-) are shown for this example.
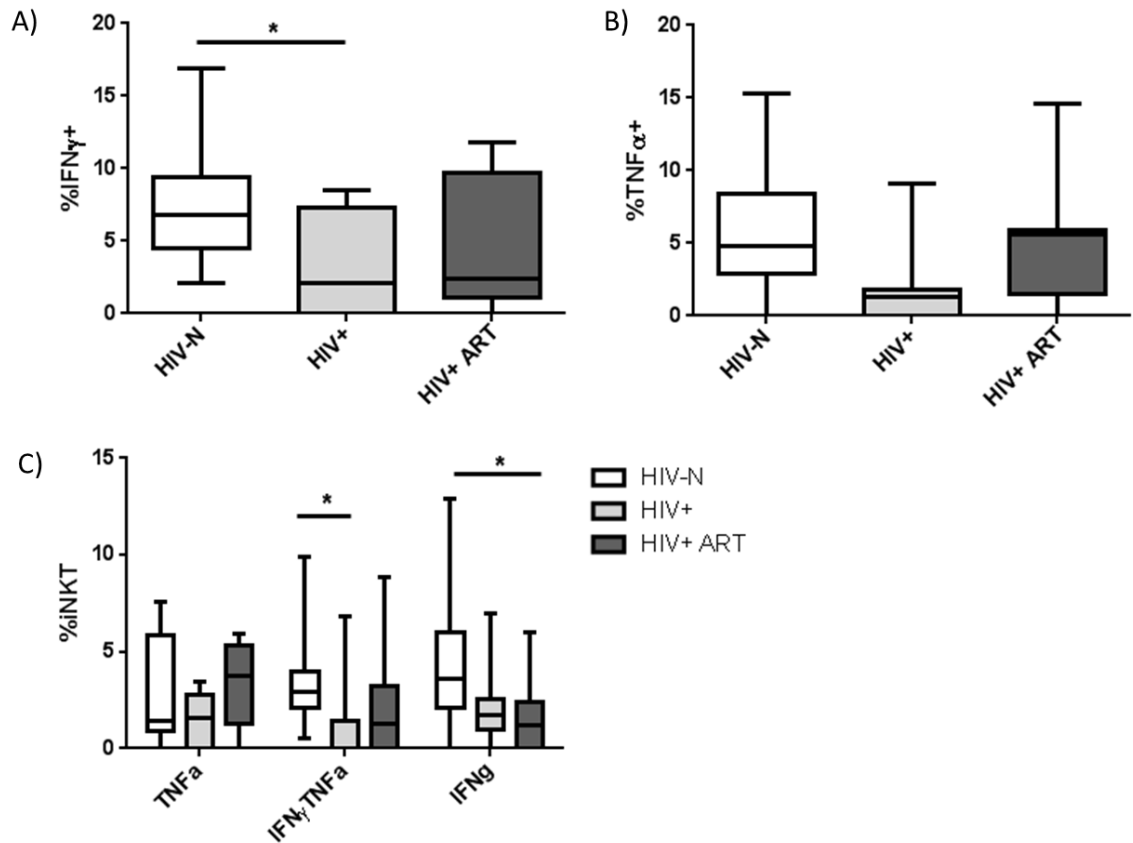
Figure 7.5. iNKT cytokine responses to αGalCer stimulation. **(A)** IFNγ production was significantly reduced among HIV+ participants compared to healthy controls (n=16 HIV-, 7 HIV+, 11 HIV+ ART). **(B)** TNFα production was similar across participant groups. **(C)** Polyfunctional analysis of αGalCer responses revealed significant decreases in IFNγ+TNFα+ and single-positive IFNγ-expressing cells among HIV-infected participants compared to healthy controls. * indicates p<0.05.

Ex vivo LAG-3 expression was associated with iNKT IFNγ, but not TNFα, secretion among HIV-infected participants. Both bulk IFNγ production and single-positive TNFα-IFNγ+ cell frequencies inversely correlated with iNKT LAG-3 expression (p=0.026, r=-0.5218, and p=0.0028, r=-0.6622, respectively, Spearman's) (Figure 7.6A). In contrast, LAG-3 expression did not correlate with bulk TNFα, TNFα+IFNγ- or TNFα+IFNγ+ responses (Figure 7.6B). *Ex vivo* PD-1 expression did not significantly correlate with either bulk IFNγ or TNFα cytokine production following stimulation (p=0.7652 and 0.8162, respectively, Spearman) (Figure 7.6C).

PMA/Io stimulation induced stronger cytokine responses compared to αGalCer among all participant groups. Interestingly, IFNγ secretion in response to PMA/Io stimulation varied significantly among groups (p=0.046, Kruskal-Wallis) (Figure 7.7A). Although no significant inter-group differences were detected by Dunn's post-test, Mann Whitney comparison of each group demonstrated significantly lower IFNγ production among both the HIV+ ART naïve and HIV+ ART groups compared to healthy controls (p=0.032 and 0.047, respectively). In contrast, PMA-induced TNFα secretion was similar among all groups (p=0.260, Krusal-Wallis) (Figure 7.7A). Analysis of polyfunctional responses to PMA/Io stimulation revealed no significant differences between participant groups other than a trend toward reduced TNFα-IFNγ+ cell frequency among HIV-infected participants (p=0.053, Kruskal-Wallis) (Figure 7.6B). *Ex vivo* LAG-3 expression did not correlate with either bulk IFNγ or TNFα production (Figure 7.7C).
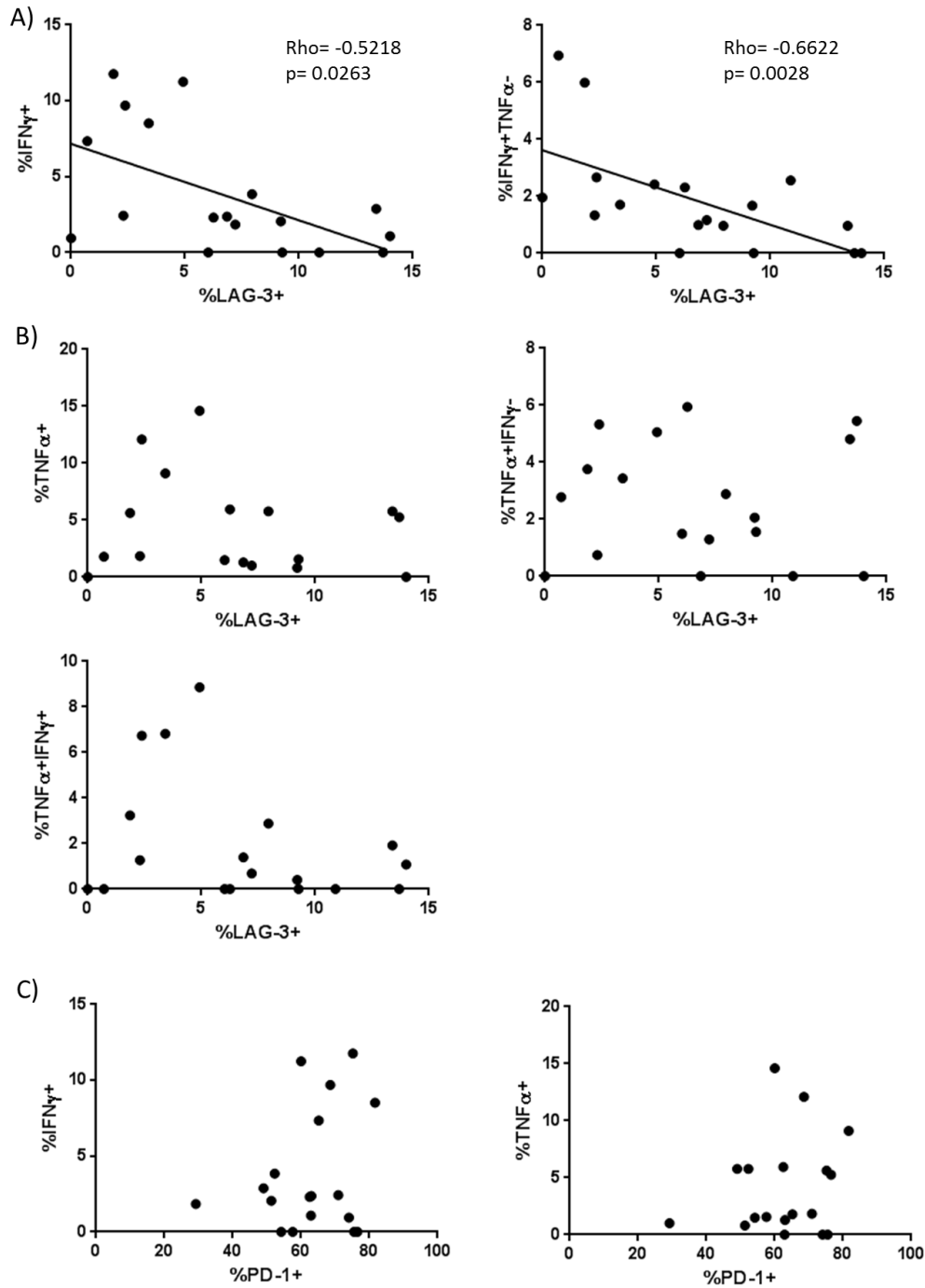
Figure 7.6. Relationship between *ex vivo* iNKT LAG-3 expression and αGalCer-induced cytokine production. (A) LAG-3 expression inversely correlated with bulk IFNγ production and single positive IFNγ+TNFα- iNKT cells among HIV-infected participants (n=18). Trend lines derived from linear regression. **(B)** LAG-3 expression was not associated with bulk TNFα production, TNFα+IFNγ- expressing cells or TNFα+IFNγ+ iNKT cells. **(C)** PD-1 expression was not associated with either IFNγ or TNFα production by iNKT cells.
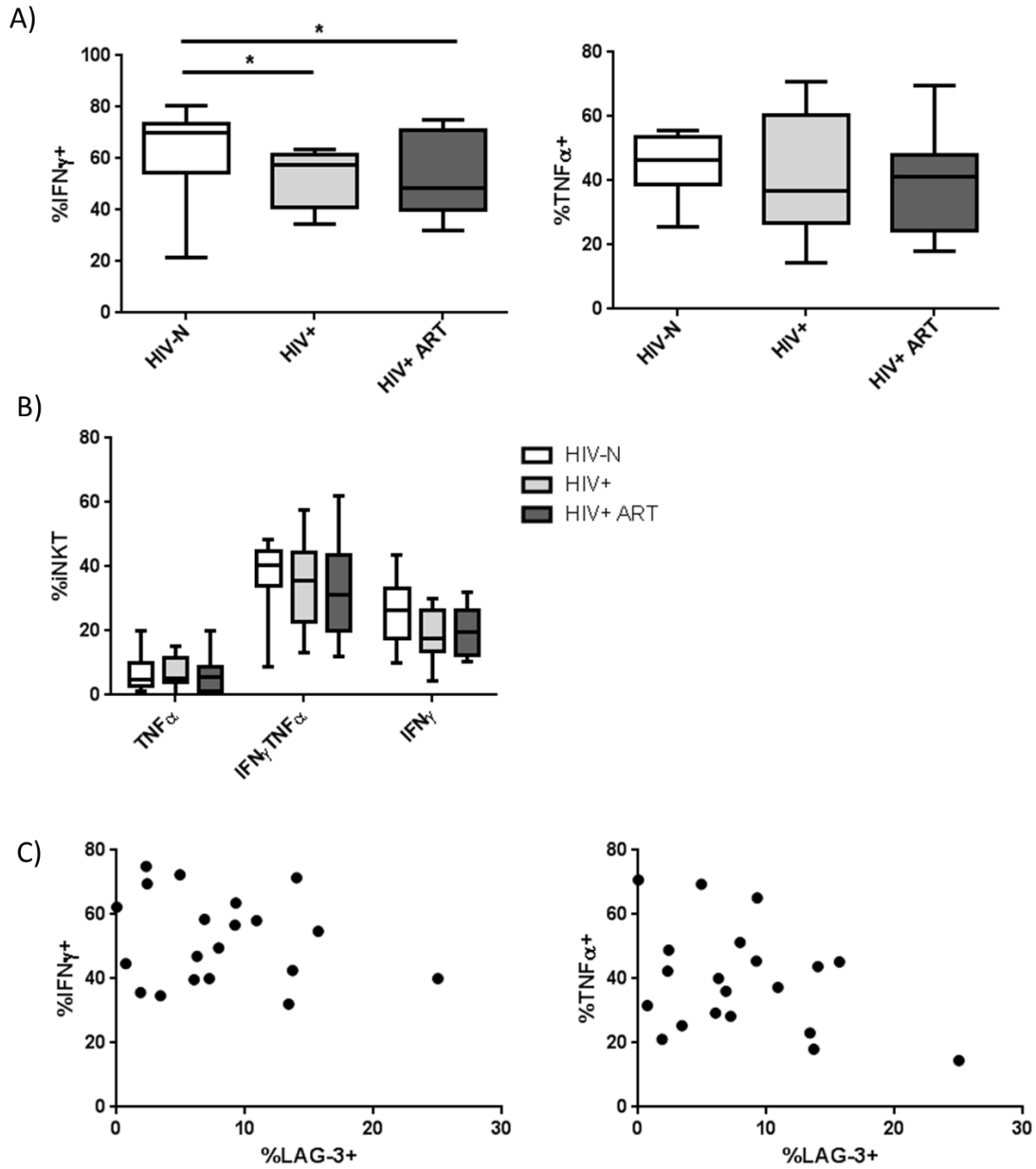
Figure 7.7. PMA/Io-induced iNKT responses. (A) PMA/Io-induced IFNγ production was significantly reduced among HIV+ (n=8) and HIV+ ART (n=12) groups compared to healthy controls (n=16), while TNFα production was similar across groups. **(B)** Polyfunctional analysis of cytokine responses revealed no significant differences in cytokine production across groups. **(C)** LAG-3 expression did not correlate with either IFNγ or TNFα production in response to PMA/Io stimulation among HIV-infected women (n=20).

In summary, αGalCer stimulation revealed defects in IFNγ and TNFα production by iNKT cells during HIV infection, while PMA stimulation demonstrated only defects in IFNγ. Baseline LAG-3 expression on iNKT cells inversely correlated with IFNγ production in response to αGalCer stimulation.

7.4.4 iNKT stimulations – Culture supernatant cytokines and chemokines

Although intracellular cytokine staining allows for the identification of individual cytokine-producing cells and their associated phenotype, the number of cytokines/chemokines analysed is limited by number of fluorescent channels available; this is especially pertinent in the case of iNKT cells, which require a high number of phenotypic markers for identification. Literature suggests, however, that iNKT cells can produce an extremely broad array of cytokines/chemokines upon stimulation (228), and it is largely unknown whether HIV infection skews the iNKT cytokine repertoire beyond a reduction in IFNγ production.

We therefore collected cell culture supernatants from 24hr and 5 day iNKT αGalCer stimulations and quantified the expression of IFNγ, IL-4, IL-10, IL-12p70, IL-13, IL-17, IP-10, MIP-1α, MIP-1β, and TNFα. IL-12 is known to play an important role in iNKT activation. With the exception of the IFN-induced protein IP-10, all other analytes have been reported to be expressed by activated iNKT cells. IL-12p70 was not detected in any samples, and is therefore not included in any analyses.

At 24 hours, very few analytes were elevated in the αGalCer-stimulated cultures relative to the unstimulated controls (Table 7.2). The most commonly expressed analytes were IL-10, MIP-1β and TNFα. Comparison of cytokine levels between groups revealed no significant differences in expression in any of these analytes (Table 7.2).

Detection of above-background cytokine expression at 5 days post-stimulation was possible for all analytes. IL-17 was expressed by a minority of participants in each group, and was excluded from further analysis. The proportion of subjects in each group demonstrating above-background expression is reported in Table 7.3. There were significant differences in the proportion of individuals with above-background IP-10 responses across groups and a trend toward differences in TNFα expression (p=0.016 and 0.104, respectively, Chi square) (Table 7.3, Figure 7.8A). In both cases, the HIV+ ART experienced group was less likely to exhibit the cytokine/chemokine response compared to the HIV-N and HIV+ ART naïve groups.

The background-subtracted concentration of each analyte is reported in Table 7.3; significant differences across groups were detected for IFNγ, IL-13 and IP-10 (p=0.009, 0.031 and 0.004, respectively, Kruskal-Wallis) (Figure 7.8B). Post-tests revealed that inter-group differences were primarily significant for the HIV-N versus HIV+ ART experienced group comparisons (p<0.01, <0.05, <0.01, respectively, Dunn's post-test) (Table 7.3).

Table 7.2. Number of subjects with above-background cytokine responses to αGalCer at 24 hours post-stimulation.

Analyte[*]	HIV-Negative (n=15)	HIV+ ART Naïve (n=9)	HIV+ ART Experienced (n=16)	Kruskal-Wallis p
IFNγ	1	1	4	
IL-4	3	2	0	
IL-10	11 (19.09; 0.0, 71.73)	4 (0.0; 0.0, 46.64)	9 (1.62; 0.0, 191.4)	0.633
IL-13	1	0	4	
IL-17	1	1	1	
IP-10	1	1	1	
MIP-1β	6 (0.0; 0.0, 50.93)	2 (0.0; 0.0, 39.39)	7 (0.0; 0.0, 383.1)	0.546
TNFα	6 (0.0; 0.0, 1.40)	2 (0.0; 0.0, 6.01)	8 (0.0; 0.0, 16.71)	0.443

[*]Analytes with above-background expression for >1 participant in each group present include the median concentration (pg/mL); IQR in parentheses.

Given that iNKT cytokine secretion can contribute to NK, B and T cell activation, these cell types likely contributed to the cytokine/chemokine milieu by 5 days post-stimulation. If the iNKT subset contributed substantially to cytokine/chemokine production, however, then iNKT frequency should correlate with cytokine expression. Indeed, *ex vivo* iNKT frequency significantly correlated with background-subtracted expression of all analytes except IL-10 (Table 7.4, Figure 7.8C).

Among participants with supernatant data available, iNKT frequency was significantly reduced among HIV+ ART participants compared to healthy controls (p=0.015, Kruskal-Wallis, post-test p<0.05) (Figure 7.9A). Background-subtracted analyte concentrations were therefore adjusted for iNKT frequency, as well as to account for the correlation between most analyte concentrations and cell frequency. Following adjustment, significant differences in IFNγ (p=0.026, Kruskal-Wallis) and IP-10 (0.014, Kruskal-Wallis) remained, as well as a trend toward differences in IL-13 (p=0.095, Kruskal-Wallis) expression (Table 7.5, Figure 7.9B).

Table 7.3. Above-background cytokine responses to αGalCer at 5 days post-stimulation.

Analyte		HIV-Negative (n=15)	HIV+ ART Naïve (n=8)	HIV+ ART Experienced (n=14)	p value[**]	Post-test differences[***]
IFNγ	N Detectible	13	7	8	0.122	
	Concentration[*]	**262.1 (75.87, 1940)**	**34.97 (4.83, 142.7)**	**2.275, (0.0, 124.8)**	**0.009**	**HIV-N vs HIV+ ART**
IL-4	N Detectible	7	3	2	0.166	
	Concentration[*]	0.0 (0.0, 21.9)	0.0 (0.0, 6.69)	0.0 (0.0, 0.18)	0.134	
IL-10	N Detectible	4	2	6	0.570	
	Concentration[*]	0.0 (0.0, 5.31)	0.0 (0.0, 4.25)	0.0 (0.0, 13.8)	0.664	
IL-13	N Detectible	11	5	6	0.243	
	Concentration[*]	**197.9 (0.0, 424.9)**	**8.26 (0.11, 77.2)**	**0.0 (0.0, 25.45)**	**0.031**	**HIV-N vs HIV+ ART**
IP-10	N Detectible	**11**	**6**	**5**	**0.016**	
	Concentration[*]	**1453 (785.8, 5764)**	**329.3 (24.5, 5351)**	**0.0 (0.0, 409.6)**	**0.004**	**HIV-N vs HIV+ ART**
MIP-1α	N Detectible	6	4	4	0.435	
	Concentration[*]	0.0 (0.0, 163)	37.2 (0.0, 158.5)	0.0 (0.0, 75.6)	0.486	
MIP-1β	N Detectible	8	4	4	0.435	
	Concentration[*]	15.11 (0.0, 366.9)	35.06 (0.0, 165.1)	0.0 (0.0, 104.6)	0.328	
TNFα	N Detectible	**10**	**7**	**6**	**0.104**	
	Concentration[*]	21.7 (0.0, 310.7)	20.2 (4.74, 115.1)	0.065 (0.0, 140.2)	0.475	

[*]Data are presented as median (IQR) in pg/mL

[**] p values obtained from Chi squared tests for N detectible data, Kruskal-Wallis tests for concentration comparisons

[***] Dunn's post-test comparisons with p<0.05 are indicated for each significant Kruskal-Wallis result

Statistical tests with p≤0.1 (trend) are indicated in bold.

191
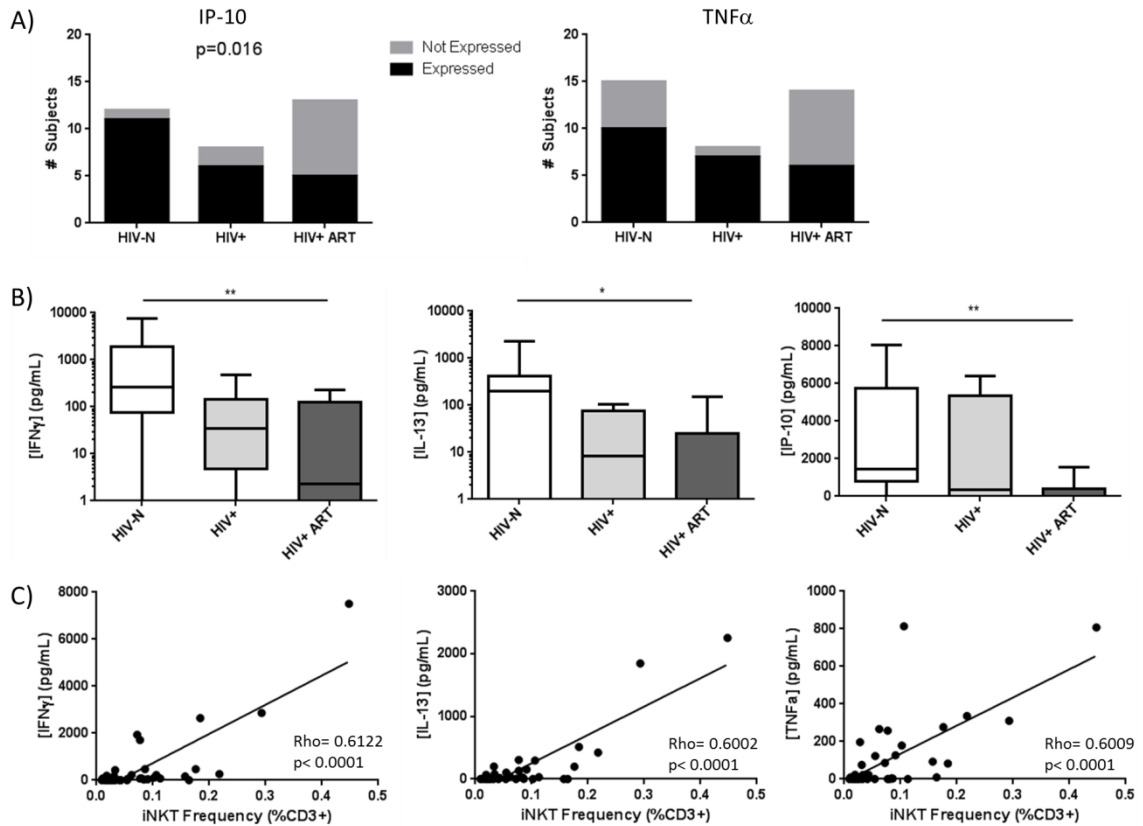
Figure 7.8. Cytokine/chemokine responses 5 days post-αGalCer stimulation among HIV-, HIV+ and HIV+ ART experienced participants. (A) The proportion of participants with IP-10 responses differed significantly across groups (n=15 HIV-, 8 HIV+, 14 HIV+ ART), while the presence of TNFα responses trended toward inter-group differences. ART-experienced participants were the least likely to exhibit a response. **(B)** The supernatant concentrations of IFNγ, IL-13 and IP-10 were significantly reduced among HIV-infected participants, particularly HIV+ ART individuals. **(C)** Correlation of *ex vivo* iNKT frequency with IFNγ, IL-13 and TNFα concentration among all participants (n=37).

Table 7.4. Correlation between *ex vivo* iNKT frequency and background-subtracted cytokine/chemokine expression.

Analyte	All participants (n=37)	
	Spearman rho	**p value**
IFNγ	**0.6122**	**< 0.0001**
IL-4	**0.3354**	**0.0424**
IL-10	0.02461	0.8850
IL-13	**0.6002**	**< 0.0001**
IP-10	**0.5119**	**0.0023**
MIP-1α	**0.3791**	**0.0247**
MIP-1β	**0.4469**	**0.0056**
TNFα	**0.6009**	**<0.0001**

Statistical tests with p<0.05 are indicated in bold.

In addition to differences in absolute levels of cytokine production, some studies have described iNKT cytokine production by expressing the contribution of each analyte as a proportion of the total cytokine production by a group (343). In this analysis, the concentration of each analyte was summed across all members of a group, and expressed as a percent of the total cytokines produced by that group (Figure 7.10). In the HIV-N group, the cytokine milieu is dominated by IP-10, IFNγ and IL-13 expression. In contrast, the HIV+ ART naïve group demonstrated a relative expansion in the contribution of IP-10, MIP-1α and MIP-1β to the total cytokine environment. Although the relative proportions of IFNγ and IL-13 were somewhat restored in the ART experienced group, there was a strong expansion in the contribution of IL-10, MIP-1α, MIP-1β and TNFα to the total cytokine/chemokine environment that did not reflect either the HIV-N or HIV+ ART naïve groups.

Correlations between cytokines/chemokines overall and within each infection group revealed differing patterns of iNKT function (Table 7.6). Among all participants, there were strong correlations between IFNγ and the IFN-induced protein IP-10 (p<0.0001, Spearman), as well as MIP-1α and MIP-1β (p<0.0001, Spearman). In fact, MIP-1α and MIP-1β expression were both tightly correlated and generally co-expressed among all participants. Notably, IFNγ, IL-13 and IL-4 significantly correlated together within the HIV-N participants, while significant correlations within the HIV+ ART experienced group revolved primarily among TNFα and MIP-1α/MIP-1β.

Table 7.5. Differences in background subtracted cytokine/chemokine concentrations adjusted for *ex vivo* iNKT frequency at 5 days post-αGalCer stimulation.

Analyte	p value[*]	Post-test significance[**]
IFNγ	**0.026**	**HIV-N vs HIV+ ART**
IL-4	0.279	
IL-10	0.636	
IL-13	**0.095**	
IP-10	**0.014**	**HIV-N vs HIV+ ART**
MIP-1α	0.513	
MIP-1β	0.328	
TNFα	0.663	

[*] p values obtained from Kruskal-Wallis tests

[**] Dunn's post-test comparisons with p<0.05 are indicated for each significant Kruskal-Wallis result

Statistical tests with p≤0.1 (trend) or <0.05 (significant) are indicated in bold.
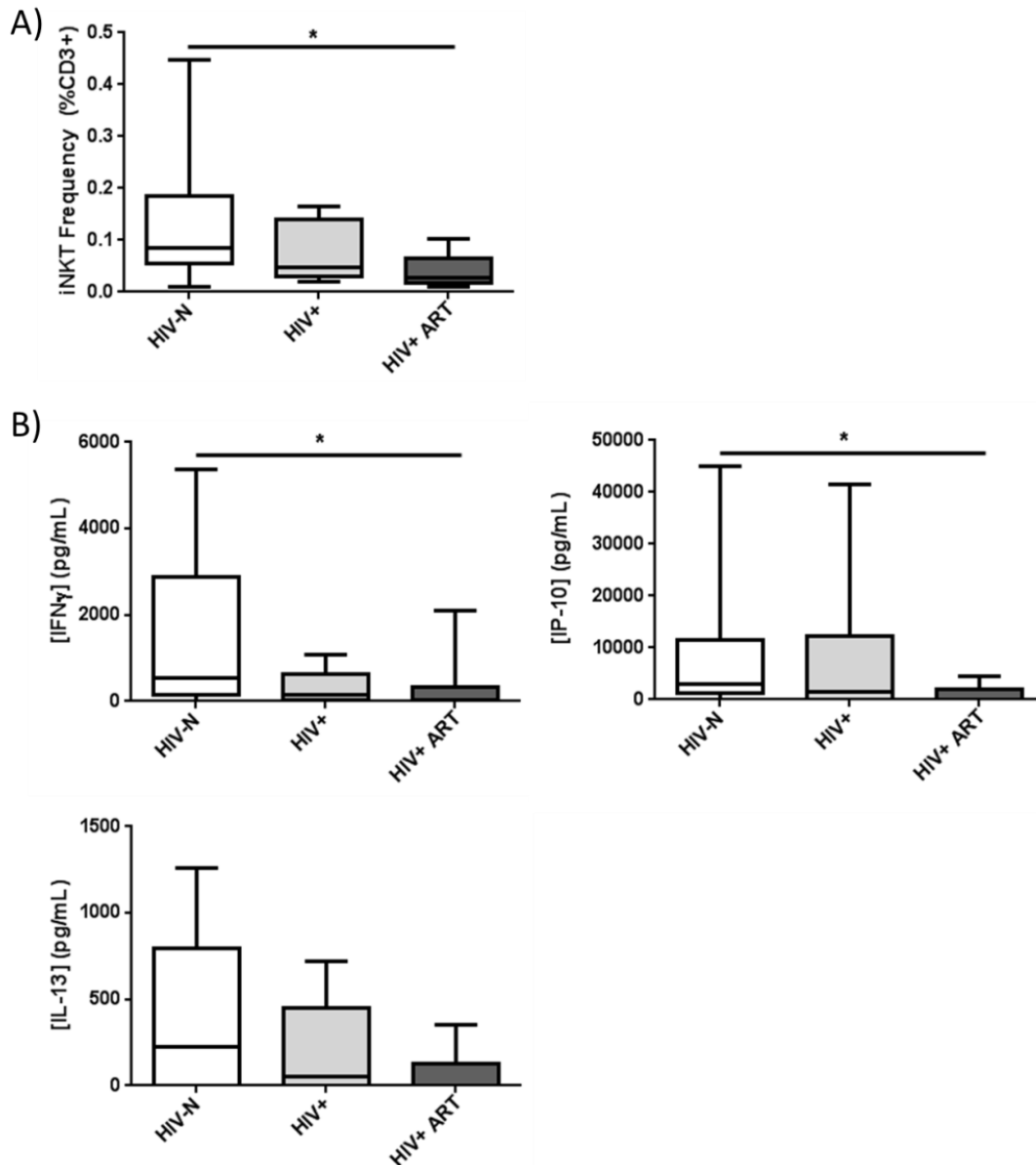
Figure 7.9. Background-subtracted αGalCer responses adjusted for iNKT frequency. (A) *Ex vivo* iNKT frequency was significantly reduced among HIV+ ART participants compared to healthy controls (n=15 HIV-, n=8 HIV+, n=14 HIV+ ART). **(B)** After adjustment for *ex vivo* iNKT frequency, expression of IFNγ and IP-10 remained significantly different between groups, while IL-13 trended toward decreased levels among HIV+ ART participants.

HIV-N

🟥	25.96%	IFNg
🟨	0.19%	IL-4
🟩	0.56%	IL-10
🟦	8.69%	IL-13
🟪	0.11%	IL-17
🟪	50.40%	IP-10
🟧	3.88%	MIP-1a
🟦	6.32%	MIP-1b
⬜	3.90%	TNFa

HIV+

🟥	3.30%	IFNg
🟨	0.08%	IL-4
🟩	4.44%	IL-10
🟦	1.13%	IL-13
🟪	0.45%	IL-17
🟪	70.66%	IP-10
🟧	10.01%	MIP-1a
🟦	7.98%	MIP-1b
⬜	1.94%	TNFa

HIV+ ART

🟥	9.28%	IFNg
🟨	0.07%	IL-4
🟩	11.29%	IL-10
🟦	4.23%	IL-13
🟪	2.09%	IL-17
🟪	37.53%	IP-10
🟧	8.60%	MIP-1a
🟦	16.38%	MIP-1b
⬜	10.52%	TNFa
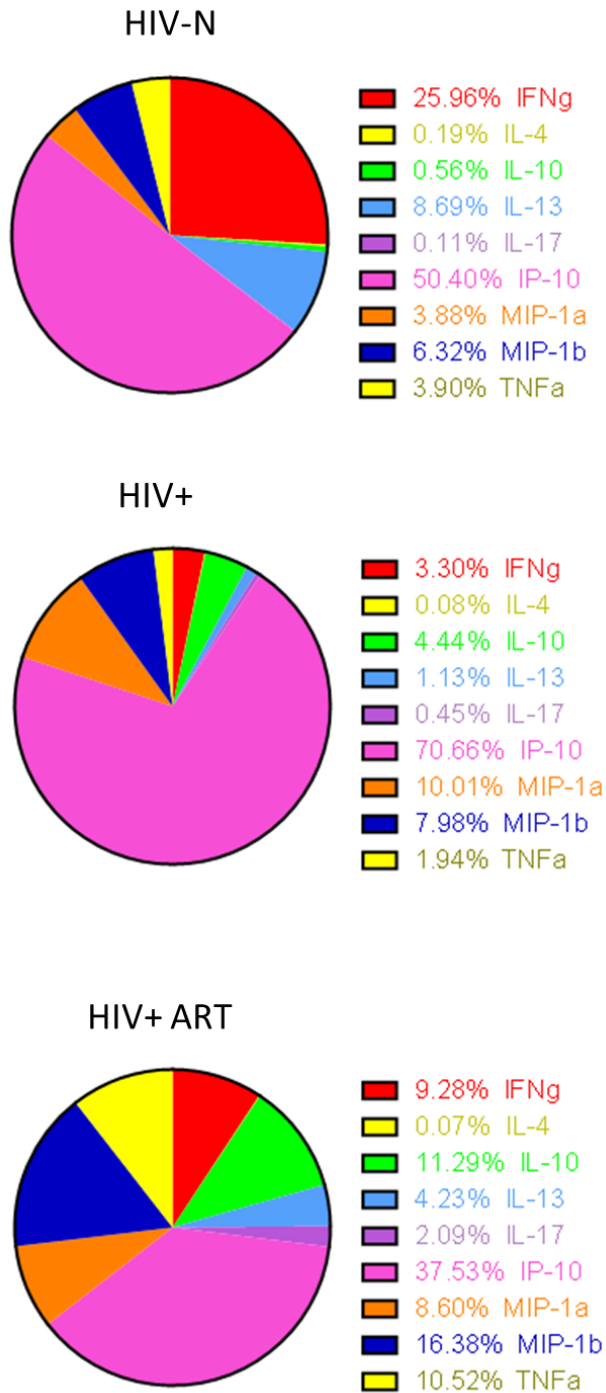
Figure 7.10. Proportional cytokine/chemokine expression following αGalCer stimulation. The proportional contribution of each analyte to total cytokine/chemokine expression among participant groups is shown.

Table 7.6. Correlations between backround subtracted day 5 αGalCer-induced cytokines and chemokines*.

Analyte		IFNγ	IL-4	IL-10	IL-13	IP-10	MIP-1α	MIP-1β	TNFα
IFNγ	Spearman rho p value	--	**0.4936** **0.0019**	0.2131 0.2054	**0.6190** **< 0.0001**	**0.7665** **< 0.0001**	**0.3021** **0.0778**	**0.5023** **0.0015**	**0.5912** **0.0001**
IL-4	Spearman rho p value		--	0.1443 0.3942	**0.4552** **0.0046**	**0.3531** **0.0438**	-0.0026 0.9881	0.1800 0.2864	0.2229 0.1847
IL-10	Spearman rho p value			--	0.2449 0.1440	-0.0059 0.9741	**0.3598** **0.0337**	**0.4081** **0.0122**	0.2224 0.1858
IL-13	Spearman rho p value				--	**0.3851** **0.0269**	0.2538 0.1412	**0.3943** **0.0157**	**0.6112** **< 0.0001**
IP-10	Spearman rho p value					--	0.0297 0.8742	0.2193 0.2201	**0.4247** **0.0138**
MIP-1α	Spearman rho p value						--	**0.8312** **< 0.0001**	**0.5919** **0.0002**
MIP-1β	Spearman rho p value							--	**0.7181** **< 0.0001**
TNFα	Spearman rho p value								--

* Red shading indicates a correlation within the HIV-N group of p<0.05, horizontal bars indicate a correlation within the HIV+ group of p<0.05, and vertical shading indicates a correlation within the HIV+ ART group of p<0.05.
Statistical tests with p≤0.1 (trend) or p<0.05 (significant) are indicated in bold.

Ex vivo iNKT LAG-3 expression inversely correlated with IFNγ and IP-10 concentrations (p=0.0029 and 0.0099, respectively, Spearman), and trended toward inverse correlations with IL-13 and TNFα (p=0.0663 and 0.0998, respectively, Spearman) among all participants (Table 7.7). Among HIV-infected women, there was a significant inverse correlation between LAG-3 and TNFα (p=0.0181, Spearman) and a trend with IL-13 (p=0.0747, Spearman). In contrast, PD-1 positively correlated with IFNγ, IL-4 and IP-10 concentrations among all participants (p=0.015, 0.002 and 0.0120, respectively, Spearman) (Table 7.7). Within the HIV-infected participants, PD-1 significantly correlated with IL-4 production (p=0.0289, Spearman) and trended toward a correlation with IL-13 (p=0.0514, Spearman).

In summary, HIV infection resulted in the perturbation of multiple cytokines and chemokines induced by αGalCer. IFNγ, IP-10 and IL-13 responses were altered during HIV infection, and the cytokine/chemokine profile was not restored by ART. HIV infection also altered which cytokines and chemokines were correlated in response to αGalCer stimulation.

Table 7.7. Correlations between *ex vivo* iNKT LAG-3 and PD-1 expression with 5 day post-αGalCer stimulation cytokine production.

Analyte		iNKT %LAG-3+		iNKT %PD-1+	
		All Participants	**HIV+**	**All Participants**	**HIV+**
IFNγ	Spearman rho	**-0.5016**	-0.4066	**0.4199**	0.3494
	p value	**0.0029**	0.1695	**0.0150**	0.2407
IL-4	Spearman rho	-0.2284	-0.3323	**0.5182**	**0.6135**
	p value	0.2010	0.1935	**0.0020**	**0.0289**
IL-10	Spearman rho	0.1876	-0.2568	-0.1462	-0.0508
	p value	0.2958	0.2549	0.4169	0.6525
IL-13	Spearman rho	**-0.3235**	**-0.5117**	0.2127	**0.5551**
	p value	**0.0663**	**0.0747**	0.2347	**0.0514**
IP-10	Spearman rho	**-0.4711**	-0.3939	**0.4604**	0.3222
	p value	**0.0099**	0.2632	**0.0120**	0.3610
MIP-1α	Spearman rho	-0.2739	-0.2053	0.06706	-0.08039
	p value	0.1359	0.3871	0.7200	0.6422
MIP-1β	Spearman rho	-0.2873	-0.4017	0.1179	-0.02604
	p value	0.1050	0.1206	0.5133	0.7972
TNFα	Spearman rho	**-0.2915**	**-0.6407**	0.1324	0.2176
	p value	**0.0998**	**0.0181**	0.4628	0.4698

Statistical tests with p≤0.1 (trend) or p<0.05 (significant) are indicated in bold.

7.4.5 sLAG-3 in culture supernatant

sLAG-3 concentrations in cell culture supernatant were quantified by in-house ELISA.

Following 5 days of αGalCer stimulation, sLAG-3 production above background was

detectible in 16/37 samples. Chi square analysis of the proportion of participants

exhibiting above-background sLAG-3 levels showed significant differences between

groups (p=0.0341, Chi square), with HIV+ ART naïve patients being highly unlikely to

produce sLAG-3 in response to stimulation (Figure 7.11A). sLAG-3 concentration varied

significantly across groups (p=0.0299, Kruskal-Wallis), with post-tests demonstrating

significant differences between HIV-N and HIV+ ART naïve groups (p<0.05) (Figure

7.11B). Following adjustment for *ex vivo* iNKT frequency, significant differences in

sLAG-3 production remained (p=0.04, Kruskal-Wallis, HIV-N vs HIV+ post-test p<0.05)

(Figure 7.11C).

Among all participants, sLAG-3 concentration significantly correlated with all analytes

except IL-10 and IL-4 (Table 7.8, Figure 7.11D). Among HIV-N participants, sLAG-3

significantly correlated with only IFNγ and TNFα (Table 7.8). Similarly, significant

correlations between sLAG-3 and IFNγ, TNFα, MIP-1β and MIP-1α were observed

among the HIV-infected participants (Table 7.8).

Table 7.8. Correlation between background-subtracted sLAG-3 concentrations at 5 days post αGalCer-stimulation and supernatant cytokines/chemokines.

Analyte	All participants (n=37)		HIV-N (n=15)		HIV+ (n=22)	
	Spearman rho	p value	Spearman rho	p value	Spearman rho	p value
IFNγ	**0.6952**	**< 0.0001**	**0.7469**	**0.0021**	**0.5332**	**0.0106**
IL-4	0.1757	0.2981	0.2576	0.3484	-0.1706	0.4479
IL-10	0.1324	0.4349	0.1191	0.6675	0.2071	0.3552
IL-13	**0.4508**	**0.0051**	0.4224	0.1173	0.2759	0.2140
IP-10	**0.5219**	**0.0018**	0.4423	0.1522	**0.3840**	**0.0857**
MIP-1α	**0.4010**	**0.0170**	0.2741	0.3373	**0.5433**	**0.0109**
MIP-1β	**0.5476**	**0.0005**	**0.5123**	**0.0544**	**0.5891**	**0.0039**
TNFα	**0.6402**	**< 0.0001**	**0.6154**	**0.0175**	**0.6984**	**0.0003**

Statistical tests with p≤0.1 (trend) or p<0.05 (significant) are indicated in bold.
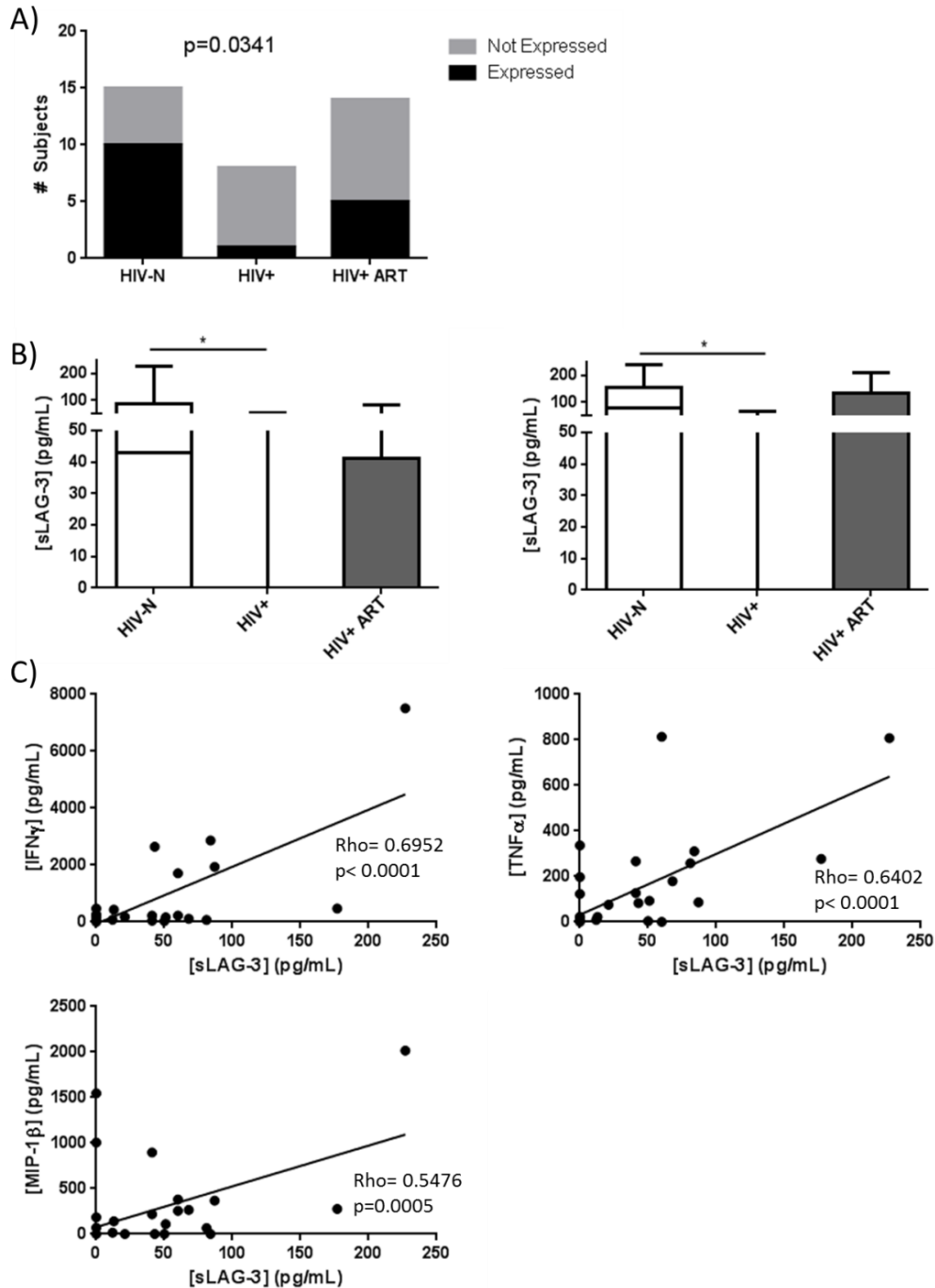
Figure 7.11. Detection of sLAG-3 5 days post-αGalCer stimulation. (A) The proportion of subjects exhibiting above-background sLAG-3 production significantly differed between groups, with HIV+ ART naïve individuals having the lowest proportion of sLAG-3 producers (n=15 HIV-, 8 HIV+, 14 HIV+ ART). **(B)** sLAG-3 concentration was significantly reduced among HIV+ ART naïve participants following stimulation, whether unadjusted or adjusted for *ex vivo* iNKT frequency. **(C)** sLAG-3 concentration significantly correlated with IFNγ, TNFα and MIP-1β among all participants.

7.5 Summary

The aim of this study was to characterize iNKT dysfunction during chronic HIV infection and treatment, and to determine whether elevated iNKT LAG-3 or PD-1 expression was associated with decreased iNKT cytokine production following lipid stimulation. The results indicated that iNKT LAG-3 expression was elevated among HIV-infected women and was not fully restored to baseline following ART. In contrast, PD-1 expression was not elevated on iNKT cells during chronic infection, unlike its elevation on CD8+ T cells. iNKT IFNγ production was impaired among HIV-infected women, and importantly, *ex vivo* iNKT LAG-3 expression inversely correlated with IFNγ production following lipid stimulation. Interestingly, sLAG-3 concentration in cell culture supernatant positively correlated with cytokine/chemokine concentrations, in contrast to the inverse correlation between LAG-3 and supernatant cytokines. These data suggest opposing roles for soluble and membrane LAG-3 in regulating cellular function. Finally, iNKT cytokine/chemokine production following long-term lipid stimulation was unique among both HIV-infected ART naïve and experienced groups compared to healthy controls.

8. Discussion

An improved understanding of the factors that influence HIV acquisition and disease progression will improve prevention and treatment strategies. This thesis investigated the contribution of 2 genes, *GNB3* and *LAG-3*, to HIV susceptibility and progression. Both genes are located in a gene-rich cluster on chromosome 12 near the *CD4* gene. *GNB3* contains a well-described SNP at position 825 that was previously reported to influence HIV progression in a single cohort (449). Within the same gene cluster, *LAG-3* encodes splice variants of soluble and cell-surface inhibitory proteins previously implicated in mediating immune exhaustion during chronic viral infections. Although other immune exhaustion markers are known to mediate T lymphocyte dysfunction during chronic HIV infection, the contribution of LAG-3 was unknown at the time that these studies were conducted.

The two main hypotheses of this thesis are that (1) *GNB3 825TT* genotype is associated with increased risk of HIV acquisition, accelerated disease progression and increased T cell immune activation in Kenyan cohorts of high- and low-risk individuals, and that (2) expression of LAG-3 on lymphocyte subsets will be increased during chronic HIV infection and will correlate with reduced T cell effector functions.

8.1 *GNB3 825* genotype and HIV acquisition and progression

To determine the epidemiological relationship between *GNB3 825* genotype and susceptibility to HIV infection and subsequent disease progression, participants in two

Kenyan cohorts were genotyped at the *GNB3 825* locus. **We hypothesized that *GNB3 825TT* genotype individuals exhibit an increased risk of HIV infection, accelerated disease progression and increased expression of T cell immune activation markers in peripheral blood.** The results of this study are also described and discussed in (443).

8.1.1 GNB3 genotype does not alter risk of HIV acquisition or rate of disease progression

In addition to previous data suggesting a link between *GNB3* genotype and HIV progression (162), a SNP in the nearby *CD4* gene (*CD4 C868T*) was previously associated with increased risk of HIV acquisition and disease progression in the FSW cohort (142). Despite their close proximity, the lack of linkage disequilibrium between the *CD4* and *GNB3* SNPs suggests that *CD4* genotype is unlikely to confound analysis of *GNB3 825* alleles and also that *GNB3 825* genotype does not contribute to the impact of *CD4* genotype on HIV acquisition. Because *CD4* genotype data was available for the FSW cohort, it was nonetheless included in the statistical model to conclusively identify any impact of *GNB3* genotype on HIV acquisition. Contrary to the hypothesis, however, *GNB3 825* genotype was not associated with an increased risk of sexual HIV acquisition in the high-risk FSW cohort (Figure 3.1), nor did it affect risk of mother-to-child HIV transmission in the PHT cohort. Furthermore, the rate of disease progression as determined by CD4 decline (in both cohorts) or viral load increase (in the PHT cohort) did not differ between *GNB3 825* genotype groups (Figure 3.2, 3.3).

Although no published studies have linked *GNB3* genotype to HIV susceptibility, Siffert *et al* reported accelerated disease progression among *GNB3 825TT* individuals (162) – an

observation that is not corroborated by this study. It is unlikely that the endpoints chosen in the analysis of disease progression affected the outcome of the analysis, as statistical models included both participants followed from the time of seroconversion as well as all HIV+ participants (with adjustment for baseline CD4 count), and included endpoints defined as CD4 < 350, CD4 < 250 and/or death, rate of CD4 decline or viral load increase over time. The major difference between the Siffert *et al* study and this thesis is likely the ethnic composition and gender of the participants. While the impact of ethnicity on *GNB3* SNPs and RNA splicing is discussed further in section 8.2, it is plausible that that the route of HIV acquisition in FSW/PHT cohorts (female genital tract, mother to child) contributed to the differences between this study and that of Siffert *et al.*

The absence of an impact of *GNB3* genotype on HIV acquisition/progression in this study does not necessarily imply that *GNB3* genotype does not affect HIV susceptibility among all populations; rather, it underscores the importance of replicating genetic association studies in populations with disparate allele frequencies (151). Studies of the *GNB3 825* SNP in African populations are generally lacking in the literature, but our results, along with others (175-177), suggest that multiple phenotypes associated with the 825T allele in Caucasian/Asian populations may not be replicated in African populations, and reinforce the observation that more diverse studies are required.

It is worthwhile to note that the association of the *825TT* genotype with increased risk of HIV progression is somewhat at odds with reports suggesting a protective effect of the T allele in infection. The *GNB3 825T* allele is associated with improved cellular responses

to Hepatitis B vaccination, and the *825CC* genotype confers a poor response to interferon α/ribavirin therapy in Hepatitis C infection as well as increased risk of infant death due to infection (164, 165, 169, 170). The 825T allele is therefore consistently associated with improved or protective immune function, rather than susceptibility to infection. Furthermore, a detailed mechanism linking *GNB3 825* genotype to immune function is currently lacking. Although the C to T mutation is associated with the production of the biologically active splice variants Gβ3s and Gβ3s2 (160, 163), data demonstrating Gβ3s/s2 expression at the protein level *in vivo* are still lacking.

8.1.2 GNB3 genotype is not associated with differential response to ART

Brockmeyer *et al* (161) reported that despite achieving lower viral load, *GNB3 825TT* individuals receiving antiretroviral therapy (ART) exhibited significantly lower CD4 T cell counts 16 – 32 weeks post-ART initiation compared to *GNB3 825CC/CT* individuals. Analysis of CD4 counts one year after ART initiation among FSW cohort participants failed to replicate this observation. Regardless of whether final CD4 count, absolute change in CD4 count or percent change in CD4 count was used as the outcome, FSW participants of varying *GNB3* genotypes responded similarly to ART (Figure 3.4). These results are generally consistent with the lack of impact of *GNB3* genotype on HIV progression among this cohort and once again underscore the importance of replicating genetic association studies in diverse populations.

8.1.3 GNB3 genotype is not associated with increased ex vivo immune activation

As Caucasian *GNB3 825T* allele carries exhibit enhanced lymphocyte chemotaxis and proliferation (164), we assessed the impact of *GNB3* genotype on cellular immune activation and plasma cytokine/chemokine levels in healthy and HIV-1-positive FSW cohort participants. The similar levels of CD4+ and CD8+ T cell immune activation (measured by CD69, CD38 and HLA DR) between genotype groups for both HIV+ and HIV-N women confirms and extends a previous report that HLA-DR expression is not altered across *GNB3* genotypes in healthy Caucasians (164) (Figure 3.5, 3.6). Similarly, expression of CCR5 and activation of CD4+CCR5+ T cells were similar between genotype groups. Lindemann *et al* also indicated that healthy Caucasian 825T allele carriers have increased CD4+ T cell counts (with no differences in B cell or CD8+ T cell counts), but did not assess the proportion of any CD4+ T cell subpopulations such as Tregs (164). In the current study, there were no differences in Treg proportion between *GNB3* 825CC/CT and TT participants regardless of HIV serostatus (Figures 3.5, 3.6). This is the first study to quantify immune activation markers among HIV-1-positive patients with respect to *GNB3* genotype.

Expression of IL-7Rα (CD127) and Fas (CD95), two known correlates of HIV disease progression, was also quantified among HIV+ FSW participants. During HIV infection, IL-7Rα inversely correlates with immune activation and apoptosis, and positively correlates with CD4 count (444), while Fas expression positively correlates with disease progression (450). Neither marker was differentially expressed on CD4+ or CD8+ T cells between GNB3 genotypes (Figure 3.6). Given the limitations of cross-sectional studies in

assessing differences between markers correlated with disease progression, all surface

markers were analysed with adjustment for CD4 count. These results are consistent with

the lack of impact of *GNB3* genotype on disease progression in this cohort, as discussed

in section 8.1.1.

GNB3 825T allele carriers demonstrate increased SDF-1α-mediated lymphocyte

chemotaxis (164) (a process mediated by G protein signaling); we therefore wondered

whether the CXCR4 ligand SDF-1α or the CCR5 ligand MIP-1β would be differentially

expressed between *GNB3* genotypes, particularly during HIV-1 infection. Plasma TRAIL

levels were also assessed due to the previously reported observation of decreased

lymphocyte apoptosis among 825TT individuals (172). No differences in

cytokine/chemokine expression were detected between genotype groups (Figure 3.7).

While these results do not assess the impact of the *GNB3* splice variants on intracellular

signaling pathways nor imply that there is no impact of the 825 SNP on signal

transduction, our data do suggest that *GNB3* genotype does not have a substantial impact

on HIV co-receptor expression, the activation of bulk or CD4+CCR5+ T cells or plasma

levels of CCR5/CXCR4 ligands. Investigation of these markers in cohorts that do exhibit

an impact of *GNB3* genotype on HIV progression may provide further insight into the

mechanism linking *GNB3* genotype with HIV disease progression.

8.1.4 Summary

Given evidence suggesting an important role for G protein signaling through the viral co-receptors in HIV entry and replication (69, 79), and the suggestion that the *GNB3 C825T* SNP is associated with altered G protein signaling activity (160, 164), it is, in fact, biologically plausible for the *GNB3 825* SNP to alter cellular permissibility to HIV infection. Any impact of *GNB3 825TT* genotype on HIV susceptibility would be particularly relevant in Africa, where the *825TT* genotype is common and HIV prevalence is high (161, 449). We demonstrated in two distinct Kenyan cohorts that *GNB3 825* genotype is not associated with increased risk of HIV acquisition or accelerated disease progression, contrary to the initial hypothesis. These cohorts included multiple modes of HIV transmission (male to female and mother-to-child) and multiple outcomes of disease progression (CD4 decline, viral load increase). Furthermore, *GNB3 825* genotype was not associated with increased *ex vivo* immune activation or plasma chemokine concentration in either healthy or HIV+ individuals, contrary to the hypothesis.

8.1.5 Limitations and Opportunities

Longitudinal studies of disease progression are most powerful when infected individuals are followed from the time of seroconversion to the defined endpoint. In the FSW cohort, the number of participants with a known date of seroconversion was limited relative to the total number of genotyped individuals. Although including participants who were HIV+ at enrolment and controlling for baseline CD4 count expanded the sample size, the study would have been strengthened by a larger number of seroconverting participants.

Cross-sectional studies of immune activation, particularly in the context of HIV infection, have inherent disadvantages compared to longitudinal studies. To control for disease progression among HIV+ participants, CD4 count was included as a covariate in the comparison of T cell activation markers between GNB3 genotypes. Nonetheless, longitudinal analysis of immune activation during the course of infection would be preferable, if the data were available. Given the lack of epidemiological evidence to support a role of GNB3 genotype in HIV infection, however, it is difficult to justify such a study.

8.2 *GNB3 825* genotype and RNA splicing

Epidemiological studies of *GNB3 825* genotype in African populations are generally underrepresented in the literature, and confirmation of *GNB3* mRNA splice variant production associated with the 825T allele (160, 163) in non-Caucasian populations is lacking entirely. Given the discrepancies between the impact of *GNB3 825* genotype on HIV progression between the Kenyan cohorts described in section 8.1 and Siffert *et al*'s cohort (449), we attempted to detect *GNB3* mRNA splicing in PBMC collected from FSW cohort participants. **We hypothesized that mRNA isolated from *GNB3 825TT* participant PBMCs contains both full-length and truncated *GNB3* RNA transcripts.**

8.2.1 Splice variant expression and exon array analysis

Exon-specific detection of *GNB3* mRNA expression revealed putative splicing differences between *GNB3 825* genotypes, but not in the probe-sets corresponding to the reported splice sites (Figure 4.1). Although unexpected, an explanation for the lack of

GNB3 splicing observed in this cohort may be found in a report of detailed *GNB3*

haplotypes among various ethnic populations. Rosskopf *et al* sought to identify additional

GNB3 SNPs that could contribute to the alternate splicing associated with the 825T allele,

based on the large distance between the 825 SNP position and the putative splice site

required to generate the Gb3s transcript (451). In Caucasian populations, the 825T allele

is in tight linkage disequilibrium with five other polymorphisms, including C1429T.

Together, these SNPs were predicted to alter the pre-mRNA folding of the *GNB3*

transcript, which the authors speculated supported alternative splicing. In African

populations, however, the linkage of the C1429T SNP to C825T is reduced compared to

Caucasian populations, and linkage with an additional SNP at position 5177 (which is

absent in Caucasians) is observed. The authors speculate that a third *GNB3* haplotype

may therefore exist in African populations that differs in its ability to promote splice

variant production. This suggestion would be consistent with the unexpected splicing

patterns observed among participants of the FSW cohort.

8.2.2 LAG-3 splicing and expression

Because the exon array data contained expression data for the genes contained within the

GNB3-CD4 locus, we compared expression and splicing of *CD4, G protein coupled*

receptor 162 (GPR162), leprecan-like 2 (LEPREL2), cell division cycle associated 3

(CDCA3), parathymosin (PTMS), lymphocyte activation gene 3 (LAG-3, CD223) and

myeloid leukemia factor 2 (MLF2) between participants with differing GNB3 genotypes

and/or HIV serostatus. *GPR162* encodes a G protein receptor expressed mainly in the

brain, *LEPREL2* encodes a collagen hydroxylase with no pre-existing link to immune

function, *CDCA3* encodes a protein involved in mitosis, *PTMS* encodes a protein involved in DNA replication, *LAG-3* encodes an inhibitory immune receptor involved in immune exhaustion, and *MLF2* encodes a protein of unknown function. Expression of *CD4* mRNA was similar between *GNB3 825* genotype groups, which is consistent with the observation that *CD4 868* genotype was neither linked to *GNB3 825* genotype nor affected CD4 expression on PBMCs (Oyugi, unpublished data). Expression of all other transcripts except *LAG-3* were similar between *GNB3* genotype groups (Figures 4.2, 4.3, 4.4), leading us to further investigate the expression and splicing patterns of *LAG-3*.

LAG-3 exhibited differences in expression of the 3' end of the RNA transcript between *GNB3* 825CC, CT and TT participants (Figure 4.4). Furthermore, *LAG-3* expression was elevated among HIV+ participants compared to HIV-N individuals (Figure 4.5). In both humans and mice, LAG-3 protein is detectible as either a full-length, membrane bound protein or a truncated, soluble protein (sLAG-3) in plasma. While murine sLAG-3 is derived from cleaved surface bound LAG-3 (395, 396), human sLAG-3 is suggested to derive from several mRNA splice variants. The differentially spliced region of the *LAG-3* transcript detected in the PBMC RNA samples corresponds closely to the exons reported to be deleted from the sLAG-3 splice variants described by Triebel *et al.* qRT-PCR amplification of two regions of the *LAG-3* transcript in a subset of samples included in the exon array anlaysis confirmed significant, differential expression of the 3' end (Figure 4.6). These results suggest both differential regulation of *LAG-3* expression among *GNB3* genotype groups and during chronic HIV infection.

At the time of this study, relatively little was known about the splicing and expression of *LAG-3* during human health and disease. There is no data regarding linkage between *LAG-3* and *GNB3* SNPs or promoter regulatory elements. *LAG-3* contains multiple SNPs resulting in missense mutations, as well as numerous intronic SNPs, that could be associated with splicing regulation. Understanding the mechanism linking *GNB3* genotype to *LAG-3* splicing patterns represents an intriguing gap in knowledge, but the expression of full length and truncated soluble LAG-3 (sLAG-3) during chronic HIV infection was more relevant to this thesis. Although several microarray experiments reported upregulation of LAG-3 expression during acute or chronic HIV/SIV infection (438-440), little data was available regarding LAG-3 protein expression on either lymphocytes or sLAG-3 levels in plasma. Activated T cells and NK cells were reported to express LAG-3, but often only following *in vitro* stimulation (388). We therefore planned to quantify LAG-3 expression on CD4+ and CD8+ T cells, CD56^{hi}CD16^{-} and CD56^{dim}CD16^{+} NK cells and invariant NKT cells among healthy and HIV-infected participants, as discussed in section 8.3.

8.2.3. Summary

Using both qRT-PCR and exon microarray analysis, we were unable to detect previously described *GNB3* splice variants in PBMC RNA derived from FSW cohort participants, in contrast to the hypothesis. mRNA splicing and expression of neighbouring genes at the *GNB3* locus were similar between *GNB3* genotype groups, with the exception of *LAG-3*, which exhibited differences in expression of the 3' end of the RNA transcript that were confirmed by qRT-PCR.

A comparison of *GNB3* RNA expression among different tissues revealed higher levels of expression in stimulated T cells and non-immune tissues compared to *ex vivo* PBMC (163). The lack of detection of *GNB3* splice variants in RNA derived from PBMC samples could therefore be related to the cellular source of the RNA, rather than a lack of splicing in all tissues of the participants. Given that this thesis is primarily concerned with the impact of *GNB3* splicing on HIV acquisition, however, unstimulated PBMC-derived RNA was a more relevant sample to use in this assay.

8.3 LAG-3 expression on lymphocyte subsets during chronic HIV infection

At the time of these studies, descriptions of LAG-3 expression on lymphocyte subsets during HIV infection were lacking in the literature; the only two published studies were inconsistent as to whether LAG-3 expression on T cells was increased (452) or unchanged (435) during chronic HIV infection. Furthermore, there was no data on LAG-3 expression on other subsets such as NK cells or iNKT cells, despite evidence that LAG-3 is expressed on these subsets *ex vivo* and/or following activation (271). Given its inhibitory activity on T cell function, LAG-3 could potentially contribute to immune exhaustion during HIV infection. We therefore performed a screening study of 90 individuals to compare LAG-3 expression on T cells, NK cells and iNKT cells between healthy, HIV+ and ARV-treated participants. **We hypothesized that LAG-3 is increased among HIV+, but not ART-experienced, individuals, primarily on CD4+ and CD8+ T cells.**

8.3.2.1 LAG-3 is expressed at low levels on bulk CD4+ and CD8+ T cells

Contrary to the hypothesis, T cell LAG-3 expression was very low (<2%) on all subjects

screened in this study (Figure 5.2). Negligible *ex vivo* LAG-3 expression on PBMC from

healthy individuals is consistent with previous observations in the literature, as well as

more recent studies (380, 388, 445). In contrast to the marked increase of exhaustion

markers such as PD-1 and Tim-3 during HIV infection (377), the statistically significant

increase in LAG-3 expression on T cells observed in this study was small in magnitude.

Subsequent to the collection of data for this study, several other reports examined LAG-3

expression on both bulk and HIV-specific CD4+ and CD8+ T cells. Although bulk CD8+

T cell LAG-3 expression was markedly higher in some individuals than observed in this

study (380), all reports concluded that LAG-3 expression was generally low on antigen-

specific T cells, was similar between CD4+ and CD8+ subsets, and did not contribute to

the major populations of exhausted antigen-specific cells (380, 436). The results from this

study are also consistent with studies of LAG-3+ T cells during other human chronic

viral infections, such as HCV (432, 453) and HBV, in which *ex vivo* LAG-3 expression

was similarly low (~2% of CD4+ and CD8+ T cells) among both healthy and HBV-

infected subjects (454).

Among all three study groups, LAG-3 expression was marginally, but significantly,

higher on CD8+ T cells compared to CD4+ T cells (Figure 5.2). This is consistent with

previous observations of *ex vivo* LAG-3 expression (445); despite a poor understanding

of the significance of LAG-3 expression on MHC class I-restricted CD8+ T cells, there is evidence to suggest that LAG-3 function on CD8+ cells may be different than CD4+ cells (410).

Although the increase in LAG-3+ T cells during chronic infection was small in this cohort, it is notable that the proportion of LAG-3+ T cells did not decrease among subjects on ART, and that, in fact, the individuals with the greatest proportion of LAG-3+ T cells were receiving ART (Figure 5.2). This expression pattern differs from those described for most other exhaustion markers including PD-1, Tim-3, 2B4 and CD160 (433). Although viral load data was not available for participants in this study, expression of HLA-DR on CD8+ T cells was significantly reduced among the ART group compared to the HIV+ group (Figure 5.4), suggesting at least some successful control of viral replication among ART recipients. Interestingly, Yamamoto *et al* noted that although bulk CD8+ T cell LAG-3 expression was reduced among ART individuals compared to ART-naïve patients, LAG-3 expression on CD8+ central memory T cells (the memory subset with highest LAG-3 expression) was not reduced by ARV therapy (380). The maintenance of LAG-3 expression during ART may, in fact, be related to the unexpected lack of correlation between LAG-3 expression and disease progression.

T cell LAG-3 expression did not correlate with CD4 count, nor was it affected by duration of ART (Figures 5.3, 5.4). Although viral load data is not available for the participants of this study, there is no evidence to suggest that LAG-3 expression is related to viral replication or disease progression. Furthermore, the correlations between LAG-3

expression and T cell activation markers were weak and inconsistent between ART naïve and experienced groups. Overall, these data suggest that HIV infection does not strongly alter LAG-3 expression on bulk CD4+ or CD8+ T cell subsets.

8.3.2.2 Ex vivo LAG-3 expression is associated with PD-1+ T cells

As LAG-3 expression was unexpectedly low among HIV+ study participants, we sought to confirm that another exhaustion marker, PD-1, would be upregulated among cohort participants in a manner consistent with the numerous published reports of PD-1 expression. Indeed, CD8+ T cell PD-1 expression was significantly increased among HIV+ participants on the bulk CD8+ T cell population (Figure 5.5) and was further enriched on antigen-specific CD8+ T cells (Figure 5.7) (further discussed below in section 8.3.2.3) in a manner consistent with previous reports (374). The lack of correlation between LAG-3 and PD-1 expression suggests that LAG-3 is not driven by the same factors known to promote PD-1 upregulation (immune activation, viral load, CD4 depletion). The increased expression of PD-1 on LAG-3+ cells, however, suggests some relationship between the two markers. Several studies now suggest that some PD-1 expression reflects T cell activation or differentiation rather than exhaustion (455), suggesting that LAG-3+PD-1+ T cells may simply mark a recently activated T cell population.

8.3.2.3 LAG-3 expression is low on HIV-specific T cells

Despite the similarities in LAG-3 expression on bulk CD4+ and CD8+ T cells in HIV-uninfected and HIV+ participants, exhaustion markers are often strongly enriched on

HIV-specific T cells. Although data from other cohorts suggests that LAG-3 expression is remarkably low on antigen specific cells (436), we sought to confirm that the low levels of LAG-3 staining on *ex vivo* T cells were not confined to HIV-specific T cells. Despite the limitation that only samples from ARV-treated participants were available for HIV peptide stimulations, gag-specific CD8+ T cell responses were readily identified by IFNγ and TNFα expression. The relationship between PD-1 expression and gag-specific responses was consistent with known literature: PD-1 expression was highly enriched on antigen-specific cells and its expression was elevated on monofunctional (exhausted) IFNγ+TNFα- cells compared to polyfunctional IFNγ+TNFα+ gag-specific cells (Figure 5.7).

In contrast, LAG-3 was not significantly enriched on gag-specific T cells, nor was there any significant difference in cytokine expression between LAG-3+ and LAG-3- antigen specific cells (Figure 5.7). Given these disparities, LAG-3 does not appear to contribute to inhibitory receptor accumulation and suppression of cytokine secretion on HIV-specific T cells in the same manner as PD-1. These results are intriguing, considering the consistency with which other inhibitory markers accumulate on antigen-specific T cells during chronic HIV infection and appear to inhibit cytokine production/proliferation. The regulation of LAG-3 expression on T cells during human chronic viral infection remains to be well defined, and represents an ongoing gap in knowledge.

8.3.3 Lymphocyte LAG-3 expression and GNB3 825 genotype

Based on the differences in 3' *LAG-3* transcript expression identified by the exon array

analysis between *GNB3* genotype groups, we compared surface LAG-3 expression

between HIV+ participants of varying 825 genotypes. LAG-3 expression was similar on

all lymphocyte subsets studied (5.8). These results highlight the importance of

confirming RNA expression changes at the protein level. Although this analysis cannot

rule out an impact of plasma sLAG-3, the exon array specifically detected expression

differences in the transmembrane/cytoplasmic tail region of the *LAG-3* transcript, which

would reflect only the full-length LAG-3 protein. It is possible that LAG-3 expression on

cell subsets not analysed by flow cytometry (i.e. monocytes) could confound the results.

The regulation of LAG-3 expression in humans is not well understood. In mice, T cells

contain large stores of intracellular LAG-3 that can be rapidly mobilized upon T cell

activation (456). Pre-formed stores of intracellular LAG-3 could argue against a direct

link between LAG-3 RNA transcription and subsequent protein production, making it

difficult to directly link the exon array data with surface protein expression data. High

quantities of intracellular LAG-3 would also confound any relationship between surface

protein and RNA expression levels.

8.3.4 LAG-3 expression is increased on NK cells during HIV infection and treatment

In this screening study, LAG-3 expression was increased among HIV+/ART individuals

compared to healthy participants on both the CD56^{hi}CD16^{-} and CD56^{dim}CD16^{+} subsets.

LAG-3 expression did not correlate with CD4 count on either NK subset, but positively

correlated with expression of acute activation marker CD69 on the CD56^{dim}CD16^{+} subset. Expression of LAG-3 on CD56^{-}CD16^{+} "dysfunctional" NK cells was similar between healthy and HIV-infected groups (Figure 5.10).

Although LAG-3 is known to be expressed on activated NK cells, little is known about its function or regulation in a subset-specific manner. In this cohort, the fold change in LAG-3 expression between HIV-N and HIV+ groups was greatest among CD56^{hi}CD16^{-} NK cells. This CD56^{hi} population is typically described as the 'immunoregulatory', cytokine-producing, NK subset. In contrast, the CD56^{dim} NK subset is highly cytotoxic, and LAG-3 is reported to have no impact on human NK cytotoxicity (418). The correlation between LAG-3 and acute activation marker CD69 raises the possibility that LAG-3 expression on this subset is indicative of increased NK activation during chronic HIV infection.

To date, no published data has demonstrated whether LAG-3 expression on CD56^{hi}CD16^{-} NK cells is associated with reduced cytokine production. Although the inhibitory activity of LAG-3 on T cell cytokine production has been demonstrated, the function of inhibitory surface receptors on different cell types is not necessarily consistent. The expression of exhaustion marker Tim-3 is differentially regulated between NK cell subsets and can display both inhibitory and activating functions depending on the cell subset (457, 458). In contrast, PD-1 expression on NK cells inhibits NK proliferation, similar to its effect on T cell proliferation (459). The lack of correlation between LAG-3 and CD69 expression on this subset suggests that the increased LAG-3 expression among HIV+ groups may

not be due primarily to increased cellular activation. Further studies will be required to determine whether increased LAG-3 expression is associated with reduced cytokine production by this subset during chronic HIV infection.

It is worthwhile to note that among both HIV-N and HIV+ participants, LAG-3 expression was significantly increased on the CD56-CD16+ NK subset relative to both other NK subsets. Indeed, among healthy individuals, LAG-3 expression declined between NK subsets with increasing CD56 expression (CD56- > CD56dim > CD56hi) (Figure 5.10). Any contribution of LAG-3 to the reduction in cytokine production among CD56- NK cells is unknown; it is currently unclear whether these NK cells exhibit molecular signatures of exhaustion similar to exhausted T cells, or whether their functional responses are skewed toward a chemokine-biased response (446). It is also possible that rather than mediating the repressed function of this subset, LAG-3 expression could mark NK differentiation/maturation stages in a manner similar to that of Tim-3 (457).

The consistent expression of LAG-3 between HIV+ and ART individuals in this study is similar to the maintenance of LAG-3 expression on the other lymphocyte subsets studied (Figure 5.11). Following initiation of ART, the NK subset often remains highly activated (460) and dysfunctional (461), thus providing a potential explanation for the maintenance of NK cell LAG-3 expression. Continual innate immune activation and dysfunction during suppressive antiretroviral therapy remains a challenge to successful treatment of HIV infection, and the contribution of LAG-3 to this dysfunctional phenotype remains a

significant gap in knowledge for future research.

8.3.5 LAG-3 expression is increased on iNKT cells during chronic HIV infection and treatment

The frequency of iNKT cells was highly variable among participants of the screening study, but the CD4+ iNKT subset was significantly depleted among HIV+ and ART individuals compared to healthy subjects (Figure 5.13). LAG-3 expression on total iNKT cells was significantly higher among the HIV+ ART group compared to the healthy subjects. While subset-specific LAG-3 expression was difficult to quantify due to the small size of the iNKT population, LAG-3 expression on the CD4+ iNKT subset was significantly increased among HIV+ ART individuals compared to healthy controls (Figure 5.14).

The depletion of iNKT cells during chronic HIV infection, particularly the CD4+ subset, has been described in multiple cohorts in the literature (243, 332, 333). The kinetics and success of CD4+ iNKT rebound during ARV, however, remain controversial and vary from cohort to cohort (332, 335, 338). Only one other study has reported on iNKT frequencies in an African cohort, where Mureithi *et al* observed CD4+ iNKT depletion that was reversed upon ARV treatment (243). Without viral load data, it is difficult to determine whether the lack of iNKT reconstitution among the ART group in this study is related to failure of viral suppression.

The expression of LAG-3 on iNKT cells during HIV infection has not been previously

described. In healthy individuals, LAG-3 is expressed at detectible, but low levels, and inversely correlates with the frequency of the CD8+ iNKT subset, suggesting a regulatory or homeostatic role for its basal expression (271). In this study, LAG-3 was similarly expressed at low, and varying, levels on CD4+, CD8+ and DN iNKT subsets among healthy subjects. In this study, we report for the first time, that LAG-3 expression was significantly increased among HIV+ ART subjects compared to uninfected individuals. The fold change increase in LAG-3 expression among both HIV+ groups compared to controls was larger than that observed for most T cell and NK cell subsets. Although modulation of LAG-3 expression on human iNKT cells has not been described in the literature, the correlation between CD69 and LAG-3 expression suggests that iNKT activation induces LAG-3 expression in a similar manner to that reported for both T and NK cells (Figure 5.15).

HIV does not encode any foreign lipid antigens capable of activating iNKT cells in a CD1d-dependent manner. The most plausible mechanism by which iNKT cells could become activated during chronic HIV infection is through increased plasma concentrations of LPS derived from microbial translocation through the depleted gut mucosa. LPS is capable of activating iNKT cells via TLR signaling on APCs, and can also drive accumulation and CD1d presentation of endogenous iNKT antigen β-GlcCer (220).

The maintenance of high LAG-3 expression among ART participants could be related to several factors. First, in this cohort, there was no reconstitution of the CD4+ iNKT subset

among the ART group, which may reflect continued iNKT dysfunction related to continuous high LAG-3 expression. Second, no data is currently available to describe the impact of lipid dysregulation during ART on iNKT function. Many ARV drugs cause side effects involving lipid metabolism (462), and mouse models indicate that lipid imbalances, including hyperlipidemia, can result in chronic iNKT activation and anergy (463). It is therefore possible that mechanisms resulting in increased LAG-3 expression among the HIV+ and ART groups are, in fact, distinct.

While the function of LAG-3 on human iNKT cell has not been demonstrated, a single report in mice demonstrated that αGalCer stimulation can result in LAG-3 upregulation on hepatic iNKT cells (420). Given the lack of data describing the functional impact of human LAG-3 expression on the iNKT subset, this study was unable to determine whether increased levels of cell surface LAG-3 simply represented iNKT activation during chronic infection, or whether the expression of this inhibitory receptor contributed to loss of iNKT cytokine producing/proliferative capacity during infection. These issues are addressed in Section 8.4.

8.3.6 Relationship between LAG-3 expression and plasma cytokines/chemokines

Correlation of LAG-3 expression on all lymphocyte subsets with plasma cytokines and chemokines revealed little about factors potentially promoting LAG-3 expression. No significant correlations were identified when all participants were included in the analysis; rather, weak correlations were observed when samples were restricted to those

with above-background cytokine levels.

The trend toward a correlation between CD8+ LAG-3 expression and plasma IFNγ among HIV+ participants was not reflected among the HIV+ ART naïve or ART treated groups separately, and exhibited a relatively low r^2 value. Although IFNγ has been reported to influence LAG-3 expression (405), plasma IFNγ levels measured by cytokine bead array are consistently quite low. The weak correlation between iNKT LAG-3 and plasma IL-10 levels was observed both among all HIV+ participants and HIV+ ART participants only. As with IFNγ, plasma IL-10 concentrations were quite low among these individuals (Figure 5.16). While iNKT cells can produce IL-10, iNKT activity also modulate other IL-10 producing lymphocytes, including Tregs, making it difficult to conclude that plasma IL-10 levels would be directly influenced by LAG-3-mediated iNKT dysfunction.

8.3.7 Detection of sLAG-3 in plasma

sLAG-3 was quantified in plasma samples by in-house ELISA. In contrast to surface LAG-3 expression, sLAG-3 concentrations were highly variable across participants in plasma did not significantly differ between HIV-N and HIV+ participants.

Among HIV+ participants, however, sLAG-3 consistently correlated with IP-10 and patient CD4 count (Figures 5.17, 5.18). Notably, IP-10 is a chemotactic protein induced by IFNγ, providing a potential link to IFNγ-induced LAG-3 expression. Although IFNγ was only reported to induce cell surface LAG-3 expression (405), rapid cleavage of

227

surface LAG-3 could influence plasma sLAG-3 concentrations. Despite the lack of

correlation between plasma IFNγ and sLAG-3, IFNγ levels measured in plasma by bead

array are extremely low. The inverse relationship between CD4 count and sLAG-3 also

argues against CD4+ T cells as a dominant source of plasma sLAG-3 during infection.

In this study, IP-10 levels were significantly higher amongst HIV+ ART naïve

participants compared to healthy controls, and there was a trend toward an inverse

correlation between CD4 count and IP-10 concentration among all HIV+ subjects. This is

consistent with numerous studies demonstrating that IP-10 inversely correlates with CD4

count, is reflective of systemic immune activation and is an independent and sensitive

predictor of disease progression and viral load (464-468). Given the relationships

between sLAG-3, IP-10 and CD4 count, sLAG-3 expression might therefore, like IP-10,

be reflective of immune activation and disease progression during infection. It is

important to note that despite the known value of IP-10 in predicting disease progression,

sLAG-3 was, in fact, a stronger correlate of CD4 count compared to IP-10 in this study.

Evaluation of sLAG-3 expression in a larger cohort of samples is therefore warranted to

determine the value of sLAG-3 as a predictor of progression.

8.3.8 Limitations and Opportunities

During this initial screening study, LAG-3 expression was assessed only on bulk CD4+

and CD8+ T cells, not HIV-specific cells. Although expression of exhaustion markers

PD-1 and Tim-3 are most strongly upregulated on antigen-specific T cells during HIV

infection, studies have also demonstrated increased expression on the bulk T cell

population, particularly in the case of Tim-3. Although we stimulated T cell samples with HIV gag peptide pools, there were limitations to the samples available for analysis. First, recall antigen responses to CEF peptide pools were generally undetectable in HIV+ participants, preventing a direct comparison LAG-3 expression on recall antigen- and HIV-specific T cells. Second, the comparison between LAG-3 and PD-1 expression on HIV-specific T cells would have been more informative in HIV+ ART naïve participants, given the reported decrease in PD-1 expression following ART. We were, nonetheless, able to detect differences in polyfunctional cytokine production between PD-1+ and PD-1- cells, even in the ART experienced participants. Given subsequent studies demonstrating negligible expression of LAG-3 on antigen-specific CD4+ and CD8+ cells and the overall low levels of expression observed in this thesis, however, it is likely that these results are representative of LAG-3 expression in ART naïve cohort participants.

The lack of viral load data available for the participants of this screening study limits the ability to correlate LAG-3 expression with disease progression. Although LAG-3 expression did not correlate with CD4 count or T cell immune activation, a correlation with viral load is possible, given a previous study demonstrating increased LAG-3 expression among HIV+ individuals with uncontrolled viremia.

The description of LAG-3 expression on CD3-CD56-CD16- NK cells is limited by the gating strategy used to identify this subset. The most stringent phenotypic definition of this subset requires additional markers (CD19-CD4-CD14-CD11c-) that were not included in this study. Given the increased in LAG-3 expression on this NK subset

relative to other NK populations even among HIV-N participants, future studies should further investigate the relationship between LAG-3 expression and expansion/function of CD56- NK cells in a more stringent manner.

The expression of LAG-3 on CD4+, CD8+ and DN iNKT subsets was limited by the number of events collected in the iNKT gate. As a result, the sample size available to compare LAG-3 expression between healthy and HIV+ groups was reduced compared to the total number of individuals screened. Individuals with <20 events in the subset gate were excluded in an effort to maintain the quality of the data, but the small sample size remains a limitation of this study.

8.4 LAG-3 expression at the female genital tract (FGT) mucosa

While LAG-3 engagement inhibits CD3-TCR signaling and inhibits effector and proliferative functions (411, 412), unique MHC class II signaling pathways are also induced that result in APC maturation and activation and the production of IL-12 and TNF-α (422-425, 427). LAG-3 expression at the genital mucosa could, therefore, play an important role in antigen processing and innate immune responses to sexually transmitted infections and normal flora. Conversely, T lymphocyte LAG-3 expression has also been proposed to limit macrophage and DC differentiation and antigen presentation at sites of inflammation (428), as well as inhibiting alloresponses among PBMC (419), making it an intriguing candidate for the modulation of immune activation at the genital mucosa, an issue of importance during HIV exposure.

Overall, little data is available to clarify the regulation and function of inhibitory markers at mucosal sites. PD-1 expression is generally increased on mucosal lymphocytes in the gut and rectal mucosa compared to peripheral blood (469, 470), but the impact of that expression on immune dysfunction/activation during HIV transmission and infection is unknown. Given the increased activation of genital tract T cells compared to peripheral blood, and evidence that PD-1 and LAG-3 mark distinct T cell populations (471, 472), we compared LAG-3 and PD-1 expression on ectocervical T lymphocyte subsets. **We hypothesized that: (1) cell surface expression of LAG-3 would be increased on CD4+ and CD8+ T cells from the female genital tract compared to peripheral blood, (2) T cell surface expression of LAG-3 would be increased in HIV+ individuals compared to healthy controls and would correlate with acute T cell activation marker CD69, and (3) sLAG-3 would be detectible in CVL samples and would be decreased among HIV+ individuals.**

8.4.1 LAG-3 and PD-1 expression on cervical mononuclear cells

This is the first study to report increased expression of LAG-3 at the female genital tract (FGT) compared to peripheral blood, but it is consistent with previous observations of increased exhaustion/activation marker expression among mucosal tissues (469, 470). Interestingly, LAG-3 expression was significantly higher across all T cell subsets (CD4+, CD8+ and CD4-CD8-, or double negative (DN) subsets), whereas PD-1 expression was only significantly increased on the CD8+ subset (Figures 6.2, 6.4, 6.5). Furthermore, the low *ex vivo* expression of LAG-3 on PBMC resulted in a significantly higher fold upregulation of LAG-3 at the mucosa compared to PD-1, particularly among DN T cells.

In the context of *ex vivo* T cell activity, LAG-3 may therefore play a far greater regulatory role at mucosal sites than in peripheral blood, a function which has not been previously explored.

The observed enrichment of LAG-3 expression on DN T cells in both PBMC and CMC is the first report of LAG-3 expression on this cell subset. Interestingly, PD-1 expression was reduced on DN T cells compared to CD4+ and CD8+ subsets at the FGT, demonstrating that not all activation/exhaustion markers are similarly enriched on this population (Figures 6.2, 6.5). In peripheral blood, DN T cells are composed primarily of γδ T cells but also include a minor population of αβ T cells. This study was unable to differentiate between these two cell types in either the FGT or peripheral blood, although the inclusion of the 6B11 iNKT marker in the flow panel allows for the exclusion of DN iNKT cells from the DN T cell population, which is a frequent confounder in studies of peripheral T cells (473).

Peripheral blood DN T cells can compensate for lost CD4+ T cell help during chronic HIV infection (195), and the frequency of DN T cells in early infection negatively correlates with T cell immune activation later in infection (474). Additionally, the DN T cell population may contain a high proportion of the infected and virus-producing cells in HIV+ individuals (359). Interestingly, αβ TCR-expressing DN T cells are associated with a regulatory/suppressive phenotype and function (including TGF-β1 and IL-10 secretion) mediated via cell-contact dependent mechanisms (193, 194), and may act to limit immune activation during HIV/SIV infection (195, 474). While the surface molecules

involved in DN T cell suppressive activity remain unknown, expression of the common Treg marker CTLA-4 is not detected on this susbset (193, 194). Given its role in mediating murine Treg suppression, it is plausible that LAG-3 could contribute to a regulatory DNT cell phenotype in PBMC.

To date, the DN T cell population at the FGT has not been described (despite reports of high proportions of DN T cells in murine genital tract samples (475)) but foreskin was recently reported to contain a significantly larger double negative (DN) T cell population than matched PBMC (196). This is consistent with the high proportions of DN T cells observed at the FGT in this study. It is unknown whether FGT DN T cells express predominantly αβ or γδ TCRs, or whether they exhibit any regulatory functions similar to peripheral blood DN T cells. Although difficult, mitogenic and antigenic stimulation of CMCs to identify DN T cell cytokine production, as well as further phenotypic characterization, will be crucial to understand the function of this mucosal cell subset.

Factors correlating with LAG-3 expression on mucosal lymphocytes were difficult to identify in this study. No cytokines or chemokines in cervical-vaginal lavage correlated with LAG-3 expression, which is consistent with the lack of correlation between peripheral blood LAG-3 expression and plasma cytokines/chemokine reported elsewhere in this thesis. LAG-3+ T cells, however, do co-express CD69 and CCR5, both of which are expressed on activated T cells (Figure 6.7). This observation is consistent with the upregulation of LAG-3 following T cell activation, but also suggests that LAG-3

expression may be preferentially associated with cells that are susceptible to HIV infection (activated and expressing the R5 tropic viral co-receptor). Whether LAG-3 engagement on CD4+LAG-3+CD69+CCR5+ T cells could inhibit viral replication is unknown, but points to a need for further phenotyping of LAG-3+ CD4+ T cells at the FGT.

8.4.2 Impact of HIV infection on LAG-3 expression

In this study, there was no difference in LAG-3 expression between HIV-N and HIV+ participants (Figure 6.6), but the study was not sufficiently powered to detect such a difference. Future studies with larger sample sizes will be required to accurately determine whether HIV infection alters LAG-3 expression. Improved phenotypic characterization of T cell subsets may also reveal smaller T cell populations where LAG-3 is up/downreglated following infection.

8.4.3 Lack of identification of iNKT cells at the FGT

Given that iNKT cells display a tissue-homing phenotype and express the mucosal homing marker α4β7 (241, 272), we sought to identify a putative iNKT population among the CMC samples collected from the FSW cohort. Despite detection of typical 6B11+ T cell populations in matched peripheral blood samples, no 6B11+ populations were detected among cervical lymphocytes (Figure 6.9). Given that CD1d is expressed at both the vaginal and cervical epithelium (274, 275), CD1d-restricted cells are likely to be recruited to the genital tract. The failure to detect cervical iNKT cells in this study may

be related to several factors: the impact of sex work and the practice of douching among cohort participants may alter the frequency of the iNKT population, and/or ectocervical scrapings may simply not be the ideal sampling site to detect iNKT cells in the genital mucosa.

8.4.4 sLAG-3 expression at the FGT

No attempts to detect sLAG-3 secretion at the FGT have been previously reported. Despite detection of plasma sLAG-3 in both healthy and HIV+ participants, sLAG-3 was detected at levels only barely above background in only 2 of 35 lavage samples screened. It is possible that any secreted sLAG-3 may be sequestered by MHC class II molecules in the genital tract or trapped in the vaginal mucous. Although the contribution of metalloprotease cleavage of surface LAG-3 to produce sLAG-3 in humans is unclear, it is possible that the increased T cell surface LAG-3 expression and reduced detectible sLAG-3 concentration are related to a reduction in LAG-3 cleavage at the genital tract compared to peripheral blood.

8.4.5 Limitations and Opportunities

Ectocervical scrapings are notoriously difficult samples from which to obtain viable lymphocyte populations, and studies are therefore often limited by sample size. Despite the small sample size of this study, we detected numerous statistically significant differences in LAG-3 expression compared to matched PBMC samples. The unexpected observation of LAG-3 expression on the DNT subset requires more intensive study. Because DNT cells are a heterogeneous subset, detailed phenotypic analysis of the

235

expression of the αβ TCR, γδ TCR and NK cell receptors is required. An advantage of this study was the inclusion of the iNKT marker 6B11, which rules out the potential for iNKT cell contamination of the DNT gate. Although functional studies of CMCs are even more difficult than *ex vivo* phenotyping, short term PMA/Io stimulation of CMCs could reveal the primary cytokines produced by the DNT subset, in order to give clues as to whether mucosal DNT cells share a similar immunoregulatory function as PBMC DNT cells.

Although LAG-3 and PD-1 expression were compared between HIV-N and HIV+ participant groups, this study was not sufficiently powered to detect differences due to serostatus. A larger sample size would be required to fully assess the impact of HIV infection on LAG-3 expression, particularly among smaller cell subsets.

The participants of the cohort enrolled in this study engage in commercial sex work and report frequent douching. The results of this study are therefore not necessarily representative of all women, especially with respect to douching practices. The inability to detect iNKT cells among the samples in this study cannot be used to conclude that this particular subset is absent from the genital tract; replication of these studies in other populations is required, and collection of biopsies and immunohistochemical staining may provide different results.

Another limitation of mucosal studies is the impact of the menstrual cycle on immunological phenotypes. A larger study with targeted recruitment for women at

similar stages in the menstrual cycle will be better suited to determine whether LAG-3 expression is altered by hormonal changes at the FGT.

8.5 LAG-3 and iNKT function

In Section 3.4.5, we demonstrated that LAG-3 expression was significantly increased on iNKT cells, particularly the CD4+ subset, among HIV+ and ART experienced participants compared to healthy individuals. No published reports have specifically determined the impact of LAG-3 expression on iNKT function in humans. To determine the impact of LAG-3 expression on the iNKT subset, we stimulated iNKT cells from healthy and HIV+ individuals to measure cytokine production and proliferation, and investigated the correlates of LAG-3 expression among plasma cytokines/chemokines. **We hypothesized that (A) iNKT LAG-3 expression correlates with pro-inflammatory plasma cytokine expression and (B) LAG-3 expression on iNKT cells negatively correlates with cytokine production.**

8.5.1 LAG-3, but not PD-1, is elevated on iNKT cells during HIV infection

The significant elevation of LAG-3 expression on the iNKT subset among HIV-infected participants is consistent with the previous study described in Chapter 3.4. Surprisingly, the increase in LAG-3 expression did not correspond to increased PD-1 expression, in contrast to another report by Moll *et al* (338) (Figure 7.2). In both cohorts, iNKT PD-1 expression was several-fold higher than T cell PD-1 expression, but PD-1 was more readily detected on both cell subsets in our cohort. Differences in cohort ethnicity could contribute to the contrasting observations, but it is also plausible that the use of the

EH12.2H7 anti-PD-1 clone coupled to the extremely bright Brilliant Violet 421 fluorochrome enabled more sensitive detection of PD-1 expression in this study than other clones and fluorochromes.

8.5.2 Correlation between plasma cytokines, soluble LAG-3 and iNKT surface-expressed LAG-3

As disease progression measured by CD4 count does not appear to be a determinant of iNKT LAG-3 expression, we hypothesized that elevated LAG-3 expression may be associated with a pro-inflammatory immune milieu. The lack of correlation between surface LAG-3 (or PD-1) expression and the majority of the selected plasma cytokines/chemokines suggests that determinants of iNKT LAG-3 expression may either act outside the periphery (i.e. in lymph nodes or tissues) or may be predominately lipid-based rather than cytokine/chemokine based. The relatively weak correlation between LAG-3 and IL-8 was statistically significant only among all participants, and was not reflected within either the HIV-N or HIV+ groups separately.

Among HIV+ participants on ART, iNKT LAG-3 expression correlated with sCD40L levels (Figure 7.3). Plasma sCD40L likely reflects levels of immune activation during HIV infection (476), but also correlates with plasma triglyceride and lipoprotein levels during ART (477) and is strongly implicated in the development of artherosclerosis (reviewed in (478)). Despite well-documented perturbation of plasma lipids (hyperlipidemia) and increased cardiovascular risk during ART (462, 479, 480) and a documented impact of hyperlipidemia on iNKT frequency among HIV-N individuals

(481), no studies to date have investigated the relationship between lipid levels and iNKT function/LAG-3 expression during ART.

In addition to surface LAG-3 expression, soluble LAG-3 protein (sLAG-3) is detectible in plasma and cell culture supernatant. As is documented in mice, regulatory cleavage of human surface LAG-3 may contribute to sLAG-3 accumulation, but human PBMC are also reported to generate mRNA splice variants encode sLAG-3 proteins. Production of sLAG-3 exhibits divergent kinetics from surface LAG-3 expression (482), raising questions about the cellular source of sLAG-3 and the factors regulating its secretion. Given that surface LAG-3 expression is negligible on T cells during HIV infection, we wondered whether iNKT surface LAG-3 expression might be related to plasma sLAG-3 levels. The trend toward a correlation between sLAG-3 and iNKT LAG-3 expression among HIV-N participants suggests some relationship between surface and soluble LAG-3 production at baseline; whether this is due to a contribution of cleaved surface LAG-3 to plasma sLAG-3, or simply an overlap in regulators of surface and sLAG-3 secretion, is unknown. In contrast, there was no evidence to suggest a relationship between surface and sLAG-3 during HIV infection, thus highlighting the need to better understand the regulators and functions of sLAG-3 in health and disease.

8.5.3 iNKT cytokine production during HIV infection and treatment

In order to determine whether LAG-3 expression could negatively impact iNKT function during chronic infection, we needed to establish whether iNKT cells derived from the FSW cohort were capable of productively responding to antigenic stimulation. Studies of

iNKT function during HIV infection and treatment in the literature suffer from inconsistent protocols and lack of replication in multiple cohorts. Furthermore, only one functional study has been performed in an African cohort (243), and that study included data only from PMA-stimulated iNKTs derived from ART-naïve subjects.

iNKT IFNγ production was significantly altered by HIV status, with HIV+ subjects exhibiting the lowest mean proportion of IFNγ+ iNKT cells in response to both PMA/Io and αGalCer stimulation (Figure 7.5, 7.7). Interestingly, the impact of HIV infection on TNFα production was less dramatic than that observed for IFNγ, suggesting that not all cytokines may be equally affected by HIV infection. These observations are generally in agreement other studies that suggest that iNKT cytokine production in response to lipid stimulation is generally compromised in ART-naïve chronically infected subjects. Defects in IFNγ production as measured by flow cytometry have been reported in two cohorts, while decreased TNFα production and proliferation were reported only once (338, 344). In contrast to TCR-mediated lipid stimulation, iNKT responses to PMA/Io are generally comparable between healthy and HIV+ groups (243, 344), although we did observe a significant decrease in PMA-induced IFNγ production among HIV-infected participants.

In this study, IFNγ production among ART-experienced patients did not fully rebound to levels of the healthy controls, with statistical analysis suggesting they exhibited intermediate responses between HIV+ ART naïve participants and HIV-uninfected women. Literature reports of restoration of iNKT function following ART initiation are

inconsistent. Some studies suggest an improvement of iNKT cytokine production following ART (336, 483), although one study initiated ART during acute infection and stimulated iNKT cultures after the depletion of CD8+ T cells, which therefore also depleted CD8+ iNKT cells, while another included an experimental IL-2 treatment in combination with ART. Conversely, other studies have failed to find ART-based improvement of iNKT function (338), or have not differentiated between treated and untreated subjects (344).

This study is therefore the first to include data on cell-specific IFNγ and TNFα production in response to both lipid and PMA/Io stimulation, particularly in an African cohort of predominately clade A HIV infections. We also assessed iNKT-driven cytokine production in PBMC cultures by multiplex bead array to further expand data regarding non-Th1 cytokines and chemokines induced by iNKT activation. Due to the experimental set up optimized for flow cytometry, above-background cytokine expression was not detected after only 24hrs of αGalCer stimulation. By 5 days post-stimulation, however, cytokine production was quite robust. For all analytes for which a significant difference in expression was detected, expression was lower or less likely among HIV+ subjects. Consistent with the ICS data obtained at 10hrs, IFNγ was the cytokine most affected by HIV status (Figure 7.8, 7.10).

The background subtracted supernatant cytokine/chemokine levels represent not only iNKT cytokine/chemokine production, but also protein expression by other cell subsets in response to iNKT activation. Although the correlation between iNKT frequency and

analyte concentration strongly suggests that the measured analyte levels are iNKT-induced (Table 7.4), defects or changes in cytokine profiles cannot be attributed solely to the iNKT population. *In vivo*, however, downstream responses to lipid ligand activation of iNKT cells (mimicked here by αGalCer) would include multiple lymphocyte/monocyte subsets, making the results obtained here relevant to immune responses during infection.

Overall, several patterns emerged from analysis of cytokine/chemokine expression levels and correlations. Among HIV-N participants, IFNγ, IL-13 and IL-4 correlated with each other (Table 7.6), and IFNγ and IL-13 were the major cytokines produced in culture after IP-10. IFN-γ and IL-4 are hallmark cytokines produced upon αGalCer stimulation. IL-13 is produced by activated iNKT cells and directs monocyte to DC differentiation (484). The loss of IL-13 secretion among HIV+ participants likely reflects the depletion of the CD4+ iNKT subset, which is reportedly the sole iNKT subset to produce IL-13 (225, 343).

In contrast, cytokine production among HIV+ ART naïve participants was mostly limited to IP-10 and MIP-1α/β production. The reduction in IFNγ, IL-13 and IL-4 production reflects defects in both Th1 and Th2 cytokines. Among the ART experienced group, there was little reconstitution of iNKT function. ART experienced patients were the most likely to lack above-background cytokine responses for all analytes studied, and never produced significantly higher levels of any analyte compared the ART naïve group. Cytokine correlations in the ART experienced group involved mostly TNFα and MIP-1α/β, which

is consistent with the increased contribution of those analytes to the total

cytokine/chemokine pool produced. These data suggest that in addition to a lack of

reconstitution of iNKT function among ART experienced patients, the cytokine

production profile is altered in comparison to both HIV-N and ART-naïve subjects.

The correlations between sLAG-3 production and cytokine/chemokine concentrations

among all study groups suggest that sLAG-3 may simply be a marker of iNKT activation

(Figure 7.11). There is no evidence that increasing concentrations of sLAG-3 in culture

results in inhibition of cytokine production. The lack of production of sLAG-3 in HIV+

ART naïve, but not ART-treated, participants is distinct compared to other

cytokine/chemokine responses, which were generally absent in the ART treated group.

The production of sLAG-3 by iNKT cells following stimulation has not been described in

the literature, and represents a significant gap in knowledge.

8.5.4 Correlation of LAG-3 and PD-1 expression with iNKT function

In this study, the *ex vivo* expression of LAG-3 on the iNKT subset inversely correlated

with IFNγ secretion as measured by ICS following αGalCer stimulation (Figure 7.6). The

association of LAG-3, but not PD-1, with iNKT dysfunction during HIV infection is

broadly consistent with a previous study of iNKT PD-1 expression (338). Although PD-1

expression was elevated among HIV-infected subjects in that cohort, its expression did

not correlate with cytokine production or proliferation, and blocking of the PD-1/PD-L1

pathway did not improve proliferation or IFNγ secretion. Despite the differing PD-1

surface expression, this study did replicate the observation that *ex vivo* PD-1 expression

was not correlated with cytokine production or proliferation among HIV+ subjects. To date, the contribution of other exhaustion markers (Tim-3, CD160, 2B4) to iNKT function during HIV infection has not been defined. The contribution of Tim-3 to iNKT inhibition during herpes simplex virus infection was assessed, but found to be not responsible for the defects in cytokine secretion (485).

The only surface marker previously demonstrated to correlate with iNKT cytokine production during HIV infection is the costimulatory molecule CD161 (Killer cell lectin-like receptor subfamily B, member 1 (KLRB1); NKR-P1A) (344). CD161 is expressed by a variable, but generally high, proportion of iNKT cells (344, 486, 487), while its expression on conventional T cells is associated with IL-17 secretion (488). The function of CD161 on NK and T cells remains relatively obscure (489, 490), but several studies now demonstrate a costimulatory function that promotes iNKT proliferation and cytokine secretion (333, 486, 487). Indeed, CD161+ iNKT cells are more likely to produce IFNγ and TNFα than CD161- cells in healthy individuals (487, 491). Snyder-Cappione *et al*'s association between high CD161 expression and poor iNKT cytokine production is therefore contrary to the current understanding of CD161 function. It is important to note, additionally, that this study did not compare CD161 levels between HIV-infected and – uninfected subjects, nor did it examine the relationship between CD161 expression and cytokine secretion on a per-cell basis. The current study, however, did not assess CD161 expression and therefore cannot confirm or rule out a contribution of CD161 upregulation to iNKT dysfunction.

The lack of correlation between LAG-3 expression and PMA-induced IFNγ expression, despite reduced PMA IFNγ responses among HIV-infected participants, is consistent with LAG-3 inhibition of TCR signaling pathways. PMA activation of lymphocytes bypasses the TCR and initiates downstream calcium signaling events; if LAG-3 were to inhibit iNKT activation via upstream TCR-activated pathways, it would have little impact on PMA responses. The reducion in IFNγ production following PMA stimulation does suggest, however, that additional factors likely contribute to the decreased IFNγ production observed by αGalCer stimulation of HIV+ participants.

The correlation between LAG-3 expression and supernatant IFNγ at 5 days post-stimulation is consistent with the ICS results described above. It is important to note, however, that changes in LAG-3 expression during culture, and the contribution of other PBMC cell subsets to cytokine production make a direct link between LAG-3 expression and long-term cytokine production difficult. The positive correlations between PD-1 expression and cytokine production also suggest that PD-1 may indicate a more activated, rather than exhausted, iNKT phenotype.

8.5.5 Limitations and Opportunities

The major limitation of the iNKT stimulation experiments lies in the small sample size of HIV+ ART-naïve participants. Recruitment of ART-naïve cohort members was much slower than for healthy and ART experienced participants. This was compounded by the need to exclude several ART naïve samples from analysis due to low iNKT frequency and an insufficient number of iNKT events following stimulation. Despite the sample

size limitation, however, significant differences in iNKT function and phenotype were still observed, underscoring the relatively strong impact of HIV infection on the iNKT subset. Issues with iNKT frequency are common among all *ex vivo* iNKT studies, and the sample sizes in this study are comparable to those published previously (243, 338, 344).

Identification and stimulation of iNKT cells can be accomplished by a variety of methods. The iNKT population can be identified using a combination of Vα24 and Vβ11 antibodies (338), CD1d-αGalCer tetramers (344, 492) or the monoclonal antibody 6B11 (248, 272, 493-498), as used in this study. There are advantages and disadvantages to each method, but 6B11-PE has been identified as an excellent antibody-fluorochrome combination (499) that strongly overlaps/correlates with tetramer staining (353), and requires only one fluorescent channel. Lipid-based iNKT stimulation can be performed using artificial αGalCer presentation (344, 500), αGalCer-pulsed DC (239) or direct addition of αGalCer to PBMC culture (250, 338, 494, 495, 501). Although addition of αGalCer directly to culture assumes comparable αGalCer presentation via CD1d across all participants, there is no evidence to suggest that CD1d-mediated lipid presentation is altered in HIV+ PBMC cultures (338, 502). As mentioned above, analysis of the iNKT subset by flow cytometry must consider the total number of iNKT events collected due to the low frequency present in peripheral blood. Many published studies do not report the threshold of events required for analysis, but those that do typically require at least 20-30 events to be collected (344, 500). In general, 300,000-500,000 lymphocyte events are collected (493, 496), which is consistent with the requirement for this study where 400,000 events were collected and at least 30 iNKT events acquired for analysis.

There are several notable caveats to the analysis of the cytokine/chemokine concentrations from the 5 day αGalCer stimulation cultures. While αGalCer specifically activates iNKT cells, iNKT cytokine production plays a major role in downstream activation of other lymphocyte subsets including NK and T cells, making it highly probable that bystander activation of other cells has contributed to the cytokine environment of the culture. Nonetheless, the correlation of almost all analytes with *ex vivo* iNKT frequency strongly suggests that cytokine production is dependent on iNKT activation, and that the resulting cytokine/chemokine levels are at least reflective of both direct and indirect effects of iNKT function. It is possible, however, that the differences observed between groups are at least partially attributable to defects in NK or T cell function among HIV+ participants. To complement this study, iNKT cells should be selected/sorted and stimulated in the absence of other lymphocytes. That data would more specifically address iNKT dysfunction during HIV infection, and could be compared to the results obtained from whole PBMC culture. It is important to note, however, that iNKT cells do not act in isolation *in vivo*, and that changes in whole PBMC culture responses to iNKT activation may be more reflective of the outcome of iNKT activation *in vivo* during infection.

8.6 General Discussion – Major Findings

8.6.1 GNB3 genotype in Africans

This thesis demonstrated that there is no evidence to link *GNB3 825* genotype to risk of HIV acquisition or disease progression. In the broader context of studies aimed identifying the impact of this SNP, which alters the expression of a widely and

constitutively expressed signaling protein, this study provides needed insight into the population-specific impact of the *GNB3 825T* allele, particularly among under-studied African populations. Perhaps one of the most intriguing implications of this work is the observation that GNB3 RNA splicing may be altered in African individuals. Further studies of the impact of various SNPs and haplotypes on Gb3s/s2 expression could yield novel insights into the mechanisms regulating splice variant production in this interesting splice variant model.

8.6.2 LAG-3 and iNKT cells

The results of this thesis suggest that iNKT cells are not irreversibly exhausted during chronic HIV infection but may instead be inhibited by increased expression of the MHCII-binding protein LAG-3. There are three major observations made by this thesis: first, the lack of LAG-3 expression on conventional T cell subests makes LAG-3 unique among the cohort of known exhaustion markers; second, the enrichment of LAG-3 on innate-like lymphocyte subsets suggests a unique role for inhibiting innate immunity during chronic infection; third, the increased expression of LAG-3 on mucosal lymphocytes suggests the potential to modulate LAG-3 activity to fine-tune immune activation at a site of HIV transmission.

The study of 'exhaustion markers' in the context of chronic viral infection, particularly HIV infection and treatment, is currently undergoing a period of upheaval and controversy. Although the expression of any one of a number of inhibitory markers is often ascribed to a state of exhaustion, recent data suggests that the functional impact of

these markers is often more complex and multifactorial than originally assumed. The function of Tim-3, originally reported to mediate stronger exhaustion than PD-1 (377), appears to be either inhibitory or costimulatory depending on the cell subset studied (457, 503), and most recently was suggested to play little to no role in T cell function and to not bind its putative ligand, galectin 9 (504). Even PD-1, the hallmark exhaustion marker, appears in some circumstances to more accurately mark cellular activation than exhaustion or inhibition (455, 505-507). Indeed, PD-1+ cells may still undergo proliferation and exhibit cytotoxic activity during chronic infection (508, 509).

Furthermore, the link between inhibitory surface receptors and immune exhaustion may be generally restricted to conventional T cells. While elevated T cell Tim-3 expression can inhibit proliferation, cytotoxicity and cytokine production during infection (377, 510), it may act as a maturation marker on NK cells, where it suppresses cytotoxicity but either has no impact on or increases cytokine production (457, 458). Similarly, a report of PD-1 upregulation on iNKT cells during HIV infection found that unlike its impact on T cells, PD-1 did not mediate inhibition of iNKT IFNγ production or proliferation. Disparities between inhibitory and activating activity on T cell and NK cell subsets have also been reported for CD160 (511-513).

In this context, prior to our study not only was little data available regarding LAG-3 expression during chronic HIV infection, but assessment of its function on non-T cell subsets was entirely lacking. The observation that LAG-3 expression is low on bulk T cells but enriched on iNKT, NK and DN T cells (innate and innate-like lymphocytes)

suggests a unique opportunity to boost immune function during HIV infection. Despite

the success of ART in restoring T cell immunity, we now understand that improvement

of T cell function does not necessarily correlate with restoration of innate immune

responses. The function of innate cell subsets including mucosal associated invariant T

cells (MAIT)(514), NK cells (460, 461), γδ T cells (515),(516) and iNKT cells (337) are

all either not restored by cART, or only partially restored. Blockade of canonical

inhibitory signaling pathways (PD-1, Tim-3) to restore immune function during HIV

infection is gaining popularity as both a treatment strategy and component of viral

eradication regimens, but there are several important drawbacks to this approach. The

wide expression of these markers on bulk T cell subsets raises the possibility of off-target

effects and the potential to exacerbate autoimmune conditions. Second, the non-inhibitory

effects of these markers on innate cell subsets suggests that blockade is unlikely to boost

innate immune responses even in the context of ART and could, potentially, further

inhibit innate immune function. In contrast, LAG-3 is negligibly expressed by peripheral

T cells, limiting the impact of LAG-3 blockade to cell subsets of interest. Given that this

thesis suggests that LAG-3 retains inhibitory activity on iNKT cells, LAG-3 blockade

could therefore selectively target and restore innate-like lymphocyte function during

chronic infection.

8.6.3 Hypotheses and conclusions

The two major hypotheses of this thesis were that:

1) *GNB3 825TT* genotype will be associated with increased risk of HIV acquisition

   and rapid disease progression compared to the *GNB3 825CC/CT* genotypes. This

will be associated with Gb3s RNA splicing and increased expression of immune activation markers among *GNB3 825TT* subjects.

2) LAG-3 protein expression will be increased on CD4+ and CD8+ T cells, NK cells and iNKT cells during chronic HIV infection compared to HIV-N subjects, and will decrease among subjects receiving ARV therapy. LAG-3 expression will be correlated with loss of T cell effector function and disease progression.

This thesis disproved the first hypothesis, demonstrating that *GNB3* genotype was not associated with HIV acquisition, disease progression, immune activation or *GNB3* RNA splicing in the Kenyan cohorts studied. Further analysis of *GNB3 825T* genotype and HIV infection or replication will be more suited to populations demonstrating a significant link between *GNB3* genotype and HIV progression.

Although LAG-3 expression was significantly higher among T cell, NK and iNKT subsets in HIV-infected study participants, its expression was relatively low on most subsets other than iNKT cells. Contrary to the hypothesis, LAG-3 expression remained high among ARV-treated patients. Importantly, iNKT LAG-3 expression negatively correlates with iNKT IFNγ secretion in response to lipid antigen stimulation, suggesting that LAG-3 may be an important negative regulator of iNKT function during chronic HIV infection.

8.7 Future Directions

8.7.1 GNB3 825 Genotype

Given the diversity of cohorts involved in this study of *GNB3 825* genotype and HIV acquisition and progression, it is difficult to justify further investigation into the impact of the *GNB3 825TT* genotype on HIV infection in African populations. Given the disparity between reported epidemiological associations of *GNB3* genotype between ethnic groups, however, further confirmation of the impact of the *GNB3 825T* allele on HIV progression in Caucasian cohorts could be considered.

Furthermore, it remains unclear why the presence of the *GNB3 825T* allele was not associated with Gb3s and Gb3s2 splice variant production in PBMC from participants in the FSW cohort. Future studies could aim to confirm whether lymphocytes derived from African *825TT* individuals do indeed exhibit increased SDF-1α-mediated chemotaxis as has been demonstrated in Caucasian populations. *GNB3* mRNA splicing patterns could also be investigated in a low-risk African cohort to better understand whether the effect of the *825* SNP is consistent among populations with diverse T allele frequencies.

While this thesis demonstrated no differences in baseline immune activation between individuals of differing *GNB3* genotypes, it did not address whether there are differences in the quantity or quality of HIV-specific T cell responses among *GNB3 825TT* subjects compared to *GNB3 825CC/CT* individuals. Previous studies have demonstrated differences in T cell responses to vaccination across genotype groups.

The studies in this thesis aimed to elucidate the contribution of LAG-3 expression to

iNKT cell dysfunction during HIV infection. The results described here suggest four

major areas of future investigations: (1) the impact of HIV/ART-mediated lipid

perturbation on iNKT function, (2) the impact of elevated iNKT LAG-3 expression on

DC maturation and activation during HIV infection, (3) the contribution of iNKT LAG-3

expression to iNKT anergy in the context of vaccination and infection, and (4) the

presence of iNKT cell populations at the female genital mucosa.

A major gap in current knowledge concerns the impact of lipid modulation during HIV

infection and treatment on iNKT activation and function. There are two major issues that

have yet to be addressed: First, the capacity of viral infection to modify host cell

endogenous lipid production is unknown. A recent study demonstrated that HBV

infection induces phospholipase-mediated production of endogenous lipid antigens that,

when presented by CD1d, activate the iNKT subset and enhance the adaptive immune

response (236). Whether HIV infection of T cells or macrophages similarly results in

perturbation of endogenous lipid production is unknown, but could represent an

additional mechanism by which the iNKT subset may become activated during acute or

chronic HIV infection. Second, the impact of dyslipidemia, a common side effect caused

by ART (517), on iNKT activation has not been investigated. In a mouse model of

dyslipidemia, the iNKT population exhibited an anergic phenotype and high levels of

PD-1 expression, which the authors attributed to chronic iNKT activation due to lipid

dysregulation (463). It is possible that aberrant iNKT responses among ARV-treated

patients, as observed in this thesis, could be related to abnormal endogenous lipid presentation in a similar manner.

While the inhibitory effect of LAG-3 expression was determined in a cell-intrinsic manner for the iNKT subset, it is important to consider the impact of LAG-3 expression on APCs during iNKT-CD1d interactions. Intriguingly, both LAG-3/MHCII interactions and iNKT/DC co-culture induce a similar upregulation of CD86 and CD40 and production of IL-12 and TNFα by DCs (422, 423, 484, 518, 519). iNKT-mediated upregulation of CD80/86 on DCs is independent of CD40/CD40L signaling (520), making it plausible that LAG-3 expression could be partially responsible for inducing the maturation program. Under normal circumstances where iNKT LAG-3 expression is low, iNKT induction of APC-derived IL-12 could induce iNKT LAG-3 upregulation, promoting further APC maturation and activation. Under conditions of high pre-existing iNKT LAG-3 expression, however, early LAG-3 engagement could inhibit monocyte-to-DC differentiation and DC antigen presentation (428), thereby contributing to DC dysfunction during chronic HIV infection.

iNKT dysfunction during HIV infection is strikingly similar to the anergic phenotype exhibited by iNKT cells following TCR stimulation. To date, the development of iNKT anergy following stimulation has not been tested or demonstrated in humans, despite the fact that the use of αGalCer as a vaccine adjuvant may be detrimental if anergy is induced. The mediators of murine iNKT anergy are not well understood, and the role of PD-1 is reported inconsistently and unconvincingly (345, 346, 521-523). Given the high

induction of LAG-3 expression by αGalCer by 5 days post stimulation, the role of LAG-3 in mediating iNKT anergy should be examined in conjunction with PD-1, especially in human PBMC.

Finally, the frequency, phenotype and function of iNKT cells at mucosal sites in humans are poorly defined. While iNKT populations were not observed in cervical mononuclear cell preparations from the FSW cohort, 6B11 staining was inconsistently detected in cervical samples from Winnipeg donors. The combination of the tissue-homing phenotype of iNKT cells with the demonstrated expression of CD1d in tissues of the FGT (274, 275) suggests that iNKT cells likely do home to the genital tract. Further characterization of the iNKT population at the FGT is required, possibly in tissue biopsies rather than cervical scrapings, to improve cell yield. The impact of the menstrual cycle must also be further taken into consideration when collecting genital mucosal samples.

Together, these studies will yield important insights into not only mechanisms of immune dysfunction during HIV infection and treatment, but also into the function of a cell subset that is becoming increasingly important in vaccination strategies. The plasticity of iNKT function and pleiotropic effects of LAG-3 on multiple cell types allows for a unique opportunity to harness these cells for use in vaccine development and to boost their function during chronic infections. A better understanding of the function and regulation of LAG-3 will be crucial in the process of developing immune-boosting therapeutics.

9. References

1.   UNAIDS. Global Report 2013.
http://www.unaids.org/en/media/unaids/contentassets/documents/epidemiology/2013/gr2013/UNAIDS_Global_Report_2013_en.pdf: 2013.
2.   Programme NAaSC. Kenya AIDS Indicator Survey 2012. 2012.
3.   Pneumocystis pneumonia--Los Angeles. MMWR Morb Mortal Wkly Rep. 1981;30(21):250-2. Epub 1981/06/05.
4.   Kaposi's sarcoma and Pneumocystis pneumonia among homosexual men--New York City and California. MMWR Morb Mortal Wkly Rep. 1981;30(25):305-8. Epub 1981/07/03.
5.   Update on acquired immune deficiency syndrome (AIDS)--United States. MMWR Morb Mortal Wkly Rep. 1982;31(37):507-8, 13-4. Epub 1982/09/24.
6.   Barre-Sinoussi F, Chermann JC, Rey F, Nugeyre MT, Chamaret S, Gruest J, et al. Isolation of a T-lymphotropic retrovirus from a patient at risk for acquired immune deficiency syndrome (AIDS). Science. 1983;220(4599):868-71. Epub 1983/05/20.
7.   Gallo RC, Sarin PS, Gelmann EP, Robert-Guroff M, Richardson E, Kalyanaraman VS, et al. Isolation of human T-cell leukemia virus in acquired immune deficiency syndrome (AIDS). Science. 1983;220(4599):865-7. Epub 1983/05/20.
8.   Sarngadharan MG, Popovic M, Bruch L, Schupbach J, Gallo RC. Antibodies reactive with human T-lymphotropic retroviruses (HTLV-III) in the serum of patients with AIDS. Science. 1984;224(4648):506-8. Epub 1984/05/04.
9.   Coffin J, Haase A, Levy JA, Montagnier L, Oroszlan S, Teich N, et al. What to call the AIDS virus? Nature. 1986;321(6065):10. Epub 1986/05/01.
10.   Campbell-Yesufu OT, Gandhi RT. Update on human immunodeficiency virus (HIV)-2 infection. Clin Infect Dis. 2011;52(6):780-7. Epub 2011/03/04.
11.   Plantier JC, Leoz M, Dickerson JE, De Oliveira F, Cordonnier F, Lemee V, et al. A new human immunodeficiency virus derived from gorillas. Nature medicine. 2009;15(8):871-2. Epub 2009/08/04.
12.   Vallari A, Holzmayer V, Harris B, Yamaguchi J, Ngansop C, Makamche F, et al. Confirmation of putative HIV-1 group P in Cameroon. Journal of virology. 2011;85(3):1403-7. Epub 2010/11/19.
13.   Sharp PM, Hahn BH. Origins of HIV and the AIDS Pandemic. Cold Spring Harbor Perspectives in Medicine. 2011;1(1).
14.   Hemelaar J. The origin and diversity of the HIV-1 pandemic. Trends Mol Med. 2012. Epub 2012/01/14.
15.   UNAIDS W. AIDS Epidemic Update 2009. Joint United Nations Programme on HIVAIDS UNAIDS and World Health Organization WHO; 2009 [cited 2011 August 10, 2011]; Available from:
http://www.unaids.org/en/media/unaids/contentassets/dataimport/pub/report/2009/jc1700_epi_update_2009_en.pdf.
16.   Boily MC, Baggaley RF, Wang L, Masse B, White RG, Hayes RJ, et al. Heterosexual risk of HIV-1 infection per sexual act: systematic review and meta-analysis of observational studies. Lancet Infect Dis. 2009;9(2):118-29. Epub 2009/01/31.

17.	Hughes JP, Baeten JM, Lingappa JR, Magaret AS, Wald A, de Bruyn G, et al. Determinants of Per-Coital-Act HIV-1 Infectivity Among African HIV-1-Serodiscordant Couples. The Journal of infectious diseases. 2012;205(3):358-65. Epub 2012/01/14.

18.	Ward H, Ronn M. Contribution of sexually transmitted infections to the sexual transmission of HIV. Current opinion in HIV and AIDS. 2010;5(4):305-10. Epub 2010/06/15.

19.	Mavedzenge SN, Van der Pol B, Weiss HA, Kwok C, Mambo F, Chipato T, et al. The association between Mycoplasma genitalium and HIV-1 acquisition among women in Zimbabwe and Uganda. AIDS (London, England). 2012. Epub 2012/01/03.

20.	Pedraza MA, del Romero J, Roldan F, Garcia S, Ayerbe MC, Noriega AR, et al. Heterosexual transmission of HIV-1 is associated with high plasma viral load levels and a positive viral isolation in the infected partner. Journal of acquired immune deficiency syndromes (1999). 1999;21(2):120-5. Epub 1999/06/09.

21.	Forbes JC, Alimenti AM, Singer J, Brophy JC, Bitnun A, Samson LM, et al. 21-year review of vertical HIV transmission in Canada (1990 to 2010). AIDS (London, England). 2012. Epub 2012/01/03.

22.	Tudor Car L, van-Velthoven MH, Brusamento S, Elmoniry H, Car J, Majeed A, et al. Integrating prevention of mother-to-child HIV transmission (PMTCT) programmes with other health services for preventing HIV infection and improving HIV outcomes in developing countries. Cochrane Database Syst Rev. 2011(6):CD008741. Epub 2011/06/17.

23.	Mofenson LM. Prevention in neglected subpopulations: prevention of mother-to-child transmission of HIV infection. Clin Infect Dis. 2010;50 Suppl 3:S130-48. Epub 2010/04/20.

24.	UNAIDS. Global HIV/AIDS Response - Progress Report 20112011 January 3 2012. Available from: http://www.unaids.org/en/media/unaids/contentassets/documents/unaidspublication/2011/20111130_UA_Report_en.pdf.

25.	Granich RM, Gilks CF, Dye C, De Cock KM, Williams BG. Universal voluntary HIV testing with immediate antiretroviral therapy as a strategy for elimination of HIV transmission: a mathematical model. Lancet. 2009;373(9657):48-57. Epub 2008/11/29.

26.	Cohen J. Breakthrough of the year. HIV treatment as prevention. Science. 2011;334(6063):1628. Epub 2011/12/24.

27.	Attia S, Egger M, Muller M, Zwahlen M, Low N. Sexual transmission of HIV according to viral load and antiretroviral therapy: systematic review and meta-analysis. AIDS (London, England). 2009;23(11):1397-404. Epub 2009/04/22.

28.	Smith K, Powers KA, Kashuba AD, Cohen MS. HIV-1 treatment as prevention: the good, the bad, and the challenges. Current opinion in HIV and AIDS. 2011;6(4):315-25. Epub 2011/06/08.

29.	Grant RM, Lama JR, Anderson PL, McMahan V, Liu AY, Vargas L, et al. Preexposure chemoprophylaxis for HIV prevention in men who have sex with men. The New England journal of medicine. 2010;363(27):2587-99. Epub 2010/11/26.

30.	van der Straten A, van Damme L, Haberer JE, Bangsberg DR. How well does PREP work? Unraveling the divergent results of PrEP trials for HIV prevention. AIDS (London, England). 2012. Epub 2012/02/16.

31.   Hontelez JA, de Vlas SJ, Tanser F, Bakker R, Barnighausen T, Newell ML, et al. The impact of the new WHO antiretroviral treatment guidelines on HIV epidemic dynamics and cost in South Africa. PloS one. 2011;6(7):e21919. Epub 2011/07/30.

32.   Kretzschmar ME, van der Loeff MF, Coutinho RA. Elimination of HIV by test and treat: a phantom of wishful thinking? AIDS (London, England). 2012;26(2):247-8. Epub 2011/12/20.

33.   Shelton JD. ARVs as HIV Prevention: A Tough Road to Wide Impact. Science. 2011;334(6063):1645-6.

34.   Siegfried N, Muller M, Deeks JJ, Volmink J. Male circumcision for prevention of heterosexual acquisition of HIV in men. Cochrane Database Syst Rev. 2009(2):CD003362. Epub 2009/04/17.

35.   Gray R, Kigozi G, Kong X, Ssempiija V, Makumbi F, Wattya S, et al. The effectiveness of male circumcision for HIV prevention and effects on risk behaviors in a post-trial follow up study in Rakai, Uganda. AIDS (London, England). 2012. Epub 2012/01/03.

36.   Shattock RJ, Rosenberg Z. Microbicides: Topical Prevention against HIV. Cold Spring Harbor Perspectives in Medicine. 2011(Journal Article).

37.   Abdool Karim Q, Abdool Karim SS, Frohlich JA, Grobler AC, Baxter C, Mansoor LE, et al. Effectiveness and safety of tenofovir gel, an antiretroviral microbicide, for the prevention of HIV infection in women. Science. 2010;329(5996):1168-74. Epub 2010/07/21.

38.   McKinnon LR, Card CM. HIV vaccine efficacy trials: A brief history, and options for going forward. AIDS reviews. 2010;12(4):209-17. Epub 2010/12/24.

39.   Rerks-Ngarm S, Pitisuttithum P, Nitayaphan S, Kaewkungwal J, Chiu J, Paris R, et al. Vaccination with ALVAC and AIDSVAX to prevent HIV-1 infection in Thailand. The New England journal of medicine. 2009;361(23):2209-20. Epub 2009/10/22.

40.   Haynes BF, Gilbert PB, McElrath MJ, Zolla-Pazner S, Tomaras GD, Alam SM, et al. Immune-correlates analysis of an HIV-1 vaccine efficacy trial. The New England journal of medicine. 2012;366(14):1275-86. Epub 2012/04/06.

41.   Koup RA, Douek DC. Vaccine Design for CD8 T Lymphocyte Responses. Cold Spring Harbor Perspectives in Medicine. 2011;1(1).

42.   Saunders KO, Rudicell RS, Nabel GJ. The design and evaluation of HIV-1 vaccines. AIDS (London, England). 2012;26(10):1293-302. Epub 2012/06/19.

43.   Frankel AD, Young JA. HIV-1: fifteen proteins and an RNA. Annu Rev Biochem. 1998;67:1-25. Epub 1998/10/06.

44.   McDougal JS, Kennedy MS, Sligh JM, Cort SP, Mawle A, Nicholson JK. Binding of HTLV-III/LAV to T4+ T cells by a complex of the 110K viral protein and the T4 molecule. Science. 1986;231(4736):382-5. Epub 1986/01/24.

45.   Maddon PJ, Dalgleish AG, McDougal JS, Clapham PR, Weiss RA, Axel R. The T4 gene encodes the AIDS virus receptor and is expressed in the immune system and the brain. Cell. 1986;47(3):333-48. Epub 1986/11/07.

46.   Freed EO. HIV-1 replication. Somat Cell Mol Genet. 2001;26(1-6):13-33. Epub 2002/12/06.

47.   Feng Y, Broder CC, Kennedy PE, Berger EA. HIV-1 entry cofactor: functional cDNA cloning of a seven-transmembrane, G protein-coupled receptor. Science. 1996;272(5263):872-7. Epub 1996/05/10.

48.	Deng H, Liu R, Ellmeier W, Choe S, Unutmaz D, Burkhart M, et al. Identification of a major co-receptor for primary isolates of HIV-1. Nature. 1996;381(6584):661-6. Epub 1996/06/20.

49.	Dragic T, Litwin V, Allaway GP, Martin SR, Huang Y, Nagashima KA, et al. HIV-1 entry into CD4+ cells is mediated by the chemokine receptor CC-CKR-5. Nature. 1996;381(6584):667-73. Epub 1996/06/20.

50.	Alkhatib G, Combadiere C, Broder CC, Feng Y, Kennedy PE, Murphy PM, et al. CC CKR5: a RANTES, MIP-1alpha, MIP-1beta receptor as a fusion cofactor for macrophage-tropic HIV-1. Science. 1996;272(5270):1955-8. Epub 1996/06/28.

51.	Choe H, Farzan M, Sun Y, Sullivan N, Rollins B, Ponath PD, et al. The beta-chemokine receptors CCR3 and CCR5 facilitate infection by primary HIV-1 isolates. Cell. 1996;85(7):1135-48. Epub 1996/06/28.

52.	Doranz BJ, Rucker J, Yi Y, Smyth RJ, Samson M, Peiper SC, et al. A dual-tropic primary HIV-1 isolate that uses fusin and the beta-chemokine receptors CKR-5, CKR-3, and CKR-2b as fusion cofactors. Cell. 1996;85(7):1149-58. Epub 1996/06/28.

53.	Gorry PR, Dunfee RL, Mefford ME, Kunstman K, Morgan T, Moore JP, et al. Changes in the V3 region of gp120 contribute to unusually broad coreceptor usage of an HIV-1 isolate from a CCR5 Delta32 heterozygote. Virology. 2007;362(1):163-78. Epub 2007/01/24.

54.	Karlsson U, Antonsson L, Ljungberg B, Medstrand P, Esbjornsson J, Jansson M, et al. Dual R3R5 tropism characterizes cerebrospinal fluid HIV-1 isolates from individuals with high cerebrospinal fluid viral load. AIDS (London, England). 2012;26(14):1739-44. Epub 2012/06/15.

55.	Ngai J, Methi T, Andressen KW, Levy FO, Torgersen KM, Vang T, et al. The heterotrimeric G-protein alpha-subunit Galphaq regulates TCR-mediated immune responses through an Lck-dependent pathway. European journal of immunology. 2008;38(11):3208-18.

56.	Herroeder S, Reichardt P, Sassmann A, Zimmermann B, Jaeneke D, Hoeckner J, et al. Guanine nucleotide-binding proteins of the G12 family shape immune functions by controlling CD4+ T cell adhesiveness and motility. Immunity. 2009;30(5):708-20. Epub 2009/05/05.

57.	Wettschureck N, Offermanns S. Mammalian G proteins and their cell type specific functions. Physiological reviews. 2005;85(4):1159-204.

58.	Dascal N. Ion-channel regulation by G proteins. Trends in endocrinology and metabolism: TEM. 2001;12(9):391-8.

59.	Rommel C, Camps M, Ji H. PI3K delta and PI3K gamma: partners in crime in inflammation in rheumatoid arthritis and beyond? Nature reviews Immunology. 2007;7(3):191-201. Epub 2007/02/10.

60.	Jones KL, Smyth RP, Pereira CF, Cameron PU, Lewin SR, Jaworowski A, et al. Early events of HIV-1 infection: can signaling be the next therapeutic target? J Neuroimmune Pharmacol. 2011;6(2):269-83. Epub 2011/03/05.

61.	Juno JA, Fowke KR. Clarifying the role of G protein signaling in HIV infection: new approaches to an old question. AIDS reviews. 2010;12(3):164-76.

62.	Balabanian K, Harriague J, Decrion C, Lagane B, Shorte S, Baleux F, et al. CXCR4-tropic HIV-1 envelope glycoprotein functions as a viral chemokine in

unstimulated primary CD4+ T lymphocytes. Journal of immunology (Baltimore, Md: 1950). 2004;173(12):7150-60.

63.   Cocchi F, DeVico AL, Garzino-Demo A, Cara A, Gallo RC, Lusso P. The V3 domain of the HIV-1 gp120 envelope glycoprotein is critical for chemokine-mediated blockade of infection. Nature medicine. 1996;2(11):1244-7.

64.   Atchison RE, Gosling J, Monteclaro FS, Franci C, Digilio L, Charo IF, et al. Multiple extracellular elements of CCR5 and HIV-1 entry: dissociation from response to chemokines. Science (New York, NY). 1996;274(5294):1924-6.

65.   Farzan M, Choe H, Martin KA, Sun Y, Sidelko M, Mackay CR, et al. HIV-1 entry and macrophage inflammatory protein-1beta-mediated signaling are independent functions of the chemokine receptor CCR5. The Journal of biological chemistry. 1997;272(11):6854-7.

66.   Alkhatib G, Locati M, Kennedy PE, Murphy PM, Berger EA. HIV-1 coreceptor activity of CCR5 and its inhibition by chemokines: independence from G protein signaling and importance of coreceptor downmodulation. Virology. 1997;234(2):340-8.

67.   Gosling J, Monteclaro FS, Atchison RE, Arai H, Tsou CL, Goldsmith MA, et al. Molecular uncoupling of C-C chemokine receptor 5-induced chemotaxis and signal transduction from HIV-1 coreceptor activity. Proceedings of the National Academy of Sciences of the United States of America. 1997;94(10):5061-6.

68.   Amara A, Vidy A, Boulla G, Mollier K, Garcia-Perez J, Alcami J, et al. G protein-dependent CCR5 signaling is not required for efficient infection of primary T lymphocytes and macrophages by R5 human immunodeficiency virus type 1 isolates. Journal of virology. 2003;77(4):2550-8.

69.   Harmon B, Ratner L. Induction of the Galpha(q) signaling cascade by the human immunodeficiency virus envelope is required for virus entry. Journal of virology. 2008;82(18):9191-205. Epub 2008/07/18.

70.   Kelly MD, Naif HM, Adams SL, Cunningham AL, Lloyd AR. Dichotomous effects of beta-chemokines on HIV replication in monocytes and monocyte-derived macrophages. Journal of immunology (Baltimore, Md: 1950). 1998;160(7):3091-5.

71.   Reckless J, Grainger DJ. Identification of oligopeptide sequences which inhibit migration induced by a wide range of chemokines. The Biochemical journal. 1999;340 (Pt 3)(Pt 3):803-11.

72.   Grainger DJ, Reckless J. Broad-spectrum chemokine inhibitors (BSCIs) and their anti-inflammatory effects in vivo. Biochemical pharmacology. 2003;65(7):1027-34.

73.   Grainger DJ, Lever AM. Blockade of chemokine-induced signalling inhibits CCR5-dependent HIV infection in vitro without blocking gp120/CCR5 interaction. Retrovirology. 2005;2(Journal Article):23.

74.   Paruch S, Heinis M, Lemay J, Hoeffel G, Maranon C, Hosmalin A, et al. CCR5 signaling through phospholipase D involves p44/42 MAP-kinases and promotes HIV-1 LTR-directed gene expression. FASEB J. 2007;21(14):4038-46. Epub 2007/07/14.

75.   Francois F, Klotman ME. Phosphatidylinositol 3-Kinase Regulates Human Immunodeficiency Virus Type 1 Replication following Viral Entry in Primary CD4+ T Lymphocytes and Macrophages. Journal of virology. 2003;77(4):2539-49.

76.   Lin YL, Mettling C, Portales P, Reant B, Clot J, Corbeau P. G-protein signaling triggered by R5 human immunodeficiency virus type 1 increases virus replication

efficiency in primary T lymphocytes. Journal of virology. 2005;79(12):7938-41. Epub 2005/05/28.

77.   Mettling C, Desmetz C, Fiser AL, Reant B, Corbeau P, Lin YL. Galphai protein-dependant extracellular signal-regulated kinase-1/2 activation is required for HIV-1 reverse transcription. AIDS (London, England). 2008;22(13):1569-76.

78.   Montes M, Tagieva NE, Heveker N, Nahmias C, Baleux F, Trautmann A. SDF-1-induced activation of ERK enhances HIV-1 expression. European cytokine network. 2000;11(3):470-7.

79.   Yoder A, Yu D, Dong L, Iyer SR, Xu X, Kelly J, et al. HIV envelope-CXCR4 signaling activates cofilin to overcome cortical actin restriction in resting CD4 T cells. Cell. 2008;134(5):782-92. Epub 2008/09/09.

80.   Cameron PU, Saleh S, Sallmann G, Solomon A, Wightman F, Evans VA, et al. Establishment of HIV-1 latency in resting CD4+ T cells depends on chemokine-induced changes in the actin cytoskeleton. Proceedings of the National Academy of Sciences of the United States of America. 2010;107(39):16934-9. Epub 2010/09/15.

81.   Evans VA, Khoury G, Saleh S, Cameron PU, Lewin SR. HIV persistence: chemokines and their signalling pathways. Cytokine & growth factor reviews. 2012;23(4-5):151-7. Epub 2012/07/04.

82.   Spear M, Guo J, Turner A, Yu D, Wang W, Meltzer B, et al. HIV-1 triggers WAVE2 phosphorylation in primary CD4 T cells and macrophages, mediating Arp2/3-dependent nuclear migration. The Journal of biological chemistry. 2014. Epub 2014/01/15.

83.   Davis CB, Dikic I, Unutmaz D, Hill CM, Arthos J, Siani MA, et al. Signal transduction due to HIV-1 envelope interactions with chemokine receptors CXCR4 or CCR5. The Journal of experimental medicine. 1997;186(10):1793-8.

84.   Weissman D, Rabin RL, Arthos J, Rubbert A, Dybul M, Swofford R, et al. Macrophage-tropic HIV and SIV envelope proteins induce a signal through the CCR5 chemokine receptor. Nature. 1997;389(6654):981-5.

85.   Iyengar S, Schwartz DH, Hildreth JE. T cell-tropic HIV gp120 mediates CD4 and CD8 cell chemotaxis through CXCR4 independent of CD4: implications for HIV pathogenesis. Journal of immunology (Baltimore, Md: 1950). 1999;162(10):6263-7.

86.   Guo J, Xu X, Yuan W, Jin T, Wu Y. HIV gp120 is an Aberrant Chemoattractant for Blood Resting CD4 T Cells. Curr HIV Res. 2012. Epub 2012/09/08.

87.   Chandrasekaran P, Buckley M, Moore V, Wang LQ, Kehrl JH, Venkatesan S. HIV-1 Nef impairs heterotrimeric G-protein signaling by targeting Galphai2 for degradation through Ubiquitinylation. The Journal of biological chemistry. 2012. Epub 2012/10/17.

88.   Hladik F, Sakchalathorn P, Ballweber L, Lentz G, Fialkow M, Eschenbach D, et al. Initial events in establishing vaginal entry and infection by human immunodeficiency virus type-1. Immunity. 2007;26(2):257-70. Epub 2007/02/20.

89.   Dezutter-Dambuyant C, Charbonnier AS, Schmitt D. [Epithelial dendritic cells and HIV-1 infection in vivo and in vitro]. Pathol Biol (Paris). 1995;43(10):882-8. Epub 1995/12/01. Cellules dendritiques epitheliales et infection par HIV-1 in vivo et in vitro.

90.   Arthos J, Cicala C, Martinelli E, Macleod K, Van Ryk D, Wei D, et al. HIV-1 envelope protein binds to and signals through integrin alpha4beta7, the gut mucosal

homing receptor for peripheral T cells. Nature immunology. 2008;9(3):301-9. Epub 2008/02/12.

91.   Zack JA, Arrigo SJ, Weitsman SR, Go AS, Haislip A, Chen IS. HIV-1 entry into quiescent primary lymphocytes: molecular analysis reveals a labile, latent viral structure. Cell. 1990;61(2):213-22. Epub 1990/04/20.

92.   Bukrinsky MI, Stanwick TL, Dempsey MP, Stevenson M. Quiescent T lymphocytes as an inducible virus reservoir in HIV-1 infection. Science. 1991;254(5030):423-7. Epub 1991/10/18.

93.   von Schwedler U, Kornbluth RS, Trono D. The nuclear localization signal of the matrix protein of human immunodeficiency virus type 1 allows the establishment of infection in macrophages and quiescent T lymphocytes. Proceedings of the National Academy of Sciences of the United States of America. 1994;91(15):6992-6. Epub 1994/07/19.

94.   Siliciano RF, Greene WC. HIV Latency. Cold Spring Harbor Perspectives in Medicine. 2011;1(1).

95.   Cohen MS, Shaw GM, McMichael AJ, Haynes BF. Acute HIV-1 Infection. The New England journal of medicine. 2011;364(20):1943-54. Epub 2011/05/20.

96.   Daar ES, Pilcher CD, Hecht FM. Clinical presentation and diagnosis of primary HIV-1 infection. Current opinion in HIV and AIDS. 2008;3(1):10-5. Epub 2008/01/01.

97.   Lavreys L, Baeten JM, Chohan V, McClelland RS, Hassan WM, Richardson BA, et al. Higher set point plasma viral load and more-severe acute HIV type 1 (HIV-1) illness predict mortality among high-risk HIV-1-infected African women. Clin Infect Dis. 2006;42(9):1333-9. Epub 2006/04/06.

98.   Fahey JL, Taylor JM, Detels R, Hofmann B, Melmed R, Nishanian P, et al. The prognostic value of cellular and serologic markers in infection with human immunodeficiency virus type 1. The New England journal of medicine. 1990;322(3):166-72. Epub 1990/01/18.

99.   1993 revised classification system for HIV infection and expanded surveillance case definition for AIDS among adolescents and adults. MMWR Recomm Rep. 1992;41(RR-17):1-19. Epub 1992/12/18.

100.   Morgan D, Mahe C, Mayanja B, Okongo JM, Lubega R, Whitworth JA. HIV-1 infection in rural Africa: is there a difference in median time to AIDS and survival compared with that in industrialized countries? AIDS (London, England). 2002;16(4):597-603. Epub 2002/03/02.

101.   Anzala OA, Nagelkerke NJ, Bwayo JJ, Holton D, Moses S, Ngugi EN, et al. Rapid progression to disease in African sex workers with human immunodeficiency virus type 1 infection. The Journal of infectious diseases. 1995;171(3):686-9. Epub 1995/03/01.

102.   Okulicz JF, Lambotte O. Epidemiology and clinical characteristics of elite controllers. Current opinion in HIV and AIDS. 2011;6(3):163-8. Epub 2011/04/20.

103.   Buchbinder SP, Katz MH, Hessol NA, O'Malley PM, Holmberg SD. Long-term HIV-1 infection without immunologic progression. AIDS (London, England). 1994;8(8):1123-8. Epub 1994/08/01.

104.   Deacon NJ, Tsykin A, Solomon A, Smith K, Ludford-Menting M, Hooker DJ, et al. Genomic structure of an attenuated quasi species of HIV-1 from a blood transfusion donor and recipients. Science. 1995;270(5238):988-91. Epub 1995/11/10.

105.   Autran B, Descours B, Avettand-Fenoel V, Rouzioux C. Elite controllers as a model of functional cure. Current opinion in HIV and AIDS. 2011;6(3):181-7. Epub 2011/04/05.
106.   Guergnon J, Dalmasso C, Broet P, Meyer L, Westrop SJ, Imami N, et al. Single-Nucleotide Polymorphism-Defined Class I and Class III Major Histocompatibility Complex Genetic Subregions Contribute to Natural Long-term Nonprogression in HIV Infection. The Journal of infectious diseases. 2012. Epub 2012/01/13.
107.   Carrington M, Walker BD. Immunogenetics of Spontaneous Control of HIV. Annu Rev Med. 2012;63:131-45. Epub 2012/01/18.
108.   Young JM, Turpin JA, Musib R, Sharma OK. Outcomes of a National Institute of Allergy and Infectious Diseases Workshop on understanding HIV-exposed but seronegative individuals. AIDS research and human retroviruses. 2011;27(7):737-43. Epub 2010/12/15.
109.   Cohen J. AIDS vaccine research. HIV natural resistance field finally overcomes resistance. Science. 2009;326(5959):1476-7. Epub 2009/12/17.
110.   Meyers AF, Fowke KR. International symposium on natural immunity to HIV: a gathering of the HIV-exposed seronegative clan. The Journal of infectious diseases. 2010;202 Suppl 3:S327-8. Epub 2010/10/05.
111.   Horton RE, McLaren PJ, Fowke K, Kimani J, Ball TB. Cohorts for the study of HIV-1-exposed but uninfected individuals: benefits and limitations. The Journal of infectious diseases. 2010;202 Suppl 3:S377-81. Epub 2010/10/05.
112.   Restrepo C, Rallon NI, Carrillo J, Soriano V, Blanco J, Benito JM. Host factors involved in low susceptibility to HIV infection. AIDS reviews. 2011;13(1):30-40. Epub 2011/03/18.
113.   Fowke KR, Nagelkerke NJ, Kimani J, Simonsen JN, Anzala AO, Bwayo JJ, et al. Resistance to HIV-1 infection among persistently seronegative prostitutes in Nairobi, Kenya. Lancet. 1996;348(9038):1347-51. Epub 1996/11/16.
114.   Card CM, McLaren PJ, Wachihi C, Kimani J, Plummer FA, Fowke KR. Decreased immune activation in resistance to HIV-1 infection is associated with an elevated frequency of CD4(+)CD25(+)FOXP3(+) regulatory T cells. The Journal of infectious diseases. 2009;199(9):1318-22.
115.   McLaren PJ, Ball TB, Wachihi C, Jaoko W, Kelvin DJ, Danesh A, et al. HIV-exposed seronegative commercial sex workers show a quiescent phenotype in the CD4+ T cell compartment and reduced expression of HIV-dependent host factors. The Journal of infectious diseases. 2010;202 Suppl 3:S339-44. Epub 2010/10/05.
116.   Songok EM, Luo M, Liang B, McLaren P, Kaefer N, Apidi W, et al. Microarray Analysis of HIV Resistant Female Sex Workers Reveal a Gene Expression Signature Pattern Reminiscent of a Lowered Immune Activation State. PloS one. 2012;7(1):e30048. Epub 2012/02/01.
117.   Burgener A, Rahman S, Ahmad R, Lajoie J, Ramdahin S, Mesa C, et al. Comprehensive Proteomic Study Identifies Serpin and Cystatin Antiproteases as Novel Correlates of HIV-1 Resistance in the Cervicovaginal Mucosa of Female Sex Workers. Journal of proteome research. 2011. Epub 2011/10/07.
118.   Lajoie J, Juno J, Burgener A, Rahman S, Mogk K, Wachihi C, et al. A distinct cytokine and chemokine profile at the genital mucosa is associated with HIV-1 protection

among HIV-exposed seronegative commercial sex workers. Mucosal immunology. 2012. Epub 2012/02/10.

119.   Plummer FA, Ball TB, Kimani J, Fowke KR. Resistance to HIV-1 infection among highly exposed sex workers in Nairobi: what mediates protection and why does it develop? Immunol Lett. 1999;66(1-3):27-34. Epub 1999/04/15.

120.   Shea PR, Shianna KV, Carrington M, Goldstein DB. Host Genetics of HIV Acquisition and Viral Control. Annu Rev Med. 2012. Epub 2012/10/02.

121.   Fellay J. Host genetics influences on HIV type-1 disease. Antivir Ther. 2009;14(6):731-8. Epub 2009/10/09.

122.   Fellay J, Shianna KV, Telenti A, Goldstein DB. Host genetics and HIV-1: the final phase? PLoS pathogens. 2010;6(10):e1001033. Epub 2010/10/27.

123.   Fellay J, Shianna KV, Ge D, Colombo S, Ledergerber B, Weale M, et al. A whole-genome association study of major determinants for host control of HIV-1. Science. 2007;317(5840):944-7. Epub 2007/07/21.

124.   Dalmasso C, Carpentier W, Meyer L, Rouzioux C, Goujard C, Chaix ML, et al. Distinct genetic loci control plasma HIV-RNA and cellular HIV-DNA levels in HIV-1 infection: the ANRS Genome Wide Association 01 study. PloS one. 2008;3(12):e3907. Epub 2008/12/25.

125.   Limou S, Le Clerc S, Coulonges C, Carpentier W, Dina C, Delaneau O, et al. Genomewide association study of an AIDS-nonprogression cohort emphasizes the role played by HLA genes (ANRS Genomewide Association Study 02). The Journal of infectious diseases. 2009;199(3):419-26. Epub 2009/01/01.

126.   Schneidewind A, Brockman MA, Yang R, Adam RI, Li B, Le Gall S, et al. Escape from the dominant HLA-B27-restricted cytotoxic T-lymphocyte response in Gag is associated with a dramatic reduction in human immunodeficiency virus type 1 replication. Journal of virology. 2007;81(22):12382-93. Epub 2007/09/07.

127.   Thomas R, Apps R, Qi Y, Gao X, Male V, O'HUigin C, et al. HLA-C cell surface expression and control of HIV/AIDS correlate with a variant upstream of HLA-C. Nat Genet. 2009;41(12):1290-4. Epub 2009/11/26.

128.   Pelak K, Need AC, Fellay J, Shianna KV, Feng S, Urban TJ, et al. Copy number variation of KIR genes influences HIV-1 control. PLoS biology. 2011;9(11):e1001208. Epub 2011/12/06.

129.   Boulet S, Kleyman M, Kim JY, Kamya P, Sharafi S, Simic N, et al. A combined genotype of KIR3DL1 high expressing alleles and HLA-B*57 is associated with a reduced risk of HIV infection. AIDS (London, England). 2008;22(12):1487-91. Epub 2008/07/11.

130.   . !!! INVALID CITATION !!!

131.   Benkirane M, Jin DY, Chun RF, Koup RA, Jeang KT. Mechanism of transdominant inhibition of CCR5-mediated HIV-1 infection by ccr5delta32. The Journal of biological chemistry. 1997;272(49):30603-6. Epub 1998/01/10.

132.   Samson M, Libert F, Doranz BJ, Rucker J, Liesnard C, Farber CM, et al. Resistance to HIV-1 infection in caucasian individuals bearing mutant alleles of the CCR-5 chemokine receptor gene. Nature. 1996;382(6593):722-5. Epub 1996/08/22.

133.   Liu R, Paxton WA, Choe S, Ceradini D, Martin SR, Horuk R, et al. Homozygous defect in HIV-1 coreceptor accounts for resistance of some multiply-exposed individuals to HIV-1 infection. Cell. 1996;86(3):367-77. Epub 1996/08/09.

134.   Dean M, Carrington M, Winkler C, Huttley GA, Smith MW, Allikmets R, et al. Genetic restriction of HIV-1 infection and progression to AIDS by a deletion allele of the CKR5 structural gene. Hemophilia Growth and Development Study, Multicenter AIDS Cohort Study, Multicenter Hemophilia Cohort Study, San Francisco City Cohort, ALIVE Study. Science. 1996;273(5283):1856-62. Epub 1996/09/27.

135.   Martin MP. Genetic Acceleration of AIDS Progression by a Promoter Variant of CCR5. Science. 1998;282(5395):1907-11.

136.   Folefoc AT, Fromme BJ, Katz AA, Flanagan CA. South African mutations of the CCR5 coreceptor for HIV modify interactions with chemokines and hiv envelope protein. Journal of acquired immune deficiency syndromes (1999). 2010;54(4):352-9.

137.   Smith MW, Dean M, Carrington M, Winkler C, Huttley GA, Lomb DA, et al. Contrasting genetic influence of CCR2 and CCR5 variants on HIV-1 infection and disease progression. Hemophilia Growth and Development Study (HGDS), Multicenter AIDS Cohort Study (MACS), Multicenter Hemophilia Cohort Study (MHCS), San Francisco City Cohort (SFCC), ALIVE Study. Science (New York, NY). 1997;277(5328):959-65.

138.   Mabuka JM, Mackelprang RD, Lohman-Payne B, Majiwa M, Bosire R, John-Stewart G, et al. CCR2-64I Polymorphism Is Associated With Lower Maternal HIV-1 Viral Load and Reduced Vertical HIV-1 Transmission. Journal of acquired immune deficiency syndromes (1999). 2009;51(2):235-7.

139.   Kostrikis LG, Huang Y, Moore JP, Wolinsky SM, Zhang L, Guo Y, et al. A chemokine receptor CCR2 allele delays HIV-1 disease progression and is associated with a CCR5 promoter mutation. Nature medicine. 1998;4(3):350-3. Epub 1998/03/21.

140.   Nakayama EE, Tanaka Y, Nagai Y, Iwamoto A, Shioda T. A CCR2-V64I polymorphism affects stability of CCR2A isoform. AIDS (London, England). 2004;18(5):729-38.

141.   Mellado M, Rodriguez-Frade JM, Vila-Coro AJ, de Ana AM, Martinez AC. Chemokine control of HIV-1 infection. Nature. 1999;400(6746):723-4. Epub 1999/08/31.

142.   Oyugi JO, Vouriot FC, Alimonti J, Wayne S, Luo M, Land AM, et al. A common CD4 gene variant is associated with an increased risk of HIV-1 infection in Kenyan female commercial sex workers. The Journal of infectious diseases. 2009;199(9):1327-34.

143.   Modi WS, Lautenberger J, An P, Scott K, Goedert JJ, Kirk GD, et al. Genetic variation in the CCL18-CCL3-CCL4 chemokine gene cluster influences HIV Type 1 transmission and AIDS disease progression. Am J Hum Genet. 2006;79(1):120-8. Epub 2006/06/15.

144.   Colobran R, Adreani P, Ashhab Y, Llano A, Este JA, Dominguez O, et al. Multiple products derived from two CCL4 loci: high incidence of a new polymorphism in HIV+ patients. Journal of immunology (Baltimore, Md : 1950). 2005;174(9):5655-64. Epub 2005/04/22.

145.   Winkler C, Modi W, Smith MW, Nelson GW, Wu X, Carrington M, et al. Genetic restriction of AIDS pathogenesis by an SDF-1 chemokine gene variant. ALIVE Study, Hemophilia Growth and Development Study (HGDS), Multicenter AIDS Cohort Study (MACS), Multicenter Hemophilia Cohort Study (MHCS), San Francisco City Cohort (SFCC). Science. 1998;279(5349):389-93. Epub 1998/02/07.

146.   Modi WS, Goedert JJ, Strathdee S, Buchbinder S, Detels R, Donfield S, et al. MCP-1-MCP-3-Eotaxin gene cluster influences HIV-1 transmission. AIDS (London, England). 2003;17(16):2357-65. Epub 2003/10/23.

147.   Liu H, Chao D, Nakayama EE, Taguchi H, Goto M, Xin X, et al. Polymorphism in RANTES chemokine promoter affects HIV-1 disease progression. Proceedings of the National Academy of Sciences of the United States of America. 1999;96(8):4581-5. Epub 1999/04/14.

148.   McDermott DH, Beecroft MJ, Kleeberger CA, Al-Sharif FM, Ollier WE, Zimmerman PA, et al. Chemokine RANTES promoter polymorphism affects risk of both HIV infection and disease progression in the Multicenter AIDS Cohort Study. AIDS (London, England). 2000;14(17):2671-8. Epub 2000/12/28.

149.   Vidal F, Peraire J, Domingo P, Broch M, Cairo M, Pedrol E, et al. Polymorphism of RANTES chemokine gene promoter is not associated with long-term nonprogressive HIV-1 infection of more than 16 years. Journal of acquired immune deficiency syndromes (1999). 2006;41(1):17-22. Epub 2005/12/13.

150.   Ioannidis JP, Rosenberg PS, Goedert JJ, Ashton LJ, Benfield TL, Buchbinder SP, et al. Effects of CCR5-Delta32, CCR2-64I, and SDF-1 3'A alleles on HIV-1 disease progression: An international meta-analysis of individual-patient data. Ann Intern Med. 2001;135(9):782-95. Epub 2001/11/06.

151.   Lama J, Planelles V. Host factors influencing susceptibility to HIV infection and AIDS progression. Retrovirology. 2007;4:52. Epub 2007/07/27.

152.   Gong Z, Tang J, Xiang T, Zhang L, Liao Q, Liu W, et al. Association between Regulated upon Activation, Normal T Cells Expressed and Secreted (RANTES) -28C/G Polymorphism and Susceptibility to HIV-1 Infection: A Meta-Analysis. PloS one. 2013;8(4):e60683. Epub 2013/04/12.

153.   Gonzalez E, Kulkarni H, Bolivar H, Mangano A, Sanchez R, Catano G, et al. The influence of CCL3L1 gene-containing segmental duplications on HIV-1/AIDS susceptibility. Science. 2005;307(5714):1434-40. Epub 2005/01/08.

154.   Bhattacharya T, Stanton J, Kim EY, Kunstman KJ, Phair JP, Jacobson LP, et al. CCL3L1 and HIV/AIDS susceptibility. Nature medicine. 2009;15(10):1112-5. Epub 2009/10/09.

155.   Urban TJ, Weintrob AC, Fellay J, Colombo S, Shianna KV, Gumbs C, et al. CCL3L1 and HIV/AIDS susceptibility. Nature medicine. 2009;15(10):1110-2. Epub 2009/10/09.

156.   Larsen MH, Thorner LW, Zinyama R, Amstrup J, Kallestrup P, Gerstoft J, et al. CCL3L gene copy number and survival in an HIV-1 infected Zimbabwean population. Infect Genet Evol. 2012. Epub 2012/04/10.

157.   Weinstein LS, Chen M, Xie T, Liu J. Genetic diseases associated with heterotrimeric G proteins. Trends Pharmacol Sci. 2006;27(5):260-6. Epub 2006/04/08.

158.   Frey UH, Eisenhardt A, Lummen G, Rubben H, Jockel KH, Schmid KW, et al. The T393C polymorphism of the G alpha s gene (GNAS1) is a novel prognostic marker in bladder cancer. Cancer epidemiology, biomarkers & prevention : a publication of the American Association for Cancer Research, cosponsored by the American Society of Preventive Oncology. 2005;14(4):871-7.

159.   Frey UH, Nuckel H, Sellmann L, Siemer D, Kuppers R, Durig J, et al. The GNAS1 T393C polymorphism is associated with disease progression and survival in

chronic lymphocytic leukemia. Clinical cancer research : an official journal of the American Association for Cancer Research. 2006;12(19):5686-92.

160.   Siffert W, Rosskopf D, Siffert G, Busch S, Moritz A, Erbel R, et al. Association of a human G-protein beta3 subunit variant with hypertension. Nature genetics. 1998;18(1):45-8.

161.   Brockmeyer NH, Potthoff A, Kasper A, Nabring C, Jockel KH, Siffert W. GNB3 C825T polymorphism and response to anti-retroviral combination therapy in HIV-1-infected patients--a pilot study. European journal of medical research. 2005;10(11):489-94.

162.   Siffert W, Esser S, Bromen K, Jockel KH, Goos M, Brockmeyer NH, editors. G Protein beta 3 subunit 825T allele is strongly predictive for accelerated progression to AIDS. Program Abstr 8th Conf Retrovir Oppor Infect Conf Retrovir Oppor Infect 8th 2001 Chic Ill; 2001.

163.   Rosskopf D, Manthey I, Habich C, Kielbik M, Eisenhardt A, Nikula C, et al. Identification and characterization of G beta 3s2, a novel splice variant of the G-protein beta 3 subunit. The Biochemical journal. 2003;371(Pt 1):223-32.

164.   Lindemann M, Virchow S, Ramann F, Barsegian V, Kreuzfelder E, Siffert W, et al. The G protein beta3 subunit 825T allele is a genetic marker for enhanced T cell response. FEBS letters. 2001;495(1-2):82-6.

165.   Virchow S, Ansorge N, Rosskopf D, Rubben H, Siffert W. The G protein beta3 subunit splice variant Gbeta3-s causes enhanced chemotaxis of human neutrophils in response to interleukin-8. Naunyn-Schmiedeberg's archives of pharmacology. 1999;360(1):27-32.

166.   Siffert W. Effects of the G protein beta 3-subunit gene C825T polymorphism: should hypotheses regarding the molecular mechanisms underlying enhanced G protein activation be revised? Focus on "A splice variant of the G protein beta 3-subunit implicated in disease states does not modulate ion channels". Physiol Genomics. 2003;13(2):81-4. Epub 2003/04/18.

167.   Ruiz-Velasco V, Ikeda SR. A splice variant of the G protein beta 3-subunit implicated in disease states does not modulate ion channels. Physiological genomics. 2003;13(2):85-95.

168.   Sun A, Ge J, Siffert W, Frey UH. Quantification of allele-specific G-protein beta3 subunit mRNA transcripts in different human cells and tissues by Pyrosequencing. European journal of human genetics : EJHG. 2005;13(3):361-9.

169.   Lindemann M, Barsegian V, Siffert W, Ferencik S, Roggendorf M, Grosse-Wilde H. Role of G protein beta3 subunit C825T and HLA class II polymorphisms in the immune response after HBV vaccination. Virology. 2002;297(2):245-52.

170.   Sarrazin C, Berg T, Weich V, Mueller T, Frey UH, Zeuzem S, et al. GNB3 C825T polymorphism and response to interferon-alfa/ribavirin treatment in patients with hepatitis C virus genotype 1 (HCV-1) infection. Journal of hepatology. 2005;43(3):388-93.

171.   Opdal SH, Melien O, Rootwelt H, Vege A, Arnestad M, Rognum TO. The G protein b3 subunit 825C allele is associated with sudden infant death due to infection. Acta Paediatrica. 2006;95(Journal Article):1129-32.

172.   Zhu H, Wang X, Lu Y, Poola J, Momin Z, Harshfield GA, et al. Update on G-protein polymorphisms in hypertension. Current hypertension reports. 2006;8(1):23-9.

173.   Rebbeck TR, Spitz M, Wu X. Assessing the function of genetic variants in candidate gene association studies. Nat Rev Genet. 2004;5(8):589-97.

174.   Siffert W, Forster P, Jockel KH, Mvere DA, Brinkmann B, Naber C, et al. Worldwide ethnic distribution of the G protein beta3 subunit 825T allele and its association with obesity in Caucasian, Chinese, and Black African individuals. Journal of the American Society of Nephrology : JASN. 1999;10(9):1921-30.

175.   Bagos PG, Elefsinioti AL, Nikolopoulos GK, Hamodrakas SJ. The GNB3 C825T polymorphism and essential hypertension: a meta-analysis of 34 studies including 14,094 cases and 17,760 controls. Journal of hypertension. 2007;25(3):487-500.

176.   Larson N, Hutchinson R, Boerwinkle E. Lack of association of 3 functional gene variants with hypertension in African Americans. Hypertension. 2000;35(6):1297-300.

177.   Tishkoff SA, Williams SM. Genetic analysis of African populations: human evolution and complex disease. Nature reviewsGenetics. 2002;3(8):611-21.

178.   Kawai T, Akira S. Toll-like receptors and their crosstalk with other innate receptors in infection and immunity. Immunity. 2011;34(5):637-50.

179.   Kawai T, Akira S. The roles of TLRs, RLRs and NLRs in pathogen recognition. International immunology. 2009;21(4):317-37.

180.   Robinson MJ, Sancho D, Slack EC, LeibundGut-Landmann S, Sousa CRe. Myeloid C-type lectins in innate immunity. Nature immunology. 2006;7(12):1258-65.

181.   Roberts TL, Idris A, Dunn JA, Kelly GM, Burnton CM, Hodgson S, et al. HIN-200 proteins regulate caspase activation in response to foreign cytoplasmic DNA. Science. 2009;323(5917):1057-60. Epub 2009/01/10.

182.   Dale DC, Boxer L, Liles WC. The phagocytes: neutrophils and monocytes. Blood. 2008;112(4):935-45. Epub 2008/08/08.

183.   Vivier E, Tomasello E, Baratin M, Walzer T, Ugolini S. Functions of natural killer cells. Nature immunology. 2008;9(5):503-10.

184.   Caligiuri MA. Human natural killer cells. Blood. 2008;112(3):461-9. Epub 2008/07/25.

185.   Lanier LL. Up on the tightrope: natural killer cell activation and inhibition. Nature immunology. 2008;9(5):495-502.

186.   LeBien TW, Tedder TF. B lymphocytes: how they develop and function. Blood. 2008;112(5):1570-80. Epub 2008/08/30.

187.   Zhu J, Paul WE. CD4 T cells: fates, functions, and faults. Blood. 2008;112(5):1557-69. Epub 2008/08/30.

188.   Yu D, Vinuesa CG. The elusive identity of T follicular helper cells. Trends Immunol. 2010;31(10):377-83. Epub 2010/09/03.

189.   Feuerer M, Hill JA, Mathis D, Benoist C. Foxp3+ regulatory T cells: differentiation, specification, subphenotypes. Nature immunology. 2009;10(7):689-95.

190.   Vignali DA, Collison LW, Workman CJ. How regulatory T cells work. Nature reviews Immunology. 2008;8(7):523-32. Epub 2008/06/21.

191.   Belz GT, Kallies A. Effector and memory CD8+ T cell differentiation: toward a molecular understanding of fate determination. Current opinion in immunology. 2010;22(3):279-85. Epub 2010/05/04.

192.   Kabelitz D. gammadelta T-cells: cross-talk between innate and adaptive immunity. Cell Mol Life Sci. 2011;68(14):2331-3. Epub 2011/05/05.

193. Fischer K, Voelkl S, Heymann J, Przybylski GK, Mondal K, Laumer M, et al. Isolation and characterization of human antigen-specific TCR alpha beta+ CD4(-)CD8-double-negative regulatory T cells. Blood. 2005;105(7):2828-35. Epub 2004/12/02.

194. Voelkl S, Gary R, Mackensen A. Characterization of the immunoregulatory function of human TCR-alphabeta+ CD4- CD8- double-negative T cells. European journal of immunology. 2011;41(3):739-48. Epub 2011/02/03.

195. Sundaravaradan V, Mir KD, Sodora DL. Double-negative T cells during HIV/SIV infections: potential pinch hitters in the T-cell lineup. Current opinion in HIV and AIDS. 2012. Epub 2012/01/14.

196. Prodger JL, Gray R, Kigozi G, Nalugoda F, Galiwango R, Hirbod T, et al. Foreskin T-cell subsets differ substantially from blood with respect to HIV co-receptor expression, inflammatory profile, and memory status. Mucosal immunology. 2012;5(2):121-8. Epub 2011/11/18.

197. Joyee AG, Qiu H, Wang S, Fan Y, Bilenki L, Yang X. Distinct NKT cell subsets are induced by different Chlamydia species leading to differential adaptive immunity and host resistance to the infections. Journal of immunology (Baltimore, Md : 1950). 2007;178(2):1048-58. Epub 2007/01/05.

198. Porcelli SA, Modlin RL. The CD1 system: antigen-presenting molecules for T cell recognition of lipids and glycolipids. Annual review of immunology. 1999;17:297-329. Epub 1999/06/08.

199. Kawano T, Cui J, Koezuka Y, Toura I, Kaneko Y, Motoki K, et al. CD1d-restricted and TCR-mediated activation of valpha14 NKT cells by glycosylceramides. Science. 1997;278(5343):1626-9. Epub 1997/12/31.

200. Tessmer MS, Fatima A, Paget C, Trottein F, Brossay L. NKT cell immune responses to viral infection. Expert Opin Ther Targets. 2009;13(2):153-62. Epub 2009/02/25.

201. van der Vliet HJ, Molling JW, von Blomberg BM, Nishi N, Kolgen W, van den Eertwegh AJ, et al. The immunoregulatory role of CD1d-restricted natural killer T cells in disease. Clinical immunology (Orlando, Fla). 2004;112(1):8-23. Epub 2004/06/23.

202. Zhou D, Mattner J, Cantu C, 3rd, Schrantz N, Yin N, Gao Y, et al. Lysosomal glycosphingolipid recognition by NKT cells. Science. 2004;306(5702):1786-9. Epub 2004/11/13.

203. Li Y, Teneberg S, Thapa P, Bendelac A, Levery SB, Zhou D. Sensitive detection of isoglobo and globo series tetraglycosylceramides in human thymus by ion trap mass spectrometry. Glycobiology. 2008;18(2):158-65. Epub 2007/12/07.

204. Christiansen D, Milland J, Mouhtouris E, Vaughan H, Pellicci DG, McConville MJ, et al. Humans lack iGb3 due to the absence of functional iGb3-synthase: implications for NKT cell development and transplantation. PLoS biology. 2008;6(7):e172. Epub 2008/07/18.

205. Porubsky S, Speak AO, Salio M, Jennemann R, Bonrouhi M, Zafarulla R, et al. Globosides but not Isoglobosides Can Impact the Development of Invariant NKT Cells and Their Interaction with Dendritic Cells. Journal of immunology (Baltimore, Md : 1950). 2012. Epub 2012/08/10.

206. Fox LM, Cox DG, Lockridge JL, Wang X, Chen X, Scharf L, et al. Recognition of lyso-phospholipids by human natural killer T lymphocytes. PLoS biology. 2009;7(10):e1000228. Epub 2009/10/28.

207.   Sriram V, Du W, Gervay-Hague J, Brutkiewicz RR. Cell wall glycosphingolipids of Sphingomonas paucimobilis are CD1d-specific ligands for NKT cells. European journal of immunology. 2005;35(6):1692-701. Epub 2005/05/26.
208.   Kinjo Y, Wu D, Kim G, Xing GW, Poles MA, Ho DD, et al. Recognition of bacterial glycosphingolipids by natural killer T cells. Nature. 2005;434(7032):520-5. Epub 2005/03/26.
209.   Wu D, Xing GW, Poles MA, Horowitz A, Kinjo Y, Sullivan B, et al. Bacterial glycolipids and analogs as antigens for CD1d-restricted NKT cells. Proceedings of the National Academy of Sciences of the United States of America. 2005;102(5):1351-6. Epub 2005/01/25.
210.   Mattner J, Debord KL, Ismail N, Goff RD, Cantu C, 3rd, Zhou D, et al. Exogenous and endogenous glycolipid antigens activate NKT cells during microbial infections. Nature. 2005;434(7032):525-9. Epub 2005/03/26.
211.   Burrows PD, Kronenberg M, Taniguchi M. NKT cells turn ten. Nature immunology. 2009;10(7):669-71. Epub 2009/06/19.
212.   Kawakami K, Yamamoto N, Kinjo Y, Miyagi K, Nakasone C, Uezu K, et al. Critical role of Valpha14+ natural killer T cells in the innate phase of host protection against Streptococcus pneumoniae infection. European journal of immunology. 2003;33(12):3322-30. Epub 2003/11/25.
213.   Kinjo Y, Illarionov P, Vela JL, Pei B, Girardi E, Li X, et al. Invariant natural killer T cells recognize glycolipids from pathogenic Gram-positive bacteria. Nature immunology. 2011. Epub 2011/09/06.
214.   Mattner J, Savage PB, Leung P, Oertelt SS, Wang V, Trivedi O, et al. Liver autoimmunity triggered by microbial activation of natural killer T cells. Cell Host Microbe. 2008;3(5):304-15. Epub 2008/05/14.
215.   Kinjo Y, Tupin E, Wu D, Fujio M, Garcia-Navarro R, Benhnia MR, et al. Natural killer T cells recognize diacylglycerol antigens from pathogenic bacteria. Nature immunology. 2006;7(9):978-86. Epub 2006/08/22.
216.   Kumar H, Belperron A, Barthold SW, Bockenstedt LK. Cutting edge: CD1d deficiency impairs murine host defense against the spirochete, Borrelia burgdorferi. Journal of immunology (Baltimore, Md : 1950). 2000;165(9):4797-801. Epub 2000/10/25.
217.   Tupin E, Benhnia MR, Kinjo Y, Patsey R, Lena CJ, Haller MC, et al. NKT cells prevent chronic joint inflammation after infection with Borrelia burgdorferi. Proceedings of the National Academy of Sciences of the United States of America. 2008;105(50):19863-8. Epub 2008/12/09.
218.   Fischer K, Scotet E, Niemeyer M, Koebernick H, Zerrahn J, Maillet S, et al. Mycobacterial phosphatidylinositol mannoside is a natural antigen for CD1d-restricted T cells. Proceedings of the National Academy of Sciences of the United States of America. 2004;101(29):10685-90. Epub 2004/07/10.
219.   Pei B, Vela JL, Zajonc D, Kronenberg M. Interplay between carbohydrate and lipid in recognition of glycolipid antigens by natural killer T cells. Ann N Y Acad Sci. 2012. Epub 2012/02/23.
220.   Brennan PJ, Tatituri RV, Brigl M, Kim EY, Tuli A, Sanderson JP, et al. Invariant natural killer T cells recognize lipid self antigen induced by microbial danger signals. Nature immunology. 2011. Epub 2011/11/01.

221.	Godfrey DI, Pellicci DG, Rossjohn J. Beta-testing NKT cell self-reactivity. Nature immunology. 2011;12(12):1135-7. Epub 2011/11/18.

222.	Kitamura H, Iwakabe K, Yahata T, Nishimura S, Ohta A, Ohmi Y, et al. The natural killer T (NKT) cell ligand alpha-galactosylceramide demonstrates its immunopotentiating effect by inducing interleukin (IL)-12 production by dendritic cells and IL-12 receptor expression on NKT cells. The Journal of experimental medicine. 1999;189(7):1121-8. Epub 1999/04/06.

223.	Nishimura T, Kitamura H, Iwakabe K, Yahata T, Ohta A, Sato M, et al. The interface between innate and acquired immunity: glycolipid antigen presentation by CD1d-expressing dendritic cells to NKT cells induces the differentiation of antigen-specific cytotoxic T lymphocytes. Int Immunol. 2000;12(7):987-94. Epub 2000/07/06.

224.	Godfrey DI, Rossjohn J. New ways to turn on NKT cells. The Journal of experimental medicine. 2011;208(6):1121-5. Epub 2011/06/08.

225.	Lee PT, Benlagha K, Teyton L, Bendelac A. Distinct functional lineages of human V(alpha)24 natural killer T cells. The Journal of experimental medicine. 2002;195(5):637-41. Epub 2002/03/06.

226.	Bendelac A, Savage PB, Teyton L. The biology of NKT cells. Annual review of immunology. 2007;25:297-336. Epub 2006/12/08.

227.	Koguchi Y, Buenafe AC, Thauland TJ, Gardell JL, Bivins-Smith ER, Jacoby DB, et al. Preformed CD40L Is Stored in Th1, Th2, Th17, and T Follicular Helper Cells as Well as CD48 Thymocytes and Invariant NKT Cells but Not in Treg Cells. PloS one. 2012;7(2):e31296. Epub 2012/03/01.

228.	Matsuda JL, Mallevaey T, Scott-Browne J, Gapin L. CD1d-restricted iNKT cells, the 'Swiss-Army knife' of the immune system. Current opinion in immunology. 2008;20(3):358-68. Epub 2008/05/27.

229.	Brigl M, Brenner MB. How invariant natural killer T cells respond to infection by recognizing microbial or endogenous lipid antigens. Seminars in immunology. 2010;22(2):79-86. Epub 2009/12/02.

230.	Reilly EC, Wands JR, Brossay L. Cytokine dependent and independent iNKT cell activation. Cytokine. 2010;51(3):227-31. Epub 2010/06/18.

231.	Brigl M, Bry L, Kent SC, Gumperz JE, Brenner MB. Mechanism of CD1d-restricted natural killer T cell activation during microbial infection. Nature immunology. 2003;4(12):1230-7. Epub 2003/10/28.

232.	Paget C, Mallevaey T, Speak AO, Torres D, Fontaine J, Sheehan KC, et al. Activation of invariant NKT cells by toll-like receptor 9-stimulated dendritic cells requires type I interferon and charged glycosphingolipids. Immunity. 2007;27(4):597-609. Epub 2007/10/24.

233.	Raftery MJ, Winau F, Giese T, Kaufmann SH, Schaible UE, Schonrich G. Viral danger signals control CD1d de novo synthesis and NKT cell activation. European journal of immunology. 2008;38(3):668-79. Epub 2008/02/07.

234.	Brigl M, Tatituri RV, Watts GF, Bhowruth V, Leadbetter EA, Barton N, et al. Innate and cytokine-driven signals, rather than microbial antigens, dominate in natural killer T cell activation during microbial infection. The Journal of experimental medicine. 2011;208(6):1163-77. Epub 2011/05/11.

235.	Wang X, Bishop KA, Hegde S, Rodenkirch LA, Pike JW, Gumperz JE. Human invariant natural killer T cells acquire transient innate responsiveness via histone H4

acetylation induced by weak TCR stimulation. The Journal of experimental medicine. 2012. Epub 2012/04/18.

236.   Zeissig S, Murata K, Sweet L, Publicover J, Hu Z, Kaser A, et al. Hepatitis B virus-induced lipid alterations contribute to natural killer T cell-dependent protective immunity. Nature medicine. 2012;18(7):1060-8. Epub 2012/06/19.

237.   Nagarajan NA, Kronenberg M. Invariant NKT cells amplify the innate immune response to lipopolysaccharide. Journal of immunology (Baltimore, Md : 1950). 2007;178(5):2706-13. Epub 2007/02/22.

238.   Tyznik AJ, Tupin E, Nagarajan NA, Her MJ, Benedict CA, Kronenberg M. Cutting edge: the mechanism of invariant NKT cell responses to viral danger signals. Journal of immunology (Baltimore, Md : 1950). 2008;181(7):4452-6. Epub 2008/09/20.

239.   Takahashi T, Chiba S, Nieda M, Azuma T, Ishihara S, Shibata Y, et al. Cutting edge: analysis of human V alpha 24+CD8+ NK T cells activated by alpha-galactosylceramide-pulsed monocyte-derived dendritic cells. Journal of immunology (Baltimore, Md : 1950). 2002;168(7):3140-4. Epub 2002/03/22.

240.   Ishihara S, Nieda M, Kitayama J, Osada T, Yabe T, Ishikawa Y, et al. CD8(+)NKR-P1A (+)T cells preferentially accumulate in human liver. European journal of immunology. 1999;29(8):2406-13. Epub 1999/08/24.

241.   Kim CH, Johnston B, Butcher EC. Trafficking machinery of NKT cells: shared and differential chemokine receptor expression among V alpha 24(+)V beta 11(+) NKT cell subsets with distinct cytokine-producing capacity. Blood. 2002;100(1):11-6. Epub 2002/06/19.

242.   Kim CH, Butcher EC, Johnston B. Distinct subsets of human Valpha24-invariant NKT cells: cytokine responses and chemokine receptor expression. Trends Immunol. 2002;23(11):516-9. Epub 2002/10/29.

243.   Mureithi MW, Cohen K, Moodley R, Poole D, Mncube Z, Kasmar A, et al. Impairment of CD1d-restricted natural killer T cells in chronic HIV type 1 clade C infection. AIDS research and human retroviruses. 2011;27(5):501-9. Epub 2010/10/15.

244.   Motsinger A, Haas DW, Stanic AK, Van Kaer L, Joyce S, Unutmaz D. CD1d-restricted human natural killer T cells are highly susceptible to human immunodeficiency virus 1 infection. The Journal of experimental medicine. 2002;195(7):869-79. Epub 2002/04/03.

245.   D'Andrea A, Goux D, De Lalla C, Koezuka Y, Montagna D, Moretta A, et al. Neonatal invariant Valpha24+ NKT lymphocytes are activated memory cells. European journal of immunology. 2000;30(6):1544-50. Epub 2000/07/18.

246.   Snyder-Cappione JE, Tincati C, Eccles-James IG, Cappione AJ, Ndhlovu LC, Koth LL, et al. A comprehensive ex vivo functional analysis of human NKT cells reveals production of MIP1-alpha and MIP1-beta, a lack of IL-17, and a Th1-bias in males. PloS one. 2010;5(11):e15412. Epub 2010/11/18.

247.   Chang YJ, Huang JR, Tsai YC, Hung JT, Wu D, Fujio M, et al. Potent immune-modulating and anticancer effects of NKT cell stimulatory glycolipids. Proceedings of the National Academy of Sciences of the United States of America. 2007;104(25):10299-304. Epub 2007/06/15.

248.   O'Reilly V, Zeng SG, Bricard G, Atzberger A, Hogan AE, Jackson J, et al. Distinct and Overlapping Effector Functions of Expanded Human CD4^{+},

CD8α^{+} and CD4^{-}CD8α^{-} Invariant Natural Killer T Cells. PloS one. 2011;6(12):e28648.

249.   Takahashi T, Nieda M, Koezuka Y, Nicol A, Porcelli SA, Ishikawa Y, et al. Analysis of human V alpha 24+ CD4+ NKT cells activated by alpha-glycosylceramide-pulsed monocyte-derived dendritic cells. Journal of immunology (Baltimore, Md : 1950). 2000;164(9):4458-64. Epub 2000/04/26.

250.   Gumperz JE, Miyake S, Yamamura T, Brenner MB. Functionally distinct subsets of CD1d-restricted natural killer T cells revealed by CD1d tetramer staining. The Journal of experimental medicine. 2002;195(5):625-36. Epub 2002/03/06.

251.   Tupin E, Kinjo Y, Kronenberg M. The unique role of natural killer T cells in the response to microorganisms. Nat Rev Microbiol. 2007;5(6):405-17. Epub 2007/05/10.

252.   Rout N, Else JG, Yue S, Connole M, Exley MA, Kaur A. Heterogeneity in phenotype and function of CD8+ and CD4/CD8 double-negative Natural Killer T cell subsets in sooty mangabeys. J Med Primatol. 2010;39(4):224-34. Epub 2010/07/14.

253.   Kuylenstierna C, Bjorkstrom NK, Andersson SK, Sahlstrom P, Bosnjak L, Paquin-Proulx D, et al. NKG2D performs two functions in invariant NKT cells: direct TCR-independent activation of NK-like cytolysis and co-stimulation of activation by CD1d. European journal of immunology. 2011;41(7):1913-23. Epub 2011/05/19.

254.   Hermans IF, Silk JD, Gileadi U, Salio M, Mathew B, Ritter G, et al. NKT cells enhance CD4+ and CD8+ T cell responses to soluble antigen in vivo through direct interaction with dendritic cells. Journal of immunology (Baltimore, Md : 1950). 2003;171(10):5140-7. Epub 2003/11/11.

255.   Joyee AG, Qiu H, Fan Y, Wang S, Yang X. Natural killer T cells are critical for dendritic cells to induce immunity in Chlamydial pneumonia. Am J Respir Crit Care Med. 2008;178(7):745-56. Epub 2008/07/04.

256.   Joyee AG, Uzonna J, Yang X. Invariant NKT cells preferentially modulate the function of CD8 alpha+ dendritic cell subset in inducing type 1 immunity against infection. Journal of immunology (Baltimore, Md : 1950). 2010;184(4):2095-106. Epub 2010/01/22.

257.   Carnaud C, Lee D, Donnars O, Park SH, Beavis A, Koezuka Y, et al. Cutting edge: Cross-talk between cells of the innate immune system: NKT cells rapidly activate NK cells. Journal of immunology (Baltimore, Md : 1950). 1999;163(9):4647-50. Epub 1999/10/21.

258.   Joshi SK, Lang GA, Devera TS, Johnson AM, Kovats S, Lang ML. Differential contribution of dendritic cell CD1d to NKT cell-enhanced humoral immunity and CD8+ T cell activation. Journal of leukocyte biology. 2012. Epub 2012/02/15.

259.   Stober D, Jomantaite I, Schirmbeck R, Reimann J. NKT cells provide help for dendritic cell-dependent priming of MHC class I-restricted CD8+ T cells in vivo. Journal of immunology (Baltimore, Md : 1950). 2003;170(5):2540-8. Epub 2003/02/21.

260.   Li X, Fujio M, Imamura M, Wu D, Vasan S, Wong CH, et al. Design of a potent CD1d-binding NKT cell ligand as a vaccine adjuvant. Proceedings of the National Academy of Sciences of the United States of America. 2010;107(29):13010-5. Epub 2010/07/10.

261.   Cerundolo V, Barral P, Batista FD. Synthetic iNKT cell-agonists as vaccine adjuvants--finding the balance. Current opinion in immunology. 2010;22(3):417-24. Epub 2010/05/18.

262.   Fujii S, Motohashi S, Shimizu K, Nakayama T, Yoshiga Y, Taniguchi M. Adjuvant activity mediated by iNKT cells. Seminars in immunology. 2010;22(2):97-102. Epub 2009/11/27.

263.   Borrow P, Shattock RJ, Vyakarnam A. Innate immunity against HIV: a priority target for HIV prevention research. Retrovirology. 2010;7:84. Epub 2010/10/13.

264.   Ko SY, Ko HJ, Chang WS, Park SH, Kweon MN, Kang CY. alpha-Galactosylceramide can act as a nasal vaccine adjuvant inducing protective immune responses against viral infection and tumor. Journal of immunology (Baltimore, Md : 1950). 2005;175(5):3309-17. Epub 2005/08/24.

265.   Youn HJ, Ko SY, Lee KA, Ko HJ, Lee YS, Fujihashi K, et al. A single intranasal immunization with inactivated influenza virus and alpha-galactosylceramide induces long-term protective immunity without redirecting antigen to the central nervous system. Vaccine. 2007;25(28):5189-98. Epub 2007/06/06.

266.   Guillonneau C, Mintern JD, Hubert FX, Hurt AC, Besra GS, Porcelli S, et al. Combined NKT cell activation and influenza virus vaccination boosts memory CTL generation and protective immunity. Proceedings of the National Academy of Sciences of the United States of America. 2009;106(9):3330-5. Epub 2009/02/13.

267.   Kopecky-Bromberg SA, Fraser KA, Pica N, Carnero E, Moran TM, Franck RW, et al. Alpha-C-galactosylceramide as an adjuvant for a live attenuated influenza virus vaccine. Vaccine. 2009;27(28):3766-74. Epub 2009/05/26.

268.   Katsikis PD, Mueller YM, Villinger F. The cytokine network of acute HIV infection: a promising target for vaccines and therapy to reduce viral set-point? PLoS pathogens. 2011;7(8):e1002055. Epub 2011/08/20.

269.   Cerundolo V, Silk JD, Masri SH, Salio M. Harnessing invariant NKT cells in vaccination strategies. Nature reviews Immunology. 2009;9(1):28-38. Epub 2008/12/17.

270.   Venkataswamy MM, Baena A, Goldberg MF, Bricard G, Im JS, Chan J, et al. Incorporation of NKT cell-activating glycolipids enhances immunogenicity and vaccine efficacy of Mycobacterium bovis bacillus Calmette-Guerin. Journal of immunology (Baltimore, Md : 1950). 2009;183(3):1644-56. Epub 2009/07/22.

271.   Montoya CJ, Pollard D, Martinson J, Kumari K, Wasserfall C, Mulder CB, et al. Characterization of human invariant natural killer T subsets in health and disease using a novel invariant natural killer T cell-clonotypic monoclonal antibody, 6B11. Immunology. 2007;122(1):1-14. Epub 2007/07/31.

272.   Thomas SY, Hou R, Boyson JE, Means TK, Hess C, Olson DP, et al. CD1d-restricted NKT cells express a chemokine receptor profile indicative of Th1-type inflammatory homing cells. Journal of immunology (Baltimore, Md : 1950). 2003;171(5):2571-80. Epub 2003/08/21.

273.   Kelly KA, Wiley D, Wiesmeier E, Briskin M, Butch A, Darville T. The combination of the gastrointestinal integrin (alpha4beta7) and selectin ligand enhances T-Cell migration to the reproductive tract during infection with Chlamydia trachomatis. American journal of reproductive immunology (New York, NY : 1989). 2009;61(6):446-52. Epub 2009/04/28.

274.   Kawana K, Matsumoto J, Miura S, Shen L, Kawana Y, Nagamatsu T, et al. Expression of CD1d and ligand-induced cytokine production are tissue specific in mucosal epithelia of the human lower reproductive tract. Infection and immunity. 2008;76(7):3011-8. Epub 2008/05/07.

275.   Miura S, Kawana K, Schust DJ, Fujii T, Yokoyama T, Iwasawa Y, et al. CD1d, a sentinel molecule bridging innate and adaptive immunity, is downregulated by the human papillomavirus (HPV) E5 protein: a possible mechanism for immune evasion by HPV. Journal of virology. 2010;84(22):11614-23. Epub 2010/09/03.

276.   van Dieren JM, van der Woude CJ, Kuipers EJ, Escher JC, Samsom JN, Blumberg RS, et al. Roles of CD1d-restricted NKT cells in the intestine. Inflamm Bowel Dis. 2007;13(9):1146-52. Epub 2007/05/04.

277.   Middendorp S, Nieuwenhuis EES. NKT cells in mucosal immunity. Mucosal immunology. 2009;2(5):393-402.

278.   Wang H, Zhao L, Peng Y, Liu J, Qi M, Chen Q, et al. Protective Role of alpha-galactosylceramide Stimulated Natural killer T cells in Genital Tract Infection with Chlamydia muridarum. FEMS Immunol Med Microbiol. 2012. Epub 2012/02/09.

279.   Lai SK, Hida K, Shukair S, Wang YY, Figueiredo A, Cone R, et al. Human immunodeficiency virus type 1 is trapped by acidic but not by neutralized human cervicovaginal mucus. Journal of virology. 2009;83(21):11196-200. Epub 2009/08/21.

280.   Kaul R, Pettengell C, Sheth PM, Sunderji S, Biringer A, MacDonald K, et al. The genital tract immune milieu: an important determinant of HIV susceptibility and secondary transmission. Journal of reproductive immunology. 2008;77(1):32-40. Epub 2007/03/31.

281.   Royce RA, Seña A, Cates W, Cohen MS. Sexual Transmission of HIV. New England Journal of Medicine. 1997;336(15):1072-8.

282.   Miller CJ, Li Q, Abel K, Kim EY, Ma ZM, Wietgrefe S, et al. Propagation and dissemination of infection after vaginal transmission of simian immunodeficiency virus. Journal of virology. 2005;79(14):9217-27. Epub 2005/07/05.

283.   Geijtenbeek TB, Kwon DS, Torensma R, van Vliet SJ, van Duijnhoven GC, Middel J, et al. DC-SIGN, a dendritic cell-specific HIV-1-binding protein that enhances trans-infection of T cells. Cell. 2000;100(5):587-97. Epub 2000/03/18.

284.   van Montfort T, Eggink D, Boot M, Tuen M, Hioe CE, Berkhout B, et al. HIV-1 N-Glycan Composition Governs a Balance between Dendritic Cell-Mediated Viral Transmission and Antigen Presentation. Journal of immunology (Baltimore, Md : 1950). 2011. Epub 2011/10/01.

285.   Ballweber L, Robinson B, Kreger A, Fialkow M, Lentz G, McElrath MJ, et al. Vaginal Langerhans cells non-productively transporting HIV-1 mediate infection of T cells. Journal of virology. 2011. Epub 2011/10/07.

286.   Keele BF, Estes JD. Barriers to mucosal transmission of immunodeficiency viruses. Blood. 2011;118(4):839-46. Epub 2011/05/11.

287.   Sagar M. HIV-1 transmission biology: selection and characteristics of infecting viruses. The Journal of infectious diseases. 2010;202 Suppl 2:S289-96. Epub 2010/09/25.

288.   Zhu T, Mo H, Wang N, Nam D, Cao Y, Koup R, et al. Genotypic and phenotypic characterization of HIV-1 patients with primary infection. Science. 1993;261(5125):1179-81.

289.   Haase AT. Early events in sexual transmission of HIV and SIV and opportunities for interventions. Annu Rev Med. 2011;62:127-39. Epub 2010/11/09.

290.   Nawaz F, Cicala C, Van Ryk D, Block KE, Jelicic K, McNally JP, et al. The genotype of early-transmitting HIV gp120s promotes alpha (4) beta(7)-reactivity,

revealing alpha (4) beta(7) +/CD4+ T cells as key targets in mucosal transmission. PLoS pathogens. 2011;7(2):e1001301. Epub 2011/03/09.

291.   Li H, Bar KJ, Wang S, Decker JM, Chen Y, Sun C, et al. High Multiplicity Infection by HIV-1 in Men Who Have Sex with Men. PLoS pathogens. 2010;6(5):e1000890. Epub 2010/05/21.

292.   Zhang Z, Schuler T, Zupancic M, Wietgrefe S, Staskus KA, Reimann KA, et al. Sexual transmission and propagation of SIV and HIV in resting and activated CD4+ T cells. Science. 1999;286(5443):1353-7. Epub 1999/11/13.

293.   King DF, Siddiqui AA, Buffa V, Fischetti L, Gao Y, Stieh D, et al. Mucosal Tissue Tropism and Dissemination of HIV-1 Subtype B Acute Envelope-Expressing chimeric virus. Journal of virology. 2012. Epub 2012/11/09.

294.   McKinnon LR, Nyanga B, Chege D, Izulla P, Kimani M, Huibner S, et al. Characterization of a Human Cervical CD4+ T Cell Subset Coexpressing Multiple Markers of HIV Susceptibility. Journal of immunology (Baltimore, Md : 1950). 2011. Epub 2011/11/04.

295.   Pudney J, Quayle AJ, Anderson DJ. Immunological microenvironments in the human vagina and cervix: mediators of cellular immunity are concentrated in the cervical transformation zone. Biol Reprod. 2005;73(6):1253-63. Epub 2005/08/12.

296.   Li Q, Estes JD, Schlievert PM, Duan L, Brosnahan AJ, Southern PJ, et al. Glycerol monolaurate prevents mucosal SIV transmission. Nature. 2009;458(7241):1034-8. Epub 2009/03/06.

297.   Blanco-Melo D, Venkatesh S, Bieniasz PD. Intrinsic Cellular Defenses against Human Immunodeficiency Viruses. Immunity. 2012;37(3):399-411. Epub 2012/09/25.

298.   Li M, Kao E, Gao X, Sandig H, Limmer K, Pavon-Eternod M, et al. Codon-usage-based inhibition of HIV protein synthesis by human schlafen 11. Nature. 2012. Epub 2012/09/25.

299.   Hrecka K, Hao C, Gierszewska M, Swanson SK, Kesik-Brodacka M, Srivastava S, et al. Vpx relieves inhibition of HIV-1 infection of macrophages mediated by the SAMHD1 protein. Nature. 2011;474(7353):658-61. Epub 2011/07/02.

300.   Laguette N, Sobhian B, Casartelli N, Ringeard M, Chable-Bessia C, Segeral E, et al. SAMHD1 is the dendritic- and myeloid-cell-specific HIV-1 restriction factor counteracted by Vpx. Nature. 2011;474(7353):654-7. Epub 2011/05/27.

301.   Goldstone DC, Ennis-Adeniran V, Hedden JJ, Groom HC, Rice GI, Christodoulou E, et al. HIV-1 restriction factor SAMHD1 is a deoxynucleoside triphosphate triphosphohydrolase. Nature. 2011. Epub 2011/11/08.

302.   Laguette N, Benkirane M. How SAMHD1 changes our view of viral restriction. Trends Immunol. 2012;33(1):26-33. Epub 2011/12/20.

303.   Baldauf HM, Pan X, Erikson E, Schmidt S, Daddacha W, Burggraf M, et al. SAMHD1 restricts HIV-1 infection in resting CD4(+) T cells. Nature medicine. 2012. Epub 2012/09/14.

304.   Sheehy AM, Gaddis NC, Choi JD, Malim MH. Isolation of a human gene that inhibits HIV-1 infection and is suppressed by the viral Vif protein. Nature. 2002;418(6898):646-50. Epub 2002/08/09.

305.   Zhang W, Du J, Evans SL, Yu Y, Yu XF. T-cell differentiation factor CBF-beta regulates HIV-1 Vif-mediated evasion of host restriction. Nature. 2011. Epub 2011/12/23.

306. Jager S, Kim DY, Hultquist JF, Shindo K, Larue RS, Kwon E, et al. Vif hijacks CBF-beta to degrade APOBEC3G and promote HIV-1 infection. Nature. 2011. Epub 2011/12/23.

307. Neil SJ, Zang T, Bieniasz PD. Tetherin inhibits retrovirus release and is antagonized by HIV-1 Vpu. Nature. 2008;451(7177):425-30. Epub 2008/01/18.

308. Stremlau M, Owens CM, Perron MJ, Kiessling M, Autissier P, Sodroski J. The cytoplasmic body component TRIM5alpha restricts HIV-1 infection in Old World monkeys. Nature. 2004;427(6977):848-53. Epub 2004/02/27.

309. Solis M, Nakhaei P, Jalalirad M, Lacoste J, Douville R, Arguello M, et al. RIG-I-mediated antiviral signaling is inhibited in HIV-1 infection by a protease-mediated sequestration of RIG-I. Journal of virology. 2011;85(3):1224-36. Epub 2010/11/19.

310. Okumura A, Alce T, Lubyova B, Ezelle H, Strebel K, Pitha PM. HIV-1 accessory proteins VPR and Vif modulate antiviral response by targeting IRF-3 for degradation. Virology. 2008;373(1):85-97. Epub 2007/12/18.

311. Borrow P. Innate immunity in acute HIV-1 infection. Current opinion in HIV and AIDS. 2011;6(5):353-63. Epub 2011/07/08.

312. Marsili G, Remoli AL, Sgarbanti M, Perrotti E, Fragale A, Battistini A. HIV-1, interferon and the interferon regulatory factor system: an interplay between induction, antiviral responses and viral evasion. Cytokine & growth factor reviews. 2012;23(4-5):255-70. Epub 2012/07/04.

313. Huang J, Yang Y, Al-Mozaini M, Burke PS, Beamon J, Carrington MF, et al. Dendritic Cell Dysfunction During Primary HIV-1 Infection. The Journal of infectious diseases. 2011. Epub 2011/10/05.

314. Chang JJ, Lacas A, Lindsay RJ, Doyle EH, Axten KL, Pereyra F, et al. Differential regulation of TLR pathways in acute and chronic HIV-1 infection. AIDS (London, England). 2012. Epub 2012/01/03.

315. Kottilil S, Chun TW, Moir S, Liu S, McLaughlin M, Hallahan CW, et al. Innate immunity in human immunodeficiency virus infection: effect of viremia on natural killer cell function. The Journal of infectious diseases. 2003;187(7):1038-45. Epub 2003/03/28.

316. Mavilio D, Lombardo G, Benjamin J, Kim D, Follman D, Marcenaro E, et al. Characterization of CD56-/CD16+ natural killer (NK) cells: a highly dysfunctional NK subset expanded in HIV-infected viremic individuals. Proceedings of the National Academy of Sciences of the United States of America. 2005;102(8):2886-91. Epub 2005/02/09.

317. Piantadosi A, Panteleeff D, Blish CA, Baeten JM, Jaoko W, McClelland RS, et al. Breadth of neutralizing antibody response to human immunodeficiency virus type 1 is affected by factors early in infection but does not influence disease progression. Journal of virology. 2009;83(19):10269-74. Epub 2009/07/31.

318. van Gils MJ, Euler Z, Schweighardt B, Wrin T, Schuitemaker H. Prevalence of cross-reactive HIV-1-neutralizing activity in HIV-1-infected patients with rapid or slow disease progression. AIDS (London, England). 2009;23(18):2405-14. Epub 2009/09/23.

319. Streeck H, Jolin JS, Qi Y, Yassine-Diab B, Johnson RC, Kwon DS, et al. Human immunodeficiency virus type 1-specific CD8+ T-cell responses during primary infection are major determinants of the viral set point and loss of CD4+ T cells. Journal of virology. 2009;83(15):7641-8. Epub 2009/05/22.

320.   Yang H, Wu H, Hancock G, Clutton G, Sande N, Xu X, et al. Antiviral inhibitory capacity of CD8+ T cells predicts the rate of CD4+ T-cell decline in HIV-1 infection. The Journal of infectious diseases. 2012;206(4):552-61. Epub 2012/06/20.

321.   Jin X, Bauer DE, Tuttleton SE, Lewin S, Gettie A, Blanchard J, et al. Dramatic rise in plasma viremia after CD8(+) T cell depletion in simian immunodeficiency virus-infected macaques. The Journal of experimental medicine. 1999;189(6):991-8. Epub 1999/03/17.

322.   Lopez M, Peris A, Soriano V, Lozano S, Vicario JL, Rallon NI, et al. The expansion ability but not the quality of HIV-specific CD8(+) T cells is associated with protective human leucocyte antigen class I alleles in long-term non-progressors. Immunology. 2011;134(3):305-13. Epub 2011/10/08.

323.   Richmond M, McKinnon LR, Kiazyk SA, Wachihi C, Kimani M, Kimani J, et al. Epitope mapping of HIV-specific CD8+ T cell responses by multiple immunological readouts reveals distinct specificities defined by function. Journal of virology. 2011;85(3):1275-86. Epub 2010/11/19.

324.   Ferre AL, Hunt PW, Critchfield JW, Young DH, Morris MM, Garcia JC, et al. Mucosal immune responses to HIV-1 in elite controllers: a potential correlate of immune control. Blood. 2009;113(17):3978-89. Epub 2008/12/26.

325.   Hersperger AR, Migueles SA, Betts MR, Connors M. Qualitative features of the HIV-specific CD8+ T-cell response associated with immunologic control. Current opinion in HIV and AIDS. 2011;6(3):169-73. Epub 2011/03/15.

326.   Belyakov IM, Ahlers JD. Functional CD8+ CTLs in mucosal sites and HIV infection: moving forward toward a mucosal AIDS vaccine. Trends Immunol. 2008;29(11):574-85. Epub 2008/10/08.

327.   Douek DC, Brenchley JM, Betts MR, Ambrozak DR, Hill BJ, Okamoto Y, et al. HIV preferentially infects HIV-specific CD4+ T cells. Nature. 2002;417(6884):95-8. Epub 2002/05/03.

328.   Paiardini M, Cervasi B, Reyes-Aviles E, Micci L, Ortiz AM, Chahroudi A, et al. Low levels of SIV infection in sooty mangabey central memory CD(4)(+) T cells are associated with limited CCR5 expression. Nature medicine. 2011;17(7):830-6. Epub 2011/06/28.

329.   Soghoian DZ, Jessen H, Flanders M, Sierra-Davidson K, Cutler S, Pertel T, et al. HIV-specific cytolytic CD4 T cell responses during acute HIV infection predict disease outcome. Science translational medicine. 2012;4(123):123ra25. Epub 2012/03/02.

330.   Ortiz AM, Klatt NR, Li B, Yi Y, Tabb B, Hao XP, et al. Depletion of CD4(+) T cells abrogates post-peak decline of viremia in SIV-infected rhesus macaques. The Journal of clinical investigation. 2011;121(11):4433-45. Epub 2011/10/19.

331.   Milush JM, Mir KD, Sundaravaradan V, Gordon SN, Engram J, Cano CA, et al. Lack of clinical AIDS in SIV-infected sooty mangabeys with significant CD4+ T cell loss is associated with double-negative T cells. The Journal of clinical investigation. 2011;121(3):1102-10. Epub 2011/02/15.

332.   van der Vliet HJ, von Blomberg BM, Hazenberg MD, Nishi N, Otto SA, van Benthem BH, et al. Selective decrease in circulating V alpha 24+V beta 11+ NKT cells during HIV type 1 infection. Journal of immunology (Baltimore, Md : 1950). 2002;168(3):1490-5. Epub 2002/01/22.

333.   Sandberg JK, Fast NM, Palacios EH, Fennelly G, Dobroszycki J, Palumbo P, et al. Selective loss of innate CD4(+) V alpha 24 natural killer T cells in human immunodeficiency virus infection. Journal of virology. 2002;76(15):7528-34. Epub 2002/07/05.

334.   Fleuridor R, Wilson B, Hou R, Landay A, Kessler H, Al-Harthi L. CD1d-restricted natural killer T cells are potent targets for human immunodeficiency virus infection. Immunology. 2003;108(1):3-9. Epub 2003/01/10.

335.   Chiappini E, Betti L, Bonsignori F, Azzari C, Galli L, de Martino M. CD4(+) and CD4(-) CD1D-restricted natural killer T cells in perinatally HIV-1 infected children receiving highly active antiretroviral therapy. Int J Immunopathol Pharmacol. 2010;23(2):665-9. Epub 2010/07/22.

336.   Vasan S, Poles MA, Horowitz A, Siladji EE, Markowitz M, Tsuji M. Function of NKT cells, potential anti-HIV effector cells, are improved by beginning HAART during acute HIV-1 infection. Int Immunol. 2007;19(8):943-51. Epub 2007/08/19.

337.   Yang OO, Wilson SB, Hultin LE, Detels R, Hultin PM, Ibarrondo FJ, et al. Delayed reconstitution of CD4+ iNKT cells after effective HIV type 1 therapy. AIDS research and human retroviruses. 2007;23(7):913-22. Epub 2007/08/07.

338.   Moll M, Kuylenstierna C, Gonzalez VD, Andersson SK, Bosnjak L, Sonnerborg A, et al. Severe functional impairment and elevated PD-1 expression in CD1d-restricted NKT cells retained during chronic HIV-1 infection. European journal of immunology. 2009;39(3):902-11. Epub 2009/02/07.

339.   Li D, Xu XN. NKT cells in HIV-1 infection. Cell Res. 2008;18(8):817-22. Epub 2008/07/23.

340.   Unutmaz D. NKT cells and HIV infection. Microbes Infect. 2003;5(11):1041-7. Epub 2003/08/28.

341.   Nowicki MJ, Vigen C, Mack WJ, Seaberg E, Landay A, Anastos K, et al. Association of cells with natural killer (NK) and NKT immunophenotype with incident cancers in HIV-infected women. AIDS research and human retroviruses. 2008;24(2):163-8. Epub 2008/02/05.

342.   Ibarrondo FJ, Wilson SB, Hultin LE, Shih R, Hausner MA, Hultin PM, et al. Preferential depletion of gut CD4-expressing iNKT cells contributes to systemic immune activation in HIV-1 infection. Mucosal immunology. 2012. Epub 2012/11/15.

343.   Rout N, Greene J, Yue S, O'Connor D, Johnson RP, Else JG, et al. Loss of effector and anti-inflammatory natural killer T lymphocyte function in pathogenic simian immunodeficiency virus infection. PLoS pathogens. 2012;8(9):e1002928. Epub 2012/10/03.

344.   Snyder-Cappione JE, Loo CP, Carvalho KI, Kuylenstierna C, Deeks SG, Hecht FM, et al. Lower cytokine secretion ex vivo by natural killer T cells in HIV-infected individuals is associated with higher CD161 expression. AIDS (London, England). 2009;23(15):1965-70. Epub 2009/07/11.

345.   Chang WS, Kim JY, Kim YJ, Kim YS, Lee JM, Azuma M, et al. Cutting edge: Programmed death-1/programmed death ligand 1 interaction regulates the induction and maintenance of invariant NKT cell anergy. Journal of immunology (Baltimore, Md : 1950). 2008;181(10):6707-10. Epub 2008/11/05.

346.   Parekh VV, Lalani S, Kim S, Halder R, Azuma M, Yagita H, et al. PD-1/PD-L blockade prevents anergy induction and enhances the anti-tumor activities of glycolipid-

activated invariant NKT cells. Journal of immunology (Baltimore, Md : 1950). 2009;182(5):2816-26. Epub 2009/02/24.

347.   Courtney AN, Thapa P, Singh S, Wishahy AM, Zhou D, Sastry J. Intranasal but not intravenous delivery of the adjuvant alpha-galactosylceramide permits repeated stimulation of natural killer T cells in the lung. European journal of immunology. 2011;41(11):3312-22. Epub 2011/08/06.

348.   Mir KD, Gasper MA, Sundaravaradan V, Sodora DL. SIV infection in natural hosts: resolution of immune activation during the acute-to-chronic transition phase. Microbes Infect. 2011;13(1):14-24. Epub 2010/10/19.

349.   Motsinger A, Azimzadeh A, Stanic AK, Johnson RP, Van Kaer L, Joyce S, et al. Identification and simian immunodeficiency virus infection of CD1d-restricted macaque natural killer T cells. Journal of virology. 2003;77(14):8153-8. Epub 2003/06/28.

350.   Fernandez CS, Chan AC, Kyparissoudis K, De Rose R, Godfrey DI, Kent SJ. Peripheral NKT cells in simian immunodeficiency virus-infected macaques. Journal of virology. 2009;83(4):1617-24. Epub 2008/12/05.

351.   Campillo-Gimenez L, Cumont MC, Fay M, Kared H, Monceaux V, Diop O, et al. AIDS progression is associated with the emergence of IL-17-producing cells early after simian immunodeficiency virus infection. Journal of immunology (Baltimore, Md : 1950). 2010;184(2):984-92. Epub 2009/12/19.

352.   Klatt NR, Silvestri G, Hirsch V. Nonpathogenic Simian Immunodeficiency Virus Infections. Cold Spring Harbor Perspectives in Medicine. 2011(Journal Article).

353.   Rout N, Else JG, Yue S, Connole M, Exley MA, Kaur A. Paucity of CD4+ Natural Killer T (NKT) Lymphocytes in Sooty Mangabeys Is Associated with Lack of NKT Cell Depletion after SIV Infection. PloS one. 2010;5(3):e9787.

354.   Cohen GB, Gandhi RT, Davis DM, Mandelboim O, Chen BK, Strominger JL, et al. The selective downregulation of class I major histocompatibility complex proteins by HIV-1 protects HIV-infected cells from NK cells. Immunity. 1999;10(6):661-71. Epub 1999/07/14.

355.   Chen N, McCarthy C, Drakesmith H, Li D, Cerundolo V, McMichael AJ, et al. HIV-1 down-regulates the expression of CD1d via Nef. European journal of immunology. 2006;36(2):278-86. Epub 2005/12/31.

356.   Cho S, Knox KS, Kohli LM, He JJ, Exley MA, Wilson SB, et al. Impaired cell surface expression of human CD1d by the formation of an HIV-1 Nef/CD1d complex. Virology. 2005;337(2):242-52. Epub 2005/05/27.

357.   Sousa AE, Carneiro J, Meier-Schellersheim M, Grossman Z, Victorino RM. CD4 T cell depletion is linked directly to immune activation in the pathogenesis of HIV-1 and HIV-2 but only indirectly to the viral load. Journal of immunology (Baltimore, Md : 1950). 2002;169(6):3400-6. Epub 2002/09/10.

358.   Haas A, Zimmermann K, Oxenius A. Antigen-dependent and -independent mechanisms of T and B cell hyperactivation during chronic HIV-1 infection. Journal of virology. 2011;85(23):12102-13. Epub 2011/08/19.

359.   Kaiser P, Joos B, Niederost B, Weber R, Gunthard HF, Fischer M. Productive human immunodeficiency virus type 1 infection in peripheral blood predominantly takes place in CD4/CD8 double-negative T lymphocytes. Journal of virology. 2007;81(18):9693-706. Epub 2007/07/05.

360.   Harper ME, Marselle LM, Gallo RC, Wong-Staal F. Detection of lymphocytes expressing human T-lymphotropic virus type III in lymph nodes and peripheral blood from infected individuals by in situ hybridization. Proceedings of the National Academy of Sciences of the United States of America. 1986;83(3):772-6. Epub 1986/02/01.

361.   Hunt PW, Martin JN, Sinclair E, Bredt B, Hagos E, Lampiris H, et al. T cell activation is associated with lower CD4+ T cell gains in human immunodeficiency virus-infected patients with sustained viral suppression during antiretroviral therapy. The Journal of infectious diseases. 2003;187(10):1534-43. Epub 2003/05/02.

362.   Brenchley JM, Price DA, Schacker TW, Asher TE, Silvestri G, Rao S, et al. Microbial translocation is a cause of systemic immune activation in chronic HIV infection. Nature medicine. 2006;12(12):1365-71. Epub 2006/11/23.

363.   Nazli A, Chan O, Dobson-Belaire WN, Ouellet M, Tremblay MJ, Gray-Owen SD, et al. Exposure to HIV-1 directly impairs mucosal epithelial barrier integrity allowing microbial translocation. PLoS pathogens. 2010;6(4):e1000852. Epub 2010/04/14.

364.   Sandler NG, Wand H, Roque A, Law M, Nason MC, Nixon DE, et al. Plasma levels of soluble CD14 independently predict mortality in HIV infection. The Journal of infectious diseases. 2011;203(6):780-90. Epub 2011/01/22.

365.   Romero-Sanchez M, Gonzalez-Serna A, Pacheco YM, Ferrando-Martinez S, Machmach K, Garcia-Garcia M, et al. Different biological significance of sCD14 and LPS in HIV-infection: importance of the immunovirology stage and association with HIV-disease progression markers. The Journal of infection. 2012;65(5):431-8. Epub 2012/06/26.

366.   Marchetti G, Cozzi-Lepri A, Merlini E, Bellistri GM, Castagna A, Galli M, et al. Microbial translocation predicts disease progression of HIV-infected antiretroviral-naive patients with high CD4+ cell count. AIDS (London, England). 2011;25(11):1385-94. Epub 2011/04/21.

367.   Bosinger SE, Sodora DL, Silvestri G. Generalized immune activation and innate immune responses in simian immunodeficiency virus infection. Current opinion in HIV and AIDS. 2011;6(5):411-8. Epub 2011/07/12.

368.   Chahroudi A, Bosinger SE, Vanderford TH, Paiardini M, Silvestri G. Natural SIV hosts: showing AIDS the door. Science. 2012;335(6073):1188-93. Epub 2012/03/10.

369.   Khaitan A, Unutmaz D. Revisiting Immune Exhaustion During HIV Infection. Current HIV/AIDS reports. 2011;8(1):4-11.

370.   Wherry EJ. T cell exhaustion. Nature immunology. 2011;12(6):492-9.

371.   Ribas A. Clinical development of the anti-CTLA-4 antibody tremelimumab. Semin Oncol. 2010;37(5):450-4. Epub 2010/11/16.

372.   Wherry EJ, Blattman JN, Murali-Krishna K, van der Most R, Ahmed R. Viral persistence alters CD8 T-cell immunodominance and tissue distribution and results in distinct stages of functional impairment. Journal of virology. 2003;77(8):4911-27. Epub 2003/03/29.

373.   Wherry EJ, Ha SJ, Kaech SM, Haining WN, Sarkar S, Kalia V, et al. Molecular signature of CD8+ T cell exhaustion during chronic viral infection. Immunity. 2007;27(4):670-84. Epub 2007/10/24.

374.   Day CL, Kaufmann DE, Kiepiela P, Brown JA, Moodley ES, Reddy S, et al. PD-1 expression on HIV-specific T cells is associated with T-cell exhaustion and disease progression. Nature. 2006;443(7109):350-4. Epub 2006/08/22.

375.   Trautmann L, Janbazian L, Chomont N, Said EA, Gimmig S, Bessette B, et al. Upregulation of PD-1 expression on HIV-specific CD8+ T cells leads to reversible immune dysfunction. Nature medicine. 2006;12(10):1198-202. Epub 2006/08/19.

376.   Leng Q, Bentwich Z, Magen E, Kalinkovich A, Borkow G. CTLA-4 upregulation during HIV infection: association with anergy and possible target for therapeutic intervention. AIDS (London, England). 2002;16(4):519-29. Epub 2002/03/02.

377.   Jones RB, Ndhlovu LC, Barbour JD, Sheth PM, Jha AR, Long BR, et al. Tim-3 expression defines a novel population of dysfunctional T cells with highly elevated frequencies in progressive HIV-1 infection. The Journal of experimental medicine. 2008;205(12):2763-79. Epub 2008/11/13.

378.   Price P, Keane N, Gray L, Lee S, Gorry PR, French MA. CXCR4 or CCR5 tropism of human immunodeficiency virus type 1 isolates does not determine the immunological milieu in patients responding to antiretroviral therapy. Viral immunology. 2006;19(4):734-40. Epub 2007/01/05.

379.   Antonelli LR, Mahnke Y, Hodge JN, Porter BO, Barber DL, DerSimonian R, et al. Elevated frequencies of highly activated CD4+ T cells in HIV+ patients developing immune reconstitution inflammatory syndrome. Blood. 2010;116(19):3818-27. Epub 2010/07/28.

380.   Yamamoto T, Price DA, Casazza JP, Ferrari G, Nason M, Chattopadhyay PK, et al. Surface expression patterns of negative regulatory molecules identify determinants of virus-specific CD8+ T-cell exhaustion in HIV infection. Blood. 2011;117(18):4805-15. Epub 2011/03/15.

381.   Jin HT, Anderson AC, Tan WG, West EE, Ha SJ, Araki K, et al. Cooperation of Tim-3 and PD-1 in CD8 T-cell exhaustion during chronic viral infection. Proceedings of the National Academy of Sciences of the United States of America. 2010;107(33):14733-8. Epub 2010/08/04.

382.   Dyavar Shetty R, Velu V, Titanji K, Bosinger SE, Freeman GJ, Silvestri G, et al. PD-1 blockade during chronic SIV infection reduces hyperimmune activation and microbial translocation in rhesus macaques. The Journal of clinical investigation. 2012. Epub 2012/04/24.

383.   Seung E, Dudek TE, Allen TM, Freeman GJ, Luster AD, Tager AM. PD-1 Blockade in Chronically HIV-1-Infected Humanized Mice Suppresses Viral Loads. PloS one. 2013;8(10):e77780. Epub 2013/11/10.

384.   Triebel F, Jitsukawa S, Baixeras E, Roman-Roman S, Genevee C, Viegas-Pequignot E, et al. LAG-3, a novel lymphocyte activation gene closely related to CD4. The Journal of experimental medicine. 1990;171(5):1393-405. Epub 1990/05/01.

385.   Bruniquel D, Borie N, Hannier S, Triebel F. Regulation of expression of the human lymphocyte activation gene-3 (LAG-3) molecule, a ligand for MHC class II. Immunogenetics. 1998;48(2):116-24. Epub 1998/06/20.

386.   Zhang Z, Duvefelt K, Svensson F, Masterman T, Jonasdottir G, Salter H, et al. Two genes encoding immune-regulatory molecules (LAG3 and IL7R) confer susceptibility to multiple sclerosis. Genes Immun. 2005;6(2):145-52. Epub 2005/01/28.

387.   Lundmark F, Harbo HF, Celius EG, Saarela J, Datta P, Oturai A, et al. Association analysis of the LAG3 and CD4 genes in multiple sclerosis in two independent populations. J Neuroimmunol. 2006;180(1-2):193-8. Epub 2006/10/06.

388.   Baixeras E, Huard B, Miossec C, Jitsukawa S, Martin M, Hercend T, et al. Characterization of the lymphocyte activation gene 3-encoded protein. A new ligand for human leukocyte antigen class II antigens. The Journal of experimental medicine. 1992;176(2):327-37. Epub 1992/08/01.

389.   Huard B, Prigent P, Tournier M, Bruniquel D, Triebel F. CD4/major histocompatibility complex class II interaction analyzed with CD4- and lymphocyte activation gene-3 (LAG-3)-Ig fusion proteins. European journal of immunology. 1995;25(9):2718-21. Epub 1995/09/01.

390.   Triebel F, Hacene K, Pichon MF. A soluble lymphocyte activation gene-3 (sLAG-3) protein as a prognostic factor in human breast cancer expressing estrogen or progesterone receptors. Cancer Lett. 2006;235(1):147-53. Epub 2005/06/11.

391.   Lienhardt C, Azzurri A, Amedei A, Fielding K, Sillah J, Sow OY, et al. Active tuberculosis in Africa is associated with reduced Th1 and increased Th2 activity in vivo. European journal of immunology. 2002;32(6):1605-13. Epub 2002/07/13.

392.   Djoba Siawaya JF, Bapela NB, Ronacher K, Veenstra H, Kidd M, Gie R, et al. Immune parameters as markers of tuberculosis extent of disease and early prediction of anti-tuberculosis chemotherapy response. The Journal of infection. 2008;56(5):340-7. Epub 2008/03/25.

393.   Triebel F. LAG-3: a regulator of T-cell and DC responses and its use in therapeutic vaccination. Trends in immunology. 2003;24(12):619-22.

394.   Triebel F, inventor; LAG-3 splice variants1999 18/06/1997.

395.   Workman CJ, Rice DS, Dugger KJ, Kurschner C, Vignali DA. Phenotypic analysis of the murine CD4-related glycoprotein, CD223 (LAG-3). European journal of immunology. 2002;32(8):2255-63. Epub 2002/09/05.

396.   Li N, Wang Y, Forbes K, Vignali KM, Heale BS, Saftig P, et al. Metalloproteases regulate T-cell proliferation and effector function via LAG-3. The EMBO journal. 2007;26(2):494-504. Epub 2007/01/25.

397.   Huard B, Mastrangeli R, Prigent P, Bruniquel D, Donini S, El-Tayar N, et al. Characterization of the major histocompatibility complex class II binding site on LAG-3 protein. Proceedings of the National Academy of Sciences of the United States of America. 1997;94(11):5744-9. Epub 1997/05/27.

398.   Workman CJ, Wang Y, El Kasmi KC, Pardoll DM, Murray PJ, Drake CG, et al. LAG-3 regulates plasmacytoid dendritic cell homeostasis. Journal of immunology (Baltimore, Md : 1950). 2009;182(4):1885-91. Epub 2009/02/10.

399.   Kisielow M, Kisielow J, Capoferri-Sollami G, Karjalainen K. Expression of lymphocyte activation gene 3 (LAG-3) on B cells is induced by T cells. European journal of immunology. 2005;35(7):2081-8. Epub 2005/06/23.

400.   Byun HJ, Jung WW, Lee DS, Kim S, Kim SJ, Park CG, et al. Proliferation of activated CD1d-restricted NKT cells is down-modulated by lymphocyte activation gene-3 signaling via cell cycle arrest in S phase. Cell Biol Int. 2007;31(3):257-62. Epub 2006/12/19.

401.   Camisaschi C, Casati C, Rini F, Perego M, De Filippo A, Triebel F, et al. LAG-3 expression defines a subset of CD4(+)CD25(high)Foxp3(+) regulatory T cells that are expanded at tumor sites. Journal of immunology (Baltimore, Md : 1950). 2010;184(11):6545-51. Epub 2010/04/28.

402. Sumitomo S, Yamamoto K. CD4+CD25-LAG-3+ T cells in mouse and human. Nihon Rinsho Meneki Gakkai Kaishi. 2010;33(2):92-8. Epub 2010/05/11.

403. Gagliani N, Magnani CF, Huber S, Gianolini ME, Pala M, Licona-Limon P, et al. Coexpression of CD49b and LAG-3 identifies human and mouse T regulatory type 1 cells. Nature medicine. 2013;19(6):739-46. Epub 2013/04/30.

404. Camisaschi C, De filippo A, Beretta V, Rini F, Tazzari M, Arienti F, et al. LAG-3 expression and role in human pDC biology. Conference Abstract - 15th International Congress of Immunology; 22 Aug 2013; Milan, Italy: Frontiers in Immunology; 2013.

405. Annunziato F, Manetti R, Cosmi L, Galli G, Heusser CH, Romagnani S, et al. Opposite role for interleukin-4 and interferon-gamma on CD30 and lymphocyte activation gene-3 (LAG-3) expression by activated naive T cells. European journal of immunology. 1997;27(9):2239-44. Epub 1997/10/28.

406. Workman CJ, Vignali DA. Negative regulation of T cell homeostasis by lymphocyte activation gene-3 (CD223). Journal of immunology (Baltimore, Md : 1950). 2005;174(2):688-95. Epub 2005/01/07.

407. Workman CJ, Cauley LS, Kim IJ, Blackman MA, Woodland DL, Vignali DA. Lymphocyte activation gene-3 (CD223) regulates the size of the expanding T cell population following antigen activation in vivo. Journal of immunology (Baltimore, Md : 1950). 2004;172(9):5450-5. Epub 2004/04/22.

408. Huard B, Prigent P, Pages F, Bruniquel D, Triebel F. T cell major histocompatibility complex class II molecules down-regulate CD4+ T cell clone responses following LAG-3 binding. European journal of immunology. 1996;26(5):1180-6. Epub 1996/05/01.

409. Sierro S, Romero P, Speiser DE. The CD4-like molecule LAG-3, biology and therapeutic applications. Expert Opin Ther Targets. 2011;15(1):91-101. Epub 2010/12/15.

410. Workman CJ, Dugger KJ, Vignali DA. Cutting edge: molecular analysis of the negative regulatory function of lymphocyte activation gene-3. Journal of immunology (Baltimore, Md : 1950). 2002;169(10):5392-5. Epub 2002/11/08.

411. Hannier S, Tournier M, Bismuth G, Triebel F. CD3/TCR complex-associated lymphocyte activation gene-3 molecules inhibit CD3/TCR signaling. Journal of immunology (Baltimore, Md : 1950). 1998;161(8):4058-65. Epub 1998/10/21.

412. Macon-Lemaitre L, Triebel F. The negative regulatory function of the lymphocyte-activation gene-3 co-receptor (CD223) on human T cells. Immunology. 2005;115(2):170-8. Epub 2005/05/12.

413. Iouzalen N, Andreae S, Hannier S, Triebel F. LAP, a lymphocyte activation gene-3 (LAG-3)-associated protein that binds to a repeated EP motif in the intracellular region of LAG-3, may participate in the down-regulation of the CD3/TCR activation pathway. European journal of immunology. 2001;31(10):2885-91. Epub 2001/10/10.

414. Okamura T, Fujio K, Shibuya M, Sumitomo S, Shoda H, Sakaguchi S, et al. CD4+CD25-LAG3+ regulatory T cells controlled by the transcription factor Egr-2. Proceedings of the National Academy of Sciences of the United States of America. 2009;106(33):13974-9. Epub 2009/08/12.

415. Huang CT, Workman CJ, Flies D, Pan X, Marson AL, Zhou G, et al. Role of LAG-3 in regulatory T cells. Immunity. 2004;21(4):503-13. Epub 2004/10/16.

416.   Miyazaki T, Dierich A, Benoist C, Mathis D. Independent modes of natural killing distinguished in mice lacking Lag3. Science. 1996;272(5260):405-8. Epub 1996/04/19.

417.   Liang B, Workman C, Lee J, Chew C, Dale BM, Colonna L, et al. Regulatory T cells inhibit dendritic cells by lymphocyte activation gene-3 engagement of MHC class II. Journal of immunology (Baltimore, Md : 1950). 2008;180(9):5916-26. Epub 2008/04/22.

418.   Huard B, Tournier M, Triebel F. LAG-3 does not define a specific mode of natural killing in human. Immunol Lett. 1998;61(2-3):109-12. Epub 1998/07/10.

419.   Subramanyam M, Wands G, Nabioullin R, Tepper MA. Soluble human lymphocyte activation gene-3 modulates allospecific T cell responses. Int Immunol. 1998;10(5):679-89. Epub 1998/06/30.

420.   Subleski JJ, Hall VL, Wolfe TB, Scarzello AJ, Weiss JM, Chan T, et al. TCR-dependent and -independent activation underlie liver-specific regulation of NKT cells. Journal of immunology (Baltimore, Md : 1950). 2011;186(2):838-47. Epub 2010/12/15.

421.   Hemon P, Jean-Louis F, Ramgolam K, Brignone C, Viguier M, Bachelez H, et al. MHC class II engagement by its ligand LAG-3 (CD223) contributes to melanoma resistance to apoptosis. Journal of immunology (Baltimore, Md : 1950). 2011;186(9):5173-83. Epub 2011/03/29.

422.   Andreae S, Buisson S, Triebel F. MHC class II signal transduction in human dendritic cells induced by a natural ligand, the LAG-3 protein (CD223). Blood. 2003;102(6):2130-7. Epub 2003/05/31.

423.   Andreae S, Piras F, Burdin N, Triebel F. Maturation and activation of dendritic cells induced by lymphocyte activation gene-3 (CD223). Journal of immunology (Baltimore, Md : 1950). 2002;168(8):3874-80. Epub 2002/04/09.

424.   Casati C, Camisaschi C, Novellino L, Mazzocchi A, Triebel F, Rivoltini L, et al. Human lymphocyte activation gene-3 molecules expressed by activated T cells deliver costimulation signal for dendritic cell activation. Journal of immunology (Baltimore, Md : 1950). 2008;180(6):3782-8. Epub 2008/03/07.

425.   Bayry J, Triebel F, Kaveri SV, Tough DF. Human dendritic cells acquire a semimature phenotype and lymph node homing potential through interaction with CD4+CD25+ regulatory T cells. Journal of immunology (Baltimore, Md : 1950). 2007;178(7):4184-93. Epub 2007/03/21.

426.   Buisson S, Triebel F. MHC class II engagement by its ligand LAG-3 (CD223) leads to a distinct pattern of chemokine and chemokine receptor expression by human dendritic cells. Vaccine. 2003;21(9-10):862-8. Epub 2003/01/28.

427.   Avice MN, Sarfati M, Triebel F, Delespesse G, Demeure CE. Lymphocyte activation gene-3, a MHC class II ligand expressed on activated T cells, stimulates TNF-alpha and IL-12 production by monocytes and dendritic cells. Journal of immunology (Baltimore, Md : 1950). 1999;162(5):2748-53. Epub 1999/03/11.

428.   Buisson S, Triebel F. LAG-3 (CD223) reduces macrophage and dendritic cell differentiation from monocyte precursors. Immunology. 2005;114(3):369-74. Epub 2005/02/22.

429.   Richter K, Agnellini P, Oxenius A. On the role of the inhibitory receptor LAG-3 in acute and chronic LCMV infection. Int Immunol. 2010;22(1):13-23. Epub 2009/11/03.

430.   Blackburn SD, Shin H, Haining WN, Zou T, Workman CJ, Polley A, et al. Coregulation of CD8+ T cell exhaustion by multiple inhibitory receptors during chronic viral infection. Nature immunology. 2009;10(1):29-37. Epub 2008/12/02.

431.   Butler NS, Moebius J, Pewe LL, Traore B, Doumbo OK, Tygrett LT, et al. Therapeutic blockade of PD-L1 and LAG-3 rapidly clears established blood-stage Plasmodium infection. Nature immunology. 2011. Epub 2011/12/14.

432.   Bengsch B, Seigel B, Ruhl M, Timm J, Kuntz M, Blum HE, et al. Coexpression of PD-1, 2B4, CD160 and KLRG1 on exhausted HCV-specific CD8+ T cells is linked to antigen recognition and T cell differentiation. PLoS pathogens. 2010;6(6):e1000947. Epub 2010/06/16.

433.   Kaufmann DE, Walker BD. PD-1 and CTLA-4 inhibitory cosignaling pathways in HIV infection and the potential for therapeutic intervention. Journal of immunology (Baltimore, Md : 1950). 2009;182(10):5891-7. Epub 2009/05/06.

434.   Sakuishi K, Jayaraman P, Behar SM, Anderson AC, Kuchroo VK. Emerging Tim-3 functions in antimicrobial and tumor immunity. Trends Immunol. 2011;32(8):345-9. Epub 2011/06/24.

435.   Lim AY, Price P, Beilharz MW, French MA. Cell surface markers of regulatory T cells are not associated with increased forkhead box p3 expression in blood CD4+ T cells from HIV-infected patients responding to antiretroviral therapy. Immunol Cell Biol. 2006;84(6):530-6. Epub 2006/09/08.

436.   Porichis F, Kwon DS, Zupkosky J, Tighe DP, McMullen A, Brockman MA, et al. Responsiveness of HIV-specific CD4 T cells to PD-1 blockade. Blood. 2011;118(4):965-74. Epub 2011/06/10.

437.   Pena J, Jones N, Bousheri S, Bangsberg DR, Cao H. LAG-3 expression defines a discrete subset of HIV-specific CD8+ T cells that is associated with lower viral load. AIDS research and human retroviruses. 2013. Epub 2013/11/05.

438.   Li Q, Smith AJ, Schacker TW, Carlis JV, Duan L, Reilly CS, et al. Microarray analysis of lymphatic tissue reveals stage-specific, gene expression signatures in HIV-1 infection. Journal of immunology (Baltimore, Md : 1950). 2009;183(3):1975-82. Epub 2009/07/15.

439.   Bosinger SE, Li Q, Gordon SN, Klatt NR, Duan L, Xu L, et al. Global genomic analysis reveals rapid control of a robust innate response in SIV-infected sooty mangabeys. The Journal of clinical investigation. 2009;119(12):3556-72. Epub 2009/12/05.

440.   Rotger M, Dalmau J, Rauch A, McLaren P, Bosinger SE, Martinez R, et al. Comparative transcriptomics of extreme phenotypes of human HIV-1 infection and SIV infection in sooty mangabey and rhesus macaque. The Journal of clinical investigation. 2011;121(6):2391-400. Epub 2011/05/11.

441.   Shankar EM, Che KF, Messmer D, Lifson JD, Larsson M. Expression of a broad array of negative costimulatory molecules and Blimp-1 in T cells following priming by HIV-1 pulsed dendritic cells. Mol Med. 2011;17(3-4):229-40. Epub 2010/11/26.

442.   Kreiss JK, Koech D, Plummer FA, Holmes KK, Lightfoote M, Piot P, et al. AIDS virus infection in Nairobi prostitutes. Spread of the epidemic to East Africa. The New England journal of medicine. 1986;314(7):414-8. Epub 1986/02/13.

443.   Juno JA, Tuff J, Choi R, Card C, Kimani J, Wachihi C, et al. The role of G Protein Gene GNB3 C825T Polymorphism in HIV-1 acquisition, progression and immune activation. Retrovirology. 2012;9(1):1. Epub 2012/01/05.

444.   Koesters SA, Alimonti JB, Wachihi C, Matu L, Anzala O, Kimani J, et al. IL-7Ralpha expression on CD4+ T lymphocytes decreases with HIV disease progression and inversely correlates with immune activation. European journal of immunology. 2006;36(2):336-44.

445.   Huard B, Gaulard P, Faure F, Hercend T, Triebel F. Cellular expression and tissue distribution of the human LAG-3-encoded protein, an MHC class II ligand. Immunogenetics. 1994;39(3):213-7.

446.   Bjorkstrom NK, Ljunggren HG, Sandberg JK. CD56 negative NK cells: origin, function, and role in chronic viral disease. Trends Immunol. 2010;31(11):401-6. Epub 2010/09/11.

447.   Bienemann K, Iouannidou K, Schoenberg K, Krux F, Reuther S, Feyen O, et al. iNKT cell frequency in peripheral blood of Caucasian children and adolescent: The absolute iNKT cell count is stable from birth to adulthood. Scand J Immunol. 2011. Epub 2011/06/16.

448.   Petrovas C, Chaon B, Ambrozak DR, Price DA, Melenhorst JJ, Hill BJ, et al. Differential association of programmed death-1 and CD57 with ex vivo survival of CD8+ T cells in HIV infection. Journal of immunology (Baltimore, Md : 1950). 2009;183(2):1120-32. Epub 2009/07/01.

449.   Siffert W, Esser S, Bromen K, Jockel KH, Goos M, Brockmeyer NH. G Protein beta 3 subunit 825T allele is strongly predictive for accelerated progression to AIDS. Program Abstr 8th Conf Retrovir Oppor Infect Conf Retrovir Oppor Infect 8th 2001 Chic Ill. 2001;8(Abstract):103.

450.   Aries SP, Schaaf B, Muller C, Dennin RH, Dalhoff K. Fas (CD95) expression on CD4+ T cells from HIV-infected patients increases with disease progression. Journal of Molecular Medicine (Berlin, Germany). 1995;73(12):591-3.

451.   Rosskopf D, Manthey I, Siffert W. Identification and ethnic distribution of major haplotypes in the gene GNB3 encoding the G-protein beta3 subunit. Pharmacogenetics. 2002;12(3):209-20. Epub 2002/04/03.

452.   Price P, Keane NM, Lee S, Lim AF, McKinnon EJ, French MA. A T2 cytokine environment may not limit T1 responses in human immunodeficiency virus patients with a favourable response to antiretroviral therapy. Immunology. 2006;119(1):74-82. Epub 2006/06/24.

453.   Kroy DC, Ciuffreda D, Cooperider JH, Tomlinson M, Hauck GD, Aneja J, et al. Liver Environment and HCV Replication Affect Human T-Cell Phenotype and Expression of Inhibitory Receptors. Gastroenterology. 2013. Epub 2013/10/24.

454.   Kennedy PT, Sandalova E, Jo J, Gill U, Ushiro-Lumb I, Tan AT, et al. Preserved T-cell function in children and young adults with immune-tolerant chronic hepatitis B. Gastroenterology. 2012;143(3):637-45. Epub 2012/06/20.

455.   Hong JJ, Amancha PK, Rogers K, Ansari AA, Villinger F. Re-Evaluation of PD-1 Expression by T Cells as a Marker for Immune Exhaustion during SIV Infection. PloS one. 2013;8(3):e60186. Epub 2013/04/05.

456.   Woo SR, Li N, Bruno TC, Forbes K, Brown S, Workman C, et al. Differential subcellular localization of the regulatory T-cell protein LAG-3 and the coreceptor CD4. European journal of immunology. 2010;40(6):1768-77. Epub 2010/04/15.
457.   Ndhlovu LC, Lopez-Verges S, Barbour JD, Jones RB, Jha AR, Long BR, et al. Tim-3 marks human natural killer cell maturation and suppresses cell-mediated cytotoxicity. Blood. 2012;119(16):3734-43. Epub 2012/03/03.
458.   Gleason MK, Lenvik TR, McCullar V, Felices M, O'Brien MS, Cooley SA, et al. Tim-3 is an inducible human natural killer cell receptor that enhances interferon gamma production in response to galectin-9. Blood. 2012;119(13):3064-72. Epub 2012/02/11.
459.   Norris S, Coleman A, Kuri-Cervantes L, Bower M, Nelson M, Goodier MR. PD-1 expression on natural killer cells and CD8(+) T cells during chronic HIV-1 infection. Viral immunology. 2012;25(4):329-32. Epub 2012/06/30.
460.   Lichtfuss GF, Cheng WJ, Farsakoglu Y, Paukovics G, Rajasuriar R, Velayudham P, et al. Virologically suppressed HIV patients show activation of NK cells and persistent innate immune activation. Journal of immunology (Baltimore, Md : 1950). 2012;189(3):1491-9. Epub 2012/06/30.
461.   Dillon SM, Lee EJ, Bramante JM, Barker E, Wilson CC. The Natural Killer Cell Interferon-gamma Response to Bacteria is Diminished in Untreated HIV-1 Infection and Defects Persist Despite Viral Suppression. Journal of acquired immune deficiency syndromes (1999). 2013. Epub 2013/10/05.
462.   Samaras K. The burden of diabetes and hyperlipidemia in treated HIV infection and approaches for cardiometabolic care. Current HIV/AIDS reports. 2012;9(3):206-17. Epub 2012/07/04.
463.   Braun NA, Mendez-Fernandez YV, Covarrubias R, Porcelli SA, Savage PB, Yagita H, et al. Development of spontaneous anergy in invariant natural killer T cells in a mouse model of dyslipidemia. Arterioscler Thromb Vasc Biol. 2010;30(9):1758-65. Epub 2010/06/12.
464.   Carsenti-Dellamonica H, Saidi H, Ticchioni M, Guillouet de Salvador F, Dufayard Cottalorda J, Garraffo R, et al. The suppression of immune activation during enfuvirtide-based salvage therapy is associated with reduced CCR5 expression and decreased concentrations of circulating interleukin-12 and IP-10 during 48 weeks of longitudinal follow-up. HIV medicine. 2011;12(2):65-77. Epub 2010/05/27.
465.   Jiao Y, Zhang T, Wang R, Zhang H, Huang X, Yin J, et al. Plasma IP-10 is associated with rapid disease progression in early HIV-1 infection. Viral immunology. 2012;25(4):333-7. Epub 2012/07/14.
466.   Liovat AS, Rey-Cuille MA, Lecuroux C, Jacquelin B, Girault I, Petitjean G, et al. Acute plasma biomarkers of T cell activation set-point levels and of disease progression in HIV-1 infection. PloS one. 2012;7(10):e46143. Epub 2012/10/12.
467.   Yao Y, Luo Y, He Y, Zheng Y, Zhang Q, Zhou H, et al. The Effect of a Year of Highly Active Antiretroviral Therapy on Immune Reconstruction and Cytokines in HIV/AIDS Patients. AIDS research and human retroviruses. 2013. Epub 2012/11/16.
468.   Gray CM, Hong HA, Young K, Lewis DA, Fallows D, Manca C, et al. Plasma Interferon-Gamma-Inducible Protein 10 Can Be Used to Predict Viral Load in HIV-1-Infected Individuals. Journal of acquired immune deficiency syndromes (1999). 2013;63(3):e115-e6. Epub 2013/06/14.

469.	Shacklett BL, Critchfield JW, Ferre AL, Hayes TL. Mucosal T-cell responses to HIV: responding at the front lines. J Intern Med. 2009;265(1):58-66. Epub 2008/12/20.

470.	Rueda CM, Velilla PA, Chougnet CA, Montoya CJ, Rugeles MT. HIV-induced T-cell activation/exhaustion in rectal mucosa is controlled only partially by antiretroviral treatment. PloS one. 2012;7(1):e30307. Epub 2012/01/26.

471.	Tian X, Zhang A, Qiu C, Yuan S, Qiu S, Hu H, et al. Up-regulation of LAG-3 Expression on T Cells in HIV-1 Infection is Correlated with Disease Progression. Abstracts from AIDS Vaccine 2011 Bangkok, Thailand 12-15 September, 2011. AIDS research and human retroviruses. 2011. Epub 2011/09/17.

472.	Grosso JF, Goldberg MV, Getnet D, Bruno TC, Yen HR, Pyle KJ, et al. Functionally distinct LAG-3 and PD-1 subsets on activated and chronically stimulated CD8 T cells. Journal of immunology (Baltimore, Md : 1950). 2009;182(11):6659-69. Epub 2009/05/21.

473.	Zloza A, Al-Harthi L. Multiple populations of T lymphocytes are distinguished by the level of CD4 and CD8 coexpression and require individual consideration. Journal of leukocyte biology. 2006;79(1):4-6. Epub 2005/12/29.

474.	Petitjean G, Chevalier MF, Tibaoui F, Didier C, Manea ME, Liovat AS, et al. Level of double negative T cells, which produce TGF-beta and IL-10, predicts CD8 T-cell activation in primary HIV-1 infection. AIDS (London, England). 2011. Epub 2011/11/03.

475.	Johansson M, Lycke N. A unique population of extrathymically derived alpha beta TCR+CD4-CD8- T cells with regulatory functions dominates the mouse female genital tract. Journal of immunology (Baltimore, Md : 1950). 2003;170(4):1659-66. Epub 2003/02/08.

476.	Sipsas NV, Sfikakis PP, Kontos A, Kordossis T. Levels of soluble CD40 ligand (CD154) in serum are increased in human immunodeficiency virus type 1-infected patients and correlate with CD4(+) T-cell counts. Clinical and diagnostic laboratory immunology. 2002;9(3):558-61. Epub 2002/05/03.

477.	Olmo M, Saumoy M, Alonso-Villaverde C, Penaranda M, Gutierrez F, Romeu J, et al. Impact of antiretroviral therapy interruption on plasma biomarkers of cardiovascular risk and lipids: 144-week final data from the STOPAR study. HIV medicine. 2012;13(8):488-98. Epub 2012/03/16.

478.	Pamukcu B, Lip GY, Snezhitskiy V, Shantsila E. The CD40-CD40L system in cardiovascular disease. Annals of medicine. 2011;43(5):331-40. Epub 2011/01/20.

479.	Boccara F, Lang S, Meuleman C, Ederhy S, Mary-Krause M, Costagliola D, et al. HIV and coronary heart disease: time for a better understanding. Journal of the American College of Cardiology. 2013;61(5):511-23. Epub 2013/02/02.

480.	Gibellini D, Borderi M, Clo A, Morini S, Miserocchi A, Bon I, et al. Antiretroviral molecules and cardiovascular diseases. The new microbiologica. 2012;35(4):359-75. Epub 2012/10/31.

481.	Nakou E, Babageorgakas P, Bouchliou I, Tziakas DN, Miltiades P, Spanoudakis E, et al. Statin-induced immunomodulation alters peripheral invariant natural killer T-cell prevalence in hyperlipidemic patients. Cardiovascular drugs and therapy / sponsored by the International Society of Cardiovascular Pharmacotherapy. 2012;26(4):293-9. Epub 2012/03/24.

482.   Li N, Workman CJ, Martin SM, Vignali DA. Biochemical analysis of the regulatory T cell protein lymphocyte activation gene-3 (LAG-3; CD223). Journal of immunology (Baltimore, Md : 1950). 2004;173(11):6806-12. Epub 2004/11/24.

483.   Kuylenstierna C, Snyder-Cappione JE, Loo CP, Long BR, Gonzalez VD, Michaelsson J, et al. NK cells and CD1d-restricted NKT cells respond in different ways with divergent kinetics to IL-2 treatment in primary HIV-1 infection. Scand J Immunol. 2011;73(2):141-6. Epub 2011/01/05.

484.   Hegde S, Chen X, Keaton JM, Reddington F, Besra GS, Gumperz JE. NKT cells direct monocytes into a DC differentiation pathway. Journal of leukocyte biology. 2007;81(5):1224-35. Epub 2007/02/22.

485.   Bosnjak L, Sahlstrom P, Paquin-Proulx D, Leeansyah E, Moll M, Sandberg JK. Contact-Dependent Interference with Invariant NKT Cell Activation by Herpes Simplex Virus-Infected Cells. Journal of immunology (Baltimore, Md : 1950). 2012. Epub 2012/05/15.

486.   Exley M, Porcelli S, Furman M, Garcia J, Balk S. CD161 (NKR-P1A) costimulation of CD1d-dependent activation of human T cells expressing invariant V alpha 24 J alpha Q T cell receptor alpha chains. The Journal of experimental medicine. 1998;188(5):867-76. Epub 1998/09/09.

487.   Chan AC, Leeansyah E, Cochrane A, Y DUDA, Mittag D, Harrison LC, et al. Ex-vivo analysis of human Natural Killer T cells demonstrates heterogeneity between tissues and within established CD4(+) and CD4(-) subsets. Clinical and experimental immunology. 2013;172(1):129-37. Epub 2013/03/14.

488.   Maggi L, Santarlasci V, Capone M, Peired A, Frosali F, Crome SQ, et al. CD161 is a marker of all human IL-17-producing T-cell subsets and is induced by RORC. European journal of immunology. 2010;40(8):2174-81. Epub 2010/05/21.

489.   Fergusson JR, Fleming VM, Klenerman P. CD161-expressing human T cells. Frontiers in immunology. 2011;2:36. Epub 2011/01/01.

490.   Aldemir H, Prod'homme V, Dumaurier MJ, Retiere C, Poupon G, Cazareth J, et al. Cutting edge: lectin-like transcript 1 is a ligand for the CD161 receptor. Journal of immunology (Baltimore, Md : 1950). 2005;175(12):7791-5. Epub 2005/12/13.

491.   Peukert K, Wingender G, Patecki M, Wagner S, Schmitt R, Ge S, et al. Invariant natural killer T cells are depleted in renal impairment and recover after kidney transplantation. Nephrology, dialysis, transplantation : official publication of the European Dialysis and Transplant Association - European Renal Association. 2013. Epub 2013/12/20.

492.   Gadola SD, Karadimitris A, Zaccai NR, Salio M, Dulphy N, Shepherd D, et al. Generation of CD1 tetramers as a tool to monitor glycolipid-specific T cells. Philos Trans R Soc Lond B Biol Sci. 2003;358(1433):875-7. Epub 2003/06/14.

493.   Jiang X, Zhang M, Lai Q, Huang X, Li Y, Sun J, et al. Restored circulating invariant NKT cells are associated with viral control in patients with chronic hepatitis B. PloS one. 2011;6(12):e28871. Epub 2011/12/24.

494.   Croudace JE, Curbishley SM, Mura M, Willcox CR, Illarionov PA, Besra GS, et al. Identification of distinct human invariant natural killer T-cell response phenotypes to alpha-galactosylceramide. BMC immunology. 2008;9:71. Epub 2008/12/06.

495.   Engelmann P, Farkas K, Kis J, Richman G, Zhang Z, Liew CW, et al. Characterization of human invariant natural killer T cells expressing FoxP3. Int Immunol. 2011;23(8):473-84. Epub 2011/06/29.
496.   Gyimesi E, Nagy G, Remenyik E, Sipka S, Zeher M, Biro T, et al. Altered Peripheral Invariant Natural Killer T Cells in Atopic Dermatitis. Journal of clinical immunology. 2011. Epub 2011/06/22.
497.   Kee SJ, Kwon YS, Park YW, Cho YN, Lee SJ, Kim TJ, et al. Dysfunction of Natural Killer T Cells in Patients with Active Mycobacterium tuberculosis Infection. Infection and immunity. 2012. Epub 2012/03/14.
498.   Lee SJ, Cho YN, Kim TJ, Park SC, Park DJ, Jin HM, et al. Natural killer T cell deficiency in active adult onset Still's disease: the correlation of its deficiency with natural killer cell dysfunction. Arthritis Rheum. 2012. Epub 2012/05/19.
499.   Metelitsa LS. Flow cytometry for natural killer T cells: multi-parameter methods for multifunctional cells. Clinical immunology (Orlando, Fla). 2004;110(3):267-76. Epub 2004/03/30.
500.   Carvalho KI, Bruno FR, Snyder-Cappione JE, Maeda SM, Tomimori J, Xavier MB, et al. Lower numbers of Natural killer T cells in HIV-1 and Mycobacterium leprae co-infected patients. Immunology. 2012. Epub 2012/01/25.
501.   Batista VG, Moreira-Teixeira L, Leite-de-Moraes MC, Benard G. Analysis of Invariant Natural Killer T Cells in Human Paracoccidioidomycosis. Mycopathologia. 2011. Epub 2011/08/02.
502.   Andersson SK, Paquin-Proulx D, Kroll M, Sandberg JK, Moll M. Technical Advance: Measurement of iNKT cell responses at the single-cell level against rare HIV-1-infected dendritic cells in a mixed culture. Journal of leukocyte biology. 2012. Epub 2012/12/25.
503.   Qiu Y, Chen J, Liao H, Zhang Y, Wang H, Li S, et al. Tim-3-Expressing CD4(+) and CD8(+) T Cells in Human Tuberculosis (TB) Exhibit Polarized Effector Memory Phenotypes and Stronger Anti-TB Effector Functions. PLoS pathogens. 2012;8(11):e1002984. Epub 2012/11/13.
504.   Leitner J, Rieger A, Pickl WF, Zlabinger G, Grabmeier-Pfistershammer K, Steinberger P. TIM-3 Does Not Act as a Receptor for Galectin-9. PLoS pathogens. 2013;9(3):e1003253. Epub 2013/04/05.
505.   Sadagopal S, Lorey SL, Barnett L, Sutherland D, Basham R, Erdem H, et al. Enhanced PD-1 expression by T cells in cerebrospinal fluid does not reflect functional exhaustion during chronic human immunodeficiency virus type 1 infection. Journal of virology. 2010;84(1):131-40. Epub 2009/10/16.
506.   Tandon R, Giret MT, Sengupta D, York VA, Wiznia AA, Rosenberg MG, et al. Age-Related Expansion of Tim-3 Expressing T Cells in Vertically HIV-1 Infected Children. PloS one. 2012;7(9):e45733.
507.   Duraiswamy J, Ibegbu CC, Masopust D, Miller JD, Araki K, Doho GH, et al. Phenotype, function, and gene expression profiles of programmed death-1(hi) CD8 T cells in healthy human adults. Journal of immunology (Baltimore, Md : 1950). 2011;186(7):4200-12. Epub 2011/03/09.
508.   Salek-Ardakani S, Schoenberger SP. T cell exhaustion: a means or an end? Nature immunology. 2013;14(6):531-3. Epub 2013/05/21.

509. Utzschneider DT, Legat A, Fuertes Marraco SA, Carrie L, Luescher I, Speiser DE, et al. T cells maintain an exhausted phenotype after antigen withdrawal and population reexpansion. Nature immunology. 2013;14(6):603-10. Epub 2013/05/07.
510. Sakhdari A, Mujib S, Vali B, Yue FY, MacParland S, Clayton K, et al. Tim-3 negatively regulates cytotoxicity in exhausted CD8+ T cells in HIV infection. PloS one. 2012;7(7):e40146. Epub 2012/07/14.
511. Le Bouteiller P, Barakonyi A, Giustiniani J, Lenfant F, Marie-Cardine A, Aguerre-Girr M, et al. Engagement of CD160 receptor by HLA-C is a triggering mechanism used by circulating natural killer (NK) cells to mediate cytotoxicity. Proceedings of the National Academy of Sciences of the United States of America. 2002;99(26):16963-8. Epub 2002/12/18.
512. Barakonyi A, Rabot M, Marie-Cardine A, Aguerre-Girr M, Polgar B, Schiavon V, et al. Cutting edge: engagement of CD160 by its HLA-C physiological ligand triggers a unique cytokine profile secretion in the cytotoxic peripheral blood NK cell subset. Journal of immunology (Baltimore, Md : 1950). 2004;173(9):5349-54. Epub 2004/10/21.
513. Peretz Y, He Z, Shi Y, Yassine-Diab B, Goulet JP, Bordi R, et al. CD160 and PD-1 Co-Expression on HIV-Specific CD8 T Cells Defines a Subset with Advanced Dysfunction. PLoS pathogens. 2012;8(8):e1002840. Epub 2012/08/24.
514. Leeansyah E, Ganesh A, Quigley MF, Sonnerborg A, Andersson J, Hunt PW, et al. Activation, exhaustion and persistent decline of the anti-microbial MR1-restricted MAIT cell population in chronic HIV-1 infection. Blood. 2012. Epub 2012/12/18.
515. Hebbeler AM, Propp N, Cairo C, Li H, Cummings JS, Jacobson LP, et al. Failure to restore the Vgamma2-Jgamma1.2 repertoire in HIV-infected men receiving highly active antiretroviral therapy (HAART). Clinical immunology (Orlando, Fla). 2008;128(3):349-57. Epub 2008/07/09.
516. Finney CA, Ayi K, Wasmuth JD, Sheth PM, Kaul R, Loutfy M, et al. HIV Infection Deregulates Tim-3 Expression on Innate Cells; Combination Antiretroviral Therapy Results in Partial Restoration. Journal of acquired immune deficiency syndromes (1999). 2013. Epub 2013/01/15.
517. Estrada V, Geijo P, Fuentes-Ferrer M, Alcalde ML, Rodrigo M, Galindo MJ, et al. Dyslipidaemia in HIV-infected women on antiretroviral therapy. Analysis of 922 patients from the Spanish VACH cohort. BMC women's health. 2011;11:36. Epub 2011/08/06.
518. Hegde S, Fox L, Wang X, Gumperz JE. Autoreactive natural killer T cells: promoting immune protection and immune tolerance through varied interactions with myeloid antigen-presenting cells. Immunology. 2010;130(4):471-83. Epub 2010/05/15.
519. Fujii S, Shimizu K, Smith C, Bonifaz L, Steinman RM. Activation of natural killer T cells by alpha-galactosylceramide rapidly induces the full maturation of dendritic cells in vivo and thereby acts as an adjuvant for combined CD4 and CD8 T cell immunity to a coadministered protein. The Journal of experimental medicine. 2003;198(2):267-79. Epub 2003/07/23.
520. Fujii S, Liu K, Smith C, Bonito AJ, Steinman RM. The linkage of innate to adaptive immunity via maturing dendritic cells in vivo requires CD40 ligation in addition to antigen presentation and CD80/86 costimulation. The Journal of experimental medicine. 2004;199(12):1607-18. Epub 2004/06/16.

521.   Parekh VV, Wilson MT, Olivares-Villagomez D, Singh AK, Wu L, Wang CR, et al. Glycolipid antigen induces long-term natural killer T cell anergy in mice. The Journal of clinical investigation. 2005;115(9):2572-83. Epub 2005/09/03.

522.   Wang J, Cheng L, Wondimu Z, Swain M, Santamaria P, Yang Y. Cutting edge: CD28 engagement releases antigen-activated invariant NKT cells from the inhibitory effects of PD-1. Journal of immunology (Baltimore, Md : 1950). 2009;182(11):6644-7. Epub 2009/05/21.

523.   Iyoda T, Ushida M, Kimura Y, Minamino K, Hayuka A, Yokohata S, et al. Invariant NKT cell anergy is induced by a strong TCR-mediated signal plus co-stimulation. Int Immunol. 2010;22(11):905-13. Epub 2010/12/02.

10. Appendices

10.1 Abbreviations

Acronym	**Definition**
aa	amino acids
AC	adenylyl cyclase
αGalCer	alpha-Galactosylceramide
AIDS	Acquired Immune Deficiency Syndrome
APC	antigen presenting cell
APOBEC3G	Apolipoprotein B mRNA editing Enzyme Catalytic peptide-like 3G
ART	Antiretroviral therapy
ARV	Antiretroviral
bp	base pairs
BSA	bovine serum albumin
CBA	cytokine bead array
CCR5	C-C chemokine receptor 5
CDC	centres for disease control
FSW	commercial sex worker
CTL	cytotoxic T lymphocyte
CTLA-4	cytoxic T lymphocyte antigen 4
CXCR4	C-X-C chemokine receptor 4
DC	dendritic cell
DC-SIGN	Dendritic-Cell-Specific ICAM3-Grabbing Non-integrin
DNA	deoxyribonucleic acid
dNTP	Deoxyribonucleotide Triphosphate
EC	elite controller
ELISA	enzyme-linked immunosorbent assay
FCS	fetal calf serum
GDP	guanosine 5'-diphosphate
GNB3	guanine nucleotide binding protein beta polypeptide 3
GPCR	G protein coupled receptor
GRK	G protein-regulated kinases
GTP	guanosine 5'-triphosphate
HAART	highly active antiretroviral therapy
HESN	HIV-exposed seronegative
HIV	Human Immunodeficiency Virus
HLA	Human leukocyte antigen
HRP	horseradish peroxidase
HTLV	Human T cell leukemia virus
IDU	Intravenous drug use
IFN	interferon
IL	interleukin
iNKT	invariant natural killer T cell

Io	ionomycine
IQ	immune quiescence
IQR	interquartile range
IRF	interferon regulatory factor
KIR	killer immunoglobulin-like receptor
LAG-3	lymphocyte activation gene 3
LD	linkage disequilibrium
LPS	lipopolysaccharide
LTNP	long term non-progressor
LTR	long terminal repeat
MAPK	mitogen-activated protein kinase
MCP	monocyte chemotactic protein
MHC	major histocompatibility complex
MIP	macrophage inflammatory protein
ml	millilitre
MSM	men who have sex with men
MTCT	mother-to-child transmission
NaOH	sodium hydroxide
NFkB	Nuclear Factor of Kappa light polypeptide gene enhancer in B-cells
ng	nanogram
NHP	non-human primate
NK	natural killer
NKT	natural killer T cell
PAMP	pathogen-associated molecular pattern
PBMC	peripheral blood mononuclear cell
PBS	phosphate buffered saline
PCR	polymerase chain reaction
PD-1	programmed death 1
PDE	phosphodiesterase
PHA	Phytohemagglutinin
PI3K	phosphatidylinositol-3-kinase
PKC	protein kinase C
PLC	phospholipase C
PMA	Phorbol 12-myristate 13-acetate
PRR	pattern recognition receptor
qRT-PCR	Quantitative Real-Time Reverse Transcriptase PCR
RANTES	Regulated upon Activation, Normal T-cell Expressed, and Secreted
RhoGEF	Rho guanine exhange factors
RM	rhesus macaques
RNA	ribonucleic acid
RP	rapid progressor
RPM	rotations per minute
RT	reverse transcriptase
SDF	stromal derived factor
SIV	Simian Immunodeficiency Virus

SM	sooty mangabey
SNP	single nucleotide polymorphism
STI	Sexually transmitted infection
TCR	T cell receptor
Tim-3	T cell immunoglobulin and mucin domain-containing molecule 3
TLR	toll-like receptor
TNF	tumor necrosis factor
Treg	Regulatory T cell
TRIM5a	Tripartite Motif 5 alpha
ug	microgram
ul	microlitre
UTR	Untranslated region
VC	viral controller
WHO	World Health Organization

10.2 Gag peptide pool

MGARASVLSGGKLDA
PQDLNTMLNTVGGH
RGNFKGQRRIVKCF
SVLSGGKLDAWEKIR
NTMLNTVGGHQAAM
RIVKCFNCGKEGHIA
GKLDAWEKIRLR
NTVGGHQAAMQMLK
FNCGKEGHIARNCRA
LDAWEKIRLRPGGKK
GHQAAMQMLKDTI
EGHIARNCRAPRKK
KIRLRPGGKKKYRLK
AAMQMLKDTINEEAA
ARNCRAPRKKGCWK
PGGKKKYRLKHLVWA
LKDTINEEAAEWDRL
RAPRKKGCWKCGK
KYRLKHLVWASREL
NEEAAEWDRLHPVHA
RKKGCWKCGKEGHQM
KHLVWASRELERFAL
EWDRLHPVHAGPI
WKCGKEGHQMKDCTER
ASRELERFALNPGLL
RLHPVHAGPIPPGQM
GHQMKDCTERQANFL
ERFALNPGLLETSEG
HAGPIPPGQMREPR
DCTERQANFLGKIW
NPGLLETSEGCQQII
IPPGQMREPRGSDIA
RQANFLGKIWPSNK
ETSEGCQQIIGQL
MREPRGSDIAGTTSTL
FLGKIWPSNKGR
EGCQQIIGQLQPAL
SDIAGTTSTLQEQI
GKIWPSNKGRPGNFL
CQQIIGQLQPAL
GTTSTLQEQIGWM
SNKGRPGNFLQSR
QIIGQLQPALQ
STLQEQIGWMTSNPPI

GRPGNFLQSRPEPTA
IIGQLQPALQTGTEEL
SNPPIPVGEIYKRWI
FLQSRPEPTAPPA
PALQTGTEELRSLY
PVGEIYKRWIILGL
SRPEPTAPPAESFGF
TGTEELRSLYNTVA
IYKRWIILGLNKIVR
TAPPAESFGFGEETT
ELRSLYNTVATLYCV
IILGLNKIVRMYSPV
ESFGFGEETTPSPK
YNTVATLYCVHQKI
NKIVRMYSPVSILDI
FGEETTPSPKQEQK
ATLYCVHQKIEVK
MYSPVSILDIRQGPK
TTPSPKQEQKDK
YCVHQKIEVKDTKEA
SILDIRQGPKEPFR
PSPKQEQKDKEPPLA
KIEVKDTKEALDKI
IRQGPKEPFRDYVDR
EQKDKEPPLASLKSL
KDTKEALDKIEEEQNK
KEPFRDYVDRFFKTL
EPPLASLKSLFGNDPL
LDKIEEEQNKSQQK
DYVDRFFKTLRAEQA
LKSLFGNDPLSQ
EEEQNKSQQKTQQAA
FFKTLRAEQATQEVK
KSQQKTQQAAADTGN
RAEQATQEVKNWM
TQQAAADTGNSSQV
EQATQEVKNWMTETL
AADTGNSSQVSQNY
EVKNWMTETLLVQNA
GNSSQVSQNYPIV
MTETLLVQNANPDCK
SQVSQNYPIVQNL
LVQNANPDCKTILKA
SQNYPIVQNLQGQMV

NPDCKTILKALGPGA
IVQNLQGQMVHQAI
TILKALGPGATLEEM
LQGQMVHQAISPRTL
LGPGATLEEMMTA
VHQAISPRTLNAWVK
GATLEEMMTACQGV
SPRTLNAWVKVIEEK
EEMMTACQGVGGPSH
NAWVKVIEEKAF
ACQGVGGPSHKARVL
WVKVIEEKAFSPEVI
GGPSHKARVLAEAM
EEKAFSPEVIPMFSA
HKARVLAEAMSQV
SPEVIPMFSALSEGA
RVLAEAMSQVTNAAI
PMFSALSEGATPQDL
AMSQVTNAAIMMQR
LSEGATPQDLNTML
VTNAAIMMQRGNFK
ATPQDLNTMLNTV
AIMMQRGNFKGQRRI

10.3. Supplementary Data.

Table 10.3.1 Median concentrations of plasma cytokines and chemokines.

Analyte	HIV-N (n=14)*	HIV+ (n=9)*	HIV+ ART (n=13)*	p value**	Post-test differences***
IL-8	5.69 (3.37, 7.99)	3.61 (0.35, 5.21)	5.02 (3.58, 5.74)	0.137	
sCD40L	3621 (2879, 5659)	4404 (3272, 5753)	3954 (2885, 6067)	0.911	
IP-10	**397.0 (331.0, 565.0)**	**1080 (472.1, 2241)**	**543.8 (365.3, 852.1)**	**0.020**	**HIV-N vs HIV+**
MCP-1	187.8 (133.2, 222.2)	171.6 (107.4, 242.2)	201.3 (133.0, 266.8)	0.568	
MIP-1β	9.47 (5.55, 16.55)	8.89 (2.40, 17.22)	12.84 (8.77, 21.37)	0.377	
IFNα2	10.67 (7.37, 13.02)	12.51 (10.33, 19.02)	13.42 (7.97, 20.72)	0.421	
IL-17F	8.0 (8.0, 40.0)	8.0 (8.0, 22.5)	35.0 (8.0, 50.0)	0.266	
IL-17A	1.40 (1.40, 12.27)	1.40 (1.40, 1.40)	1.40 (1.40, 16.43)	0.170	
IFNγ	**2.47 (1.20, 4.85)**	**1.92 (1.20, 3.65)**	**5.90 (1.84, 7.80)**	**0.050**	
MIP-3α	46.88 (26.50, 62.26)	34.08 (19.38, 38.78)	36.85 (27.99, 54.99)	0.250	
IL-12p70	3.85 (1.10, 17.68)	6.02 (1.10, 7.35)	10.23 (3.27, 24.70)	0.153	
IL-22	112.5 (28.25, 163.8)	50.0 (16.0, 75.0)	75.0 (16.0, 160.0)	0.341	
IL-23	360.0 (84.50, 1329)	207.3 (84.50, 380.0)	1038 (84.5, 1241)	0.431	
TNFα	18.61 (14.73, 21.30)	7.48 (7.01, 24.47)	17.14 (11.23, 24.42)	0.336	

*Data are presented as median (IQR).

**Intra-group differences were assessed by Kruskal-Wallis test,

***post-test differences determined by Dunn's post-test.